PHOTOCHEMICAL DEGRADATION

OF POLYSTYRENE

by

ASHLEY SCOTT

A Thesis Submitted for the Degree

of

Doctor of Philosophy

of

The University of Aston in Birmingham

June 1976

SUMMARY

In this work the oxidative degradation of pure polystyrene, polybutadiene and butadiene-modified polystyrene (normally called high-impact polystyrene or HIPS) have been studied using a variety of physical and chemical techniques. The changes in dynamic-mechanical properties occurring during the ultra-violet light accelerated weathering of these polymers were followed by a visco-elastometric technique (Rheovibron) in the solid phase over a wide temperature range. Selective cross-linking of the polybutadiene in high-impact polystyrene caused the depression of the low temperature damping peak (tan δ) with a corresponding sharp peak in tan δ at ambient temperature accompanied by an integral rise in complex modulus. During the same period of photoxidation, the hydroperoxide concentration and gel content increased rapidly, reaching a maximum before decomposing photolytically with the destruction of unsaturation and with the formation of stable oxidation products. Infra-red spectroscopy showed the formation of carbonyl and hydroxyl groups. α,β-unsaturated carbonyl was also identified and was formed by decomposition of both allylic hydroperoxide and initial peroxidic gel by β-scission of the graft between polybutadiene and polystyrene. With further photoxidation a more stable ether gel was formed involving the destruction of the conjugating double bond of α, β-unsaturated carbonyl.

Addition of saturated and unsaturated ketones which are potential sensitisers of photoxidation to high-impact polystyrene and polybutadiene failed to photo-initiate the oxygen absorption of the polymers. A prior thermal oxidative treatment on the other hand eliminated the auto-

accelerating stage leading to linear kinetics as the concentration of thermally-produced hydroperoxide approached a maximum. Antioxidants which act by destroying hydroperoxide lengthened the induction period to rapid oxygen absorption, whilst a phenolic antioxidant behaved as a weak photo-activator initially and a retarder later. Prior photolysis of high-impact polystyrene photo-activated the unsaturated component and caused similar changes in dynamic-mechanical properties to those found during photoxidation although at a much lower rate. Polybutadiene behaves as a photo-pro-oxidant for the destruction of polystyrene in high-impact polystyrene.

The work described herein was carried out at the University of Aston in Birmingham between October 1972 and October 1975.

It has been done independently and submitted for no other degree.

June 1976

A. Scott

ACKNOWLEDGEMENTS

For supervision and inspiration throughout the course of research I am obliged to Professor G. Scott and Dr.A. Ghaffar.

For provision of a research grant and payment of fees I am indebted to Scott, Son & Partners Ltd.

I am especially grateful to my wife, Mrs. E. Scott for maintenance and moral support.

Finally I am grateful to Mrs. D. Scott for showing both proficiency and patience in typing this thesis.

CONTENTS

Page

SUMMARY

INTRODUCTION 1

CHAPTER 1: EXPERIMENTAL 11

1.1 Materials 11

1.2 Sample Preparation 12

1.2.1 Melt Procedure 12

1.2.1.1 Extrusion 12

1.2.1.2 Torque rheometer/compression moulding 13

1.2.2 Special Procedure for Polybutadiene 13

1.2.3 Solution Casting 14

1.2.4 Purification of Chemicals 14

1.2.4.1 Cumene 14

1.2.4.2 Cumene hydroperoxide 15

1.2.4.3 Other reagents 15

1.3 Actinometry 15

1.3.1 Procedure 15

1.3.2 Theory and Evaluation of Results 16

1.3.3 Quantum yield for Photoxidation 18

1.3.3.1 High Impact Polystyrene 18

1.3.3.2 Crystal Polystyrene 19

1.4 Oxygen absorption 20

1.4.1 Design of Apparatus 20

1.4.2 Calibration 20

1.4.3 Oxygen diffusion limitation 22

1.4.3.1 High Impact Polystyrene 22

1.4.3.2 Crystal Polystyrene 22

1.4.3.3.Cumene 26

Page

CHAPTER 1: continued

1.4.4 Partial Pressure Dependence 26

1.4.5 Overall Energy of Activation 30

1.5 Measurement of Dynamic Mechanical Properties 34

1.5.1 Procedure 34

1.5.2 Theory and Evaluation 35

1.6 Measurement of Carbonyl, Hydroxyl, 1,2- and 1,4-polybutadiene absorbances by IR spectroscopy 36

1.6.1 Polymer Films 36

1.6.2 Difference spectra of polymer solutions 37

1.6.3 Verification of Beer-Lambert's Law 37

1.7 Microscopy 37

1.7.1 Electron microscopy (EM) 37

1.7.2 Optical Microscopy (phase contrast) 39

1.8 Chemical determination of hydroperoxides 40

1.9 Determination of gel content 41

1.10 Cross-link Density (CLD) determination by swelling 42

1.11 Pre-irradiation of HIPS 45

1.12 Oven Ageing 45

1.13 Ozone Testing 45

1.14 Singlet Oxygen 46

1.15 Synthesis and Characterisation of metal complexes 46

1.15.1 Procedure 46

1.15.2 C, H, N, analysis 47

1.15.3 UV Spectroscopy 48

1.15.4 EDTA Analysis 49

Page

CHAPTER 2: EFFECT OF PROCESSING AND THERMAL TREATMENT ON UV STABILITY OF HIGH IMPACT POLYSTYRENE 50

2.1 RESULTS 50

2.1.1 Determination of hydroperoxide and other functional groups 50

2.1.1.1 Oven ageing 50

2.1.1.2 Processing 52

2.1.1.3 Photoxidation 55

2.1.1.4 Photolysis 60

2.1.2 Oxygen absorption 62

2.1.2.1 Oven aged films 62

2.1.2.2 Processed material 64

2.1.3 IR Spectroscopy 64

2.1.3.1 Oven aged films 64

2.1.3.2 Processed material 71

2.1.4 Spectroscopy 71

2.1.5 Correlation between hydroperoxide, carbonyl, hydroxyl, trans-1,4-polybutadiene and gel content 75

2.2 DISCUSSION 77

Page

CHAPTER 3: CHEMICAL AND PHYSICAL CHANGES OCCURRING DURING THE UV DEGRADATION OF HIGH IMPACT POLYSTYRENE, CRYSTAL POLYSTYRENE AND POLYBUTADIENE 106

3.1 RESULTS 106

3.1.1 Dynamic-mechanical properties 106

3.1.1.1 High impact polystyrene 106

3.1.1.2 Polybutadiene 118

3.1.1.3 Crystal polystyrene 122

3.1.2 Microscopy 124

3.1.3 IR spectroscopy 133

3.1.3.1 High impact polystyrene 133

3.1.3.2 Crystal polystyrene 139

3.1.3.3 Polybutadiene 142

3.1.4 Correlation between gel content, cross-link density and peak height for polybutadiene 151

3.1.5 Correlation between oxygen absorption trans-1,4-polybutadiene and peak height for high impact polystyrene 153

3.1.6 Correlation between damping and complex modulus at ambient temperature with peak height for high impact polystyrene. 155

3.2 DISCUSSION 158

Page

CHAPTER 4: ACTIVATION AND STABILISATION IN MODEL SYSTEMS AND POLYMER SOLUTIONS 182

4.1 RESULTS 182

4.1.1 Effect of purification 182

4.1.2 Photoxidation of cumene by oxygen absorption 184

4.1.2.1 Cumene hydroperoxide 184

4.1.2.2 Cumyl alcohol 184

4.1.2.3 Dinonyl ketone 187

4.1.2.4 Mesityl oxide 187

4.1.2.5 Acetophenone 190

4.1.2.6 Benzaldehyde 190

4.1.2.7 Benzoic acid 193

4.1.2.8 Phenyl acetic acid 195

4.1.2.9 β-carotene 195

4.1.2.10 3-methyl-1-butene 198

4.1.3 Photoxidation of polybutadiene in chlorobenzene by oxygen absorption 200

4.1.3.1 Cumene hydroperoxide, cumyl alcohol and acetophenone 200

4.1.3.2 Dinonyl ketone 202

4.1.3.3 Mesityl oxide 204

4.2 DISCUSSION 207

Page

CHAPTER 5: INITIATION OF PHOTOXIDATION OF HIGH IMPACT POLYSTYRENE AND ACTIVATION OF POLYSTYRENE BY POLYBUTADIENE 237

5.1 RESULTS 237

5.1.2 Activation of high impact polystyrene by photolysis 237

5.1.2.1 Unstabilised 237

5.1.2.2 Stabilised 240

5.1.3 Activation of polystyrene by polybutadiene 250

5.1.3.1 High impact polystyrene film 250

5.1.3.2 Polybutadiene/polystyrene solution 252

5.1.4 Exposure of high impact polystyrene to ozone 254

5.1.5 Exposure of high impact polystyrene and polybutadiene to singlet oxygen 258

5.2 DISCUSSION 259

Page

CHAPTER 6: INITIATION AND STABILISATION OF HIGH IMPACT POLYSTYRENE WITH METAL COMPLEXES AND OTHER ADDITIVES 276

6.1 RESULTS 276

6.1.1 Metal complexes of thiocarbamic acid 276

6.1.1.1 Nickel 276

6.1.1.2 Cobalt 278

6.1.1.3 Copper 278

6.1.1.4 Zinc 278

6.1.1.5 Iron 282

6.1.2 Alkyl nitroxide 286

6.1.3 Mono-(o-hydroxy-phenyl) phosphoric acid 288

6.1.4 Cloranil 290

6.1.5 Dinonyl ketone 290

6.2 DISCUSSION 293

CONCLUSIONS 309

SUGGESTIONS FOR FURTHER WORK 314

REFERENCES 317

SUPPORTING PUBLICATION

A.Ghaffar, A.Scott and G.Scott, Eur.Poly.J., 11, 271 (1975).

INTRODUCTION

Commercial polystyrene is an atactic polymer; the random spatial position of the phenyl side groups render it incapable of crystallisation. Polystyrene (PS) is a hard, rigid, transparent thermoplastic with good electrical insulation properties and mouldability namely injection moulding and vacuum forming. The principal limitation of polystyrene is its brittleness, although the molecular weight will alter this parameter. A viable way of increasing impact strength and toughness is attained by incorporation of rubber into polystyrene. Blending of polybutadiene (PBD) or styrene-butadiene rubber (SBR), results in only marginally improved impact strength. However, if the rubber is first dissolved in styrene monomer and then polymerised, a graft co-polymer of short polystyrene side chains attached to SBR is obtained. A high impact polystyrene (HIPS) may have several times the impact strength of polystyrene but only half the tensile strength. Hardness and softening point are also reduced, and clarity is replaced by opacity.

Data obtained from bond dissociation energies[1] suggests that the tertiary benzylic hydrogen of polystyrene should be as reactive as allylic hydrogen and more reactive than the tertiary hydrogen of a polymer with a pendent methyl group, polypropylene (PP). Polystyrene is, however, more stable than PP towards oxidative attack. The acquisition of an impact modifier drastically reduces the oxidative stability of HIPS and subsequently the glassy polystyrene matrix. Oxidative deterioration of

a polymer is accompanied by cross-linking and finally chain scission leading to embrittlement and loss of mechanical properties, notably impact strength, elongation, tensile strength, modulus and tear resistance. In the case of polystyrene and HIPS, yellowing is also apparent.

Autoxidation, which has been used mainly to describe thermal oxidation[2], is a free radical chain process and in polymers is typically auto-accelerating. Autoxidation is characterised by an initial slow period of oxygen uptake followed by an accelerating portion attaining linear kinetics and possibly concluded by auto-retardation. Bolland's[3] original kinetic scheme for autoxidation of low molecular weight hydrocarbons also accounts for the thermal degradation of polymers:

initiation	RH	$\rightarrow$	$R^{\bullet}$	(1)
	$2\ ROOH$	$\rightarrow$	$RO^{\bullet} + ROO^{\bullet} + H_2O$	(2)
chain branching	$RO^{\bullet} + RH$	$\rightarrow$	$ROH + R^{\bullet}$	(3)
	$ROO^{\bullet} + RH$	$\rightarrow$	$ROOH + R^{\bullet}$	(4)
propagation	$R^{\bullet} + O_2$	$\rightarrow$	$ROO^{\bullet}$	(5)
	$ROO^{\bullet} + RH$	$\rightarrow$	$ROOH + R^{\bullet}$	(6)
termination	$2ROO^{\bullet}$	$\rightarrow$	$ROOR + O_2$	(7)

Cleavage of carbon-carbon (335 $k.J.mol^{-1}$) or carbon-hydrogen bond (418 $k.J.mol^{-1}$) to produce alkyl radicals (1) is unlikely on the basis of the bond energies involved. The bi-molecular breakdown of hydroperoxide may be considered to dominate the initiation once hydroperoxides are present. Peroxy radicals are believed to be the main chain carriers as illustrated in the propagation reactions (5) and (6). From kinetic[4] studies on the thermal autoxidation of natural rubber it was deduced that

on reaching a stationary hydroperoxide concentration linear kinetics are obtained. This was substantiated by work involving the simultaneous study of oxygen absorption and hydroperoxide formation for the autoxidation of tetralin[5]. The attainment of a critical concentration of hydroperoxide has been reported for the thermal oxidation of atactic polypropylene[6].

Autoxidation was considered to be exclusive to thermal oxidation[2], the auto-accelerating portion being absent in photoxidation. However, it is now generally believed that similar free radical mechanisms occur[7,8] in both thermal and photoxidation. The slow bi-molecular breakdown of hydroperoxide is subsequently replaced by a much faster homolysis,

$$ROOH \xrightarrow{h\nu} RO\bullet + \bullet OH$$

giving rise to a shorter kinetic chain length. The presence of hydroperoxides during photoxidation has been confirmed for rubbers[9] and low molecular weight hydrocarbons[10] but the expected maximum concentration attained during autoxidation for polymers has not been reported. In the present work evidence is provided to suggest that a maximum concentration of hydroperoxide is concomitant with auto-acceleration of HIPS during photoxidation.

Pure hydrocarbons do not absorb substantially in the region of the solar spectrum reaching the earth's surface[11]. However, unstabilised HIPS film degrades under ambient conditions of natural weathering after approximately 50 hours (one week) of sunshine. The apparent degradability of HIPS can not be accounted for by primary photochemical initiation, because of low quantum yields, in which ultra violet (UV)

radiation is absorbed by the "pure" polymer, or oxygen-polymer complexes (similar to those described for low molecular weight hydrocarbon[12]) leads to free radical chain reactions. Absorption of UV by impurities contained in the polymer is more likely. This secondary photochemical initiation will act as a precursor to autoxidation. Polymer manufacture, including polymerisation, thermal processing and possibly contamination will result in the incorporation of peroxidic and carbonyl compounds, and perhaps transition metal ions into the polymer before exposure to UV. Transition metal ions act as sensitisers for the photoxidation of polyolefins[13].

Alkyl hydroperoxides have a maximum absorption at 210 nm[14] but the tail extends into the solar spectrum. Absorption leads to photochemical cleavage of the peroxidic bond with a quantum efficiency approaching unity[15]. Similarly carbonyl groups, whose absorption maxima occur at higher wavelengths[16], 270 to 290 nm, and extends beyond 300 nm, are known to undergo photochemical reactions leading to the formation of free radicals[17,18]. This absorption arises from promotion of a non-bonding, n-orbital electron localised on the oxygen to a delocalised antibonding, π^*-orbital, delocalised over the entire carbonyl group[16]. The excited singlet state, $^1(n - \pi^*)$, may by intersystem crossing (ISC) change to the excited triplet state, $^3(n - \pi^*)$, both of which may lead to chain-scission reactions in the polymers[19]. Breakdown of carbonyl may occur by both radical and non-radical paths, designated by Norrish[20] as type I and type II:

$$RCH_2 - CH_2 - \overset{\overset{O}{\|}}{C} - R' \rightarrow RCH_2 - CH_2 - \overset{\overset{\cdot O}{|}}{\underset{\cdot}{C}} - R' \text{ (triplet)}$$

Type I $\rightarrow$ $RCH_2 - CH_2^{\cdot} + R'CO^{\cdot}$

Type II $\rightarrow$ $RCH = CH_2 + CH_3 - \overset{\overset{O}{\|}}{C} - R'$

The quantum yields for the two types of breakdown differ considerably and the difference is of importance in the photodegradation of polymers. Hartley and Guillet[18,21] have found that Norrish type II is favoured relative to Norrish type I, although the quantum yield for type II decreases with increasing chain length to give 0.06 (tritetracontan-22-one). The quantum yield for type I also decreased with increasing chain length to a value of 0.012. However, low molecular weight aldehydes and ketones produced by Norrish type II breakdown of triplet carbonyl will themselves favour type I homolysis relative to type II. Consequently, photo-initiation by radicals produced by Norrish type I will only be of importance after an appreciable amount of carbonyl has built up in the polymer.

Kautsky[22] has reported that excited states of molecules may be quenched by oxygen to produce excited state oxygen. Trozzlo and Winslow[23] have proposed that the formation of hydroperoxide occurs via singlet oxygen ($^1O_2$) produced by quenching triplet carbonyl. Their mechanism has four steps: absorption of light by carbonyl chromophore; Norrish II involving n-π^* excited states; quenching to form singlet oxygen, and subsequent reaction with vinyl to form hydroperoxide with a corresponding shift of the double bond.

$$^1(>C = O) \xrightarrow[n\text{-}\pi^*]{h\nu} {}^1(>C = O)^* \xrightarrow{ISC} {}^3(>C = O)^*$$

$$\text{Norrish II} \rightarrow \quad CH_3 - \overset{O}{\overset{\|}{C}} - R + RCH_2 - CH = CH_2 \quad \text{vinyl}$$

$$^3(>C = O)^* + {}^3O_2 \rightarrow {}^1(>C = O) + {}^1O_2 \quad \text{singlet oxygen}$$

$$^1O_2 + RCH_2 - CH = CH_2 \rightarrow RCH = CH - CH_2 - OOH$$

allylic hydroperoxide

Further support for the production of singlet oxygen by quenching of excited triplet molecules has been provided by Kearns[24], although no conclusive evidence has been adduced to show that hydroperoxides involved in the photo-initiation of polymer photoxidation occur via the singlet oxygen intermediate.

Quenching of a triplet sensitiser produces two states of singlet oxygen[23], $^1\Sigma_g^+$ state (156.9 k.J.mol^{-1}) and $^1\Delta_g$ state (94.1 k.J.mol^{-1}) which lie above the ground state, $^3\Sigma_g^-$. Attempts have been made to demonstrate the reactivity of singlet oxygen towards polymers by exposure to singlet oxygen produced externally by either chemical or electrical discharge techniques. MacCallum[25] failed to observe reaction of polystyrene with singlet oxygen but found atomic oxygen, also produced by microwave generation, to be reactive. Kaplan and Kelleher[26] have shown by IR that chemically produced singlet oxygen treatment of cis-polybutadiene results in hydroperoxide formation plus conjugation. Similar results were obtained by other workers[27]. Both cis- and trans-polybutadiene reacted with singlet oxygen to give peroxides measured by iodimetry and ATR.

George[28] presents evidence that aromatic carbonyl units are responsible for the phosphorescence of polystyrene observed and suggests they are possible initiators of photoxidation. "Pure" polystyrene containing no hydroperoxide or carbonyl, detectable by IR, may be initiated by acetophenone-type chromophores as a precursor to hydroperoxidation. Klöpffer[29] has reported the phosphorescence spectrum of weakly degraded polystyrene to arise from acetophenone-type end-groups, and fluorescence in the blue spectral region to be a possible consequence of chromophores formed by conjugated double bonds and phenyl groups. However, in this work hydroperoxides are likely to be formed during the prior thermal treatment. Ranby[30] has cited the benzene ring of pure polystyrene as a possible chromophore, leading to formation of singlet oxygen via excitation of the benzene ring and interaction with molecular oxygen. Initiation by this mechanism under environmental conditions is unlikely, considering the very short wavelengths used in these experiments and that singlet oxygen shows no reactivity towards polystyrene[25].

During the UV irradiation of polystyrene Weir[31] has reported an initial stage of rapid chain scission associated with selective fission of "weak links"; a purely photolytic process independent of oxygen. The photolysis of peroxide bonds formed during polymerisation was proposed. Alkoxy radicals produced will initiate free radical chain mechanisms occurring during photoxidation, although no evidence has been provided to demonstrate the presence or relative importance of peroxidic groups produced during polymerisation of commercial polystyrene.

Shimada[32] has studied the photoxidation of ABS and has reported

a decrease in trans-1,4-polybutadiene, although this band overlaps the phenyl group in the IR the change was only that of the trans-1,4-polybutadiene because the phenyl group does not alter. The decay of trans-1,4-polybutadiene was considered to be a result of photolysis which initiates autoxidation:

$$R - CH = CH - CH_2 - CH_2 - CH = CH - R \xrightarrow{h\nu}$$

$$2 \quad R - CH = CH - \dot{C}H_2$$

Direct cleavage of this activated methylene-methylene resulting in chain scission is unlikely to precede tertiary-hydrogen abstraction from 1,2-polybutadiene as mentioned for thermal degradation of ABS[33]:

$$R - CH_2 - \underset{\displaystyle R}{\overset{\displaystyle H \quad \dot{O} - \dot{O}}{\overset{\displaystyle |}{\underset{\displaystyle |}{C}}}} - CH = CH_2 \xrightarrow{\Delta} R - CH_2 - \underset{\displaystyle R}{\overset{\displaystyle \dot{}}{\overset{\displaystyle |}{\underset{\displaystyle |}{C}}}} - CH = CH_2 + \cdot OOH$$

Phillips[34,35] has shown the absorption spectrum of residual products of thermally oxidised polybutadiene to be identical to those formed in photoxidation. The assumption that UV absorption results from α,β-unsaturated carbonyl was supported by the decrease in absorption on vacuum photolysis of thermally oxidised films. Phosphorescence excitation and emission spectra of photoxidised polybutadiene was claimed to be a result of saturated aldehydes and α,β-unsaturated ketones. These are strongly absorbing chromophores in the UV and are possible sources of initiation, but their formation without first forming allylic hydroperoxide is difficult to envisage.

ESR offers a powerful tool for identifying radicals produced by UV irradiation at liquid nitrogen temperature although the relative preponderance of these radicals at ambient conditions of photoxidation is

difficult to assess. Tsuji and co-workers[36] have reported radicals produced during the UV irradiation of polystyrene at -196°C with wavelengths above 250 nm, and have attributed the spectrum to the tertiary-carbon of phenyl radicals. Similarly the ESR spectrum of irradiated cis-1,4-polybutadiene has been attributed to radicals formed by scission of the carbon-carbon bond. A less intense spectrum was formed by hydrogen-abstraction from one of the α-methylene groups.

For most applications of polymers it is necessary to stabilise the polymer against the adverse effects of oxidative degradation. Antioxidants have been divided into two groups[37]: (1) preventive antioxidants, which reduce the rate of chain initiation including peroxide decomposers, metal ion deactivators and UV deactivators and (2) chain-breaking antioxidants, which interfere with chain propagation by removing active free radicals by donation of hydrogen or an electron. For photoxidation the rate of initiation is higher than for thermal oxidation, thus the rate of termination is higher and the kinetic chain length is shorter; kinetic chain breaking antioxidants which act by removing chain propagating alkylperoxy radicals will therefore have little effect[37]. However, antioxidants which act by destroying hydroperoxides produced during melt-processing will also be effective UV stabilisers because of their ability to decompose hydroperoxides formed during photoxidation[38]. Retardation of UV degradation may be attained by the incorporation of UV screens, or UV absorbers which absorb all UV but no visible light and dissipate the absorbed energy in a harmless manner[39].

The objectives of the present work

In the present study attention has been focused on the photoxidation of impact modified polystyrene (HIPS); this being a most interesting and complex system because the rubber accelerates the degradation[40]. It will become clear that the polybutadiene (PBD) moiety dominates and behaves as a photo-pro-oxidant for polystyrene. It is believed that the same photochemical processes occur during the photoxidation of commercial, "crystal" polystyrene thus an insight may be obtained from the behaviour of polystyrene initiated by PBD in HIPS. This approach necessitated a study of pure PBD. Polybutadiene of known microstructure was used; not the "impact modifier" of "uncontrolled" polymerisation used in the manufacture of HIPS. In conjunction with the mechanistic study on the above system a correlation between chemical and dynamic-mechanical properties occurring during UV degradation of polystyrene, HIPS and PBD was attempted. The affect of various activating and stabilising additives was also investigated for HIPS.

CHAPTER 1

EXPERIMENTAL

1.1 Materials

Two samples of high impact polystyrene (HIPS) and one of "crystal" polystyrene (PS) were kindly donated by Badische Anilin and Soda-Fabrik A.G. (BASF), Ludwigshafenrheim. The following information was provided:

Commercial grade (Bi 1003), HIPS

6.5% polybutadiene rubber

3.0% paraffin oil

0.1% phenolic antioxidant

traces of residual monomer and processing aids.

Laboratory sample (B 1003), HIPS

6.5% polybutadiene rubber

3.0% paraffin oil

traces of residual monomer and processing aids.

no antioxidant.

Crystal polystyrene (168 N), PS

molecular weight average

approximately 300 000

commercial antioxidant.

A sample of polybutadiene rubber, Intene 55 NFA, of known microstructure, prepared by lithium butyl catalysed polymerisation, was donated by The International Synthetic Rubber Company Ltd., (ISR), Southampton. The composition was as follows:

51% trans-polybutadiene

11% vinyl-polybutadiene

37% cis-polybutadiene

Sodium salts of dibutyl dithiocarbamate(45% w/v aq. solution) were donated by Robinson Brothers Ltd., West Bromwich.

1.2 Sample preparation

1.2.1 Melt Procedure

1.2.1.1 Extrusion

Continuous film of even thickness was extruded using an 18 mm Betol, (Betol Machinery Ltd, Luton, Bedfordshire). Both HIPS and "crystal" PS were extruded. Fixed temperature settings were used throughout all operations. These were as follows: barrel zone 3 at 220°C, barrel zone 2 at 180°C, barrel zone 1 at 160°C, die zones 1 and 2 at 220°C. A 10°C temperature gradient was used on the take-off rollers. The top roller was set at 60°C and the bottom at 40°C. Take-off speed was fixed at 2.3 $m.min^{-1}$ (7.5 ft/min) and screw speed (approximately 20 rpm) was adjusted to produce various thicknesses of extrudate, ranging from 15 to 100 μm. It is believed that the above conditions are similar to commercial processing of HIPS (BASF) material, albeit on a reduced scale. The incorporation of additives into HIPS by

extrusion mixing produced films of good homogenerity and little pre-mixing of chip with additive was necessary.

1.2.1.2 Torque rheometer/compression moulding

A full charge (36 g) of polymer chip was used in the chamber, left open to air (ram withdrawn) of the variable RAPRA torque rheometer[41]. A temperature of 200°C was used throughout processing operations for various times at high shear rate (72 rpm). The hot melt was chilled rapidly in water on removal from the rheometer to avoid uncontrolled thermal oxidation.

The appropriate weight of material was compression moulded (using steel plates with aluminium backing-plates) to obtain even films of desired thickness between 50 and 100 μm. The platterns of the mould were set at 180°C. Maximum pressure was maintained for one minute before water-cooling the mould to room temperature.

1.2.2 Special procedure for polybutadiene

Normal melt extrusion or compression moulding of PBD proved impossible owing to the unfavourable visco-elastic properties of the original uncross-linked material and the rapidity of oxidative attack. Consequently useful films of PBD were obtained only when specific conditions were observed. 8 g of PBD were compression moulded using a good quality cavity mould (76.2 μm). The mould was maintained at 120°C under a pressure of 10.9 $M.Nm^{-2}$ for two minutes then water-cooled to 15°C before removing the mould. The moulded film was then sandwiched between two frames and kept below 0°C until required.

1.2.3 Solution Casting

Films were cast from solution of polymer in either toluene or dichloromethane (1% w/v up to 20% w/v) onto a clean glass plate. An atmosphere of nitrogen at reduced pressure was maintained for up to 72 hours by passing a steady stream of nitrogen over the film and removing the vapour/nitrogen with the aid of a water-jet vacuum line. Cast films were then floated off under water and dried in vacuo.

1.2.4 Purification of Chemicals

1.2.4.1 Cumene

Crude cumene (BDH) was first distilled under argon between 148°C and 153°C; only the middle fraction was retained. This was then shaken with an equal volume of 10% sodium carbonate solution in distilled water to destroy traces of hydroperoxides; this procedure was repeated five times. The cumene was washed with distilled water until the pH returned to neutrality then dried over anhydrous calcium sulphate and distilled from molecular sieves under argon at 151°C at atmospheric pressure. Only the middle fraction was collected. This "final" distillation was repeated three to four times; the pure cumene was kept under argon, below 0°C.

Passing the pure cumene through an alumina column[42] served only to contaminate the hydrocarbon and lead to spurious photo-oxygen absorption results.

1.2.4.2 Cumene hydroperoxide

Cumene hydroperoxide (CHP), obtained from BDH (stabilised with 6% of a 15% w/w slurry of sodium bicarbonate with water) was purified by the method of Kharasch[43]. The final distillation was effected with the aid of a Perkin triangle; the temperature of the CHP being kept below 60°C at 0.01 mm Hg. The pure colourless liquid was stored below 0°C.

1.2.4.3 Other Reagents

Distillation over molecular sieves under argon was found to be the most effective means of purification and was adopted for all other liquids. Dinonyl ketone (Koch-Light) was used without further re-crystallisation.

1.3 Actinometry[44]

1.3.1 Procedure

A calibration graph for ferrous ions was prepared by using 0.4×10^{-6} mol. ml^{-1} of Fe^{2+} in 0.1 N H_2SO_4 -(a) (freshly prepared by dilution from standardised 0.1 M $FeSO_4$ in 0.1 N H_2SO_4), 0.1% O-phenanthroline monohydrate in water-(b) and buffer solution, 600 ml of N sodium acetate plus 360 ml of N H_2SO_4 diluted to 1 litre - (c). Into a series of 25 cm^3 volumetric flasks the following volumes of (a) were added: 0, 0·5, 1·0 ... 4·5, 5·0 ml. 0·1 N H_2SO_4 was added so as to make the total acidity equivalent to 10 ml of 0·1 N H_2SO_4. 2 ml of (b) and 5 ml of (c) were then added (mixing after each addition) and made up to the mark and allowed to stand for half an hour. The optical

density (OD) was measured at 510·5 mm in a 1 cm cell. A correction for each OD for the value obtained with the solution to which no ferrous ions had been added was made and the results plotted against the amount of ferrous ions added.

25 ml of 0·006 M potassium ferrioxalate, $K_3Fe(C_2O_4)_3$, (V_1) was irradiated in a quartz tube, internal diameter of 2.5 cm for up to 40 sec.,(t). During irradiation the actinometer was stirred by a current of oxygen-free nitrogen to facilitate mixing and prevent oxidation of ferrous ions. After irradiation a 10 ml aliquot (V_2) was pipetted into a 25 cm^3 volumetric flask; 2 ml 0·1% O-phenanthroline solution was added, followed by 5 ml of buffer solution and made up to the mark with distilled water. The solution was well mixed and allowed to stand for half an hour IN THE DARK. An identical solution for use as a blank in the reference beam was prepared using unirradiated solution. The OD was measured at 510·5 mm in a 1 cm cell.

1.3.2 Theory and Evaluation of results[45]

From the above data the number of ions of Fe^{2+} formed during photolysis ($n_{Fe^{2+}}$) was calculated by using:

$$n_{Fe^{2+}} = \frac{\log_{10} Io/I \times V_1 \times V_3 \times N}{V_2 \times 1 \times \varepsilon_\lambda}$$

where V_1 = vol. of actinometer solution irradiated (ml)

V_2 = vol. of aliquot taken for analysis (ml)

V_3 = final vol. to which aliquot V_2 is diluted (ml)

$\log_{10} Io/I$ = measured OD of the solution at 510·5 nm.

l = path length of spectrophotometer cell used (1 cm)

ε_λ = experimental value of molar extinction coefficient of Fe^{2+} complex as determined from the slope of the calibration plot (ca. $1{\cdot}1 \times 10^4$ $\ell.mol^{-1}.cm^{-1}$)

N = Avogadro's Number

Thus knowing $n_{Fe^{2+}}$ from the above equation, the value of the quantum yield ($Q_{Fe^{2+}}$) for Fe^{2+} ion formation was selected from tables[44], the light intensity I_o^i, incident just inside the front window of the actinometer tube was calculated using the equation:

$$I_o^i = \frac{n_{Fe^{2+}}}{Q_{Fe^{2+}} \times t \times (1-10^{-\varepsilon[A]\ell})}$$

where $(1 - 10^{-\varepsilon[A]\ell})$ is the fraction of incident light absorbed by the actinometer solution.

where $\varepsilon = 1{\cdot}05 \times 10^4$ $\ell.mol^{-1}.cm^{-1}$ (experimental data)

$[A] = 6 \times 10^{-3}$ $mol.\ell^{-1}$

$\ell = 2{\cdot}5$ cm

Therefore $(1 - 10^{\varepsilon[A]\ell}) \simeq 1$

t = time of irradiation (sec.).

Thus I_o, the incident light intensity measured in photons (or einsteins) $cm^{-2}.s^{-1}$ may be calculated by:

$$I_o^i = I_o.S$$

where S = area of the front window of the actinometer tube (cm^2)

Thus $I_o = \frac{I_o^i}{S} \equiv \frac{\text{quanta}.s^{-1}}{cm^2}$

$\equiv$ quanta. s^{-1}. cm^{-2}

However, 1 mol of photons (i.e. Avogadro's Number)

$\equiv$ 1 einstein

ie. $6{\cdot}023 \times 10^{20}$ photons $\equiv$ 1 einstein

Therefore $I_o = \frac{\text{quanta}.\ s^{-1}.cm^{-2}}{6{\cdot}023 \times 10^{20}}$

$\equiv$ einsteins. s^{-1}. cm^{-2}

Results:

Exposure time t (sec)	Absorbance with blank in ref. beam	I_o (quanta. $^{-1}.cm^{-2}$)	I_o (einstein. $^{-1}cm^{-2}$)
10	0·161	$0{\cdot}385 \times 10^{16}$	$6{\cdot}39 \times 10^{-6}$
20	0·373	$0{\cdot}446 \times 10^{16}$	$7{\cdot}40 \times 10^{-6}$
30	0·533	$0{\cdot}425 \times 10^{16}$	$7{\cdot}05 \times 10^{-6}$
40	0·765	$0{\cdot}457 \times 10^{16}$	$7{\cdot}59 \times 10^{-6}$

1.3.3 Quantum yield for photoxidation[46]

1.3.3.1 High Impact Polystyrene

The initial rate of photoxidation by oxygen absorption in oxygen (25°C) of unstabilised HIPS extruded film, 50 μm thickness, was $11{\cdot}25 \times 10^{-12}$ mol. s^{-1}. cm^{-2}. Assuming 100% absorbance

of incident radiation, (O D of HIPS, 50 μm, was > 1·5 for wavelengths used), the corresponding rate of absorption of quanta is $7{\cdot}11 \times 10^{-6}$ einsteins. s^{-1}. cm^{-2}. Hence the quantum yield (ϕ_{yield}) for photo-xidation of HIPS is $1{\cdot}58 \times 10^{-6}$.

1.3.3.2 Crystal polystyrene

The initial rate of photoxidation of "crystal" polystyrene in oxygen (25°C), 25 μm thickness, was $2{\cdot}66 \times 10^{-12}$ mol. s^{-1}. cm^{-2}. The optical density (OD) of "crystal" PS, 10 μm thick-ness, was 1·5 at 260 nm corresponding to nearly 100% absorption of UV. Consequently, for 25 μm film, 100% absorbance of incident radiation was assumed. Therefore, the quantum yield for photoxidation of "crystal" PS is $3{\cdot}74 \times 10^{-7}$. A value of $8{\cdot}73 \times 10^{-2}$ has been reported for shorter wavelengths[47].

1.4 Oxygen absorpton

1.4.1 Design of apparatus

Two systems were used (see photograph) for measurement of photoxidation by oxygen absorption (photo-oxygen absorption) of thin polymer films, and model compounds or polymer solutions. The principle used in both cases being the same. For polymer films, two identical sets of tubes were arranged on the reciprocating rack (10 cm) in front of alternate Westinghouse/Atlas fluorescent sun lamps, the intensity of which approximates to a normal distribution centred at a maximum intensity of 317 nm and 350 nm with a cut-off at 280 nm and 300 nm respectively[48]. Samples (up to 30 cm^2) were fixed onto the face of the inner (pyrex) tube.

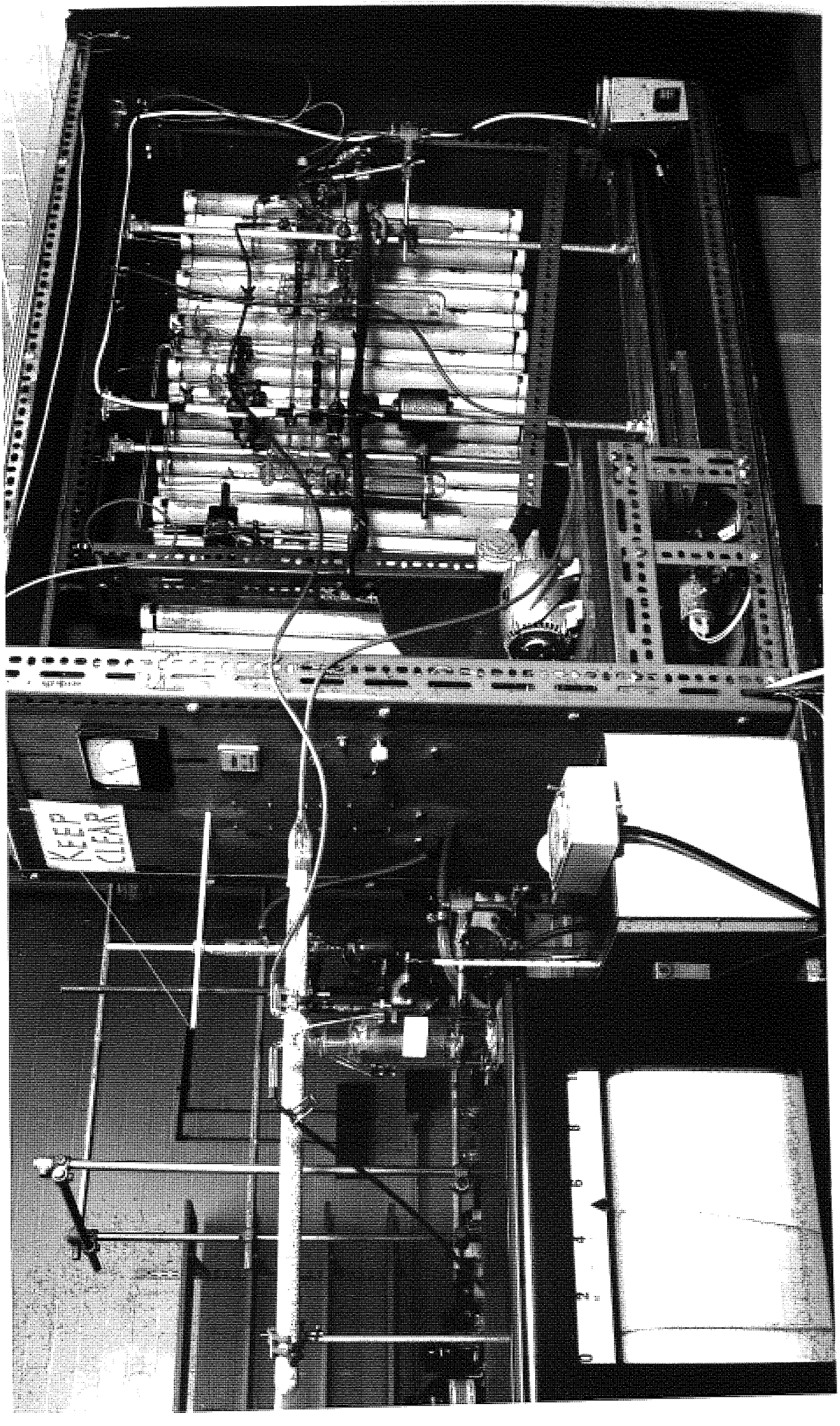
KEEP
CLEAR

This was enclosed in a larger (fused quartz) tube. The atmosphere of the cavity (126 cm^3) containing the sample was purged with oxygen, via a drying tube, or left as air. 2 g of freshly activated molecular sieves were placed in the sample tube to absorb molecular products of photoxidation (CO_2, CO and H_2O, found by mass spectroscopy) which would otherwise detract from oxygen absorption results. The change in volume of oxygen, absorbed by the polymer during photoxidation, and hence pressure was recorded on a chart recorder via a pressure transducer, (maintained at 2·0 volts) Pye Ether Ltd.,Stevenage, Hertfordshire, type UP-3TC ± 34·5 $k.Nm^{-2}$ (which was internally temperature compensated). The film was maintained at constant temperature by pumping thermostatically controlled water through the inner tube and cooling the returning water by means of a water condenser. This arrangement enabled the reaction temperature to be varied from 15°C to 70°C. For most experiments a temperature of 25·0 ± 0·5°C was used.

A similar system of quartz tubes (95·5 cm^3) was designed for model compounds. However, an uncompensated transducer was used (UP-3), although this was partially rectified by copious lagging; no control of reaction temperature was possible. The liquid in the reaction tube was stirred continuously during photoxidation by small inert magnetic stirrer and motor mounted on the rack directly below the sample tube. Rate of stirring was controlled by a Variac unit.

1.4.2 Calibration

Calibration of the chart recorder was attained for both systems by extracting a known volume of gas isothermally, at the

Calibration curves for oxygen absorption

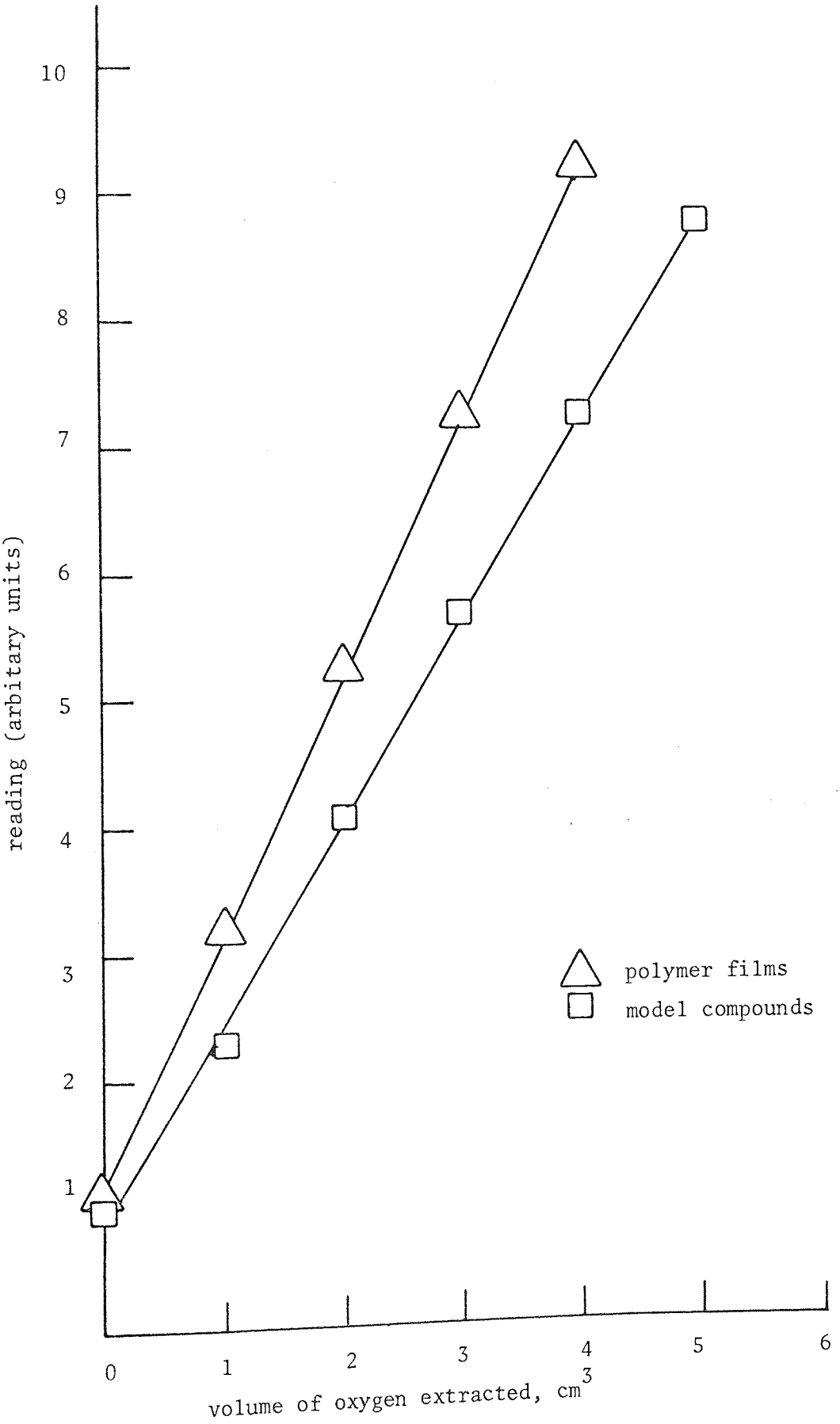

Figure 1.

temperature of operation, from the sample vessel and reading the corresponding value on the recorder. Zero suppression was set at a reading of "one" on the chart paper. A graph of reading against extracted volume was plotted for each series, figure 1.

1.4.3 Oxygen diffusion limitation

1.4.3.1 High Impact Polystyrene

Before reliable information could be obtained from photo-oxygen absorption measurements on HIPS it was essential to select a standard thickness of film whose rate of photoxidation was not limited by the rate of oxygen diffusion into the polymer. Also a very thin sample, because of restrictions imposed by the dimensions of the tubes, would be of insufficient mass to absorb enough oxygen to be recorded accurately. Figure 2 shows the effect of film thickness on oxygen absorption in oxygen of samples cast from solution (see 1.2.3). Maximum rates were plotted against inverse thickness in the manner described[49], figure 3. An inverse linear relationship holds for the rate of photoxidation and film thickness down to 55 μm, below this the rate is independent of oxygen diffusion. Consequently films of 50 μm thickness were used for oxygen absorption measurements on HIPS. This thickness was adopted as standard for most experiments involving a variety of other techniques.

1.4.3.2 Crystal Polystyrene

A similar procedure was used for "crystal" PS; the photoxidation rate is considerably slower, figure 4. No inflexion point is apparent, although it is believed that the inherently slower

Effect of thickness on the photoxidation of unstabilised HIPS cast film (oxygen absorption in oxygen).

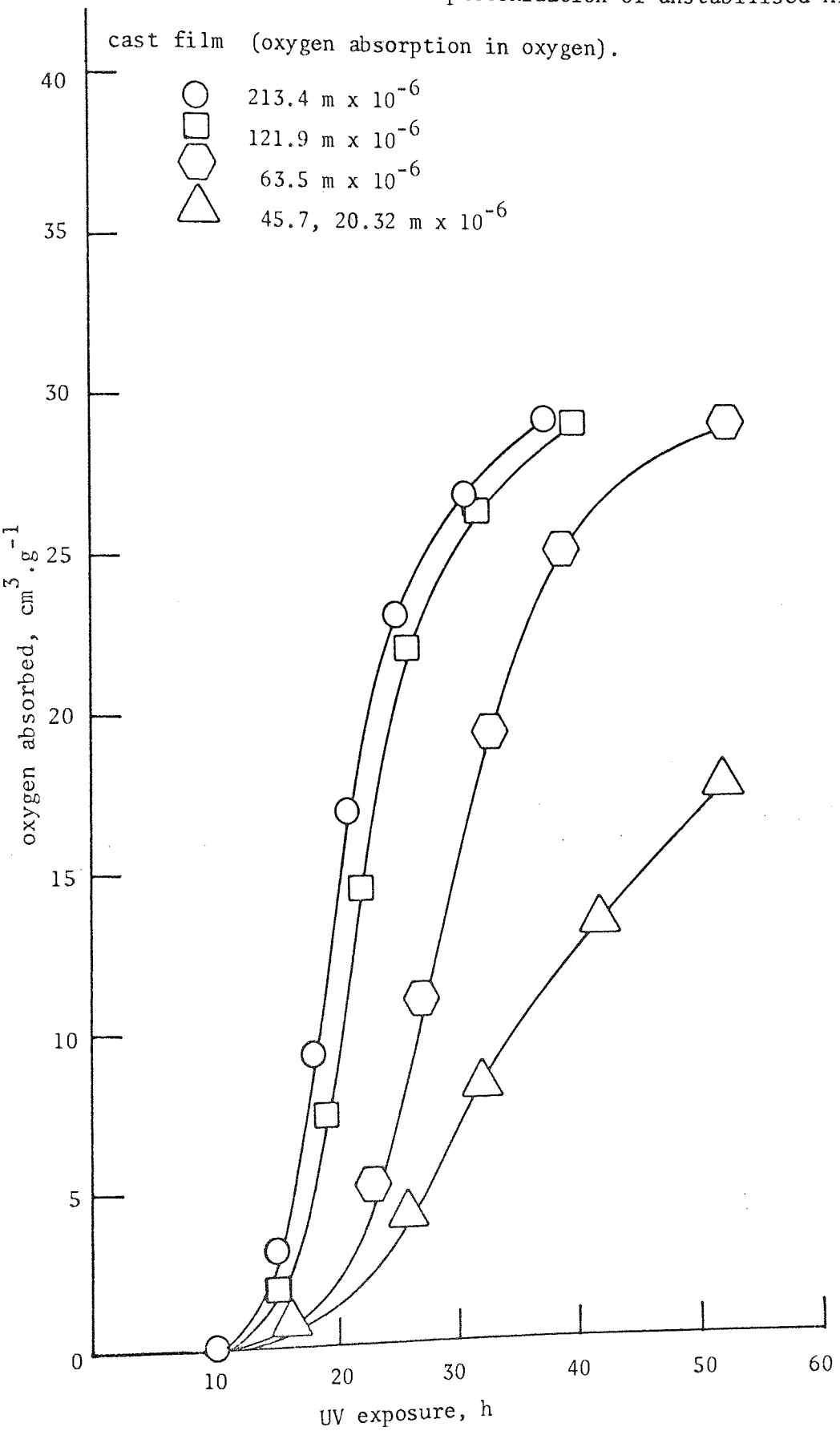

Figure 2.

Variation of rate of photoxidation of unstabilised HIPS cast film with decreasing film thickness.

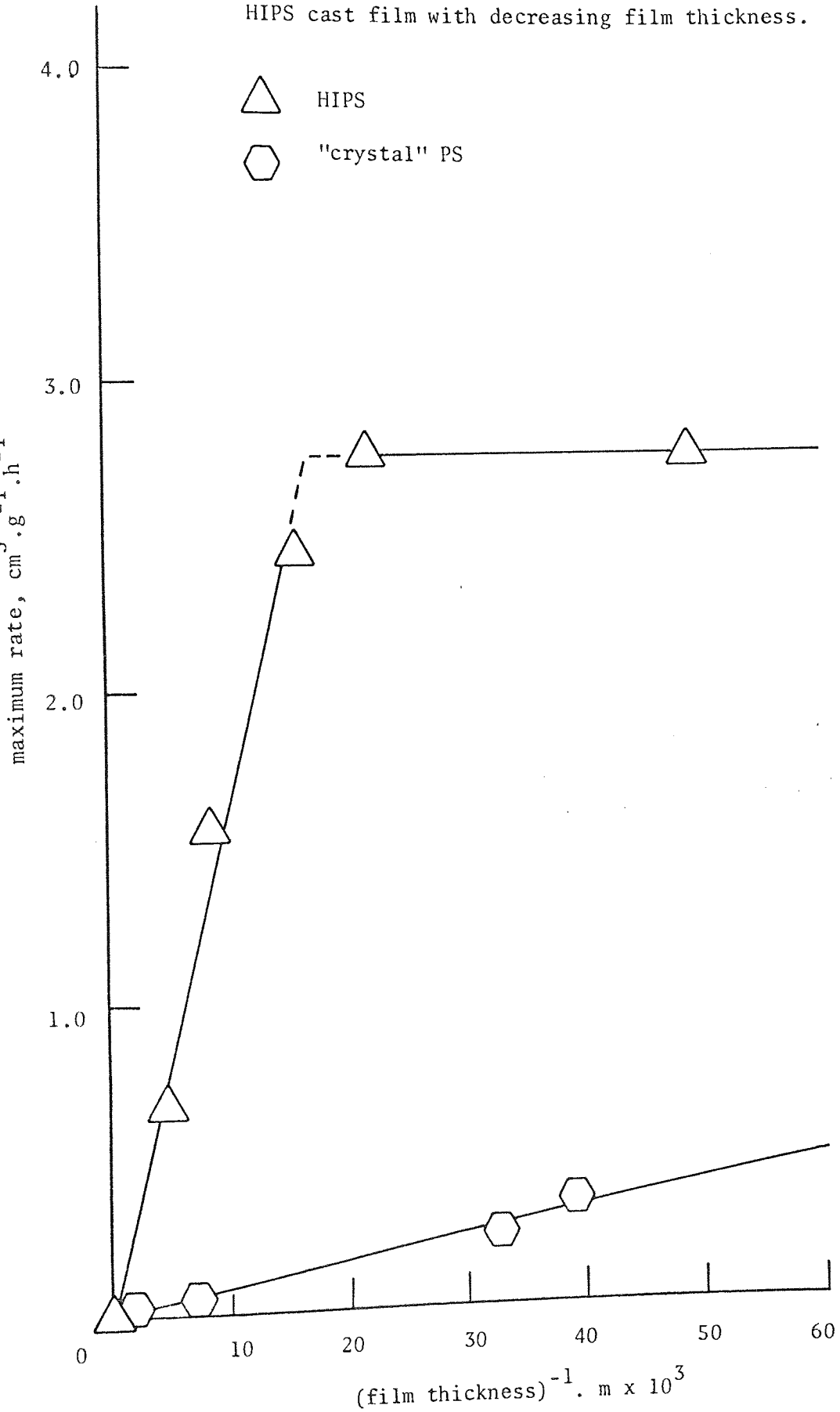

Figure 3.

Effect of thickness on the photoxidation of "crystal" PS cast film (oxygen absorption in oxygen).

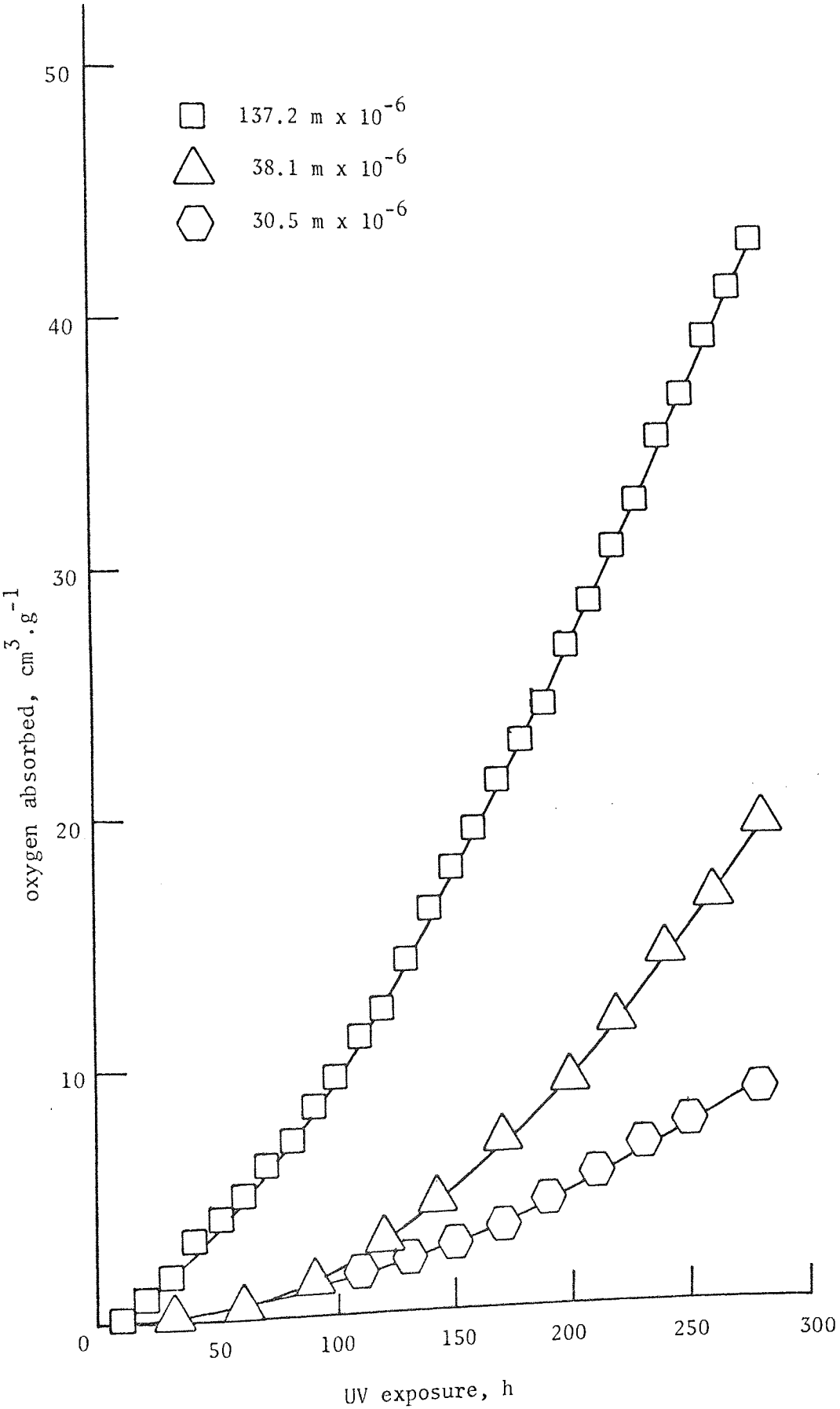

Figure 4.

oxidation rate will lessen the importance of oxygen diffusion limitation. Nevertheless films of thickness down to 15 μm were used for oxygen absorption and up to 50 μm for other techniques. A diffusion path of 5 μm, that is a film of 10 μm thickness, has been reported in the literature for "crystal" PS[50].

1.4.3.3 Cumene

The difficulty in obtaining reliable kinetic measurements on liquid-phase autoxidations because of the problem of maintaining oxygen saturation in the liquid has been reported[51]. Figure 5 shows the effect of stirring rate on the photoxidation of pure cumene; the initial rate increases with increasing rate of stirring. However, this apparent dependence of initial rate on oxygen diffusion may be a combination of several factors, namely, increased mixing of activating species formed during photoxidation of cumene (CHP), and an increase in the area under irradiation. Nevertheless, all reactions subsequently performed were stirred at moderate speed as standard. In the case of solutions of polymer in chlorobenzene, stirring is essential to ensure complete mixing.

1.4.4 Partial pressure dependence

The atmosphere used in polymer photo-oxygen absorption is of decisive importance. From figure 6 it is clear that the initial and maximum rate of photoxidation is faster for a sample exposed in pure oxygen than air. The induction period is also shorter. For this reason when correlation between oxygen absorption and other techniques necessitating UV exposure of HIPS film in air was desired, the cavity

Effect of rate of stirring on the photoxidation of 1 ml of cumene (oxygen absorption in oxygen)

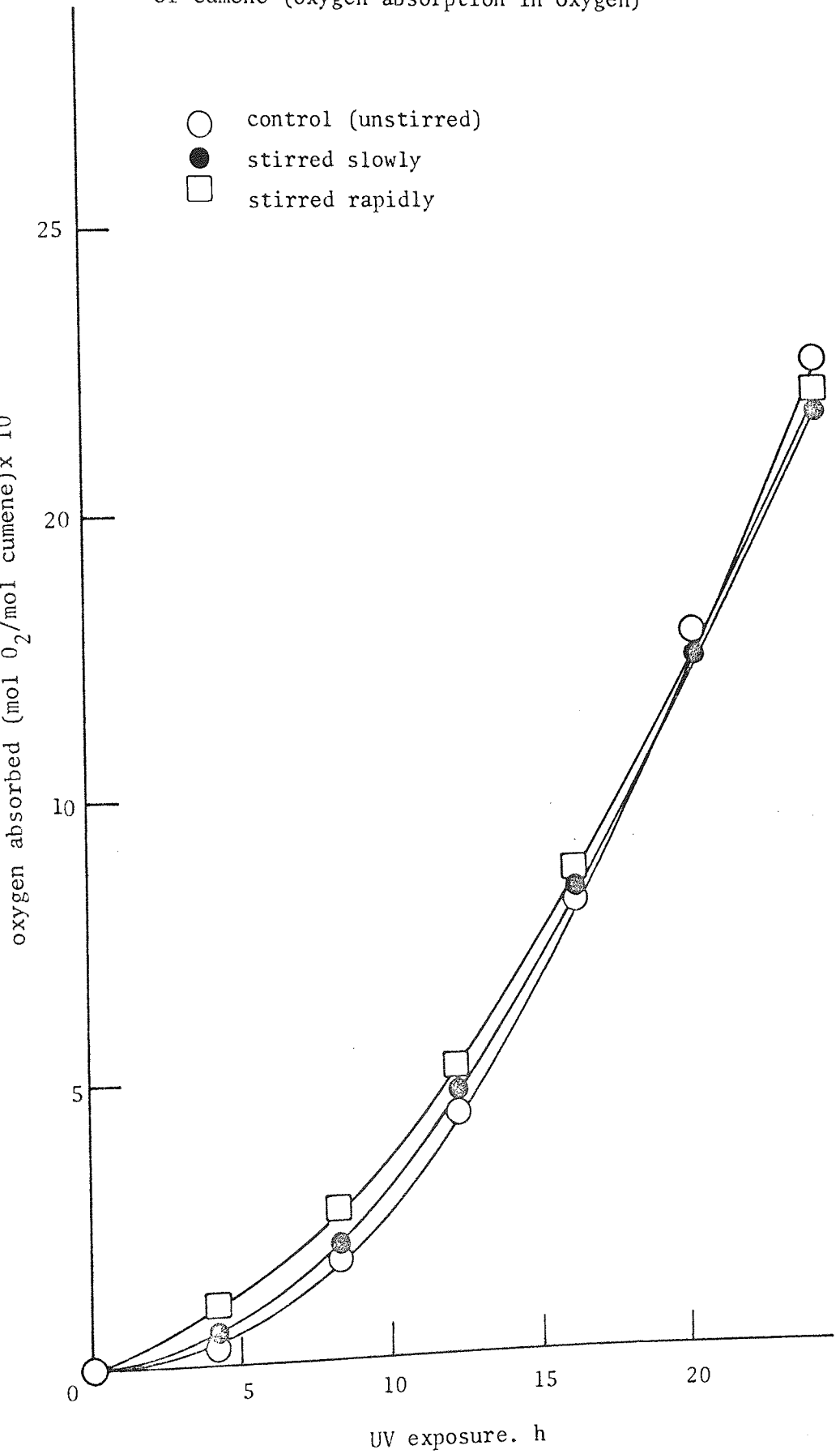

Figure 5.

Effect of atmosphere on the photoxidation of stabilised HIPS extruded film.

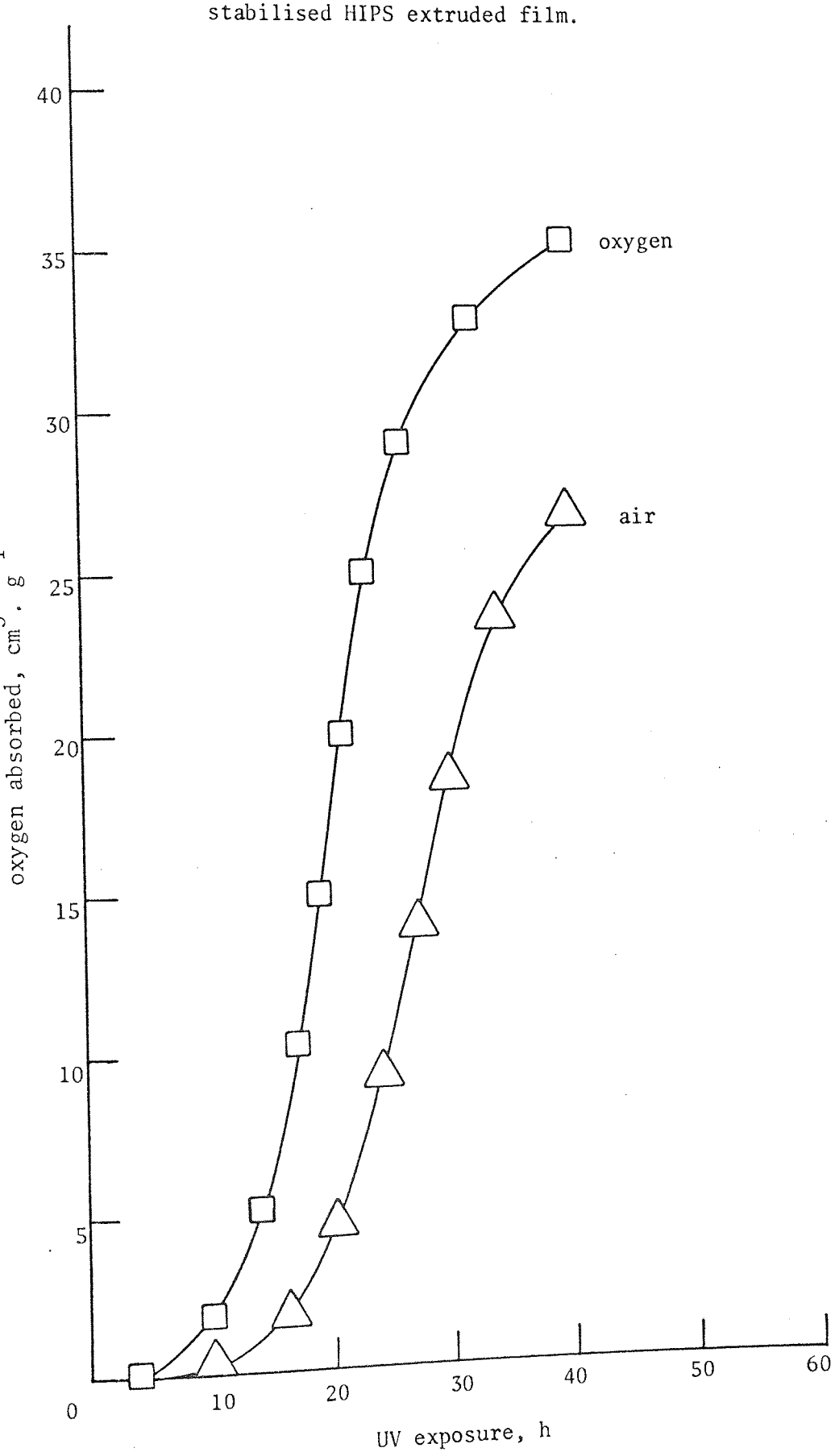

Figure 6.

Dependence of initial rate of photoxidation of stabilised HIPS extruded film on the partial pressure of oxygen

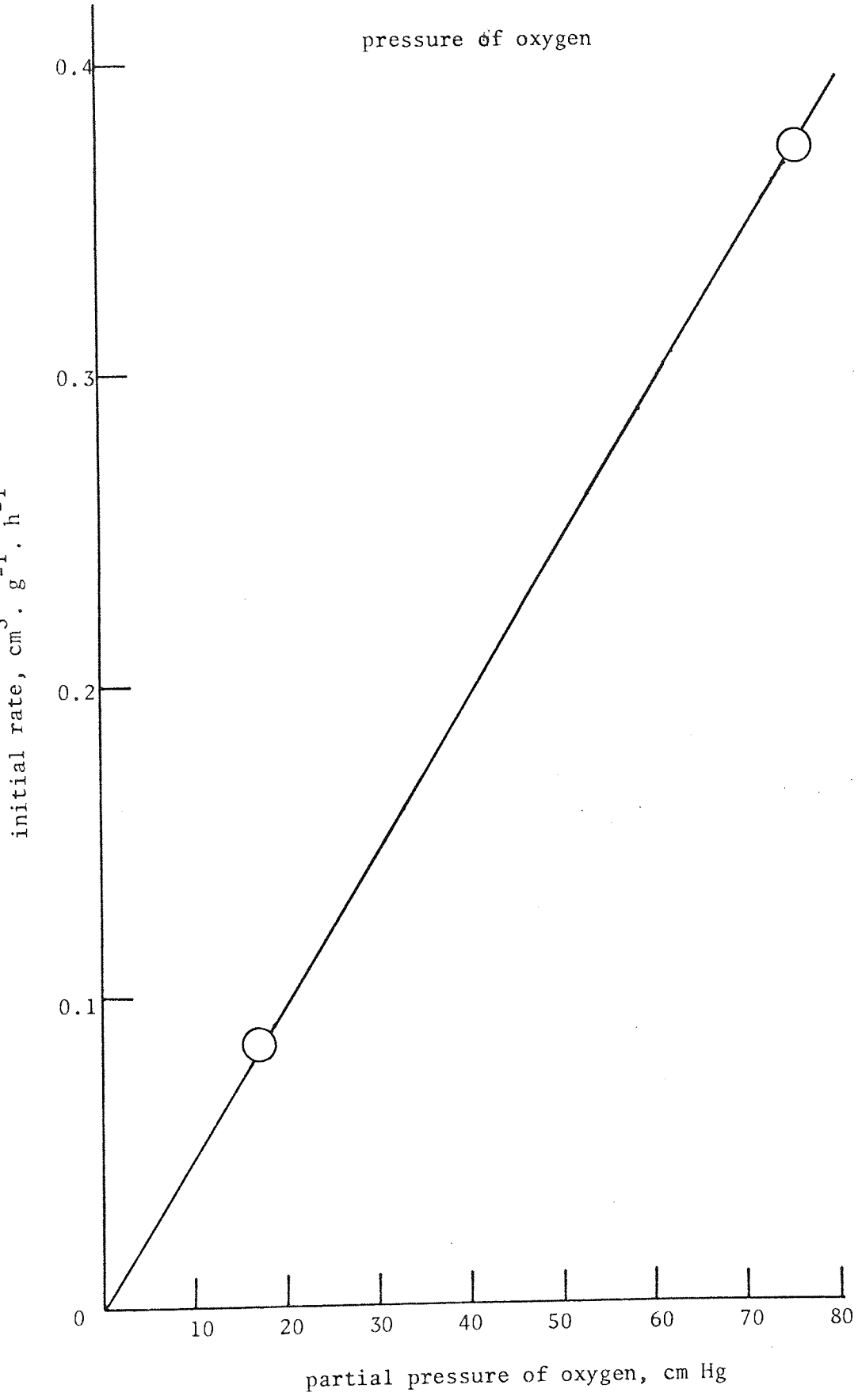

Figure 7.

(see 1.4.1) was left to acquire a fresh supply of ambient air. Oxygen was used for all other work including model compound experiments. From figure 7 a linear dependence, passing through the origin, is apparent between initial rate of oxygen absorption and partial pressure of oxygen present initially. These results are in good agreement with data obtained for the photo-oxygen absorption of "crystal" PS by other workers[47]. It might be expected that during the course of photo-xidation absorption of oxygen would decrease the partial pressure of an air-filled vessel and reduce the rate. However, the maximum pres-sure change obtainable from this system is 3·6 cm.Hg, with negligible affect on rate (see figure 7).

1.4.5 Overall Energy of Activation

The effect of temperature on the photo-oxygen absorption of HIPS containing no antioxidant is illustrated in figure 8. These results were converted into extent of reaction ,$(n_o - n_1)\mu$ mol.g^{-1} (where n is the number of mols of oxygen) by using the experimental fact that 1 mol of an ideal gas occupies 22·4 ℓ at STP. Other workers have derived a relationship which takes into consideration small changes in volume of the vessel arising from displacement of the manometric liquid[52]. When the mercury manometer is replaced by a pressure transducer no change in volume occurs (see 1.4.1).

The photoxidation of HIPS was interpreted in accordance with first order kinetics, figure 9. Reasonable straight lines were obtained. The derived rate constants (k) increased with reaction temperature in agreement with Arrhenius; $\log_{10}k$ was plotted against the inverse of

Effect of temperature on the photoxidation of unstabilised HIPS extruded film. (oxygen absorption in oxygen)

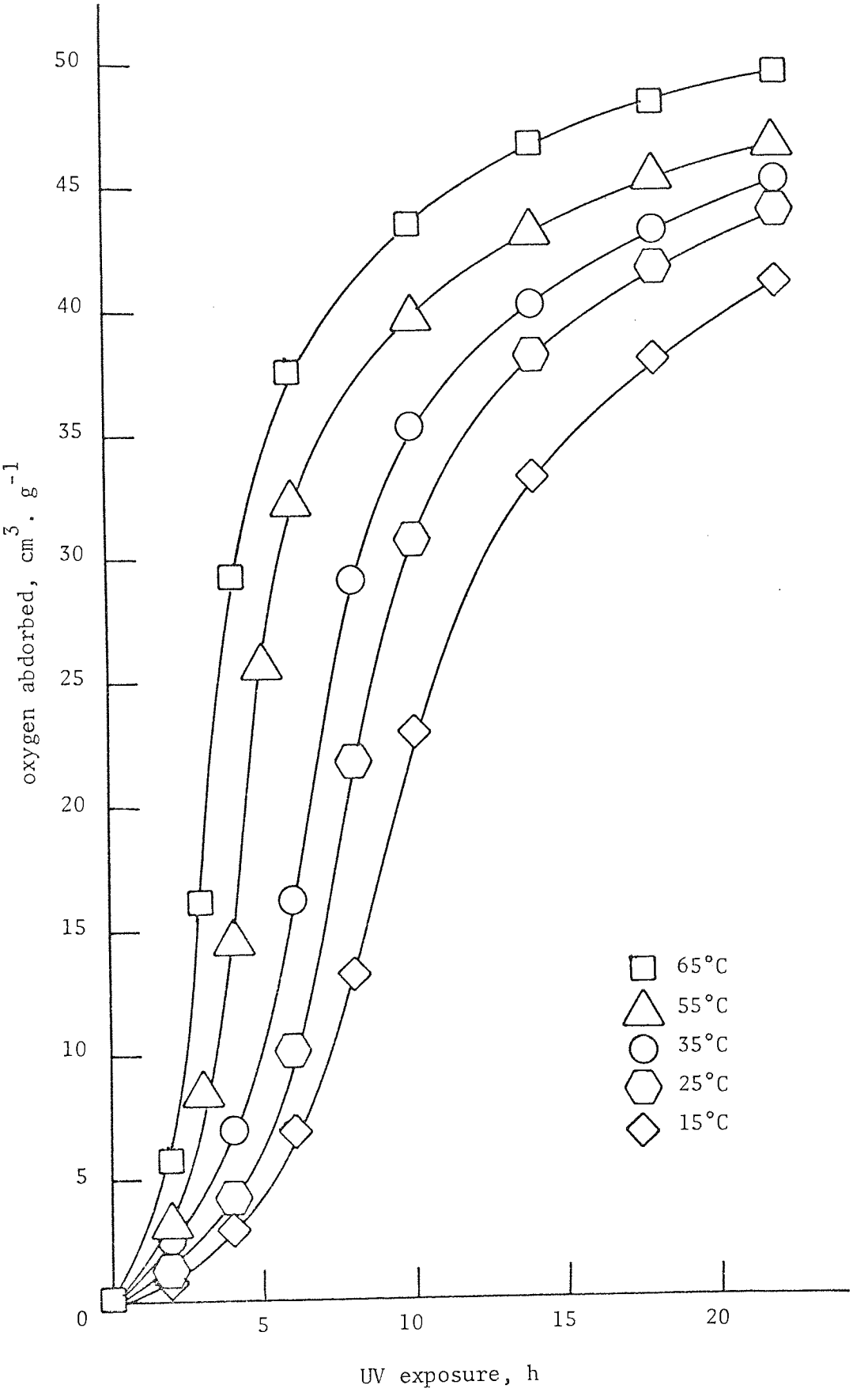

Figure 8.

Photoxidation of unstabilised HIPS extruded film interpreted as a first order reaction.

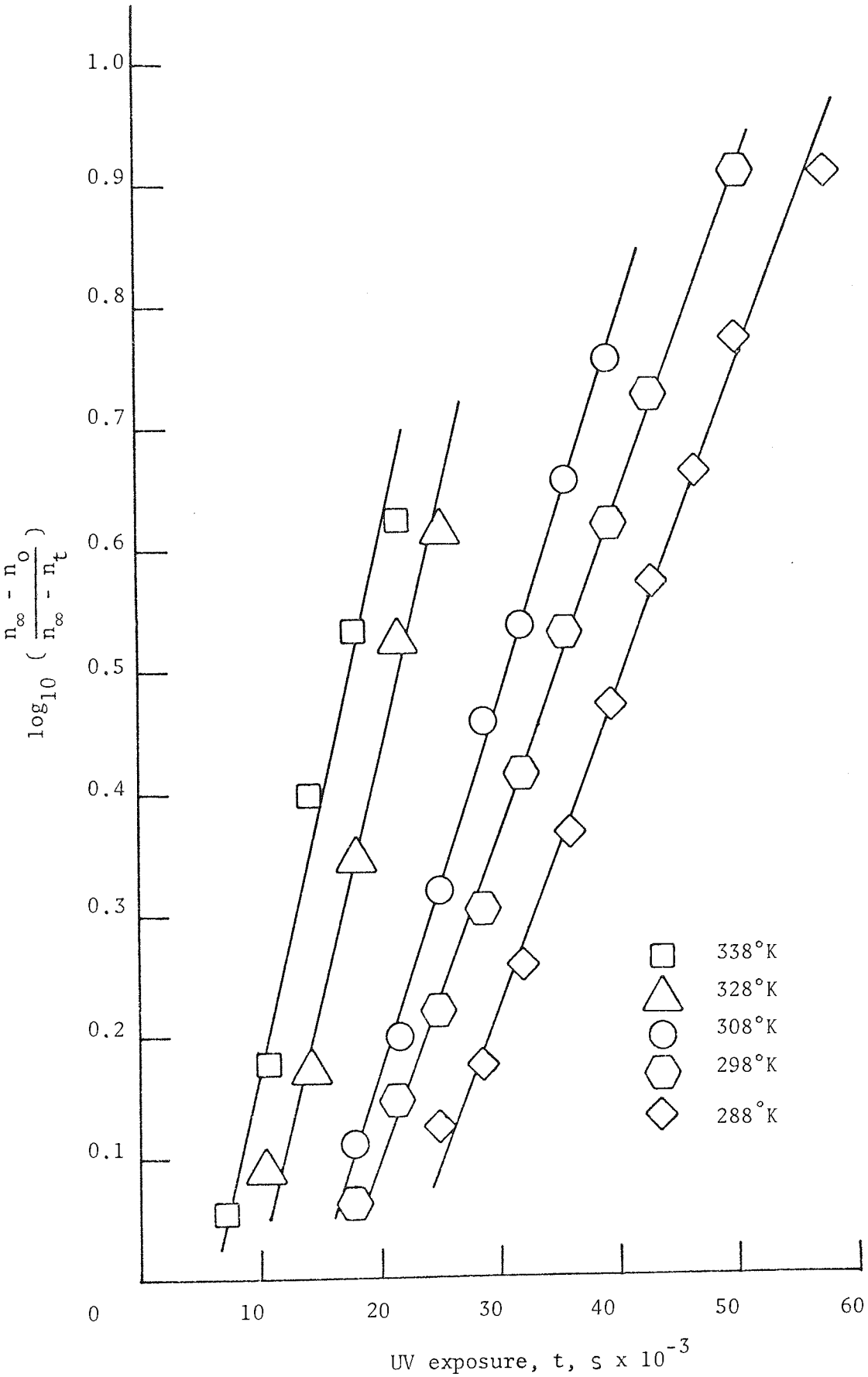

Figure 9.

Plot of $\log_{10}k$ against $^{1}/_{T}$ for the photoxidation of unstabilised HIPS extruded film.

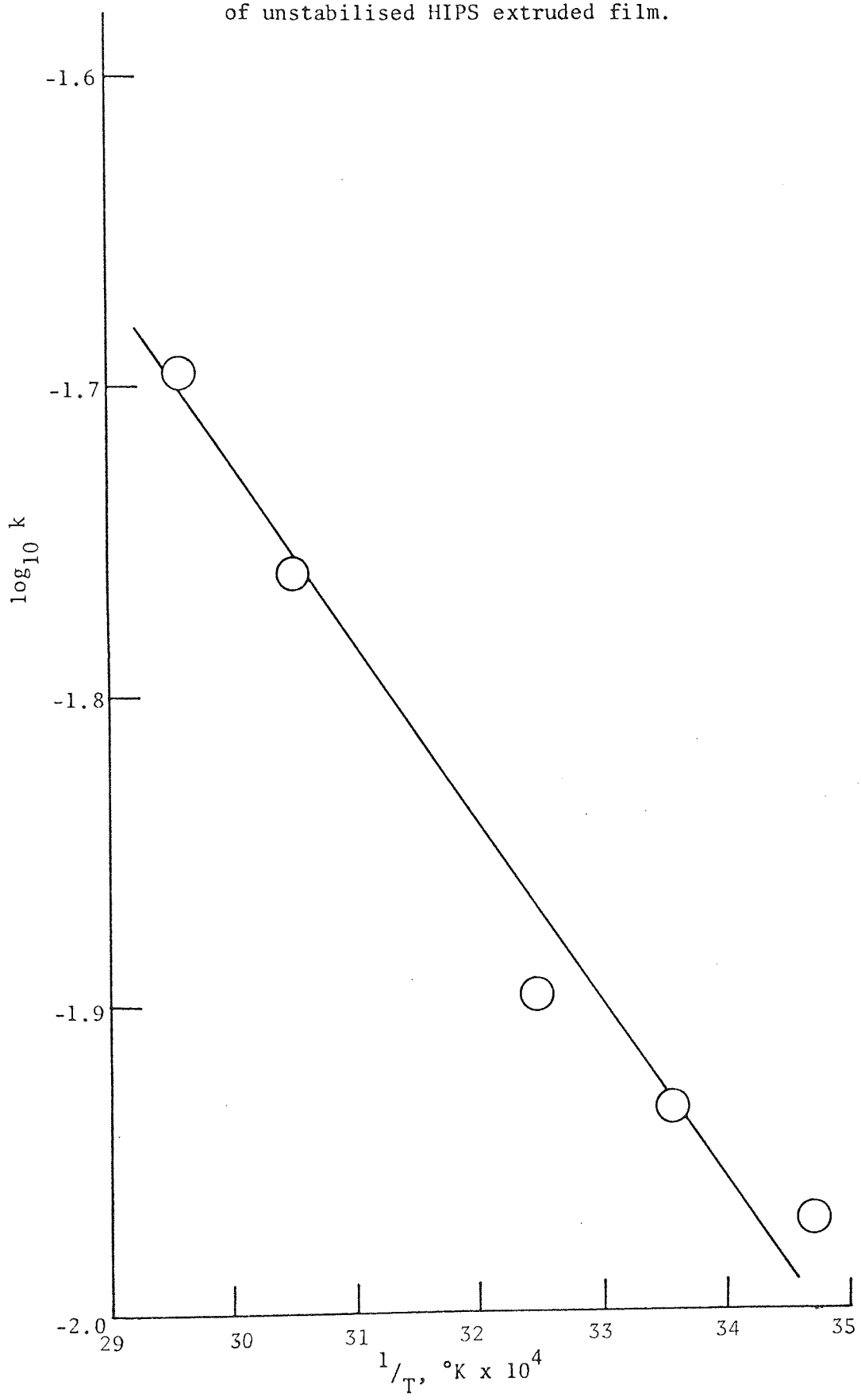

Figure 10.

the absolute temperature (T), figure 10. The overall energy of photo-activation for HIPS was calculated from the slope and found to be 11•1 $k.J.mol^{-1}$ (2•64 $k.cal.mol^{-1}$). A value 25•1 $k.J.mol^{-1}$ (6•0 $k.cal.mol^{-1}$) has been reported for "crystal" PS[47]. HIPS, therefore, requires less energy for activation; this is to be expected.

1.5 Measurement of Dynamic Mechanical Properties

1.5.1 Procedure

The Rheovibron Model DDVII, Toyo Measuring Instruments Co.Ltd., (TMI), Tokyo[53], was used at ambient temperature and over a temperature range from -130°C up to + 100°C. All measurements were made at a frequency of 110 hertz (Hz). Specimens (3 mm x 60 mm) were stamped out using a steel cutter from either cast or extruded film. The sample chamber was cooled by maintaining a steady stream of dry air which was cooled by a liquid nitrogen reservoir. Two techniques were used for taking readings at low temperatures. The sample chamber was either cooled to - 130°C fairly quickly, maintaining constant tension in the sample to prevent "kinking" or fracture. After reaching equilibrium the liquid nitrogen was allowed to boil off and readings were taken as the chamber slowly returned to ambient conditions; the air flow being adjusted as required. Or secondly, readings were taken during the cooling operation. The former method was found to give more accurate results owing to better temperature control. For high temperature work a different chamber was used equipped with an electrical heating device. The simplicity of this arrangement presented no problems of temperature control.

1.5.2 Theory and Evaluation

The purpose of the Rheovibron is to measure the temperature dependence of the complex modulus of high polymers at a definite frequency. Both ends of the specimen are clamped to two transducers; one being a stress (force) gauge, T-1, and the other a strain (displacement) gauge, T-7. A sinusoidal tensile strain is applied to one end of the sample in a viscoelastic state and a sinusoidal stress is generated at the other end of the sample. Stress and strain are out of phase by an angle delta (δ). After the absolute values of the electrical vectors transduced from T-1 and T-7 have been adjusted to unity by attaining full scale deflection, vector substraction is made by changing the output circuits of the two gauges. This enables the value of $\tan\delta$ to be read directly from the meter. The storage modulus, E', (elastic component) and the loss modulus, E'', (viscous component) are calculated from the amplitude of stress and strain and the value of δ. Derivation of basic equations are explained fully elsewhere[53]. Complex modulus, embracing both viscous and elastic components may be calculated from the following equation:

$$|E^*| = 2{\cdot}0 \times \frac{1}{AxD} \times \frac{L}{S} \times 10^8 \ N.m^{-2}$$

where L = sample length (cm)

S = cross-sectional area (cm^2)

A = value corresponding to amplitude factor selected[53] (usually A was equal to 1·0)

D = dynamic force reading on dial.

An error correction (K) may be included in the value of dynamic force:

$$|E^*| = 2{\cdot}0 \times \frac{1}{Ax(D-K)} \times \frac{L}{S} \times 10^8 \ N.m^{-2}$$

The value of K was found to be diminished and consequently had negligible affect on the final calculation of complex modulus. Thus the dynamic-mechanical spectra of HIPS, "crystal" PS and PBD were obtained, with respect to photoxidation and photolysis.

1.6 Measurement of Carbonyl, Hydroxyl, 1,2- and 1,4-polybutadiene absorbances by IR Spectroscopy

1.6.1 Polymer Films

Standard procedure was adopted on films either cast from solution or extruded (see 1.2.1 and 1.2.3) using the Perkin Elmer Model 457, IR spectrophotometer. Films of 50 μm thickness were found to be consistent with the requirements for no interference and to give measurable absorption peaks. Two instrument settings were used, each for qualitative or quantitative analysis. For qualitative observations the spectrum from 4000 cm^{-1} to 250 cm^{-1} was recorded at slow or medium scan speeds. Whereas for quantitative kinetic measurements, only selected peaks were recorded at an expansion of $2\frac{1}{2}$ times on continuous chart paper. In both cases the peak at 1940 cm^{-1} was taken as the reference peak for HIPS and "crystal" PS. The appropriate indexes were defined as the ratio of the absorbance of growing or decaying peak to that of the reference.

1.6.2 Difference spectra of polymer solutions

For this work a pair of sodium chloride variable path cells were used. 1% polymer (HIPS or "crystal" PS) solution in dichloromethane gave measurable peaks at a path length of approximately 2 mm. Samples in the form of films were exposed to UV prior to dissolution. By judicious adjustment of the cell containing unexposed sample in the reference beam, all peaks including those corresponding to dichloromethane were compensated for, leaving only those of the oxidation products and cross-linking. Consequently identification of the peaks that would otherwise have been masked by "background" absorption was possible.

1.6.3 Verification of Beer-Lambert's Law

Beer-Lambert's Law states that light is exponentially attenuated during its passage through the film or that $I_t = I_o.e^{-k\ell}$ where Io and I_t are the incident and transmitted intensities and ℓ is the film thickness. This was found to be so and is illustrated in figure 11 for both "crystal"PS and HIPS. Both lines pass through the origin indicating that very little (if any) light is scattered or reflected at the film surface. HIPS attenuates more readily then "crystal" PS; this is to be expected considering the opacity introduced by impact modification with rubber, resulting in a two phase system.

1.7 Microscopy

1.7.1 Electron Microscopy (EM)

The grafted rubber phase of HIPS was examined by transmission EM(AEI, EM 6B) using the procedure reported in the literature[54,55]. Samples of HIPS film (3 mm x 1 mm) were placed in stoppered bottles

Verification of Beer-Lambert's Law for the photoxidation of stabilised HIPS and "crystal" PS cast films

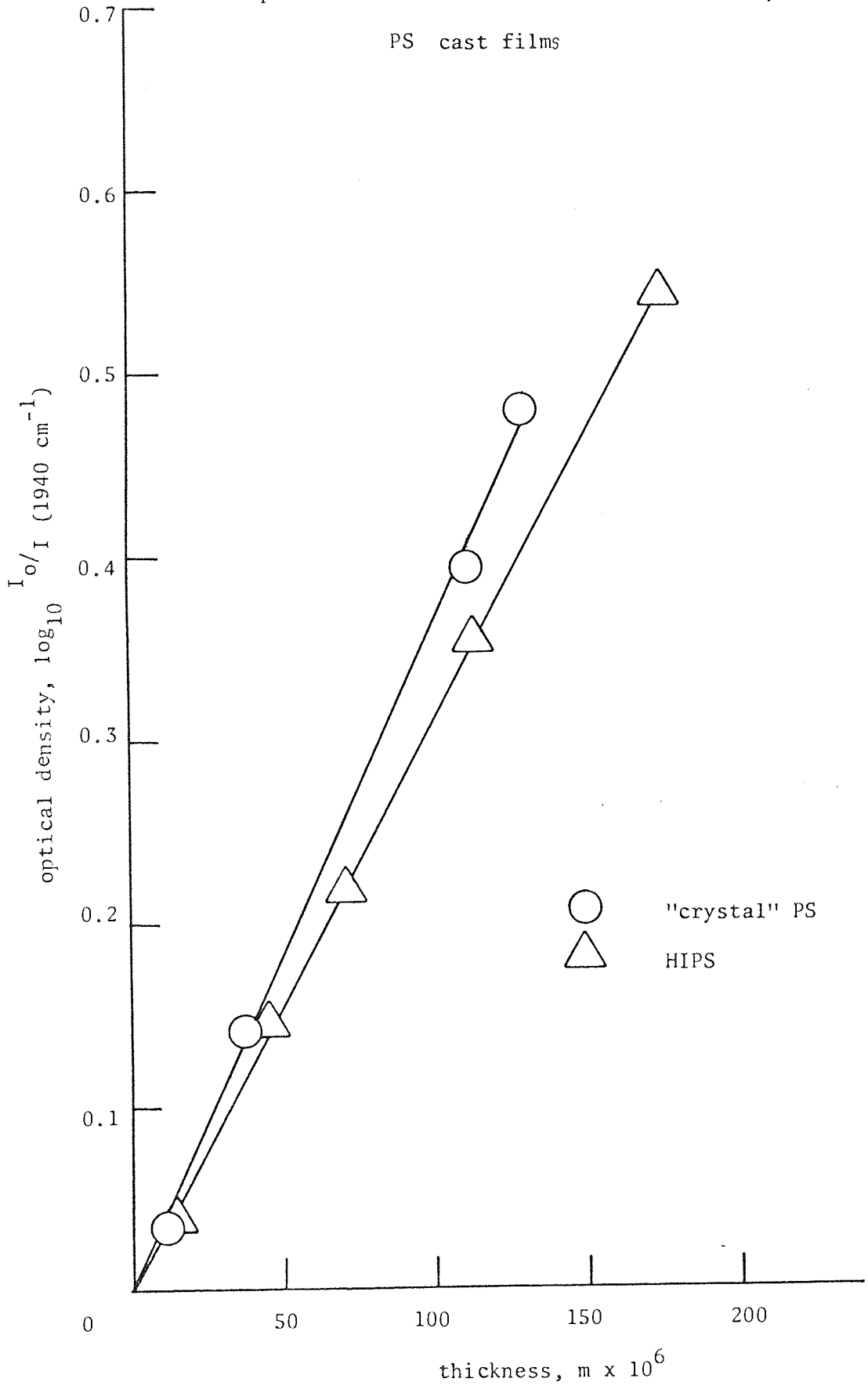

Figure 11.

containing osmium tetroxide solution (2% aq.) and allowed to stand for 48 hours, washed with distilled water and dry alcohol. The stained samples were placed in capsules, filled with resin and baked in an oven for 48 hours at 60°C. Microtomed sections of polymer were then examined by EM.

1.7.2 Optical Microscopy (phase contrast)

Phase contrast microscopy has become a viable method of studying the nature and uniformity of rubber dispersion in impact modified polymers[56,57]. It is based on the principle of magnifying the differences in the amplitude of waves which combine at the eye piece of the microscope to form the image; with the effect of modifying the relative intensities of background and object to increase contrast. This is attained by illuminating the sample with a hollow cone of light from a substage condenser having a special annular lens. Light from the specimen passes through a special diffraction plate situated behind the focal plane of the objective; light unaffected by the specimen is advanced in phase by one quarter of the wavelength. The two wave fronts, diffracted and undiffracted, interfere at the final image plane to produce an image of enhanced contrast.

A solid block of HIPS was microtomed using a sledge microtome set at 2 μm. Good sections were transferred with a soft-bristle brush onto the surface of hot glycerol, to uncoil the specimen. After mounting on a slide and after dying excess glycerol a drop of glycerol-potassium mercuric iodide solution was added to increase the refractive index of the medium[57]. In addition to ultra thin microtomed specimens

obtained from the processed material, films of similar thickness were cast from very dilute solutions in toluene. (see 1.2.3).

1.8 Chemical determination of hydroperoxides

Hydroperoxides play a key role in the degradation of polymers, consequently a reliable method of quantitative determination is of great value. Iodiometry has been used to measure hydroperoxides formed in nylon 66 during UV exposure[58].

With the use of hydriodic acid as a strong reducer total peroxidic oxygen present including alkyl peroxide, cyclic and hydroperoxide has been determined[59]. Other methods based on complex formation using O-phenanthroline measure hydroperoxide content only[60], although this technique was found to be too sensitive leading to poor reproducibility. In the present study, polymer hydroperoxides, and possibly peroxides, produced by either thermal ageing or UV exposure of HIPS extruded film were determined quantitatively by an iodiometric method[61]. Samples, approximately 1 g, were placed in a flask equipped with a gas inlet tube. 40 ml of Analar isopropyl alcohol and 2 ml of glacial acetic acid were added through the reflux condenser. Carbon dioxide was passed for 3 minutes, before heating to reflux. 10 ml of isopropyl alcohol saturated with sodium iodide was introduced through the condenser and the refluxing continued for 15 minutes. Carbon dioxide flow was maintained for a further 3 minutes. After cooling, the flask was disconnected and the contents, titrated with standardised 0·01 N sodium thiosulphatesolution to the disappearance of the yellow. It was necessary to establish the effect of reflux time on peroxide estimation to ensure reaction completion. Polymer which was UV oxidised

under standard conditions (8·0 hours) was refluxed for various times and hydroperoxide concentration measured. A broad maximum around 75 minutes of refluxing was obtained. Hydroperoxide reacts very rapidly with iodide ion:

$$ROOH + 2I^- + H_2O \rightarrow I_2 + ROH + 2OH^-$$

$$2I^- \rightarrow I_2 + 2e^-$$

$$ROOH + 2H^+ + 2e^- \rightarrow H_2O + ROH$$

therefore:

$$2I^- \equiv 2e^- \equiv ROOH \equiv I_2$$

This would explain the asymtopic rise in iodine concentration observed during the initial period of reflux. The slower increase to maximum may either be a consequence of diffusion of iodide ion into the polymer (50 μm thickness) at reflux temperature (see 1.4.3), or a slower reduction of polymeric peroxides formed during photoxidation. For the latter reason a reflux time of 15 minutes was used as standard for the determination of hydroperoxides. The more gradual fall off with extended periods of reflux may be a result of absorption of iodine as triiodide by diolefinic structures. Volatilisation of iodide ion is unlikely owing to the solubility of sodium iodide forming the less volatile triodide ion:

$$I_2 + I^- \rightleftharpoons I_3^-$$

1.9 Determination of gel content

HIPS containing no antioxidant was exposed to UV and the cross-linked phase, mainly rubber, was separated by centrifuging[62].

1 g of polymer film was divided into four 50 cm^3 centrifuge tubes and 25 ml of dichloromethane was pipetted into each tube. This prevented loss of irradiated sample by eliminating the usual stage of "dissolving" the polymer prior to placement in the centrifuge tubes. The tubes were capped securely to prevent spillage or volatilisation and centrifuged for half an hour at 15 000 rpm using an MSE ultra centrifuge. After removing the caps carefully to prevent mixing, the solution of uncross-linked material (sol) mainly PS was pipetted into a sample container. Approximately 0·5 ml was left containing the gel, which was less dense than the sol thus separating during centrifuging on the surface of the liquid. The tubes were allowed to dry at ambient temperature overnight before adding 25 ml of fresh dichloromethane and the phase separation procedure repeated. The remaining gel was dried for up to 72 hours at ambient temperature then removed and stored in a weighed sample bottle. The last stage of removing the gel from the tube presented some problems and may have introduced inaccuracy in measurement.

1.10 Cross-link Density (CLD) determination by swelling

Gel (see 1.9) formed during photoxidation of HIPS results largely from carbon-carbon, ether or peroxide bond formation in the rubber (PBD) phase. For this reason PBD was UV irradiated and the inter cross-link molecular weight (M_c) and hence the parameter defined as $1/2M_c$ known as cross-link density (CLD) was obtained from the relationship due to Flory and co-workers[63] swelling measurements. CLD thus obtained is an estimate of physical cross-links only; this may be converted to chemical cross-link values, using a semi-empirical relationship by Mullins et al.[64,65].

Heptane was chosen as the swelling liquid because of the ease with which excess liquid may be removed from the swollen rubber, although it is a relatively poor solvent for PBD. The interaction constant (χ) characteristic of heptane - PBD systems was calculated from data obtained in the literature using the Flory-Rehner equation[66]:

$$\ell n(1 - \nu_r) + \nu_r + \chi.\nu_r^2 + \frac{1}{m_c}\ \nu_r^{\frac{1}{3}} = 0$$

where $m_c = \frac{V_c}{V_o}$, $\quad M_c = V_c \rho_r$

and $\quad \nu_r = \frac{1}{Q+1}$

ν_r = equilibrium swelling ratio

χ = polymer-solvent interaction content.

ρ_r = density of rubber (0·976[66])

Q = maximum imbibition (1·48 [66])

V_o = molar volume of solvent (145·54 for heptane)

V_c = molar volume between cross-links (4200[66])

m_c = ratio of V_c to V_o

M_c = inter cross-link molecular weight.

By substituting into the Flory-Rehner equation a value of χ for heptane-PBD was found to be 0·54. The Flory-Huggins equation[63] was then deduced by substituting, $m_c = \frac{M_c}{V_o.\rho_r}$:

$$\ell n(1 - \nu_r) + \nu_r + \chi.\nu_r^2 + \rho_r.V_o.M_c^{-1}.\nu_r^{\frac{1}{3}} = 0$$

PBD film (see 1.2.2) was mounted on glass to prevent sticking, and UV irradiated. At various intervals strips (0·02g) were cut off and placed in weighing bottles, filled with heptane and kept in a water bath at 25°C for 4 hours till equilibrium swelling was attained. The excess heptane was removed with filter paper and swollen PBD weighed immediately. The PBD was then de-swollen by applying vacuum for half an hour at 60°C to constant weight; the difference between the swollen and de-swollen weight giving the weight of heptane absorbed. The equilibrium swelling ratio, ν_r, also defined as:

$$\nu_r = \frac{\text{volume of rubber in swollen sample}}{\text{volume of rubber in swollen sample} + \text{volume of swelling solvent absorbed.}}$$

was substituted into the Flory-Huggins equation together with the value for χ and M_c and hence CLD was obtained for different degrees of cross-linking.

It has been reported that the physical cross-link value is always greater than the chemical value and the divergence apparently increases with increasing degree of cross-linking[65]. The divergence between physical and chemical determinations of cross-linking is manifest as an intercept value of approximately $0{\cdot}3 \times 10^{-4}$ on the axis of the physical determination of $1/2M_c$ at zero degree of chemical cross-linking, and may be accounted for by chain entanglement. Flory[67] has suggested that a correction should be made for the non-elastic contribution from cross-links at chain ends by substituting $(1 - 2M_cM^{-1})$ for M_c^{-1} where M is the number-average molecular weight of the rubber before cross-linking. Hence, the absolute (chemical) degree of cross-linking may

be determined by combining the above corrections[65]:

$$\frac{1}{2M_{c,phy}} = \left(\frac{1}{2M_{c,chem}}\right)\left(1 - 2M_{c,chem}.M^{-1}\right) + 0{\cdot}3\left(1 - 2M_{c,chem}.M^{-1}\right) \times 10^{-4}$$

1.11 Pre-irradiation of HIPS

Samples of extruded film, approximately 30 cm^3 and 50 μm thickness, were placed in either a pyrex (borosilicate glass, cut-off at 290 nm) or quartz tube, fitted with a suba-seal. Argon was introduced via syringe needles. The apparatus was purged for at least 24 hours prior to UV exposure; the gas flow being maintained during photolysis. The sample was irradiated for various times and subsequently exposed to air for 2 hours in the dark before commencing with oxygen absorption studies or other techniques.

1.12 Oven ageing

HIPS extruded film was mounted on stiff cardboard or sandwiched between two frames of similar material, to prevent distortion during thermal ageing. Samples were heated in separate cells of the Wallace forced air ageing block (H.W.Wallace Co.Ltd., Croydon) set at 98°C.

1.13 Ozone testing

1 g of HIPS extruded film, 50 μm thickness, was suspended from the revolving rack of the Hampden Shawbury ozone tester, Hampden Test Equipment Ltd., Rugby, Model MTPC-1. An ozone concentration of 2500 pphm at 25°C was used as standard. Samples were examined for carbonyl

content and peroxide concentration was determined (see 1.8). Also photo-oxygen absorption studies were carried out on ozone-exposed film.

1.14 Singlet Oxygen

Excited oxygen was generated using a microwave discharge apparatus described elsewhere[68]. Cylinder oxygen was used in place of the air inlet. Atomic oxygen also generated was removed by a warmed mercury trap. The microwave generator, Microtron 200, mark 3, Electro-Medical Supplies (Greenham) Ltd., Berkshire, was adjusted to produce an incident power of 30 - 50 watts during discharge. The reflected power was maintained at a minimum by tuning the microwave cavity. Samples of HIPS extruded film or PBD cast from dichloromethane onto a KBr disc were exposed 30 cm downstream for up to 10 hours and then examined by IR. Formation of hydroperoxide was also investigated using iodiometric analysis (see 1.8) for HIPS.

1.15 Synthesis and characterisation of metal complexes

1.15.1 Procedure

0·02 mols of the appropriate metal salt were dissolved in 75 ml of distilled water at 70°C. 0·04 (or 0·06)mols of sodium di-butyl dithiocarbamate were dissolved in 100 ml of distilled water at 70°C. The two solutions were then mixed with stirring; the resulting precipitate was filtered through a Buchner funnel and washed with warm distilled water. The filtrate was then dried under vacuum and re-crystallised from 50 ml of heptane at 70°C. The solution was cooled in an ice bath and the crystals filtered and dried under vacuum. For some complexes it was necessary to carry out reactions at 0°C under

nitrogen to reduce the chances of obtaining oxidation products of thiocarbamates, mainly oils. Cobalt^{II}, pink complex, was readily oxidised to form the more stable cobalt^{III}, green complex, which was easily isolated. Complexometric titration confirmed this (see 1.15.4). Manganese^{II}, white complex, could not be isolated from the inert atmosphere of the separating funnel, although readily obtainable in situ, on contact with air it immediately oxidised to higher oxidation states and finally to the black oxide.

1.15.2 C, H, N, analysis

Metal Complex	N		C		H	
	expt.	cal.	expt.	cal.	expt.	cal.
Nickel^{II}	5·79%	5·99%	46·05%	46·25%	8·18%	7·76%
Iron^{III}	5·79	6·03	45·67	46·53	8·01	7·81
Copper^{II}	5·69	5·93	46·15	45·78	8·29	7·68
Cobalt^{III}	5·92	6·25	43·07	48·25	8·10	8·10
Zinc^{II}	5·69	5·91	42·30	45·60	7·75	7·65

1.15.3 UV Spectroscopy

metal complex concentration	λ_{max} absorbance	λ_{max} absorbance	λ_{max} absorbance
Nickel^{II} $4x10^{-5}$M/$CHCl_3$	254 nm 0·79	329 nm 1·07	400 nm 0·19
Iron^{III} $4x10^{-5}$M/$CHCl_3$	254 nm 1·50	312·5 nm 0·83	449 nm 0·35
Copper^{II} $4x10^{-5}$M/$CHCl_3$	274 nm 1·29	290 nm* 0·77	442·5 nm 0·52
Cobalt^{III} $3x10^{-5}$M/$CHCl_3$	255 nm* 0·75	279 nm 0·96	326 nm 0·59
Zinc^{II} $4x10^{-5}$M/$CHCl_3$	267 nm 1·22	312 nm 0·23	———

* shoulder

Note: Solvent cut-off for chloroform at 245 nm.

1.15.4 EDTA analysis[69]

To 0·1 g of accurately weighed cobalt complex, concentrated nitric acid (10 - 20 ml) was added. The solution was warmed to expel fumes of nitrogen oxides, after which distilled water was added and the solution warmed. Indicator, Xylenol Orange, was added followed by sufficient hexamine till a deep red (pH - 6) was obtained. This was again warmed and titrated against standard (0·01 M) EDTA solution. The percentage of cobalt was determined from the following relationship:

$$\% \text{ Co} = \frac{0{\cdot}01 \,.\, 58{\cdot}93 \,.\, x \,.\, 100}{1000 \,.\, y}$$

where x = EDTA added (ml)

y = weight of complex (g)

x	y	% Co
18·0 ml	0·1265 g	8·39%
17·0 ml	0·1168 g	8·58%
15·7 ml	0·1091 g	8·48%
14·7 ml	0·0999 g	8·67%

The calculated percentage cobalt is 8·77 for Co^{III} complex and 12·6 in the case of Co^{II}. Therefore the stable complex isolated is evidently $cobalt^{III}$.

CHAPTER 2

EFFECT OF PROCESSING AND THERMAL TREATMENT ON UV STABILITY OF HIGH IMPACT POLYSTYRENE

2.1 RESULTS

2.1.1 Determination of hydroperoxide

2.1.1.1 Oven ageing

Hydroperoxide concentration, determined by iodiometry (see 1.8) and other functional groups measured by IR (see 1.6) for unstabilised HIPS extruded film (50 μm) are shown in figure 12 during thermal ageing at 98°C in the Wallace forced air oven (see 1.12). A small quantity of hydroperoxide was detected in the control sample, less than $0{\cdot}1 \times 10^{-6}$ mol.g^{-1}; this increased linearly without an induction period up to about 30 hours of heating reaching a maximum concentration of $6{\cdot}4 \times 10^{-6}$ mol.g^{-1}. With further heating the hydroperoxide concentration fell at a similar rate to that of its formation. Estimation of hydroperoxide after 50 hours of ageing became irreproducible, although the peroxide concentration continued to fall it never reached zero or even the initial low concentration of hydroperoxide. Unsaturation, namely trans-1,4-polybutadiene decayed from the onset of thermal ageing of HIPS, although it did not attain maximum rate of decay until 15 hours of heating. Figure 12 shows that the mid-point of this linear portion does not correspond exactly to the maximum concentration of hydroperoxide but is shifted by 5 hours to shorter thermal duration. After

Changes in concentration of functional groups in unstabilised HIPS extruded film (50 μm) on oven ageing at 98°C in air.

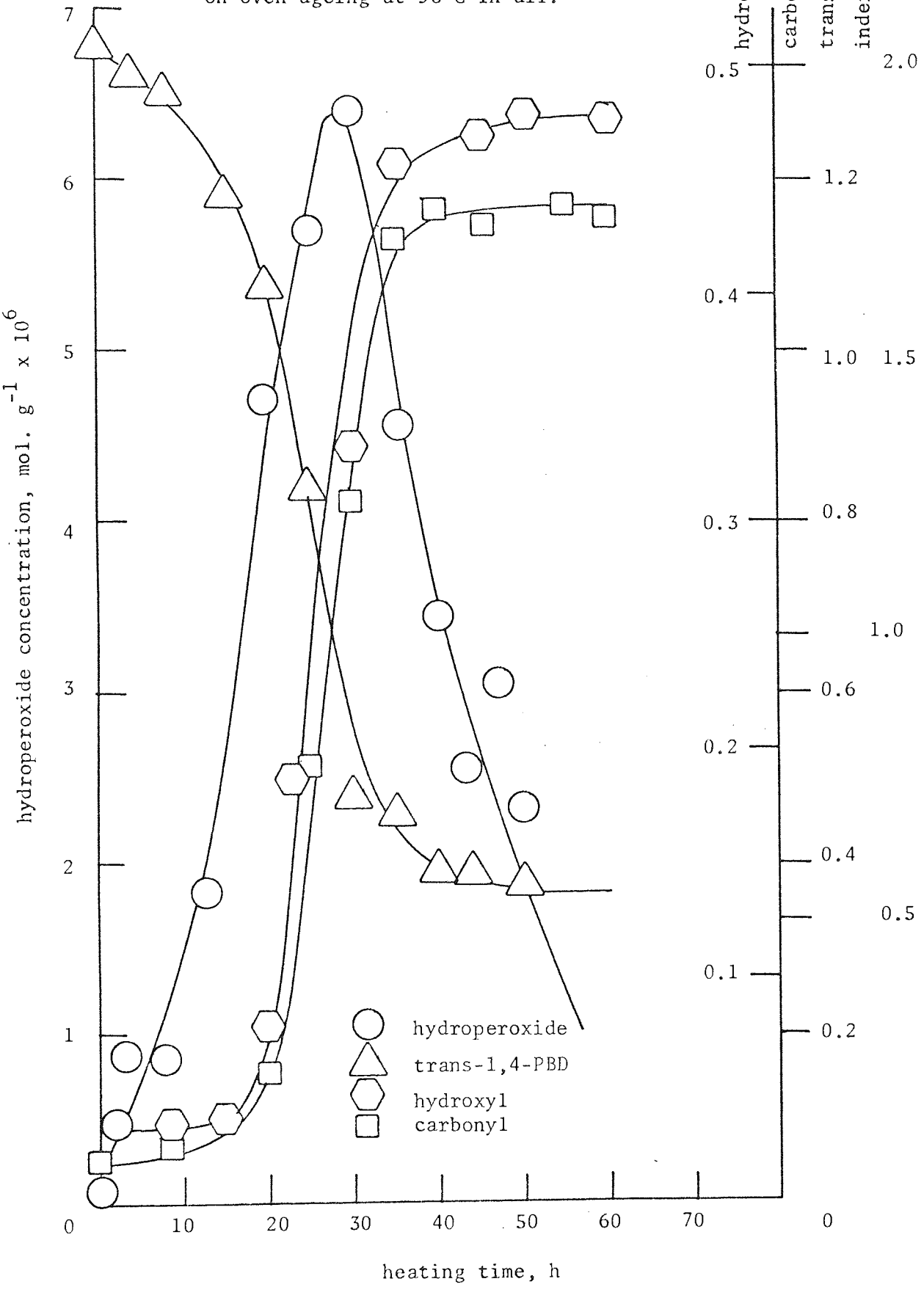

Figure 12.

40 hours of heating the unsaturation reaches a constant value of 0·55 indicating zero concentration.

The concentration of carbonyl groups (1720 cm^{-1}) built up slowly for the first 15 to 20 hours of ageing reaching a maximum rate after approximately 30 hours, corresponding to the maximum concentration of hydroperoxide. Extrapolation of the linear portion of carbonyl formation to the abscissa implies an induction period of nearly 20 hours, defined as the time required to reach linear kinetics, maximum rate. Carbonyl concentration remained constant after 40 hours thermal treatment. Similarly hydroxyl formation increased very slowly up to 15 hours of ageing then rose rapidly parallel to carbonyl build-up; the induction period being 2 hour shorter. However, at the end of 40 hours heating, hydroxyl concentration continued to increase gradually.

2.1.1.2 Processing

HIPS chip containing no antioxidant was processed in an open torque rheometer (see 1.2.1.2) and films made by compression moulding were analysed for hydroperoxide and groups detectable by IR. Figure 13 shows a rapid, linear increase in hydroperoxide up to 3 hours of processing, reaching a maximum of 4×10^{-6} $mol.g^{-1}$, after which it dropped to $0{\cdot}85 \times 10^{-6}$ $mol.g^{-1}$ corresponding to 6 hours of processing. Trans-1,4-polybutadiene was destroyed very rapidly without induction period with a linear decay which continued for up to 5 hours of processing, thereafter it tended to level out but did not reach zero concentration. The mid-point of the PBD decay curve in figure 13 occurs 1 hour before the maximum concentration of hydroperoxide;

Changes in concentration of functional groups in unstabilised HIPS on processing in the open chamber of the torque rheometer at 200°C.

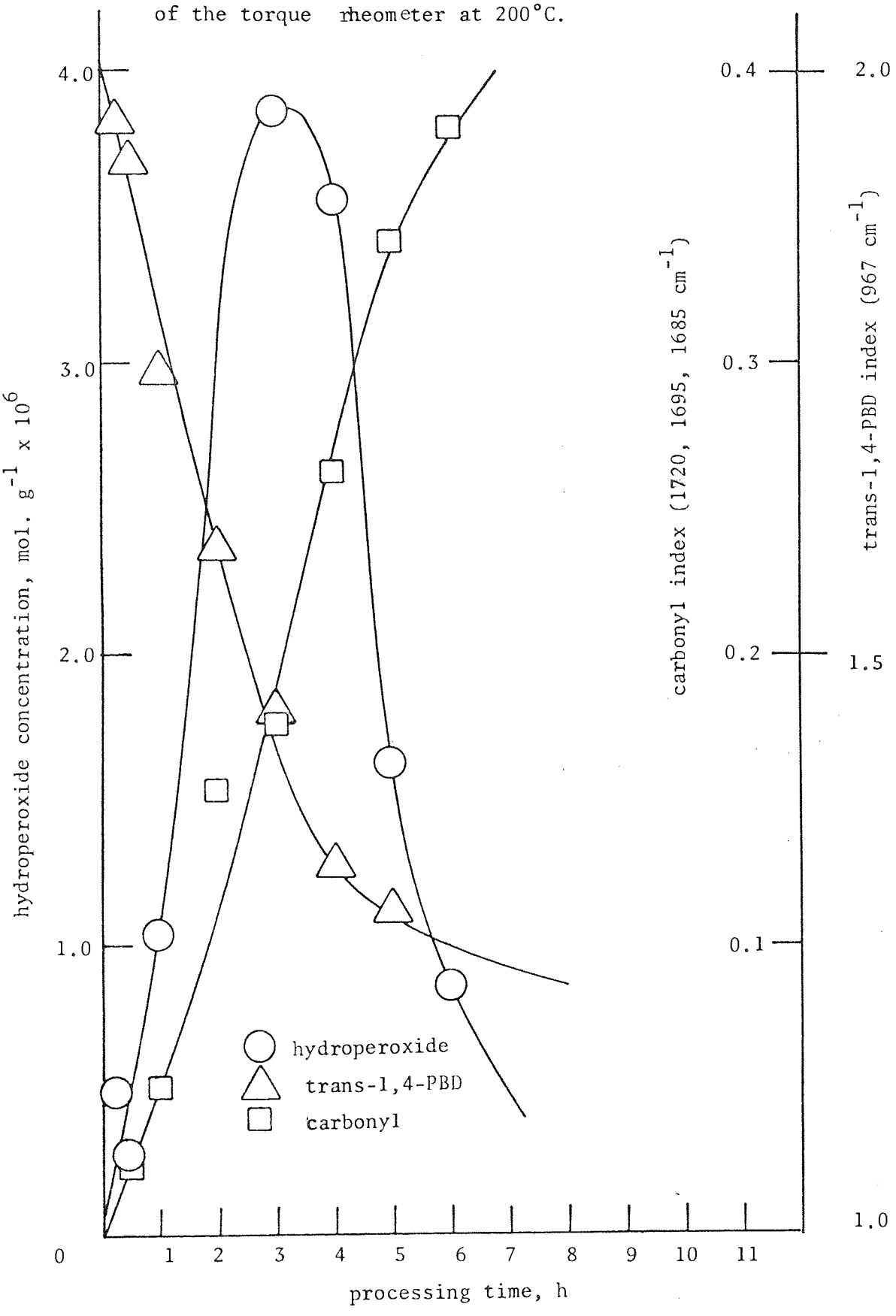

Figure 13.

Changes in the carbonyl region of the IR spectra of unstabilised HIPS on processing in the open chamber of the torque rheometer at 200°C.

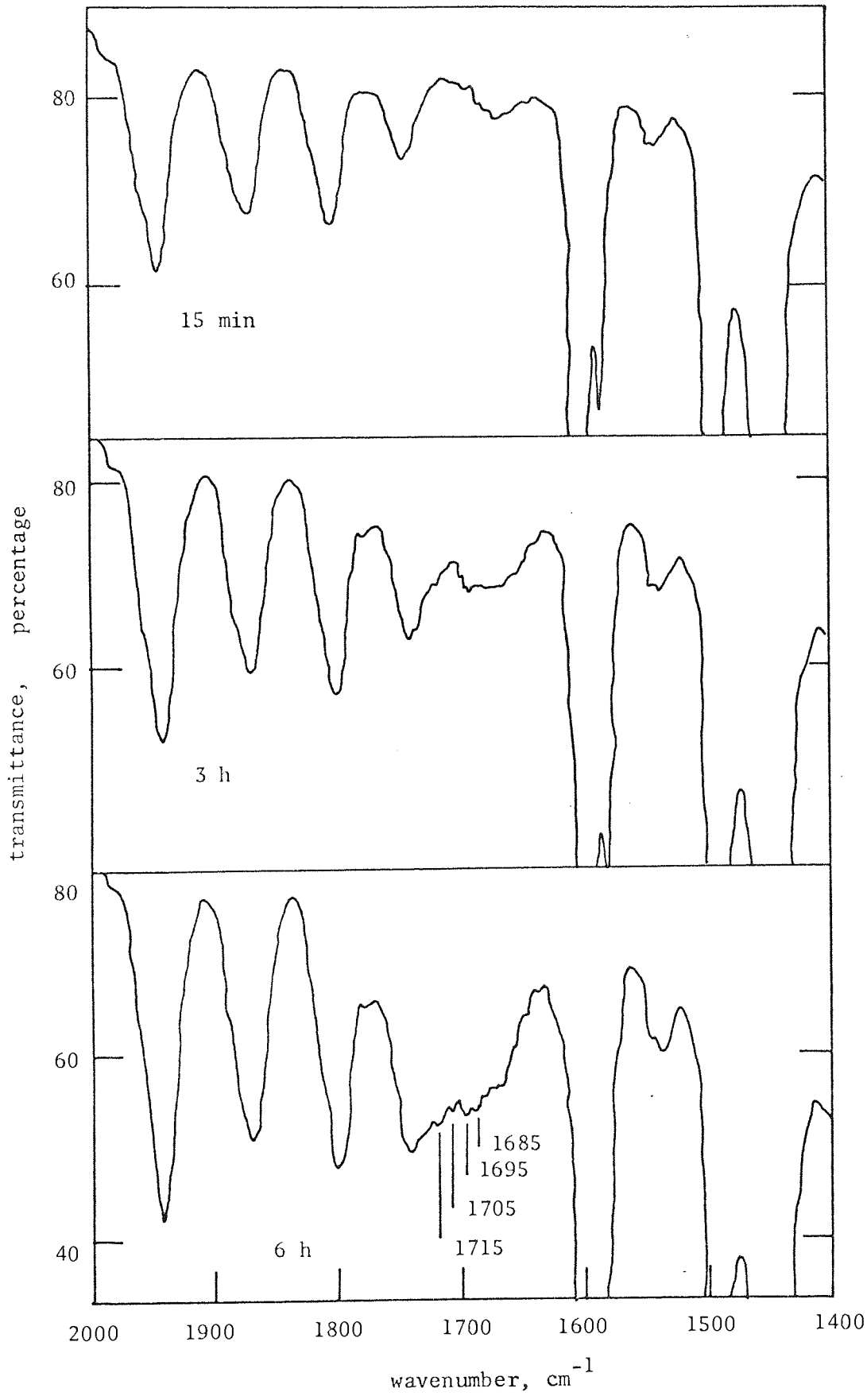

Figure 14 .

this shift being consistent with the results obtained during oven ageing (see 2.1.1.1). Under the conditions of melt-processing carbonyl groups increased, without induction period, in a linear manner, extrapolating to the origin for unprocessed material. However, the maximum rate in figure 13 coincides with the maximum hydroperoxide concentration, and retards only slightly after 6 hours processing. Hydroxyl concentration followed the same path as carbonyl and is represented in figure 13 by the same curve. It was observed that the colour of melt-processed material changed gradually to dark brown at 6 hours processing.

Both conjugated and non-conjugated carbonyl were oberved during the processing of HIPS. Figure 14 shows the IR spectra of films produced by compression moulding of material which has been processed for 15 minutes, 3 hours and 6 hours in the open chamber of the torque rheometer. The spectrum representing 15 minutes of processing in figure 14 has a small peak at 1695 cm^{-1} corresponding to conjugated aldehyde and a small shoulder around 1720 cm^{-1} indicating the presence of a saturated carbonyl. Absorbance of both saturated and conjugated carbonyls increase with further processing for 3 hours, figure 14. The increase in concentration of conjugated and non-conjugated carbonyl during processing is represented by a single curve in figure 13. The intense peak at 1695 cm^{-1} observed after 6 hours of processing implies a high concentration of conjugated carbonyl, figure 14.

2.1.1.3 Photoxidation

HIPS extruded film, 55 μm, containing no antioxidant was exposed to UV radiation at ambient temperature and the changes in

Changes in concentration of functional groups in unstabilised HIPS extruded film (55 μm) on UV irradiation

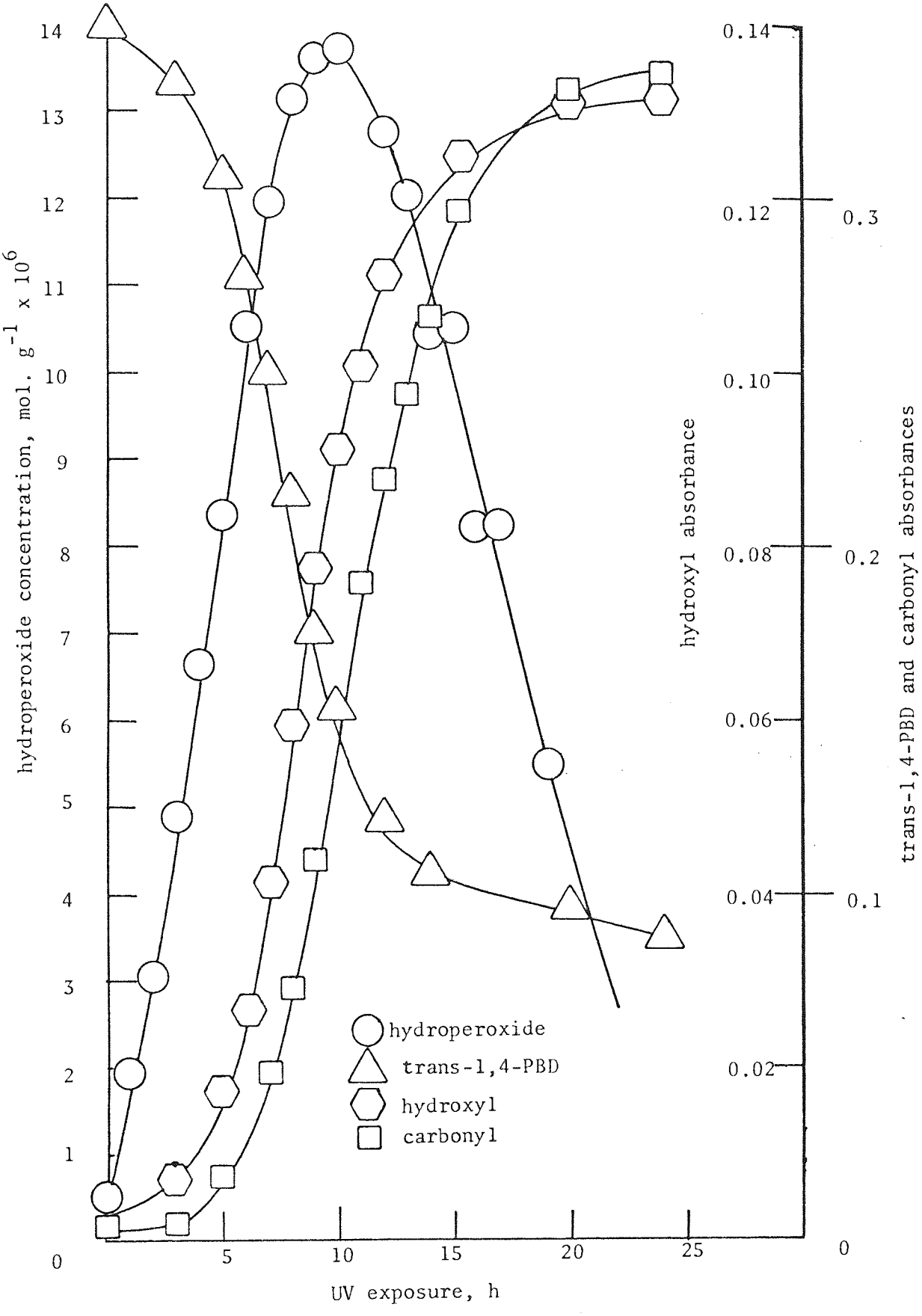

Figure 15.

concentration of functional groups were monitored by iodiometry and IR. The initial concentration of hydroperoxide, $0{\cdot}5 \times 10^{-6}$ mol.g^{-1}, increased very rapidly in a linear manner, displaying no induction period, up to 10 hours of UV exposure, figure 15. After 10 hours the maximum hydroperoxide concentration, 14×10^{-6} mol.g^{-1}, fell at a slightly slower rate than that experienced during its formation, leading to an asymmetric concentration profile. Trans-1,4-polybutadiene showed similar behaviour to that encountered during oven ageing (see 2.1.1.1); an initial slow decay leading to a faster, linear depletion after 5 hours UV exposure. After 10 to 15 hours the rapid rate of decay returned to that of the initial 5 hours. As in the case of thermal ageing the mid-point of the linear stage occurred prior to reaching the maximum concentration of hydroperoxide. Both carbonyl and hydroxyl exhibit an induction period of 6 and 4 hours respectively. The two curves are parallel and in turn parallel to the formation of hydroperoxide. After 15 hours UV exposure the rate of formation of both carbonyl and hydroxyl decrease. The maximum rate of formation of carbonyl and hydroxyl corresponds to the integral curve representing hydroperoxide. Estimation of hydroperoxide was not reliable after 20 hours UV exposure (see 2.1.1.1).

The relationship between formation of hydroperoxide and oxygen absorption for the same polymer film under identical conditions is shown in figure 16, expressed in μ mol.g^{-1} of HIPS (see 1.4.5). The quantity of oxygen absorbed followed the increase in hydroperoxide, described above, up to 4 hours of UV exposure after which it increased rapidly reaching 90×10^{-6} mols of oxygen absorbed per g corresponding

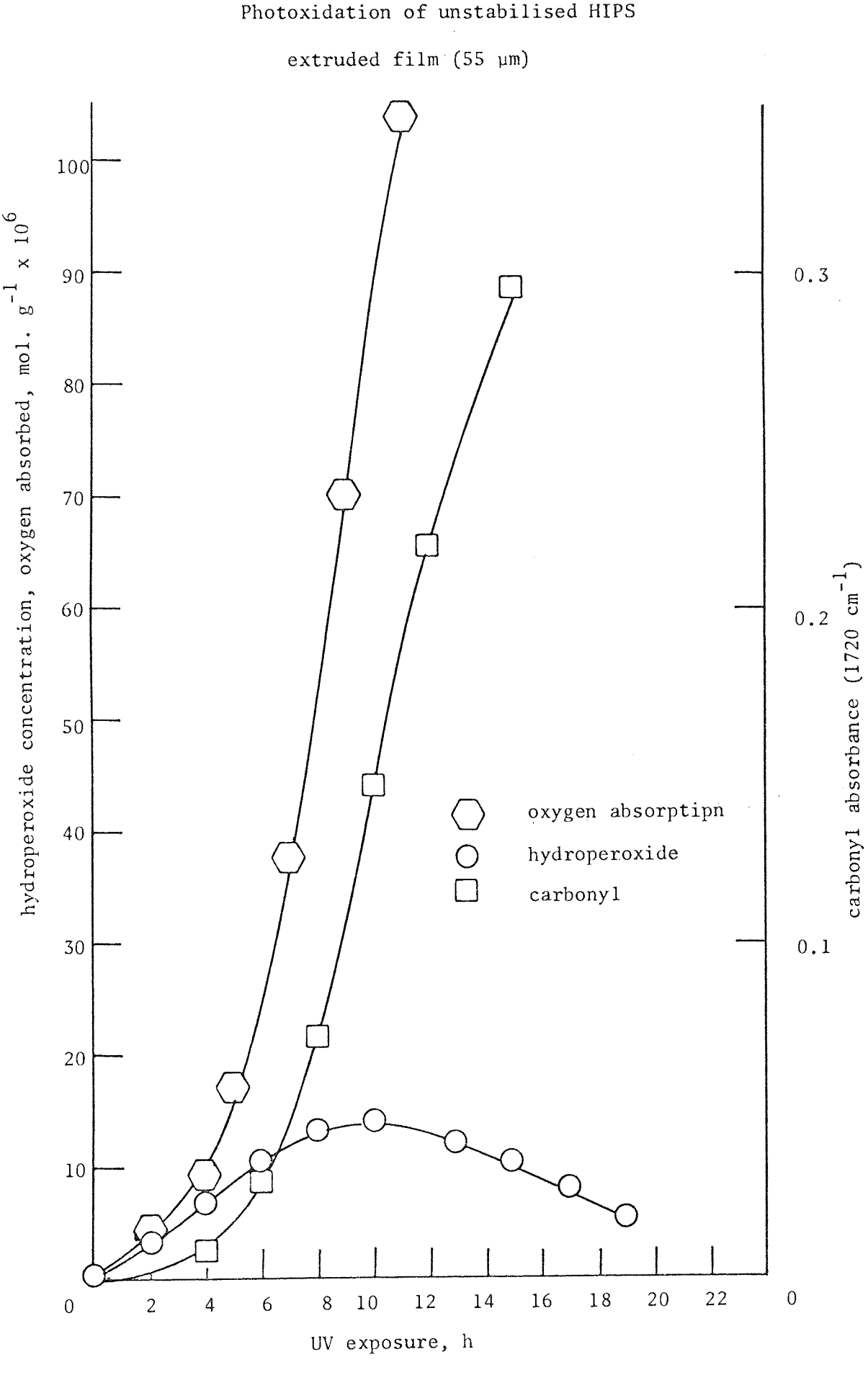
Photoxidation of unstabilised HIPS
extruded film (55 µm)
hydroperoxide concentration, oxygen absorbed, mol. g^{-1} x 10^{6}
carbonyl absorbance (1720 cm^{-1})
UV exposure, h
oxygen absorptipn
hydroperoxide
carbonyl
0
10
20
30
40
50
60
70
80
90
100
0.1
0.2
0.3
2
4
6
8
10
12
14
16
18
20
22

Figure 16.

Changes in concentration of function groups as a function of hydroperoxide concentration in unstabilised HIPS extruded film (55 μm) on photoxidation

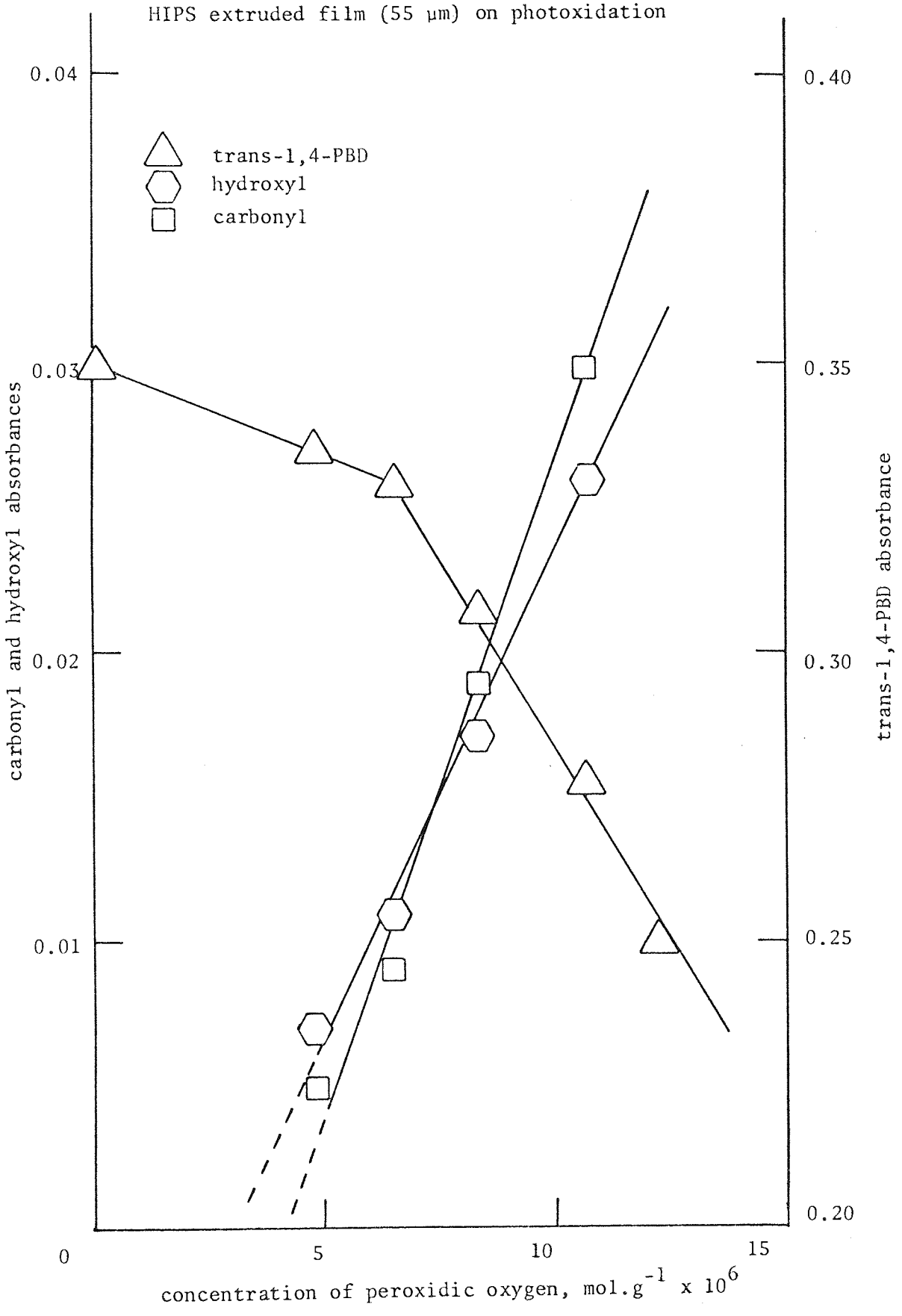

Figure 17.

to 14 x 10^{-6} mols of hydroperoxide after 10 hours exposure to UV. In figure 16 it is clear that during UV exposure the concentration of hydroperoxide is always less than the concentration of oxygen absorbed, apart from the initial concentration of hydroperoxide present before oxygen absorption measurements were made. Extrapolation of the rapid, linear rise in oxygen absorption to the abscissa conferred an induction period of 5 hours, 1 hour less than that for carbonyl absorbance, figures 15 and 16.

The relationship between formation of peroxidic oxygen and other chemical groups is depicted in figure 17, showing a dual rate curve for trans-1,4-polybutadiene. The rate of decay of unsaturation is moderately fast up to a hydroperoxide concentration of nearly 7 x 10^{-6} mol.g^{-1}, thereafter a more rapid decay is observed. After a hydroperoxide concentration of approximately 5 x 10^{-6} mol.g^{-1} (figure 17) a linear relationship holds for both carbonyl and hydroxyl build-up. The above linear concentration inter-dependence is apparent only up to the maximum concentration obtained in hydroperoxide.

2.1.1.4 Photolysis

HIPS extruded film, 50 μm, containing no antioxidant was pre-irradiated in a large quartz tube (200 cm^3), (see 1.11), and the hydroperoxide concentration estimated by iodiometry after exposure to air for 2 hours in the dark. Figure 18 contrasts the rise and fall of hydroperoxide during photoxidation (from figure 15) and after photolysis. The concentration profile for pre-irradiated HIPS appears to follow the same shape as that obtained during photoxidation, although

Changes in concentration of hydroperoxide in unstabilised HIPS extruded film

(1) during photoxidation and

(2) after photolysis and exposure to air for 2 hours

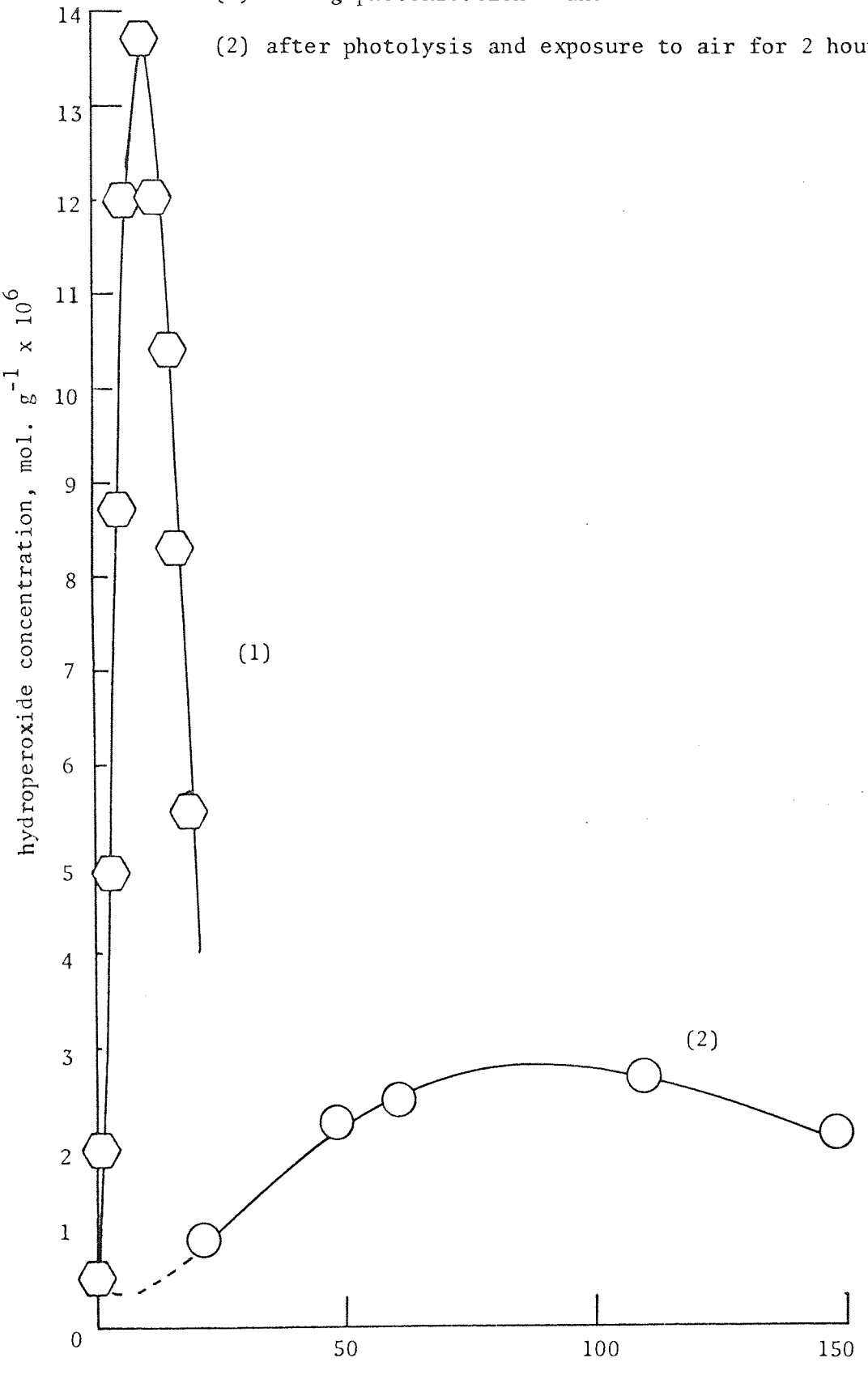

Figure 18.

the maximum concentration of hydroperoxide is considerably less, below 3×10^{-6} mol.g^{-1} and the duration of UV necessary to reach this maximum is extended by nearly 10 fold. Estimation of hydroperoxide up to the first 30 hours UV exposure was irreproducible; the sample size being restricted by the volume of the photolysis tube.

2.1.2 Oxygen absorption

2.1.2.1 Oven aged films

Samples of HIPS extruded film, 55 μm, which had been oven aged at 98°C(see 1.12) for various heating times were subsequently examined for UV stability by photo-oxygen absorption in oxygen (see 1.4). Figure 19 illustrates the response to UV exposure of samples containing increasing amounts of hydroperoxide up to the maximum, slightly less than 30 hours thermal ageing (see 2.1.1.1). Oxygen absorption studies on samplesheated for extended periods proved impossible owing to the extreme brittleness and subsequent handling difficulties. However, several noteworthy features are displayed in figure 19. The control sample gave the lowest initial rate of oxygen uptake reaching the (maximum) steady-state rate after an induction period of 5 hours. It also absorbed the greatest amount of oxygen. The induction period was rapidly diminished until it was completely removed after 20 hours of thermal ageing prior to UV exposure; corresponding to an increase in initial rate. With samples that had been aged for longer periods the initial rate fell, but did not reach that of the control. All thermally treated samples showed a decreasing maximum rate and absorbed progressively lower quantities of oxygen.

Photoxidation of unstabilised HIPS extruded film (55 μm) oven aged at 98°C in air (oxygen absorption in air)

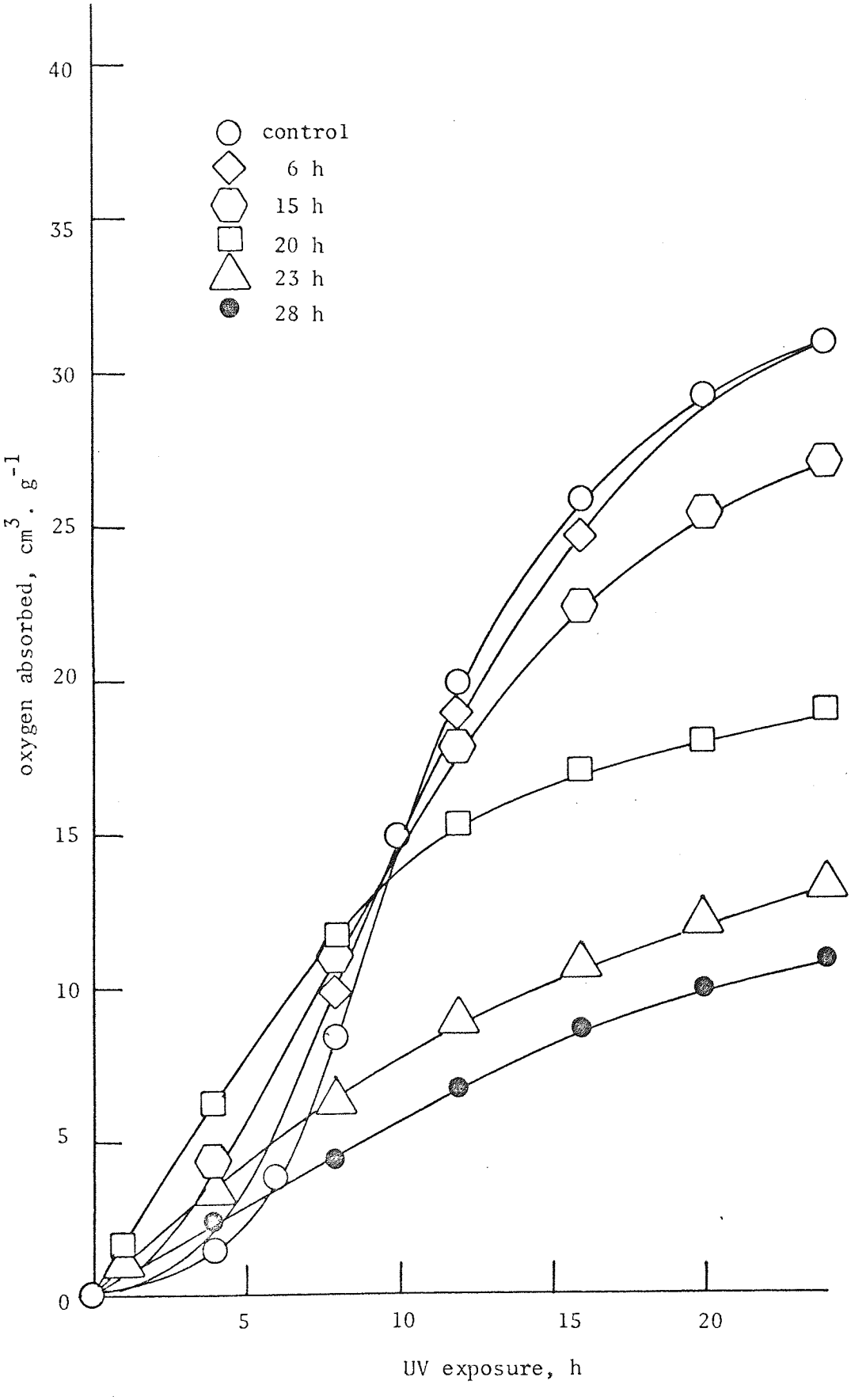

Figure 19.

2.1.2.2 Processed material

Films obtained by compression moulding of unstabilised HIPS which was processed at 200°C (see 1.2.1.2) for various times (see 2.1.1.2) were examined by photo-oxygen absorption in oxygen. After 4 hours of processing the corresponding films were too brittle to be used for oxygen absorption studies. Figure 20 shows that a sample processed for 15 minutes has an induction period of approximately 4 hours; 1 hour less than the control film in figure 19, which was not produced by the same drastic processing operation (see 1.2.1.1). With increasing processing time the initial rate increases and the induction period is progressively removed. However, in this case the maximum rate appears to be unaltered. The fastest initial rate corresponds to the maximum concentration of hydroperoxide obtained, after 3 hours processing (see 2.1.1.2), and with further processing decreases slightly. Samples which have been processed for longer than 30 minutes prior to photo-oxygen absorption consumed progressively lower quantities of oxygen.

2.1.3 IR Spectroscopy

2.1.3.1 Oven aged films

HIPS extruded film, 55 μm, containing no antioxidant was mounted on frames and aged at 98°C in the Wallace oven (see 1.12) for various times up to 60 hours. The subsequent affect on UV stability was followed by IR (see 1.6.1). The final destruction of unsaturation by UV exposure is shown in figure 21. Because these films for IR measurements were supported on frames it was possible to use samples taken from the Wallace oven that were extremely brittle. The

Photoxidation of unstabilised HIPS compression moulded film (55 μm) processed in the open chamber of the torque rheometer at 200°C (oxygen absorption in oxygen)

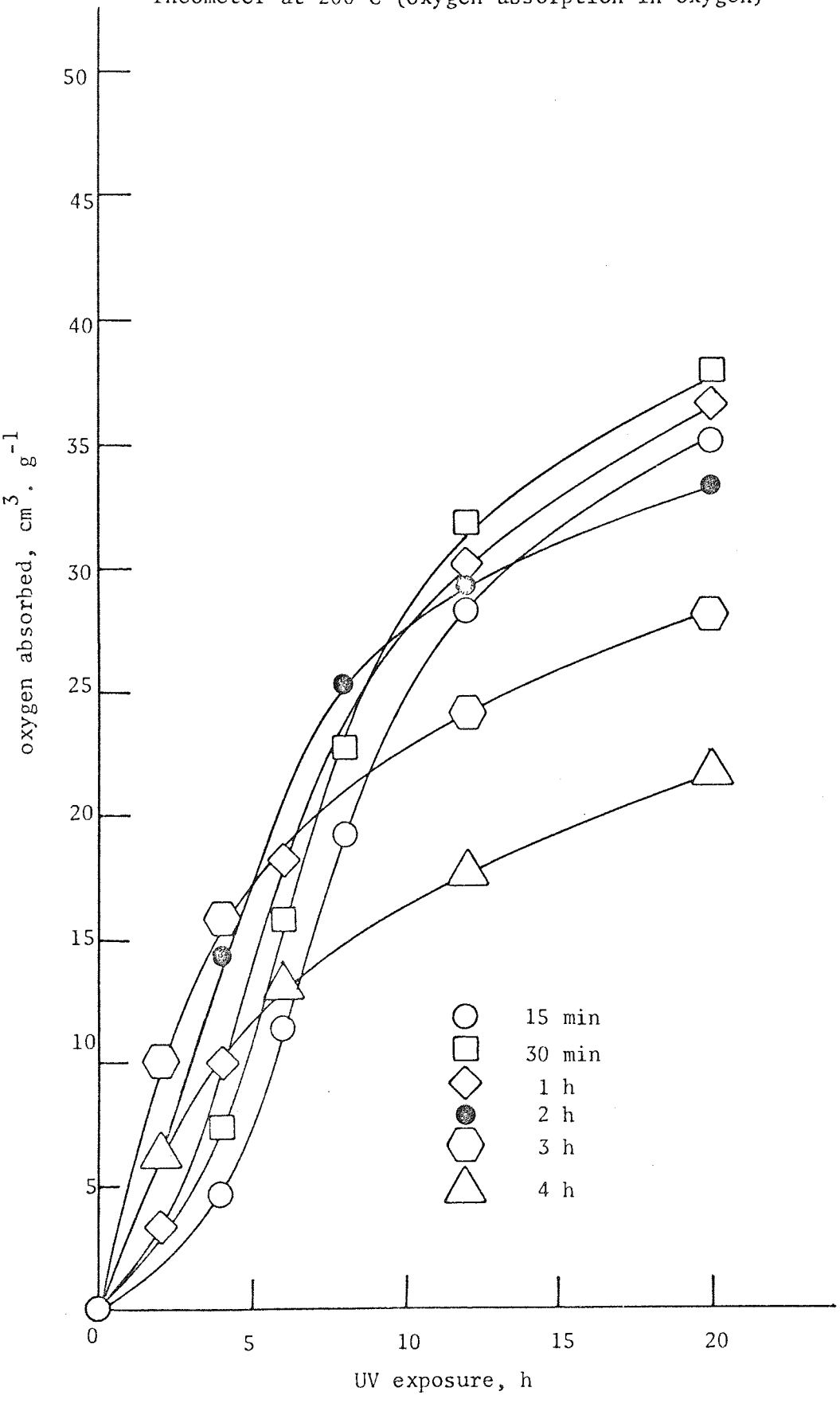

Figure 20.

Decay of unsaturation during photoxidation of unstabilised HIPS extruded film (55 μm) oven aged at 98°C in air.

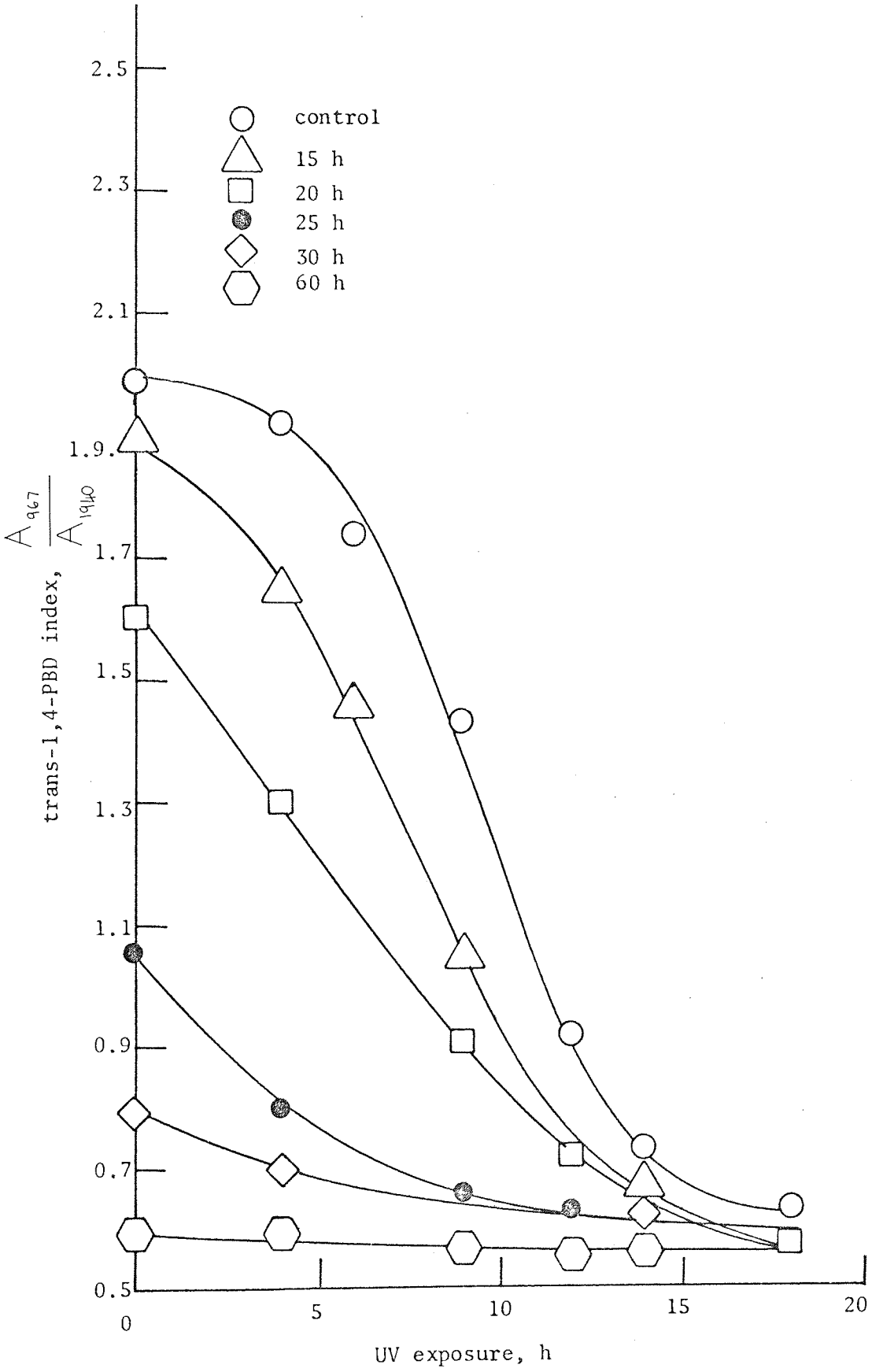

Figure 21.

progressively diminished starting concentration of trans-1,4-polybutadiene corresponds to the decay during ageing depicted in figure 12. The control curve exhibits an initial slow rate of decay reaching a maximum after 5 hours of UV exposure; after 15 hours nearly all the trans-1,4-polybutadiene has been destroyed. (An index of 0·55 implies zero concentration of trans-1,4-polybutadiene). With increasing duration of thermal treatment prior to UV exposure the initial rate of decay increased up to 20 hours of heating, representing the maximum rate of depletion of unsaturation in figure 12. For samples heated for 30 and 60 hours, the initial rate approaches zero. In all samples the maximum rate of decay is less than that of the control.

Figure 22 shows the growth of carbonyl during UV exposure. Similarly, the increase in starting concentration corresponds to the curve representing carbonyl build-up during oven ageing, figure 12. Virtually no carbonyl is formed in the control sample for 5 hours UV exposure, thereafter carbonyl increases rapidly, conferring an induction period of 8 hours, the time required to attain maximum rate. With increasing duration of thermal treatment prior to UV exposure the induction period is rapidly removed and the initial rate increases leading to linear kinetics between 20 and 25 hours of heating. At extended periods of oven ageing resulting in a very high starting concentration of carbonyl a different behaviour is apparent. The curves tend to flatten during the initial exposure to UV before carbonyl concentration increases rapidly. All curves appear to converge on the same carbonyl index after 20 hours of UV exposure.

Growth of carbonyl during photoxidation of unstabilised HIPS extruded film (55 μm) oven aged at 98°C in air

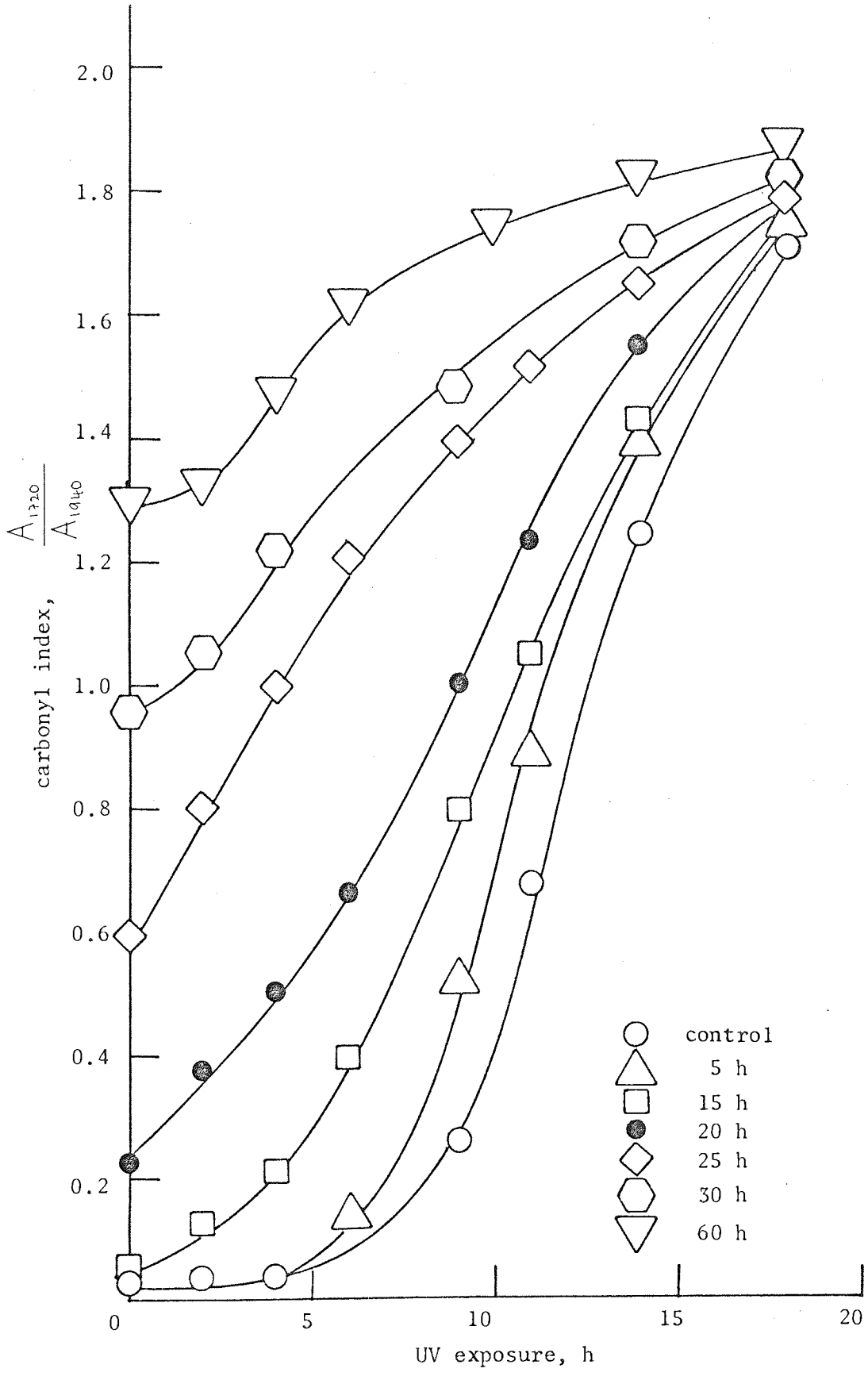

Figure 22.

An entirely analogous behaviour is illustrated in figure 23 for hydroxyl. The only difference being a shorter UV exposure required for convergence, less than 20 hours, although the samples containing the highest initial concentration of hydroxyl lie below this point.

Complementary to the experiments described above, a sample of HIPS extruded film (50 μm) containing no antioxidant was heated in the Wallace oven for 24 hours in air at 98°C. Part of this film was then examined for hydroperoxide by iodiometry; carbonyl, trans-1,4-polybutadiene and hydroxyl indexes were determined by IR. The above heat treatment in air resulted in a hydroperoxide concentration of $4{\cdot}1 \times 10^{-6}$ $mol.g^{-1}$ and carbonyl, trans-1,4-polybutadiene and hydroxyl indexes of 0·13, 1·81 and 0·085 respectively. A section of this film containing $4{\cdot}1 \times 10^{-6}$ $mol.g^{-1}$ of hydroperoxide was heated in a sealed tube (purged with argon) for 14 hours by submersion in an oil bath at 125°C to 130°C. The sample was allowed to cool in its argon atmosphere before it was characterised as above.

The hydroperoxide concentration fell to a level below detection. Trans-1,4-polybutadiene index dropped markedly to 1·23 and carbonyl index increased slightly to 0·23. However, hydroxyl increased by a relatively smaller amount to 0·095.

Subsequent exposure to UV of the polymer film containing $4{\cdot}1 \mu mol.g^{-1}$ of hydroperoxide and the sample heated in argon was performed under identical conditions and the results monitored by IR. The sample containing no hydroperoxide exhibited a slightly lower initial rate, a considerably slower maximum rate and retarded earlier.

Growth of hydroxyl during photoxidation of unstabilised HIPS extruded film (55 μm) oven aged at 98°C in air.

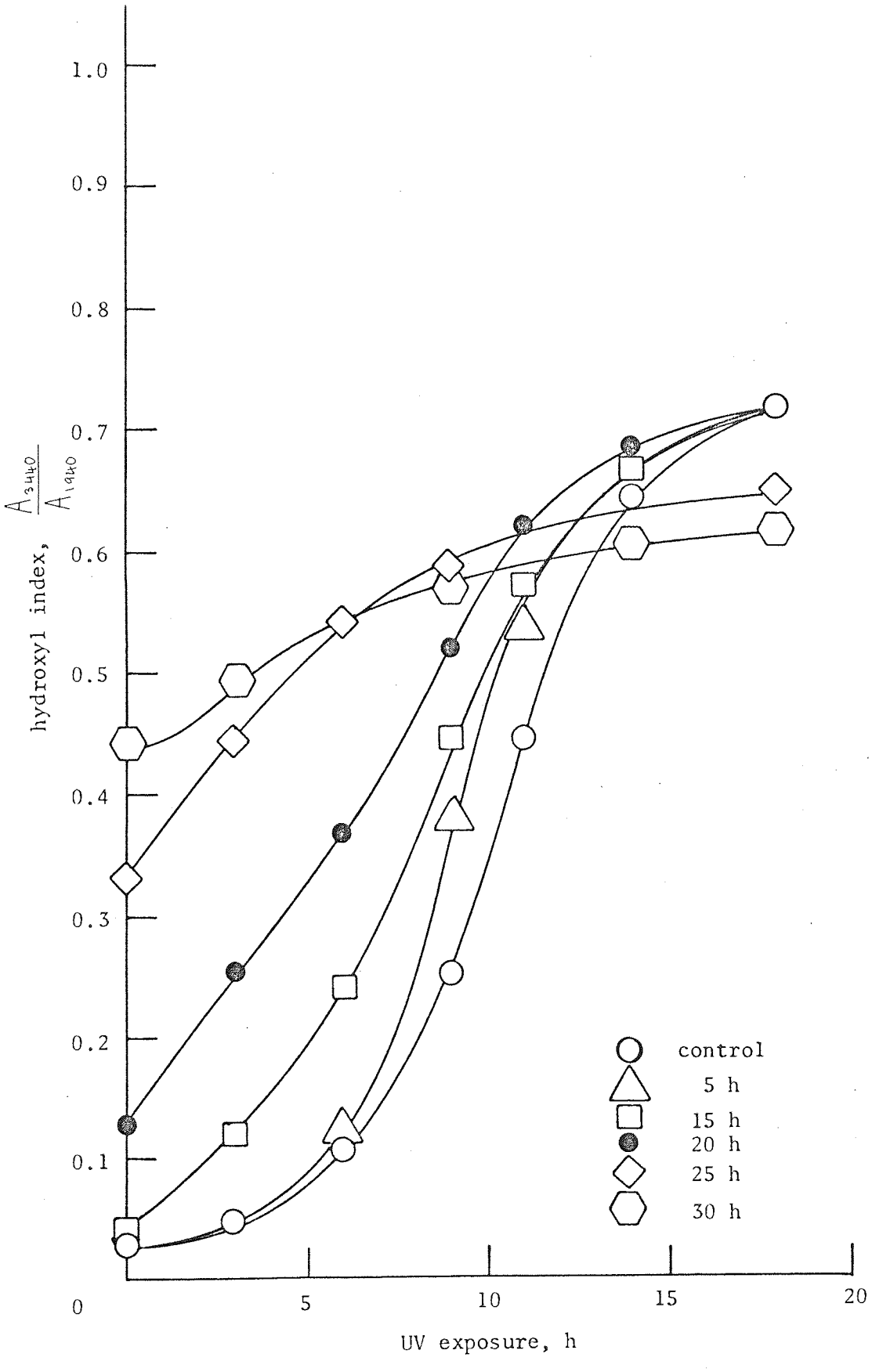

Figure 23.

2.1.3.2 Processed material

Films produced by compression moulding of HIPS processed material used for photo-oxygen absorption studies (see 2.1.2.2) were also examined by IR during subsequent UV exposure. Figure 24 shows the changes occurring in the concentration of carbonyl during UV exposure of processed material. The starting concentration, corresponding to the curve in figure 13, is considerably less than that obtained by oven ageing (see 2.1.3.1), figure 22. Consequently, the anomalous behaviour observed at high concentrations of carbonyl for oven aged films was not apparent here.

2.1.4 UV Spectroscopy

The UV absorbance at 286 nm of HIPS extruded film, 50 μm, containing no antioxidant, was obtained by difference using a control film, 50 μm, in the reference beam. The sample film was exposed to UV under ambient conditions and the resultant absorbance curve is shown in figure 25, superimposed on the hydroperoxide concentration profile for this batch of film measured under identical conditions by iodiometry and the corresponding changes in carbonyl concentration measured by IR. No UV absorbance was detected until 4 hours exposure; thereafter it increased rapidly following the growth of carbonyl and reached a maximum rate around 10 hours corresponding to the maximum concentration of hydroperoxide, 15×10^{-6} mol.g^{-1}. After 20 hours UV exposure no further increase in UV absorbance was apparent.

The UV absorbance at 280 nm of "crystal" PS extruded film, 50 μm, was also obtained by difference, for longer periods of UV exposure,

Growth of carbonyl during photoxidation of unstabilised HIPS compression moulded dilm (55 μm) processed in the open chamber of the torque rheometer at 200°C.

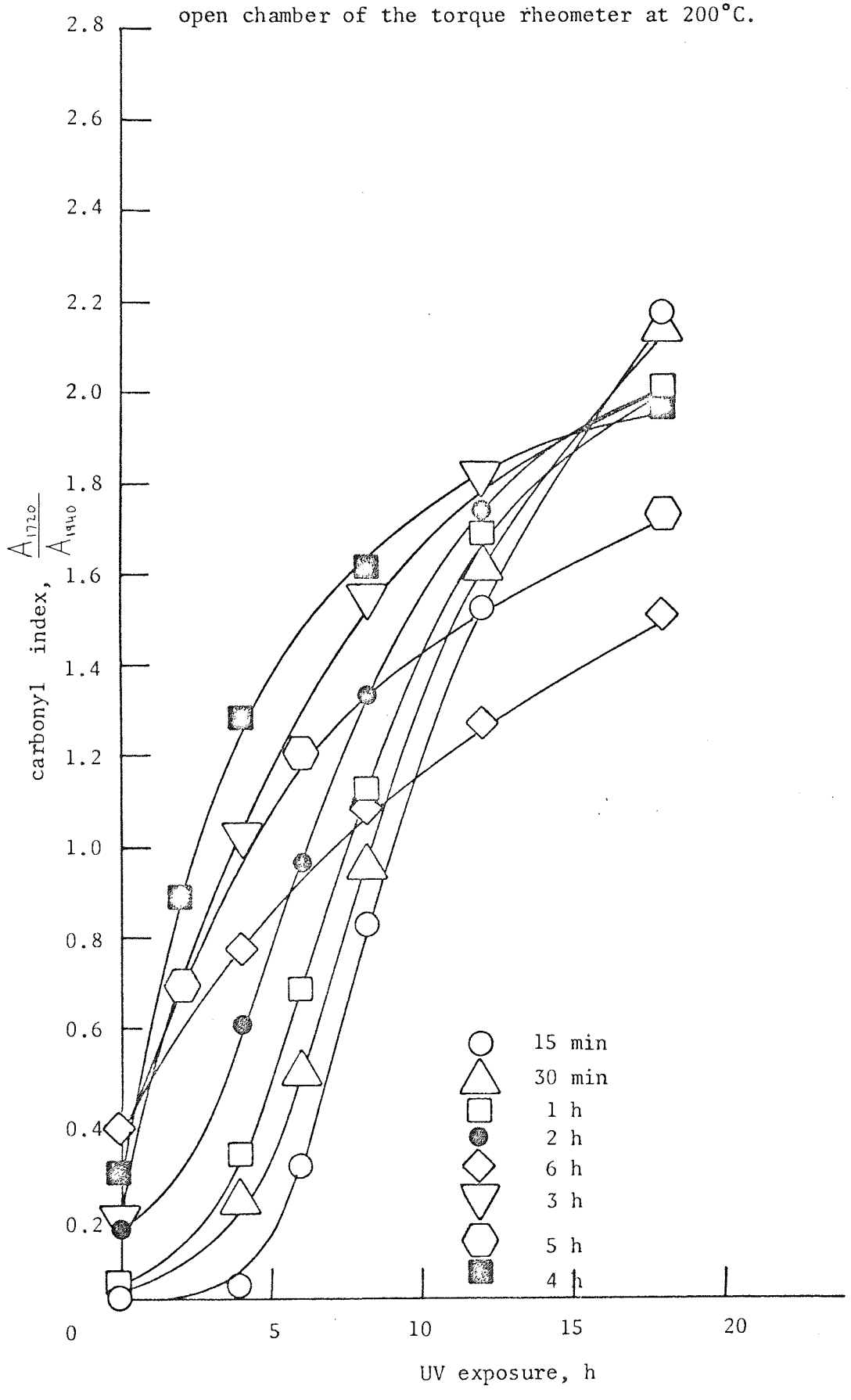

Figure 24.

Changes in concentration of hydroperoxide and UV and IR absorbances of carbonyl in unstabilised HIPS extruded film (50 μm) on photoxidation

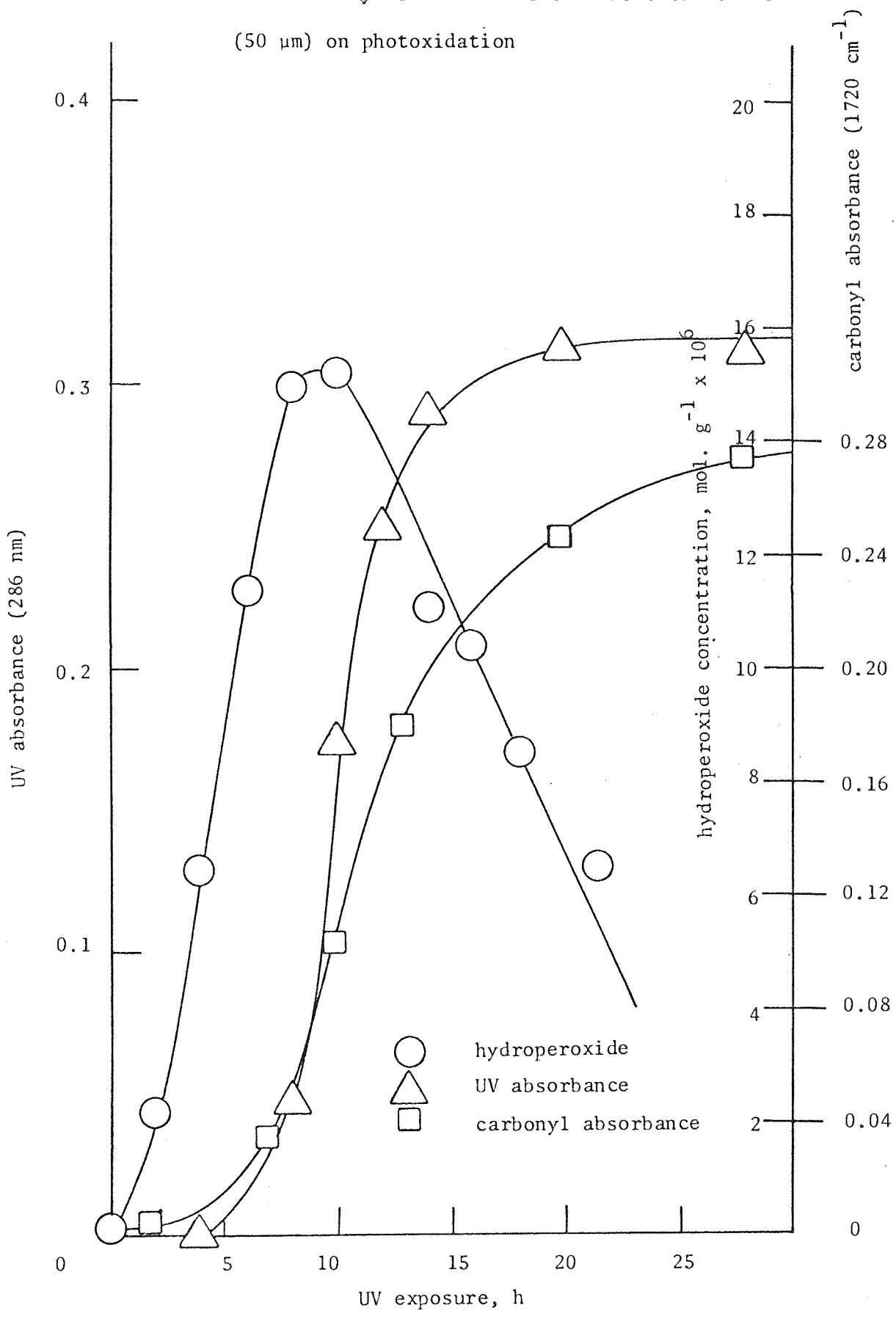

Figure 25.

Development of UV absorbance at 275 nm in "crystal" PS film (50 μm) on photoxidation.

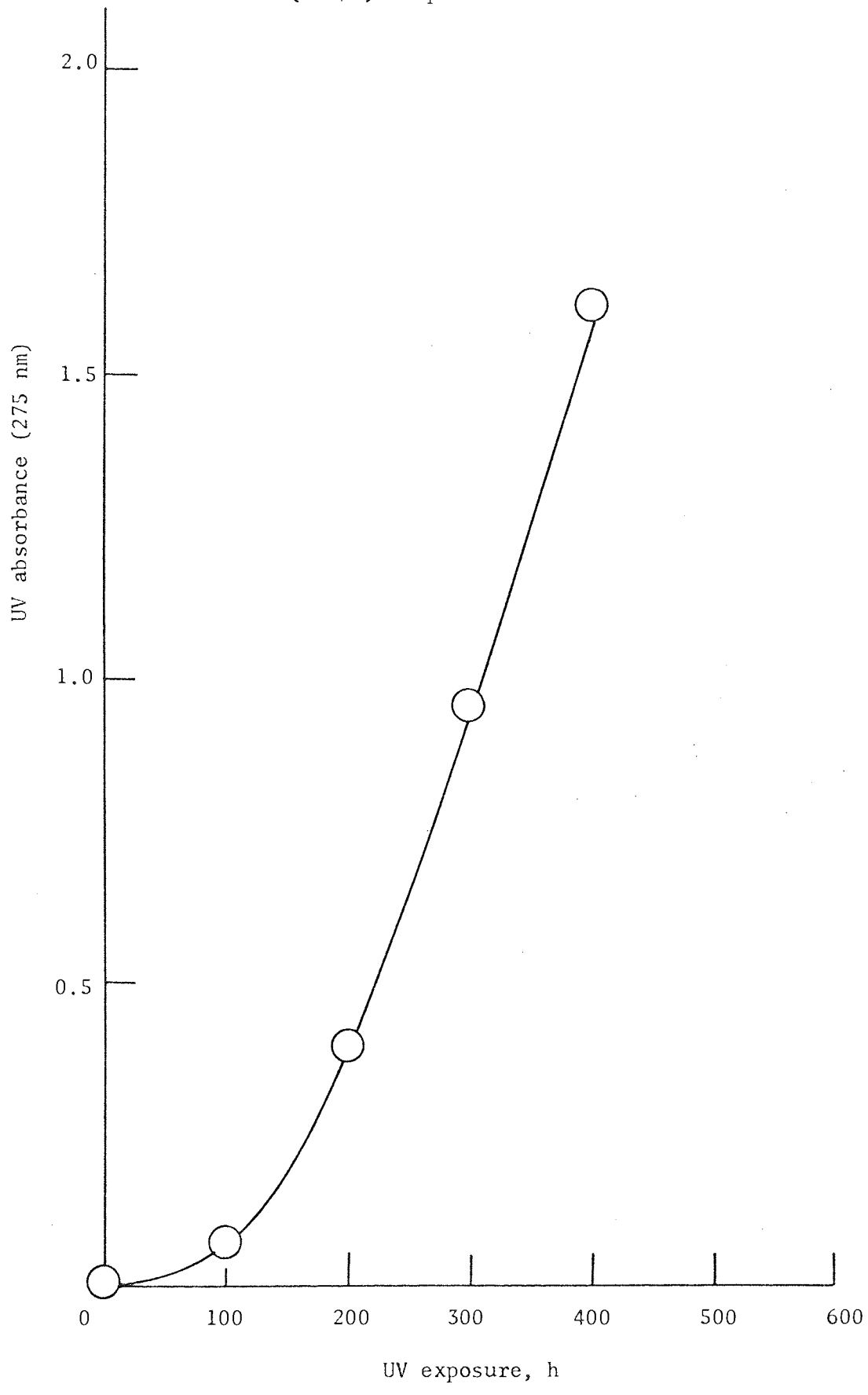

Figure 26.

figure 26. The concentration of chromophores build up at a much slower rate and attain linear kinetics after an induction period of 150 hours (found by extrapolation to zero absorbance) of exposure to UV. There appears to be no retardation even after 400 hours of UV exposure.

2.1.5 Correlation between hydroperoxide, carbonyl, hydroxyl, trans-1,4-polybutadiene and gel content

HIPS extruded film, 50 μm, containing no antioxidant was exposed to UV for intervals up to 30 hours and the concentration of functional groups was determined by IR spectroscopy (see 1.6.1) and chemical analysis (see 1.8). Under identical conditions gel content was estimated (see 1.9) and the results superimposed, figure 27. The most important curve is that representing gel content, this rises immediately at a very rapid rate bearing a linear relationship with UV exposure and reaches a maximum of 18•5% gel by weight. After 6 hours exposure to UV the gel content drops, at the same rate as its formation, to 6% corresponding to 10 hours UV exposure. It continues to fall gradually reaching a minimum of approximately 4•5% gel between 15 and 20 hours, after which it increases slightly at the same rate up to 6% towards 30 hours UV exposure. During these 30 hours the colour of the gel obtained changed from opaque (during the attainment of the maximum gel content from 0 to 10 hours) to bright yellow (from 10 to 30 hours).

The hydroperoxide concentration increases more slowly than gel content, although a linear relationship with UV exposure still holds.

Correlation of gel formation and decay with the formation and decay of functional groups in unstabilised HIPS film (50 μm) on photoxidation

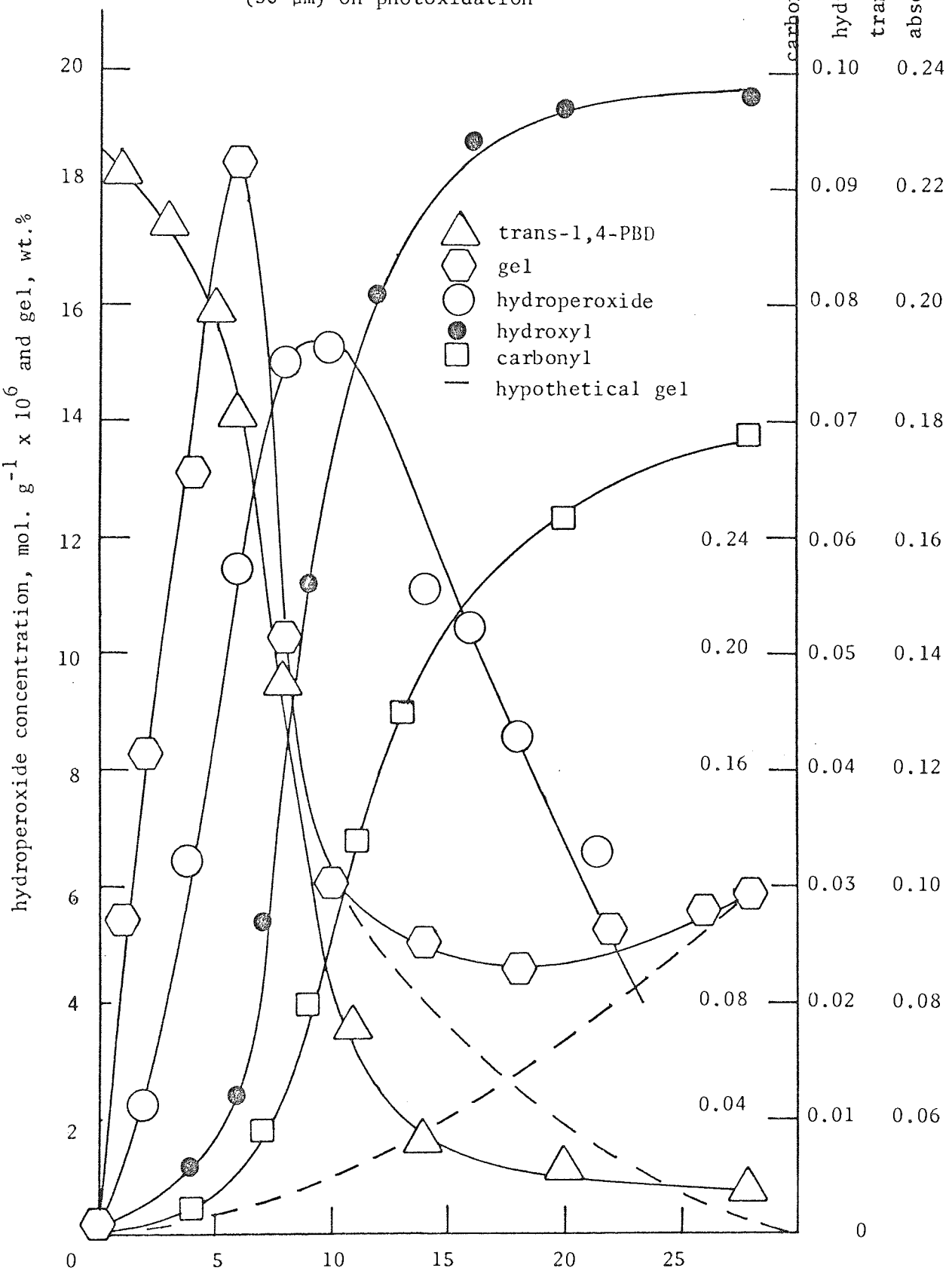

Figure 27.

The maximum observed for hydroperoxide occurs after 10 hours UV exposure (see 2.1.1.3), 4 hours after that of gel content. Hydroperoxide concentration fell after 10 hours in a similar manner already described for film 55 μm thickness (see 2.1.1.3), producing an asymmetric profile.

Unsaturation decreases from the onset of UV exposure in a linear manner up to approximately 5 hours then drops very rapidly, levelling out after 10 to 15 hours and becoming almost completely flat towards 30 hours UV exposure. The maximum rate of decay of trans-1,4-polybutadiene occurs 2 hours after the maximum weight of gel recovered.

Carbonyl and hydroxyl both build up slowly during the first 6 hours of UV exposure reaching maximum rate around 10 hours corresponding to the hydroperoxide maximum (see 2.1.1.3), and tend to level out towards 30 hours. Carbonyl formation has a longer induction period than hydroxyl.

2.2 DISCUSSION

The fate of HIPS during photoxidation may be described by following four chemical groups, namely, trans-1,4-polybutadiene, carbonyl, hydroxyl and hydroperoxide (figure 15). It would appear that hydroperoxide is the most important because of its rapid formation prior to carbonyl and hydroxyl. Indeed, only hydroperoxide was detected in extruded film, containing no antioxidant. To understand more about photo-initiation of HIPS, samples that contain different concentrations and relative proportions of hydroperoxide, hydroxyl, trans-1,4-polybutadiene, carbonyl and conjugated carbonyl were studied under conditions of photo-

oxidation. This was achieved by either increasing the severity of the melt procedure by processing or by thermal oven ageing of mildly-oxidised extruded film. During thermal oxidation analogous concentration profiles for hydroperoxide and other chemical groups were obtained, figures 12 and 13, confirming that the same free radical chain reactions occur in both photo and thermal oxidative degradation. Consequently HIPS which has had a prior thermal oxidative treatment however mild will contain hydroperoxides. Subsequent exposure to UV will cleave the oxygen-oxygen bond with a quantum efficiency approaching unity[15] with the production of active alkoxy and hydroxyl radicals capable of hydrogen abstraction[14]. It is pertinent to this discussion to consider mechanistically the removal of the trans-1,4-polybutadiene from the system. Hydrogen abstraction will occur at an α-methylenic position (owing to the low dissociation energy of the carbon-hydrogen bond[1]) producing an allylic alkyl radical (see scheme 1). This is stabilised by resonance[65] with an equal likelihood of further reactions taking place from either radical centre. It is mechanistically more rewarding to consider the isomer with the shifted double bond, although in the polymer many reaction paths will be followed simultaneously.

Atmospheric oxygen will react with an alkyl radical rapidly leading to an alkylperoxy radical; this is capable of several immediate reactions of which the most important will be considered here. Hydrogen abstraction (A) from a labile hydrogen in the polymer chain will produce allylic hydroperoxide, evidenced by iodiometry (see 1.8), and another alkyl radical. The allylic hydroperoxide may either break

down losing water with the formation of conjugated carbonyl (1685 cm^{-1}) through a possible cage intermediate[70] or undergo homolysis producing an alkoxy radical and a hydroxyl radical. The alkoxy radical may in turn either abstract a hydrogen forming allylic alcohol (3400 cm^{-1}) or undergo β-scission[71] forming an alkyl radical and conjugated aldehyde (1695 cm^{-1}).

As an alternative (B) to inter-hydrogen abstraction, the peroxy radical may abstract a hydrogen from the doubly activated methylenic centre[51,72] to produce an allylic hydroperoxide and an alkyl radical capable of stabilisation by resonance. Both isomers of hydroperoxide may be photolysed losing water to produce conjugated (1685 cm^{-1}) and saturated carbonyl (1720 cm^{-1}) respectively. The alkyl radical associated with the saturated ketone may terminate by abstraction of a hydrogen from another chain. However, the reactive methylene radical associated with the conjugated carbonyl will be stabilised by resonance with a shift of the double bond to produce a conjugated system. Addition of oxygen to the alkyl radical will give a peroxy radical capable of hydrogen abstraction from another chain to produce allylic hydroperoxide and subsequently decompose to conjugated carbonyl.

Complementary to β-scission other chain cleavage reactions may involve Norrish I or II photolysis[20] of carbonyl. In the case of trans-1,4-polybutadiene Norrish II producing an olefinic chain end is unlikely because of neighbouring unsaturation anticipating an allene structure. However, Norrish I cleavage (a) may readily occur producing both alkyl and acyl radicals. The acyl radical may undergo

various reactions with radicals to produce different functional groups. An illustrative reaction involves the addition of triplet oxygen followed by hydrogen abstraction from the polymer chain leading to a conjugated peracid (1775 cm^{-1}). Homolysis of the oxygen-oxygen bond results in an alkoxy radical capable of abstracting a hydrogen to produce conjugated carboxylic acid (1703 cm^{-1}) or cross-linking with an alkyl radical forming a conjugated ester (1723 cm^{-1}).

Conjugated carbonyl (1685 cm^{-1}) may be removed from the system by addition of an alkoxy radical to the conjugating double band (b) producing an alkyl radical and saturated ketone (1720 cm^{-1}). This reaction also constitutes gel formation through an ether linkage. Other workers have suggested that conjugation with carbonyl may be destroyed by a shift of the double bond via photoexcitation of the carbonyl group[34]. A more general mechanism (C) involves peroxy radicals producing initially a labile peroxidic linkage, 150 kJ. mol^{-1} [73,74]. This will undergo homolysis resulting in alkoxy radicals and will subsequently be involved in the formation of a secondary ether linkage which is more stable towards UV, 360 kJ. mol^{-1}[73,74].

SCHEME 1

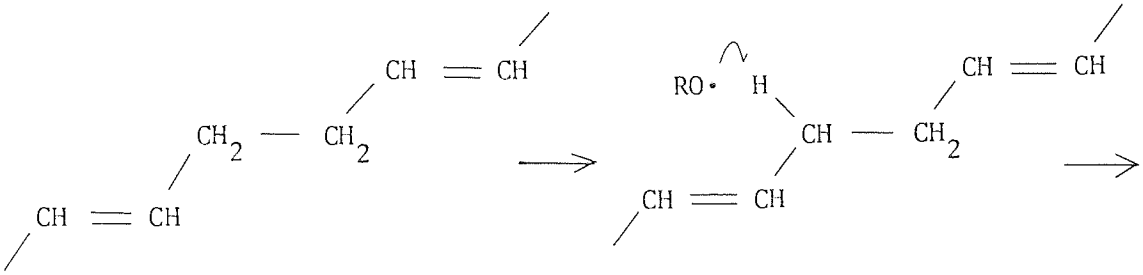

trans-1,4-polybutadiene ($967\ cm^{-1}$)

hydrogen abstraction by alkoxy radical

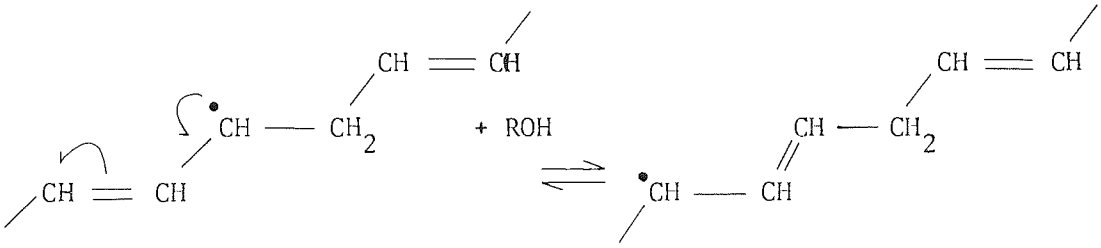

allylic radical

stablilised by resonance

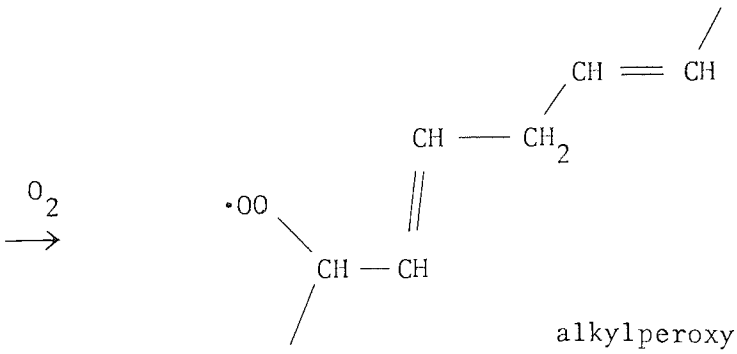

alkylperoxy radical

The alkylperoxy radical can then react further by alternative processes, A, B, C and D:

A.

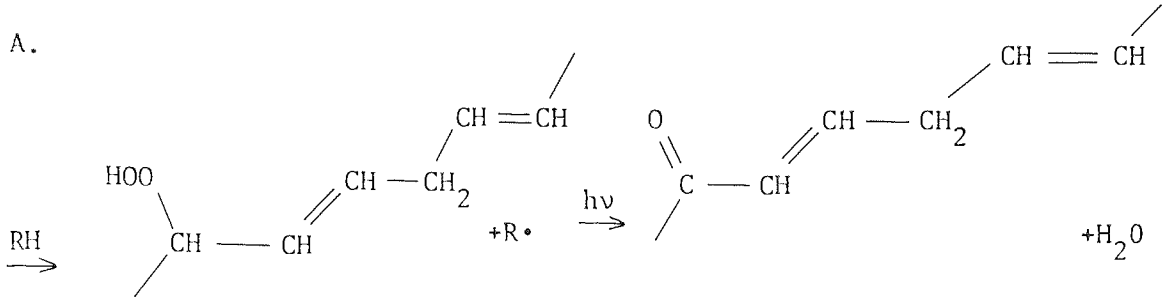

allylic hydroperoxide
(idiometry)

conjugated carbonyl
(1685 cm^{-1})

↓ hν

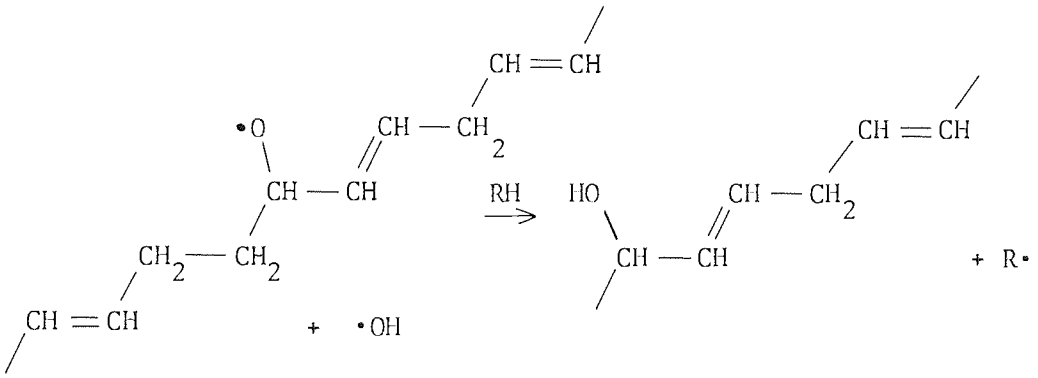

alkoxy radical

allylic alcohol
(3400 cm^{-1})

↓ β-scission

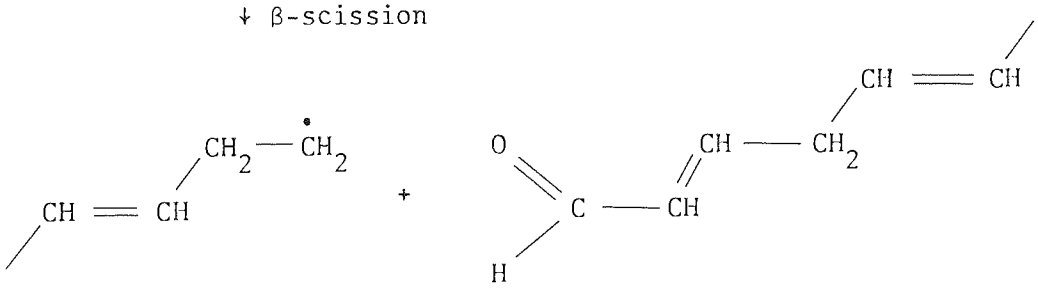

conjugated aldehyde (1695 cm^{-1}) +
alkyl radical

B.

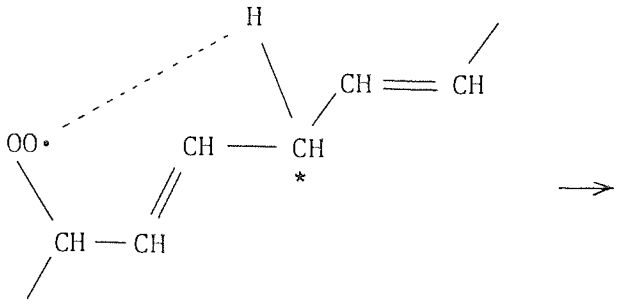

* doubly activated methylene

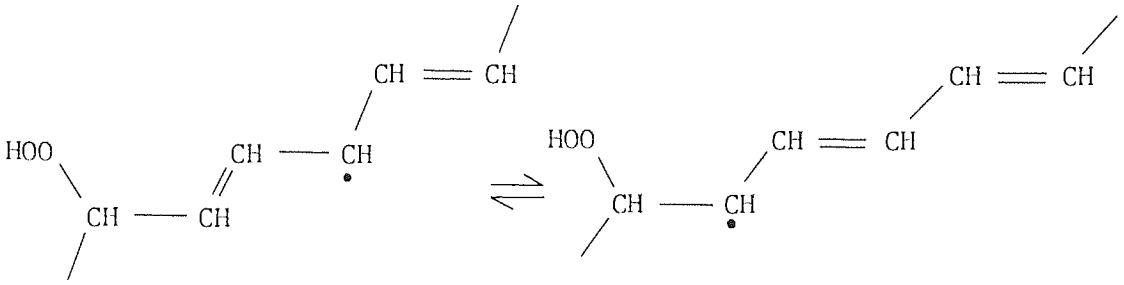

allylic hydroperoxide + allylic radical

stabilised by resonance

↓hν ↓hν

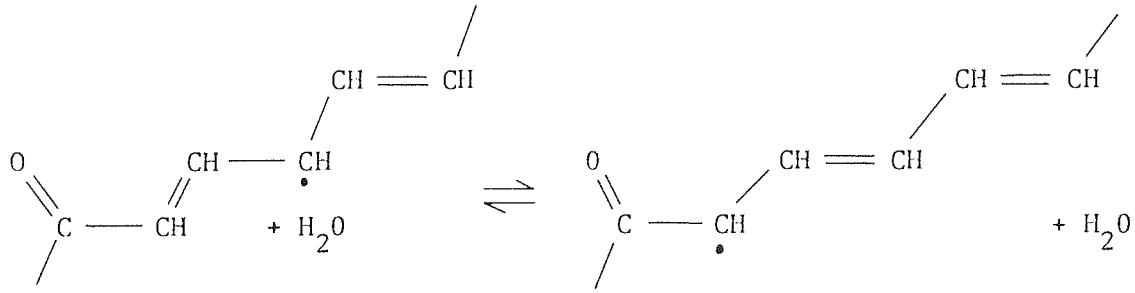

conjugated carbonyl (1685 cm^{-1})

saturated carbonyl (1720 cm^{-1})

↑↓

↓ RH

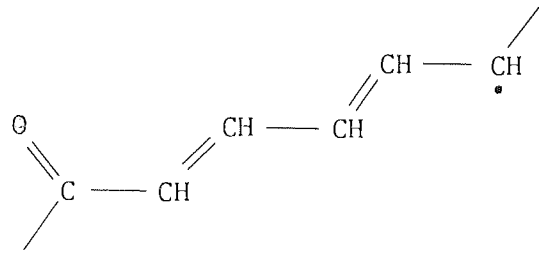

stabilised by resonance

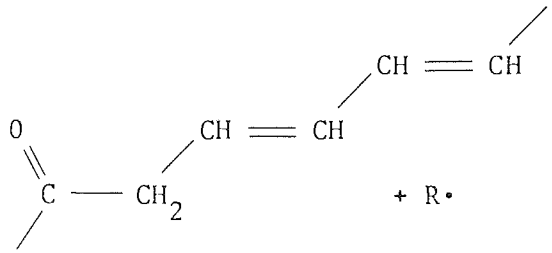

saturated ketone

(1720 cm^{-1})

$+O_2$

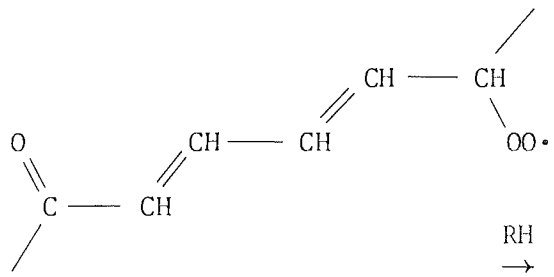

peroxy radical

RH →

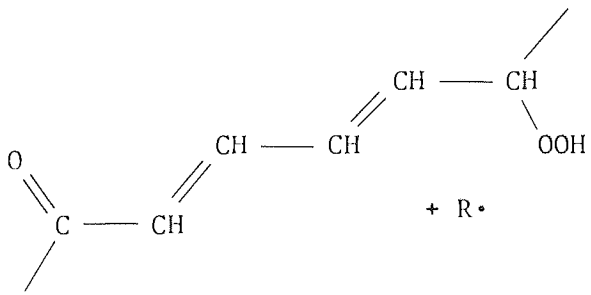

allylic hydroperoxide

hν →

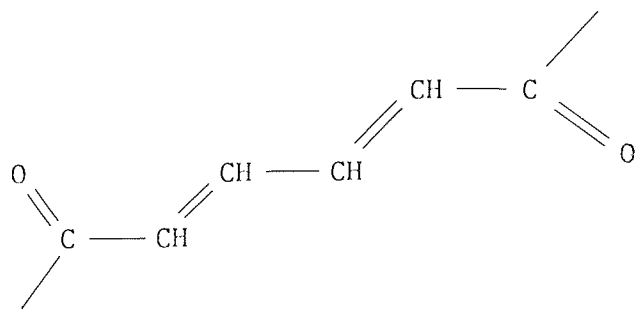

$+ H_2O$

α, β, γ, δ - unsaturated ketone

(1667 cm^{-1})

(a) Norrish I photolysis:

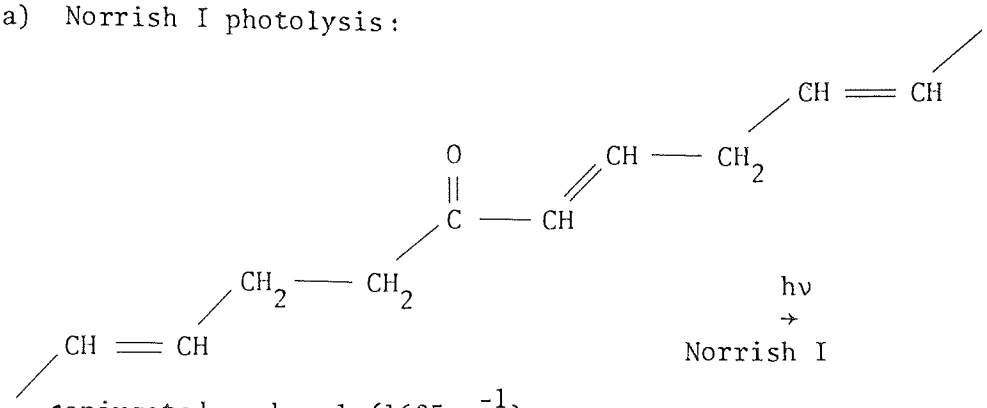

conjugated carbonyl ($1685 cm^{-1}$)

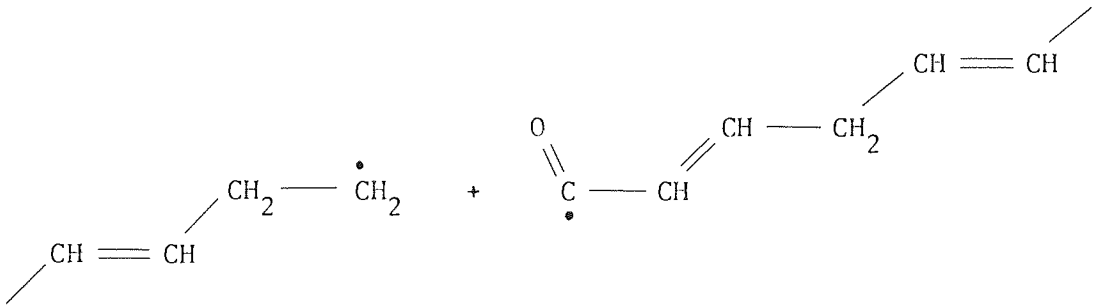

alkyl and acyl radicals (chain scission)

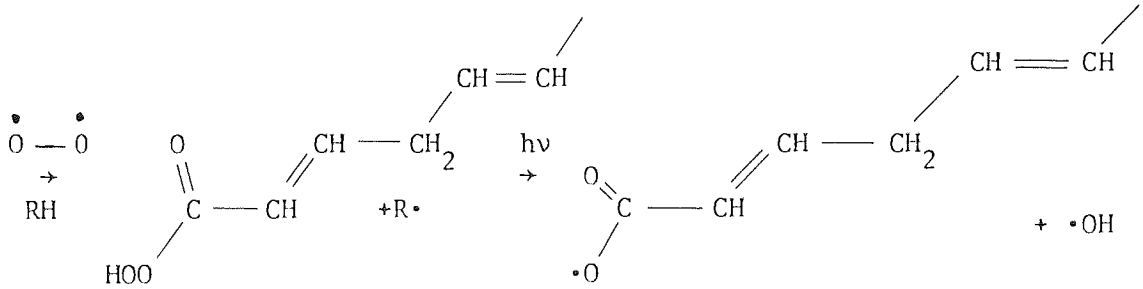

conjugated peracid ($1775 cm^{-1}$)

acyloxy radical

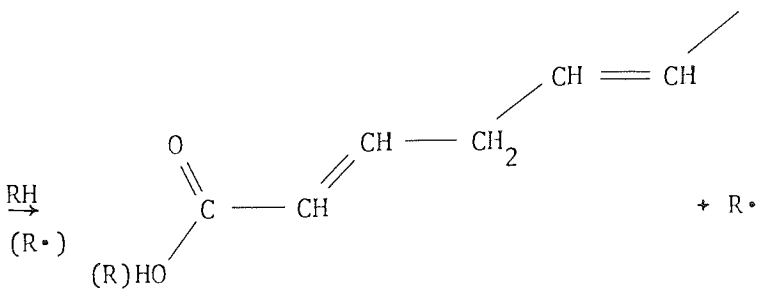

conjugated carboxylic acid ($1703 cm^{-1}$) or ester ($1723 cm^{-1}$)

(b) destruction of conjugation:

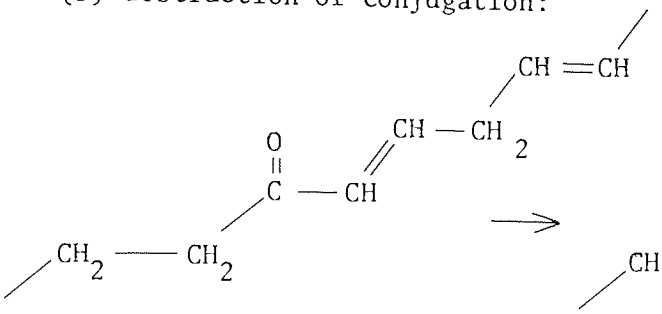

conjugated carbonyl

(1685 cm^{-1})

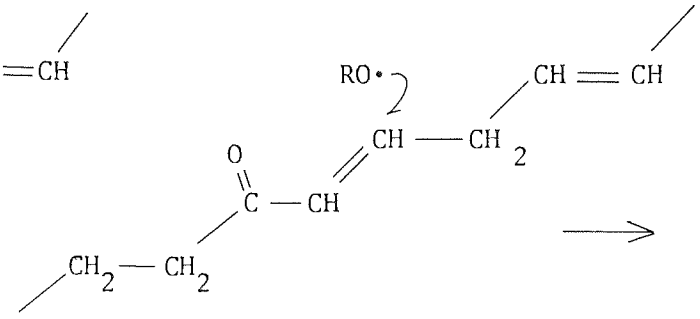

addition of alkoxy

radical to double bond

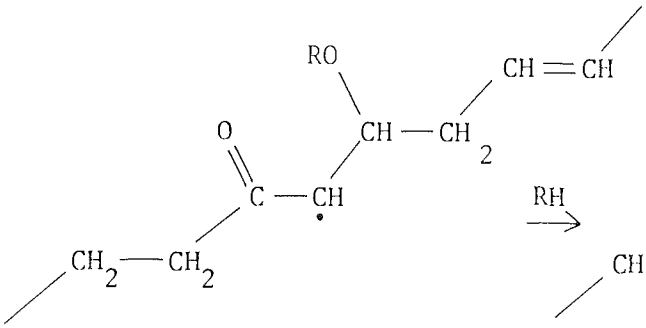

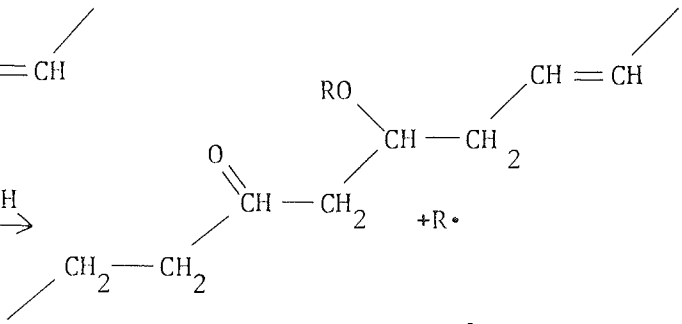

saturated ketone (1720 cm^{-1})

C_1 formation of peroxidic gel:

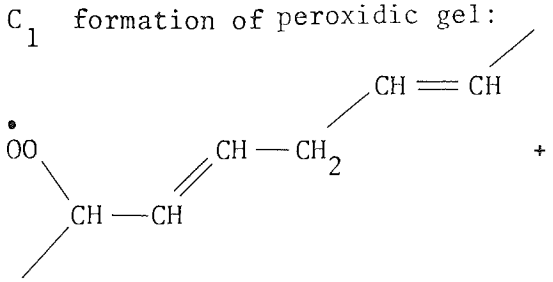

alkylperoxy radical

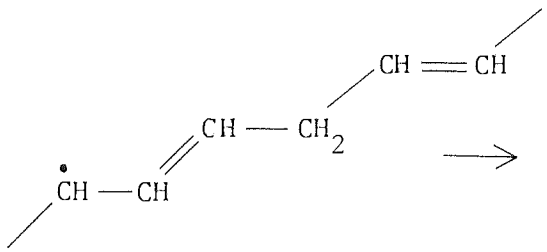

alkyl radical

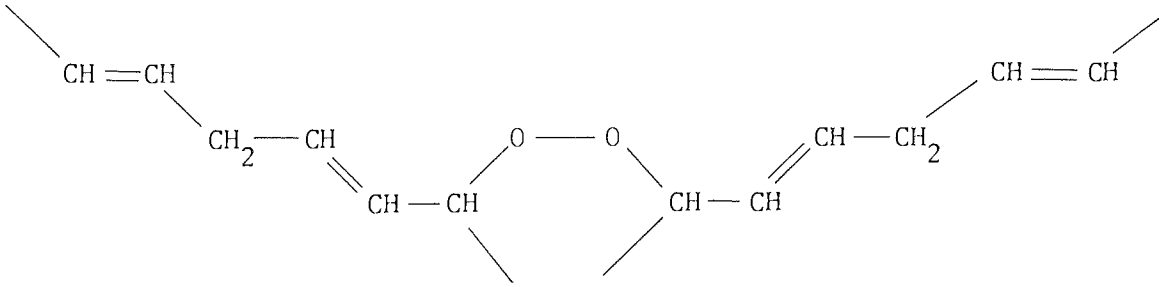

peroxide gel (termination)

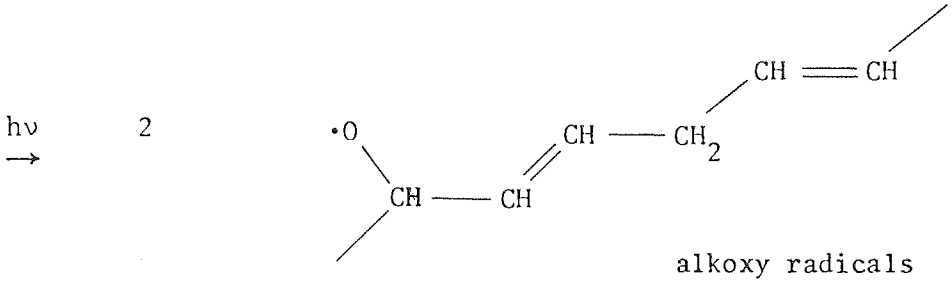

alkoxy radicals

C_2 formation of ether linkage:

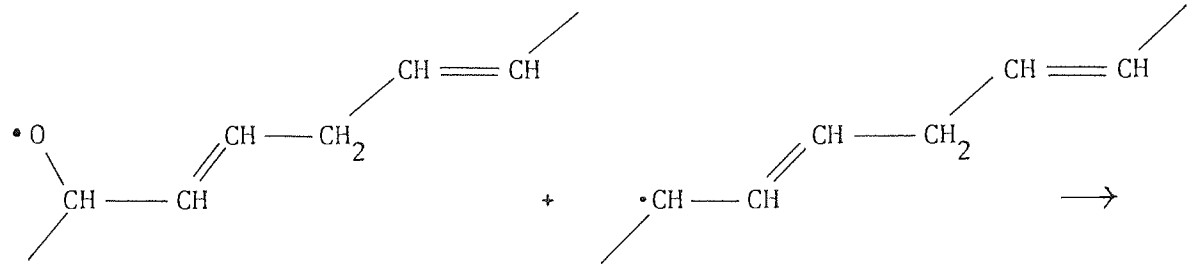

alkoxy radical alkyl radical

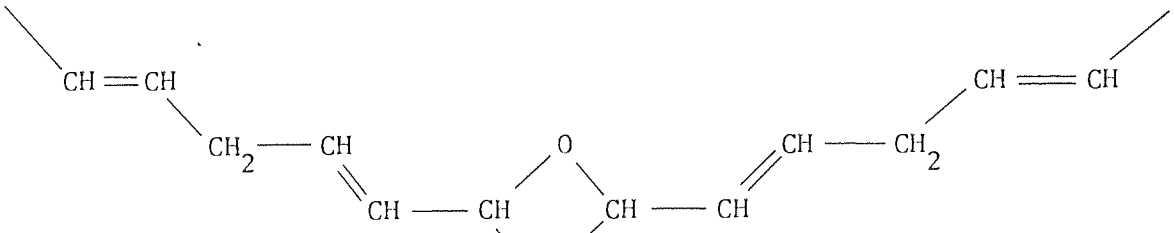

ether linkage (termination)

(1105 - 1000 cm^{-1})

C_3 formation of peroxidic gel by addition to 1,4-polybutadiene :

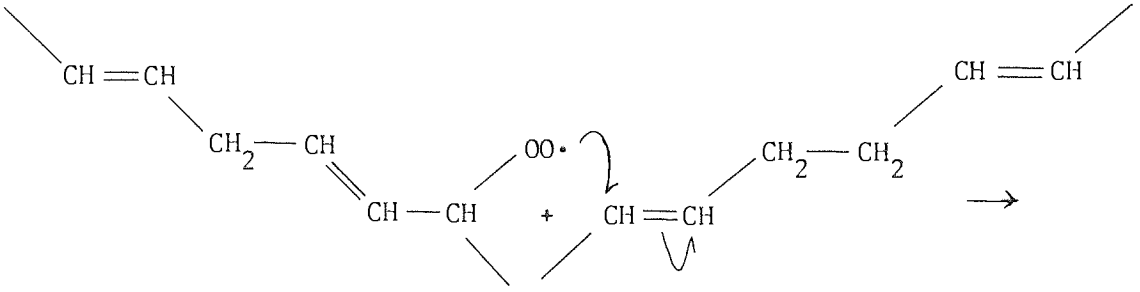

alkylperoxy radical

trans-1,4-polybutadiene

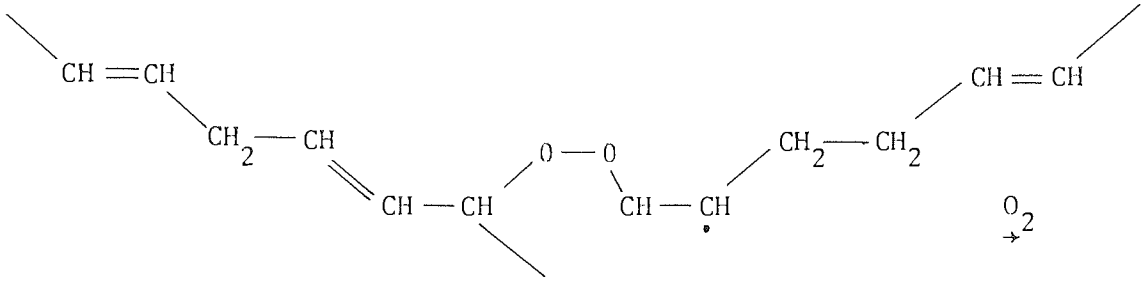

peroxidic linkage + alkyl radical

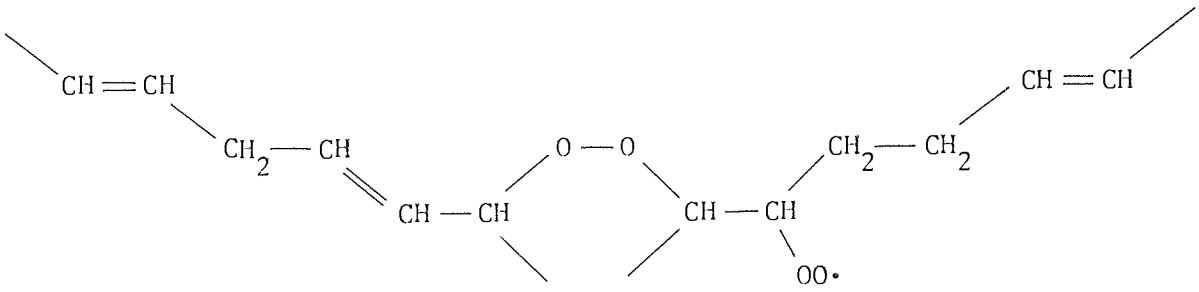

peroxy radical

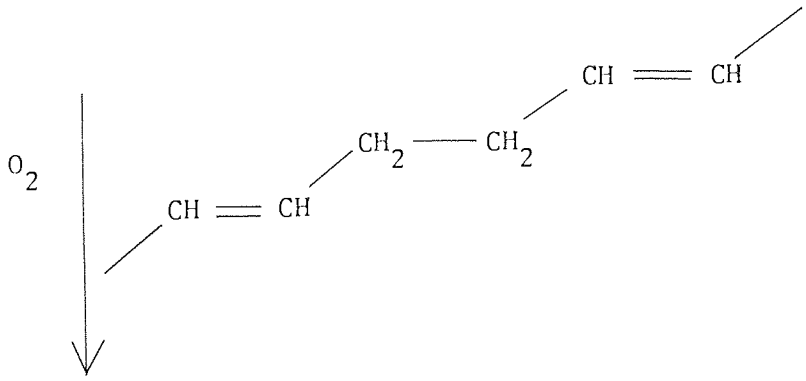

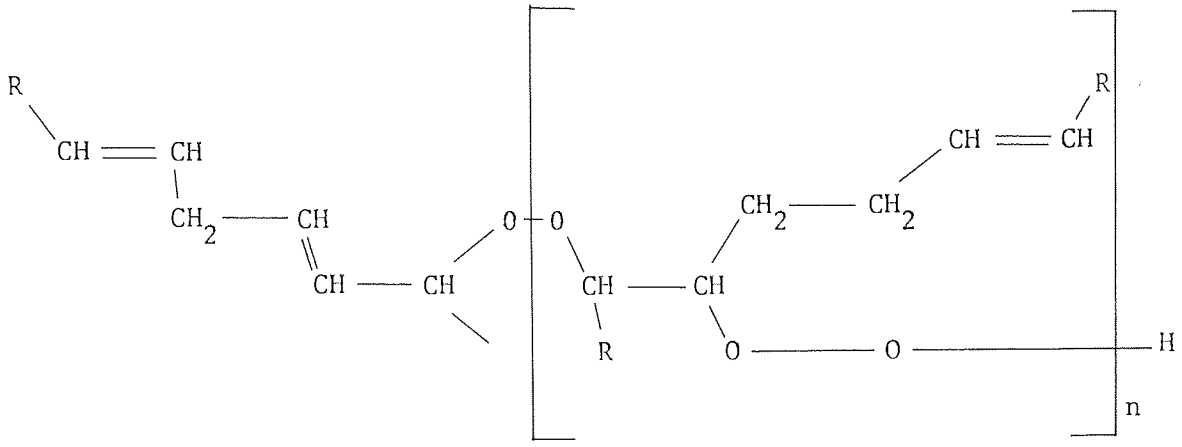

polyperoxide

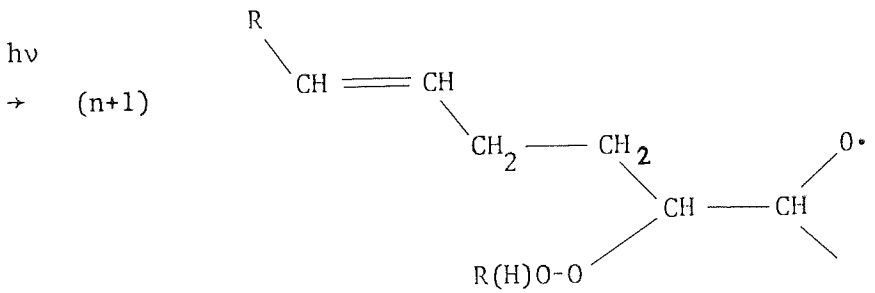

alkoxy radicals

C_4 formation of perodidic gel by addition to pendant double bond:

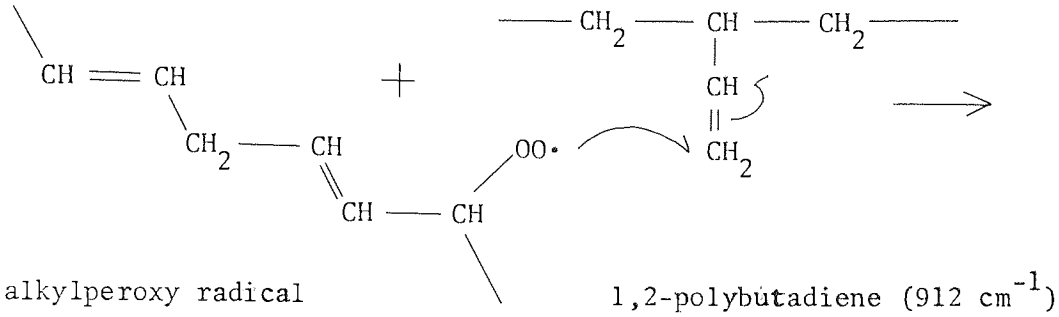

alkylperoxy radical — 1,2-polybutadiene (912 cm^{-1})

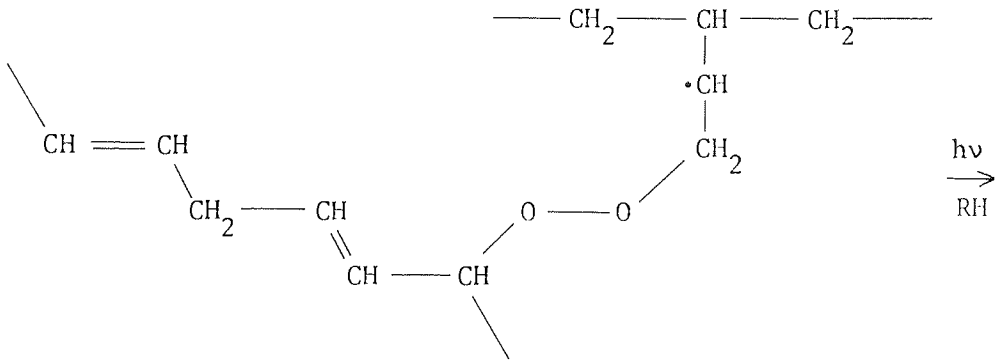

peroxidic linkage + alkyl radical

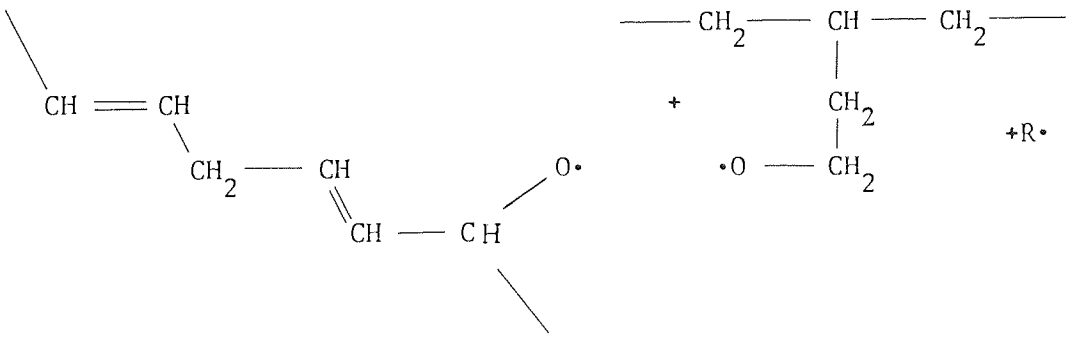

alkoxy radicals (RO•)

C_5 formation of ether linkage by addition to 1,2-or 1,4-polybutadiene :

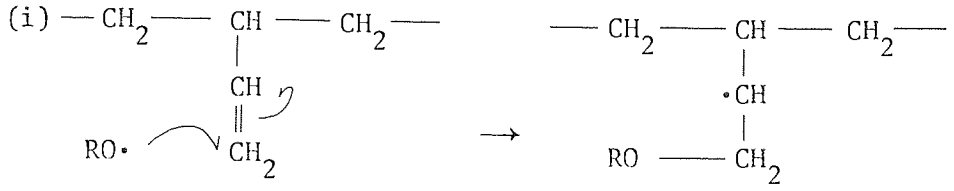

1,2-polybutadiene ether linkage

(ii)

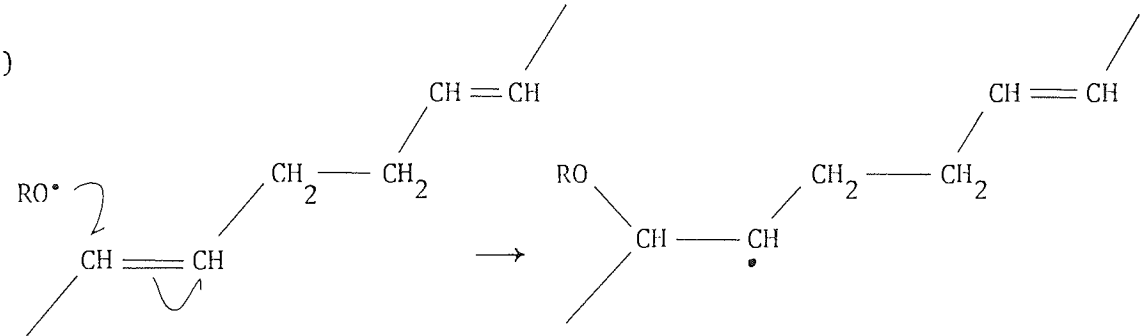

1,4-polybutadiene ether linkage

D formation of epoxide by addition to double bond:

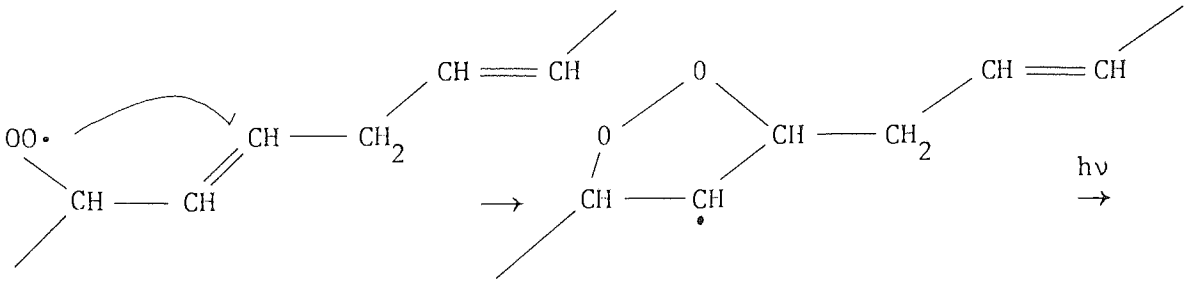

1,4-polybutadiene

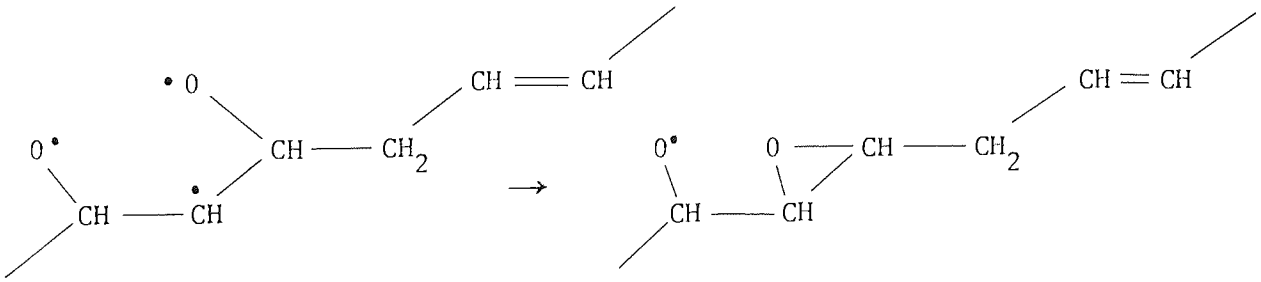

epoxide

A general mechanism for the destruction of trans-1,4-polybutadiene having been proposed it is now possible to explain the formation of hydroperoxide, hydroxyl and carbonyl during photoxidation of HIPS and conversely to substantiate the mechanistic schemes discussed in this chapter. The relative importance of 1,2-polybutadiene, cis- and trans-1,4-polybutadiene will be discussed in Chapter Three.

During processing (see 2.1.1.2) of HIPS more conjugated carbonyl was formed than during the analogous oven ageing (see 2.1.1.1). The intense peak in figure 14 attributed to conjugated aldehyde (1695 cm^{-1}) was not observed during oven ageing or during photoxidation of HIPS. It is clear from the proposed mechanisms that allylic hydroperoxide is formed as a pre-requisite to degradation and that breakdown of allylic hydroperoxide by either thermal or UV irradiation will produce a predominance of conjugated carbonyl. Conjugated aldehyde (1695cm^{-1}) produced via β-scission was observed as a more intense peak than conjugated ketone (1685 cm^{-1}), figure 14, resulting from dehydration of allylic hydroperoxide, for a sample processed for 6 hours. Even though the chamber of the torque rheometer was open to air (see 1.2.1.2) the availability of oxygen to the oxidising melt is likely to be considerably less than that for oven aged films (see 1.12).

Consequently, destruction of conjugated carbonyl by addition of alkoxy radical to the conjugating double bond will not occur so frequently. On exposure to UV and oxygen the conjugated carbonyl of processed films failed to dominate the carbonyl region of the IR and was superceded by saturated carbonyl (1720 cm^{-1}). The colour

associated with processing is considered to be a consequence of the predominance of conjugated systems including carbonyl even though relatively little consumption of trans-1,4-polybutadiene has occurred relative to oven ageing; both indexes start at 2·0 and fall to 0·55 for oven ageing but only 1·25 for processing. Similarly the UV spectrum shows a progressive increase in absorbance of conjugated chromophores around 280 nm with respect to processing time; the tail of which extends into the visible region.

The linear build-up of carbonyl, representing both conjugated and non-conjugated ketone and aldehyde (figure 13) for processed material is consistent with similar work involving high density polyethylene (HDPE) also at 200°C using the torque rheometer[75]. Similarly at lower temperature (160°C) an induction period was observed for HDPE[75]; this being analogous to thermal ageing at 98°C for HIPS, figure 12.

Evidence from both thermal and UV degradation, figures 12, 13 and 15, implies that destruction of unsaturation is concurrent with hydroperoxide formation. Indeed allylic hydroperoxide is one of the initial products derived from alkylperoxy radicals. Under conditions of UV and thermal oxidation this will breakdown very rapidly to produce chain propagating radicals. However, when there is an abundance of unsaturation, at the start of degradation, hydroperoxide formation will exceed decomposition resulting in a measurable stationary concentration of hydroperoxide, this being higher for photoxidation than for thermal oxidation[76]. It is apparent from the mechanisms

described earlier (see scheme 1) that trans-1,4-polybutadiene is consumed very rapidly thus diminishing the supply of reactive methylene groups which lead to the replenishing of the supply of radicals. The processes of decomposition will thus supercede leading to a net reduction in the hydroperoxide concentration. The consequence of these competing reactions is a maximum concentration as the differential of the unsaturation concentration. It must be appreciated that the allylic hydroperoxide formed initially from the PBD will be replaced by hydroperoxide resulting from photoxidation of the remaining polystyrene of HIPS. This will be of a much lower concentration necessary to sustain the slower degradation and thus explains the slightly higher values obtained for hydroperoxide concentration after the maximum, figure 15.

An alternative explanation for an observed maximum in hydroperoxide concentration during the thermal oxidation of low molecular weight polypropylene has been proffered by other workers[77]. This concerns the possibility of induced decomposition of hydroperoxide by formation of a transitory complex with carboxylic acid through hydrogen-bonding. Similarly it was suggested[78] that the observed hydroperoxide maxima obtained during the thermal oxidation of atacticpolypropylene film[6] was a result of induced peroxide decomposition by acidic products of degradation. The hydrogen-bonded association of hydroperoxide with carboxylic acid discussed above is analogous to that required for the bimolecular decomposition postulated for hydroperoxide during (thermal) oxidation[78,79] of hydrocarbon polymers. The bimolecular decomposition of hydroperoxide will occur in preference to the mono-molecular

reaction after a critical concentration of hydroperoxide has built up in the polymer and may similarly account for the maximum concentration of hydroperoxide observed during thermal oxidation[78]. The transition from mono-molecular to bi-molecular decomposition of hydroperoxide has also been invoked to explain the observed maximum in hydroperoxide concentration during the thermal oxidation of polyisoprene[80]. From kinetic studies of autoxidation of hydrocarbon[4] attainment of linear kinetics requires that the hydroperoxide concentration reaches a limiting value only; a decrease in hydroperoxide concentration during oxidation is not essential.

In the present study on HIPS evidence for hydrogen-bonded association is deduced from the broad band observed in the oxygen-hydrogen (O-H) stretching frequency of the IR during photoxidation; typical spectra will be shown in Chapter Three. However, it is not possible to differentiate between hydrogen bonding involving hydroperoxide and carboxylic acid and hydroperoxide with itself. During thermal oxidation of HIPS the concentration of hydroperoxide falls after a substantial build up of carbonyl groups, figures 12 and 13. Similar results were obtained for the photoxidation of HIPS, figure 15. It is likely that carboxylic acid is one of the main constituents in the carbonyl region of the IR. Therefore the evidence would suggest that carboxylic acid induced hydroperoxide decomposition is a possible candidate for the maximum observed in the hydroperoxide concentration curves. The inhibitory effect of carboxylic acids on the photoxidation of cumene initiated by hydroperoxide will be illustrated in Chapter Four. Consequently it is believed that the concentration

of polybutadiene in HIPS dominate the course of oxidative degradation in both thermal and photoxidation producing the observed maximum hydroperoxide concentration, figures 12, 13 and 15, in conjunction with accelerated decomposition of hydroperoxide by carboxylic acid induced decomposition.

During the initial 3 to 5 hours of UV exposure of HIPS nearly all the oxygen absorbed is converted into hydroperoxide (or peroxide), after which carbonyl and hydroxyl are formed[9]. This is evident from figure 16 in which the curve representing the total quantity of oxygen absorbed is supplemented by formation of carbonyl and hydroxyl through the breakdown of hydroperoxide. Consequently carbonyl (or hydroxyl) follows the oxygen-absorption curve in a parallel manner.

Similarly in figure 17 the deflection of the curve relating unsaturation and hydroperoxide,showing increasing slope implies that more trans-1,4-polybutadiene is consumed to produce hydroperoxide; in other words allylic hydroperoxide decomposes to produce carbonyl and hydroxyl. This is confirmed by the two linear relationships between carbonyl and hydroxyl with hydroperoxide concentration. Both of which extrapolate to the abscissa with a finite concentration of hydroperoxide. It is apparent that hydroxyl groups are produced slightly before carbonyl during thermal and especially during UV oxidation, figures 12 and 15 respectively; this would suggest that IR spectrum attributed to hydroxyl receives a complement from bonded hydroperoxide[81]. This is substantiated in figure 12 for heat aged HIPS resulting in a smaller shift of hydroxyl corresponding to a lower concentration of hydroperoxide compared with figure 15 for photoxidation.

In competition with hydrogen abstraction by alkylperoxy radical to produce hydroperoxide is a termination reaction (see scheme 1) involving recombination with an alkyl radical to form a dialkyl peroxide. Moreover, allylic hydroperoxide formation will involve production of alkyl radicals to furnish the peroxide build-up. The alkyl radicals themselves will be in competition with oxygen to produce peroxy radicals. The combination of alkyl and peroxy radicals constitutes a possible first stage of gel formation (C_1). With further exposure to UV homolysis of the oxygen-oxygen bond will occur producing alkoxy radicals. Termination with an alkyl radical will result in an ether linkage (C_2) representing the second stage of the gel formation.

Evidence supporting an initial formation of peroxide gel is obtained from figure 27 in which the maximum weight of gel occurs before the maximum hydroperoxide concentration; only alkylperoxy radicals will be available in these early stages before homolysis of hydroperoxide yields a supply of alkoxy radicals for possible ether linkages. Carbon-carbon cross-linking is unlikely when the supply of oxygen is high. Another route for peroxidic gel formation involving 1,4-(or 1,2-) polybutadiene, is addition of a peroxy radical to a double bond (C_3); this being more favourable when the polymer is saturated with oxygen. Addition of oxygen to the alkyl radical formed adjacent to the peroxide bridge will produce a further peroxy radical capable of similar additions to 1,4-(or 1,2-) polybutadiene. This polymerisation will result in a polyperoxide[82,83] terminated with a hydroperoxide.

With further UV irradiation this will break down to form alkoxy radicals. The above gel formation provides an explanation for the observed maximum rate of destruction of trans-1, 4-polybutadiene occurring before the maximum hydroperoxide concentration is reached; addition of peroxy radicals to double bands will remove a finite quantity of unsaturation. However, because this is a relatively small and transitory concentration compared to hydroperoxide, the continuity of the hydroperoxide profile measured by iodiometry (see 1.8) was not distorted by possible reduction of polyperoxides.

Addition of an alkylperoxy radical to the pendent double bond of 1,2-polybutadiene to produce peroxidic gel[84] (C_4) is also favoured under condition of atmospheric photoxidation and is similarly more likely to prevail over the termination reaction C_1. UV exposure will cleave the peroxidic bond with the production of alkoxy radicals associated with 1,4- and 1,2-polybutadiene. The alkoxy radical itself may undergo addition reactions with either 1,2- or 1,4-polybutadiene resulting in an ether gel[84], C_5(i) and C_5(ii) respectively. Addition of an alkoxy radical to a pendent double bond is more likely than addition to 1,4-polybutadiene. However, from the evidence presented in 2.1.3.1 concerning the destruction of thermally-produced hydroperoxide by heating in an atmosphere of argon, and by comparing the results with those obtained for oven ageing shown in figure 12, it is evident that the decrease in concentration of trans-1,4-polybutadiene after heating in argon is greater than would be expected considering the corresponding small increase in carbonyl and hydroxyl. This evidence suggests that alkoxy radicals produced by thermal

breakdown of allylic hydroperoxide undergo addition reactions with trans-1,4-polybutadiene in an atmosphere of argon. The destruction of hydroperoxide by heating in argon should have rendered the sample as stable as a control film which has had no thermal treatment whatsoever. However, addition of an alkoxy radical to a double bond (C_5) produces an alkyl radical capable of further reactions unless it is terminated by dimerisation in the inert atmosphere.

Addition of an alkylperoxy radical of 1,4-polybutadiene to an adjacent double bond (D) will lead to a ring structure and formation of a radical centre. Under conditions of photoxidation homolysis of the oxygen-oxygen bond will occur with the production of alkoxy radicals. Combination with one of these alkoxy radicals with the adjacent alkyl radical will result in an epoxide[85].

The gel curve shown in figure 27 for photoxidised HIPS may be considered to represent the summation of two hypothetical curves (depicted as broken lines). The first curve corresponds to the destruction by UV of a predominantly peroxidic gel tending towards zero concentration after 30 hours UV exposure, and the second curve to represent the gradual formation of an ether linkage. The colour change of the gel occurring after 10 hours UV exposure is synchronous with the breakdown of the opaque peroxide gel and formation of an unsaturated branched ether linkage (1105 - 1000 cm^{-1}). The chemical changes occurring during photoxidation will be discussed more fully in Chapter Three. The initial peroxide gel must encompass polystyrene and polybutadiene chains because HIPS contains only 6·5%PBD; the maximum

weight of gel recovered reached 18·5%. It is known that the PBD is present as a grafted co-polymer, namely styrene-butadiene rubber (SBR)[54] and therefore initial cross-linking would certainly involve styrene chains. Furthermore, the weight of gel recovered after 10 hours UV exposure was below 6%, suggesting that the polystyrene may not be involved. This was confirmed by IR and UV spectroscopic evidence on the gel; the complement from polystyrene was progressively diminished and after 16 hours of UV exposure gels consisted of nearly 100% PBD rubber. This evidence suggests that chain scission occurs at the graft points[40] eliminating polystyrene which cannot enter readily into gel formation, in other words the tie-bonds connecting the polystyrene and polybutadiene phases are cleaved. Conversely if β-scission occurs at the middle of the PBD chain in HIPS then the gel would consist of a greater proportion of polystyrene, contrary to evidence.

Hydrogen abstraction by an alkoxy radical will take place from the reactive tertiary allylic graft point (see scheme 2) with the formation of an alkyl radical stabilised by resonance. However, combination with atmospheric oxygen will take place very rapidly to give a peroxy radical capable of hydrogen abstraction with the formation of a tertiary allylic hydroperoxide. This will be very unstable breaking down under UV to form a tertiary alkoxy radical which will undergo β-scission[14] by alternate paths (a) and (b). β-scission at the polystyrene chain end, (a), will result in the immediate separation of the polystyrene and polybutadiene chains with the formation of conjugated ketone (1685 cm^{-1}) and radical chain ends which may

terminate by dimerisation. β-scission at position (b) leads to separation of a polybutadiene segment from a styrene-butadiene chain with formation of conjugated ketone. However, Norrish I photolysis will cleave the styrene-butadiene chain producing alkyl and acyl radicals. The acyl radical may form conjugated peracid or ester.

SCHEME 2

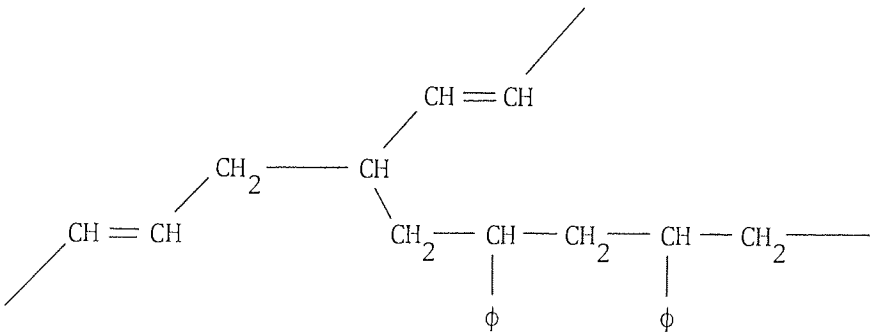

graft co-polymer of styrene - butadiene rubber

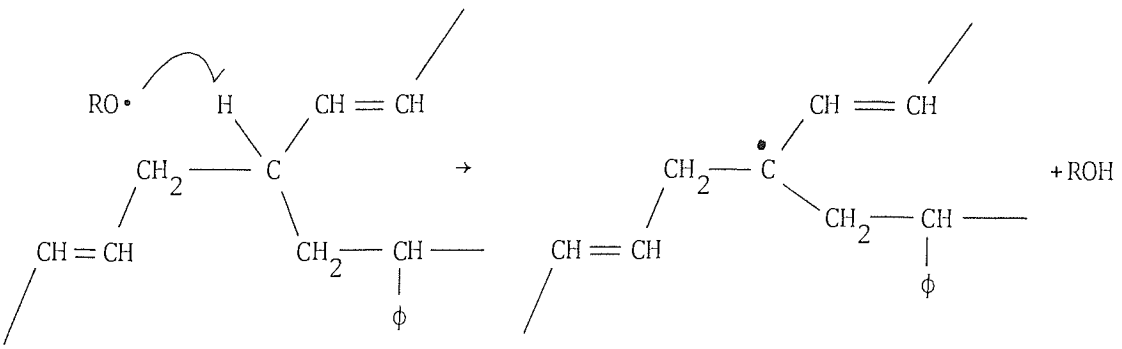

abstraction of tertiary allylic hydrogen by alkoxy radical

alkyl radical (stabilised by resonance)

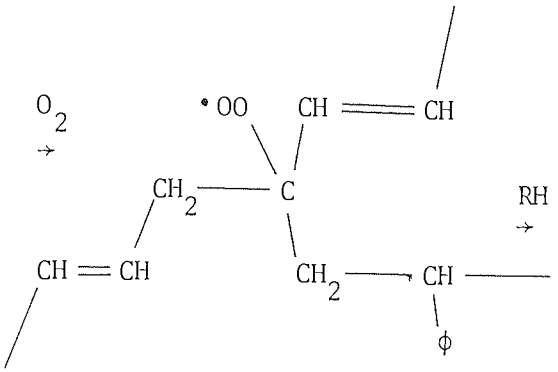

peroxy radical

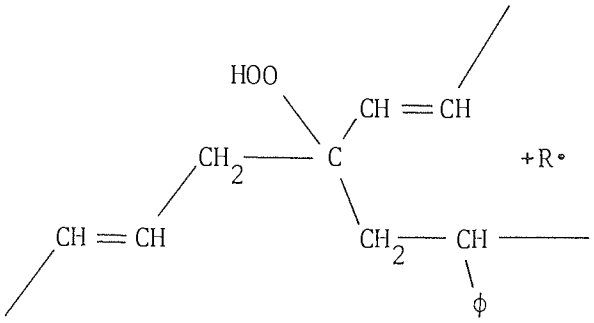

tertiary allylic hydroperoxide

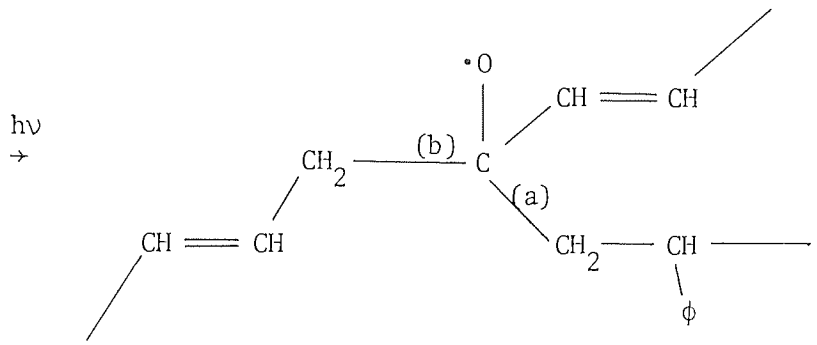

alkoxy radical

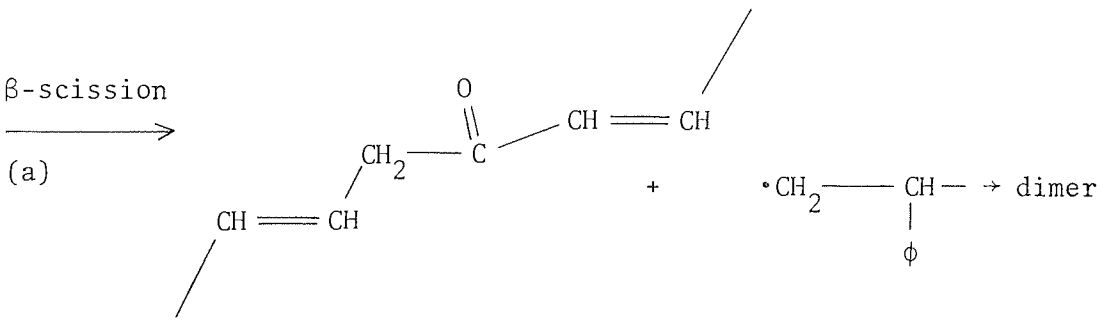

conjugated ketone (1685 cm^{-1}), (separation of polybutadiene and polystyrene chains)

β-scission

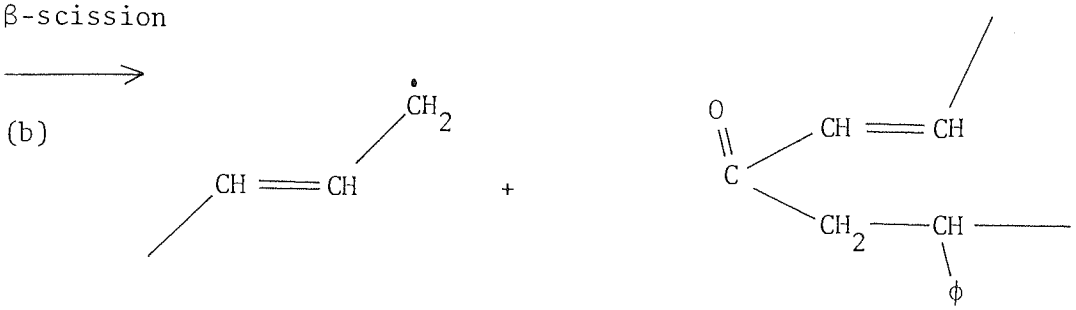

(b)

(separation of polybutadiene segment from styrene-butadiene chain)

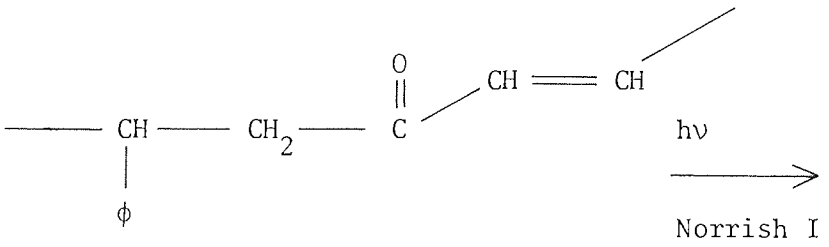

conjugated ketone (1685 cm^{-1})

alkyl and acyl radicals (separation of polystyrene and polybutadiene chains)

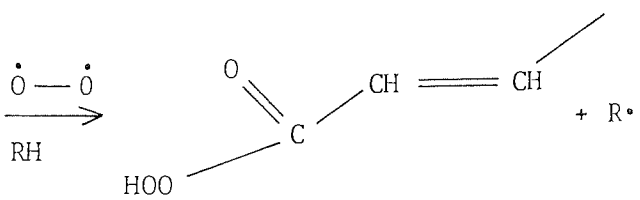

peracid

The inseparable relationship between unsaturation, namely trans-1,4-polybutadiene and allylic hydroperoxide during thermal and UV degradation has been discussed fully and the effect of relative concentration of these two entities on UV stability may now be explained. Samples of thermally oxidised polymer that contain a concentration of hydroperoxide approaching the maximum exhibit the fastest initial rate, confirming that allylic hydroperoxides are the principal initiators in photoxidation of HIPS. However, the rate of photoxidation is also a function of oxidisable substrate remaining, notably trans-1, 4-polybutadiene. Hence competition between destruction of unsaturation and build-up of allylic hydroperoxide will necessitate an optimum for maximum initial rate of photoxidation occurring just before half of the trans-1, 4-polybutadiene has been consumed. This is evident from figure 19 where the maximum initial rate corresponds to a PBD index of 1·6 (figure 21) for a film oven-aged for 20 hours containing a hydroperoxide concentration of approximately $4{\cdot}6 \times 10^{-6}$ $mol.g^{-1}$, figure 12. For processed material the maximum initial rate of photoxidation (figure 20) does actually correspond to the maximum concentration of hydroperoxide ($3{\cdot}9 \times 10^{-6}$ $mol.g^{-1}$), figure 13, although this corresponds to a PBD index of 1·4 implying that just less than half of the unsaturation has been consumed. The PBD index ranges from 2·0 to 0·55, the latter corresponding to zero concentration, figure 21. Because the depletion of unsaturation occurs prior to UV exposure the final maximum rate attained (even if greater than the initial rate) will be less than maximum rate of the control possessing nearly all its unsaturation. Similarly the total quantity of oxygen absorbed will be diminished.

The anomalous behaviour of carbonyl in figure 22 for a sample which has been thermally oxidised for 60 hours at 98°C in air (see 2.1.3.1) may be partly accounted for by the low starting concentration of hydroperoxide, approximately 1 x 10^{-6} $mol.g^{-1}$ (estimated from figure 12). This would explain the relatively slow initial rate observed in figure 22. However, this sample contains the highest concentration of ketone (index of 1·3) and the lowest concentration of trans-1,4-polybutadiene (index of 0·6, figure 21), consequently Norrish I photolysis of carbonyl will lead to an accumulation of free radicals which act as photo-initiators in the absence of unsaturation conferring an apparent induction period of 2 to 3 hours. An actual decrease in carbonyl concentration under analogous conditions has been reported by other workers[86,87]. Photo-initiation by Norrish I photolysis of carbonyl during the early stages of photoxidation is unlikely because of the very low concentration of UV absorbing chromophore, figure 25; hydroperoxide shows no induction period.

CHAPTER 3

CHEMICAL AND PHYSICAL CHANGES OCCURRING DURING THE UV DEGRADATION OF HIGH IMPACT POLYSTYRENE, CRYSTAL POLYSTYRENE AND POLYBUTADIENE

3.1 RESULTS

3.1.1 Dynamic-mechanical properties

3.1.1.1 High impact polystyrene

The low temperature dynamic-mechanical properties of HIPS containing a phenolic antioxidant are shown in figure 28. Unprocessed material was cast from toluene (see 1.2.3) and annealed for two hours at 85 - 90°C in air. Specimens (55μm) were then pressed out using a steel cutter (see 1.5.1) and subjected to a further two hours of annealing. Readings were taken from room temperature (20°C) down to -120°C. Figure 28 illustrates the changes in the low temperature damping peak (tan δ) of HIPS during UV exposure. The control sample reaches a maximum in tan δ of 0.052 at -82°C. The height of the peak is rapidly diminished during exposure to UV and after 14 hours it is almost extinct. Similarly the width of the peak increases and the apex shifts to higher temperatures during UV irradiation. Consequently the area under the damping curve is reduced. All the tan δ curves are asymmetric, tending to "lean" towards lower

Changes in low temperature damping peak (Tg) of stabilised HIPS cast film (55 μm) during photoxidation (temperature run from + 20° to - 120°C)

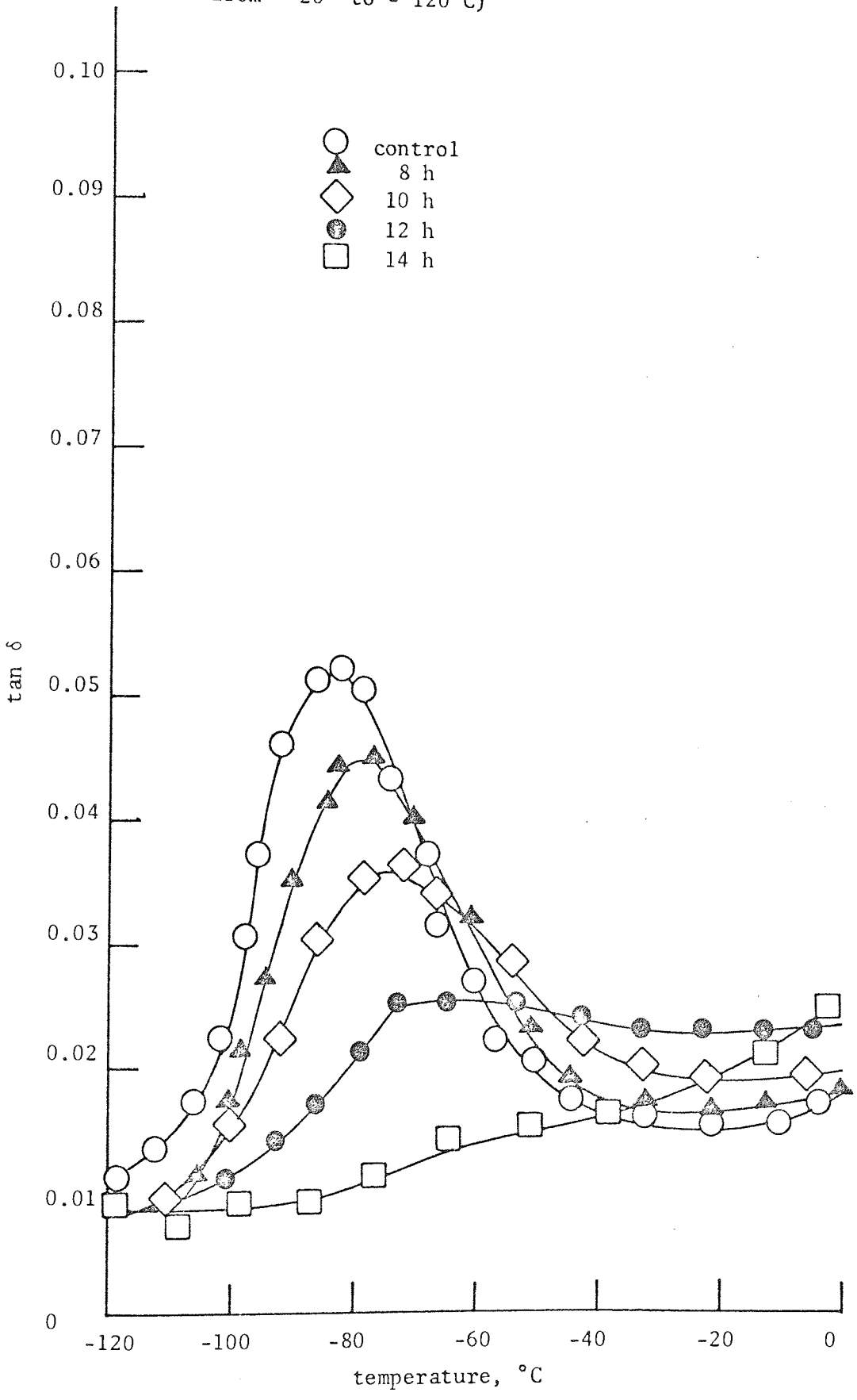

Figure 28.

Changes in low temperature damping peak (Tg) of unstabilised HIPS estruded film (50 μm) during photoxidation (temperature run from -130° to + 20°C)

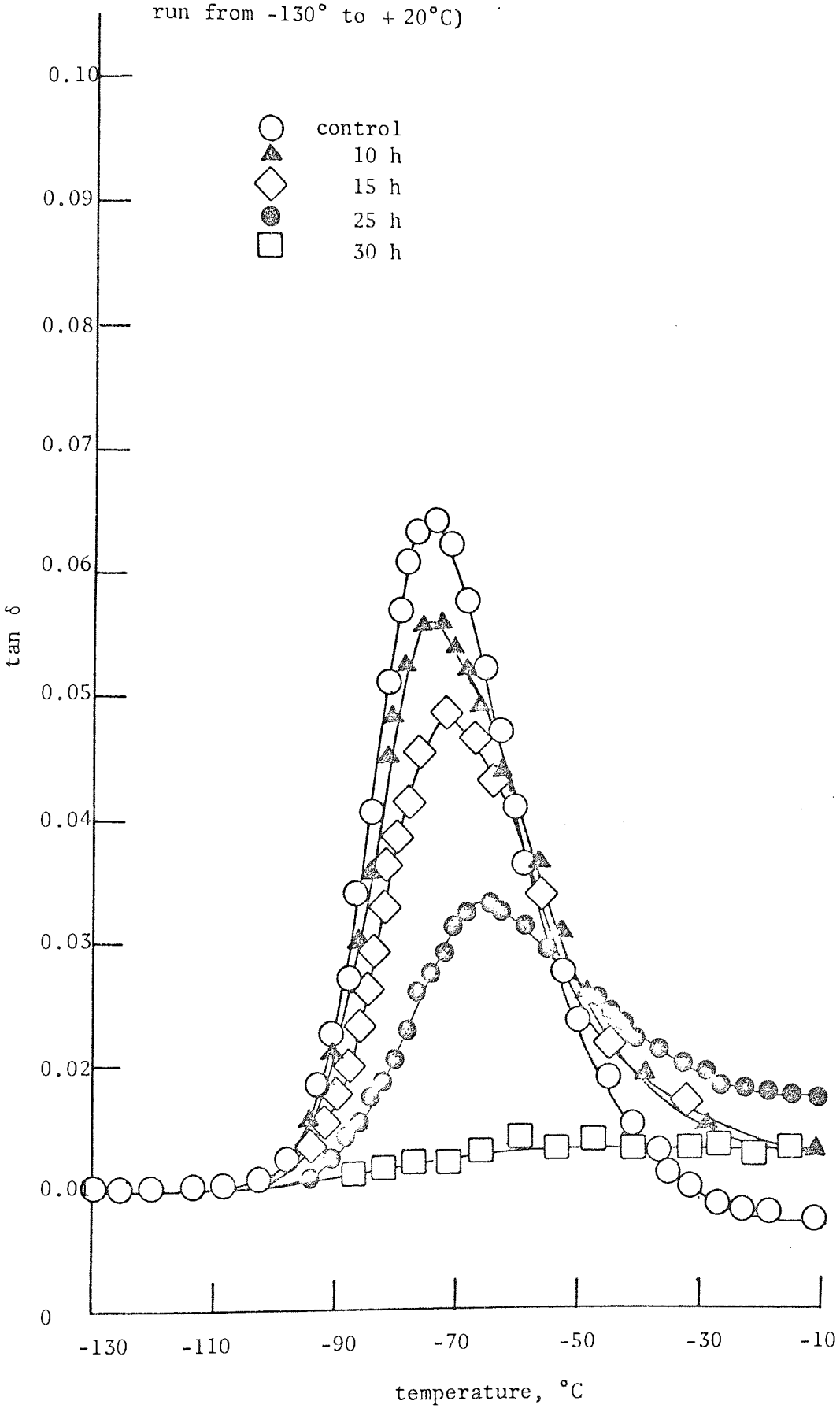

Figure 29.

temperatures. A change is also apparent in the plateau region above -40°C. During photoxidation tanδ in this region increases from 0.015 up to 0.023. However, when the destruction of the peak around -80°C is complete, tanδ at -40°C drops sharply.

Similar results were obtained using unstabilised HIPS extruded film (50 μm) (see 1.2.1.1). No additional annealing was employed on these samples, and the readings were taken on the Rheovibron from -130°C to +20°C (see 1.5.1). This procedure produced less scatter of tanδ readings as shown in figure 29. There are several notable differences between figures 28 and 29. The region between -130°C to -100°C is completely flat and is little changed by UV exposure. The control curve in figure 29 is symmetric about the peak at -75°C reaching a height of 0.064 and falls well below the base line of 0.01 as the temperature is raised to -10°C. Exposure to UV results in the same general alterations in the low temperature damping peak and up to -10°C. However, the disappearance of the peak requires considerably longer exposure to UV, up to 30 hours. The influence of the peak on the plateau region above -30°C is seen clearly as a raising and lowering of tanδ readings during the destruction of the low temperature damping peak, although the range at which this occurs is somewhat lower, figure 29.

The complex modulus of HIPS extruded film was calculated (see 1.5.2) from readings obtained during the measurement of tanδ shown in figure 29. Figure 30 shows the value of complex modulus associated with the peak height (tanδ) at the appropriate temperature, during UV

Decay of peak height (tan δ) and associated changes in complex modulus during photoxidation of unstabilised HIPS extruded film (50 μm)

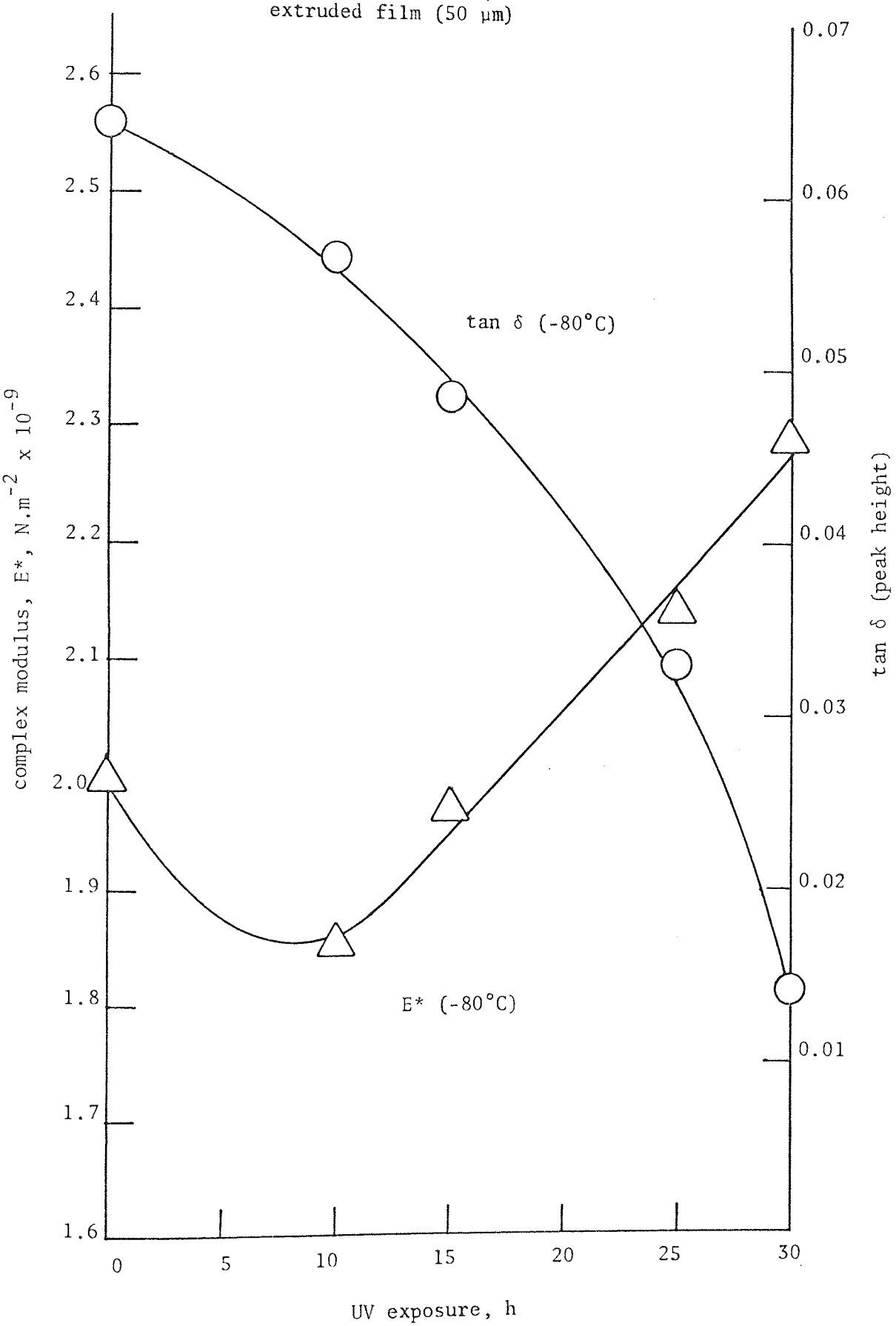

Figure 30.

exposure. The suppression of the tanδ peak described for figure 29 appears as a continuous curve of increasing slope up to 30 hours exposure to UV. However, complex modulus shows a distinctive drop after 10 hours UV exposure, after which it increases almost linearly up to 30 hours, figure 30.

To understand fully the affect of destroying the low temperature damping peak on the physical properties of HIPS, it was essential to view the whole spectrum from -130°C up to +100°C. This requires a change of the ancillary equipment of the Rheovibron (see 1.5.1) and may account for apparent discontinuity in readings. However, to obtain acceptable results the samples used for low temperature runs were employed in high temperature work. Figure 31 illustrates the complete dynamic-mechanical spectra of HIPS cast film. The asymptopic curve at 95°C for the control represents the shoulder of the main transition in HIPS, Tg of polystyrene. The far side of this peak can not be measured with the Rheovibron even after extensive UV exposure. However, the broadening of the peak (or shifting of the shoulder) is clearly visible. It will be appreciated that there are no discrete peaks growing or decaying between the two major ones at -80°C and +95°C. After the low temperature peak has been destroyed, tanδ increased linearly from -120°C up to the shoulder beginning at +50°C. Moreover, the curve representing 14 hours UV exposure attains the highest tanδ reading at 20°C; the significance of this will be seen later (figure 51). Inspection of the control curve and that representing 8 hours UV exposure between 10°C and 60°C does, however, suggest the presence of a broad peak around 30°C, although this was soon masked on further irradiation.

Changes in dynamic-mechanical spectra of stabilised HIPS cast film (55 μm) during photoxidation

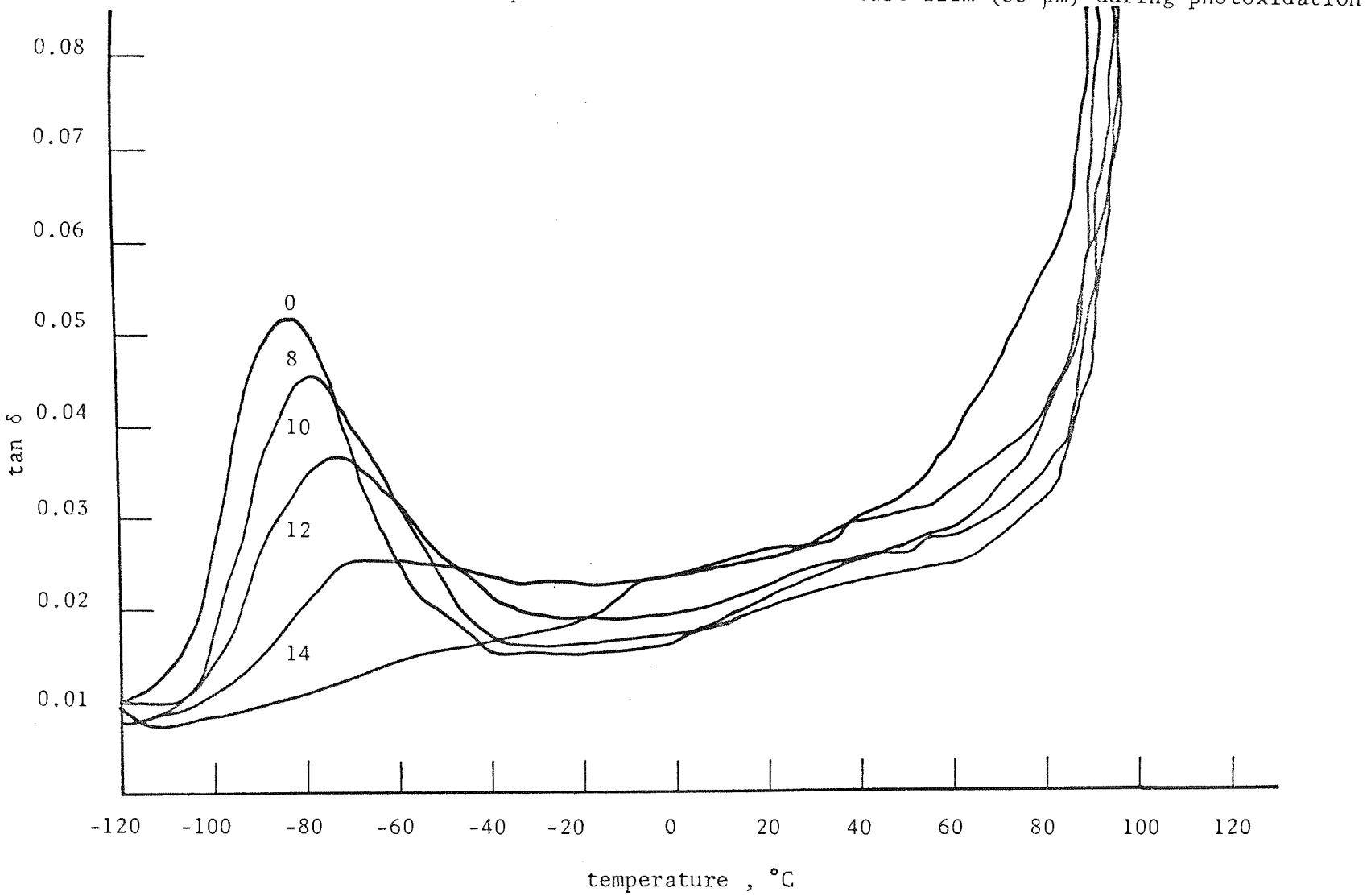

Figure 31.

Figure 32 shows the complete dynamic-mechanical spectra for HIPS extruded film. In this case different samples were used for high temperature runs. The consequences of this are seen in the lack of continuity around 20°C. However, the method of taking readings for high temperature work was identical with that used in figure 31. HIPS extruded film displays a slightly higher, asymptopic shoulder for the control at 100°C. A 5°C shift is apparent in all samples with analogous irradiation damage. Similarly the sample representing complete destruction of the low temperature peak gives the highest tanδ value at 20°C.

The complex moduli calculated from results obtained during the reading of tanδ from the Rheovibron (figure 32) for HIPS extruded film are shown in figure 33. The overall effect of raising the temperature from -130°C to +100°C is to alter the physical properties of the HIPS resulting in a substantial fall in complex modulus culminating at 100°C. A small dip in complex modulus may be seen around 70°C in the control sample and the sample exposed to UV for 30 hours.

To account for the differences described earlier between figures 28 and 29 a series of low temperature runs were performed on pertinent samples. Figure 34 demonstrates the effect of direction of temperature run on peak height and position, on cast film. For readings taken from +20°C down to -120°C a tanδ peak of 0.052 at -83°C was observed. However, when the sample was first frozen and readings taken from -120°C up to +20°C a larger peak height of 0.062 occurred at a higher temperature of -76.5°C. A 5 - 6°C shift is apparent

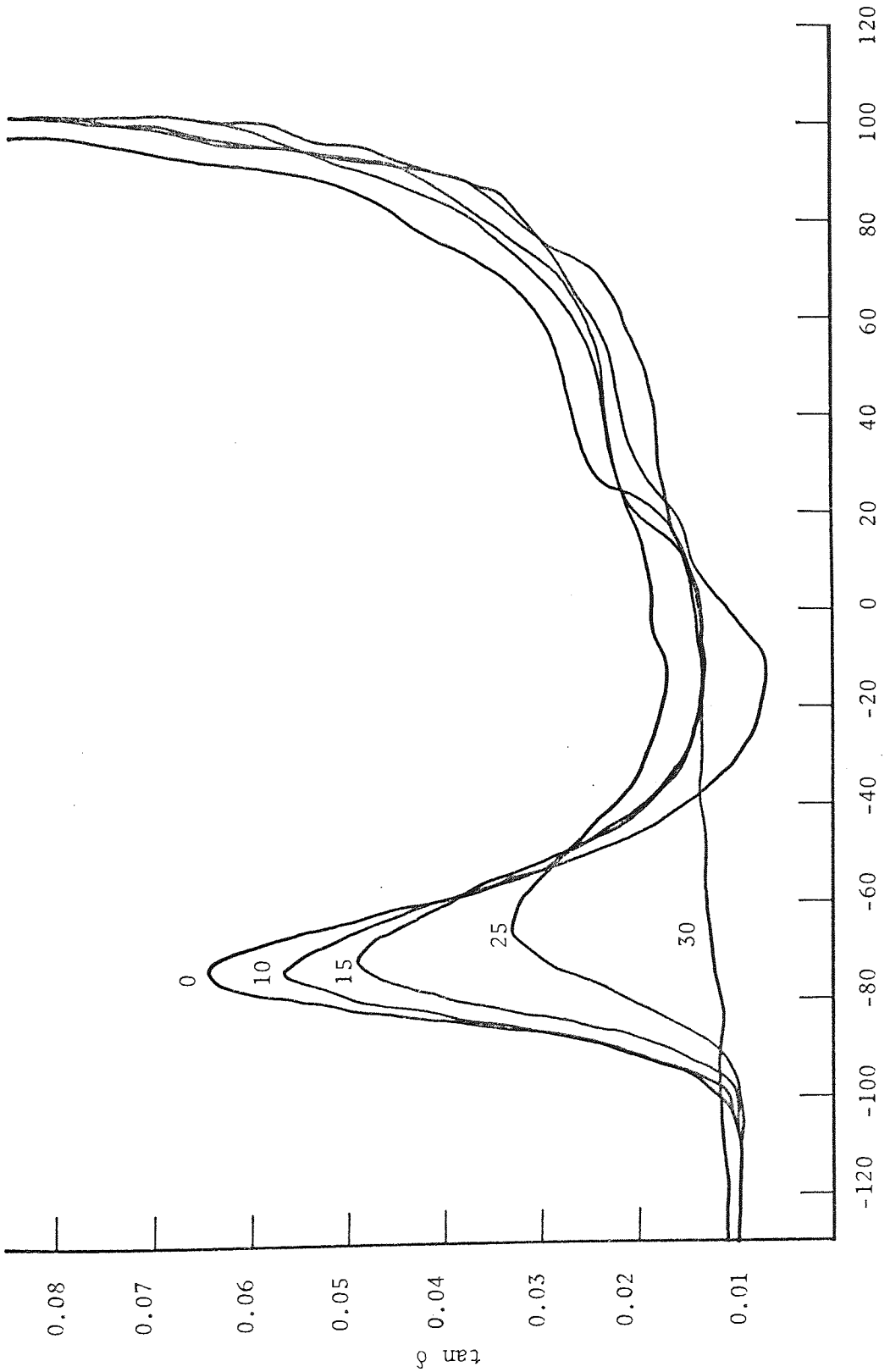

Changes in dynamic-mechanical spectra (tan δ) of stabilised HIPS extruded film (50 μm)during photoxidation.

Figure 32.

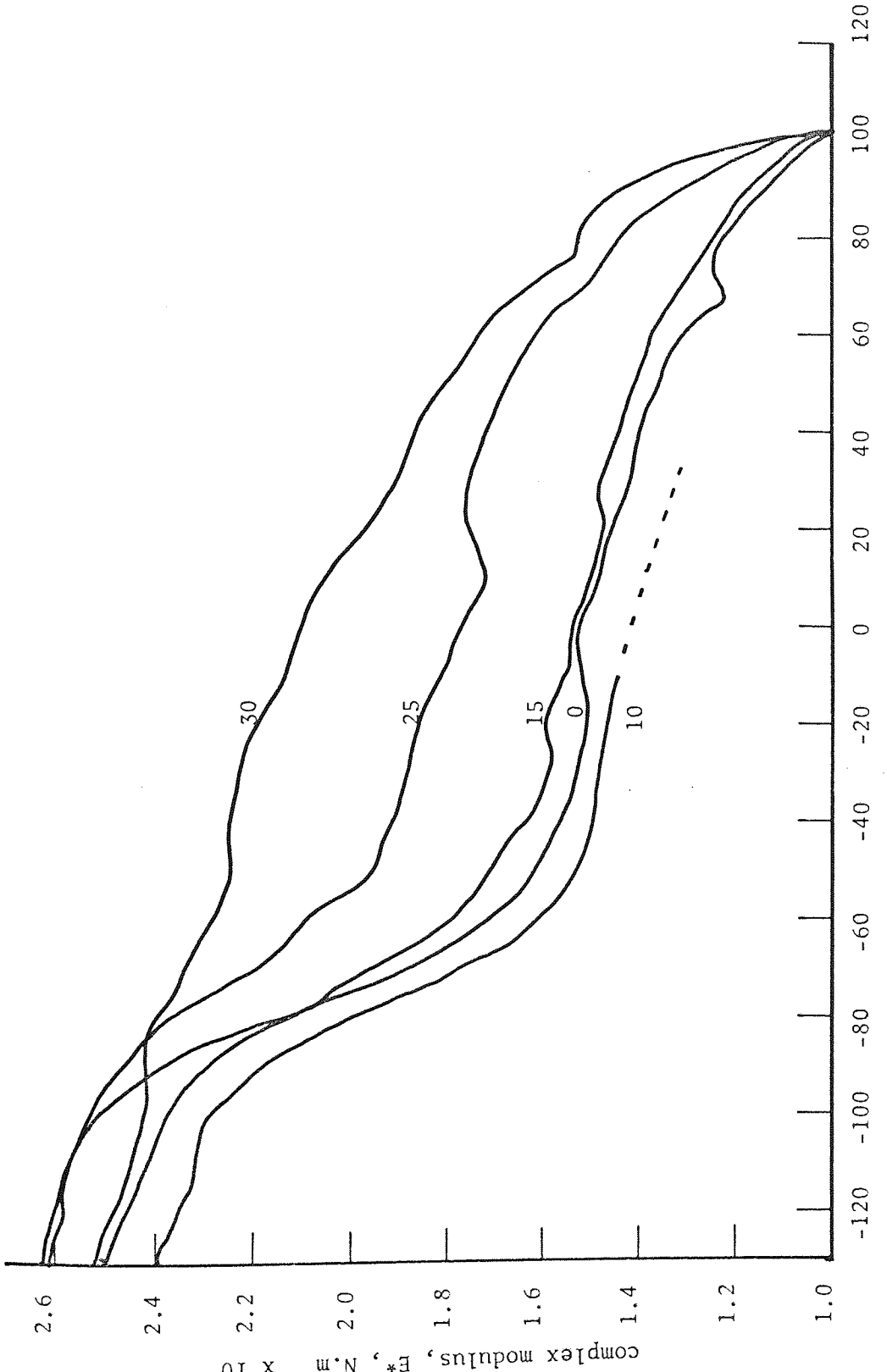
Changes in dynamic-mechanical spectra (E*) of stabilised HIPS extruded film (50 μm) during photoxidation
complex modulus, E*, N.m^{-2} x 10^{-9}
2.6
2.4
2.2
2.0
1.8
1.6
1.4
1.2
1.0
-120
-100
-80
-60
-40
-20
0
20
40
60
80
100
120
temperature, °C
30
25
15
0
10

Figure 33.

Effect of experimental technique on position and height of damping peak of unirradiated, stabilised HIPS cast film (55 μm),(temperature run from (a) + 20° to -120°C, (b) - 120° to + 20°C)

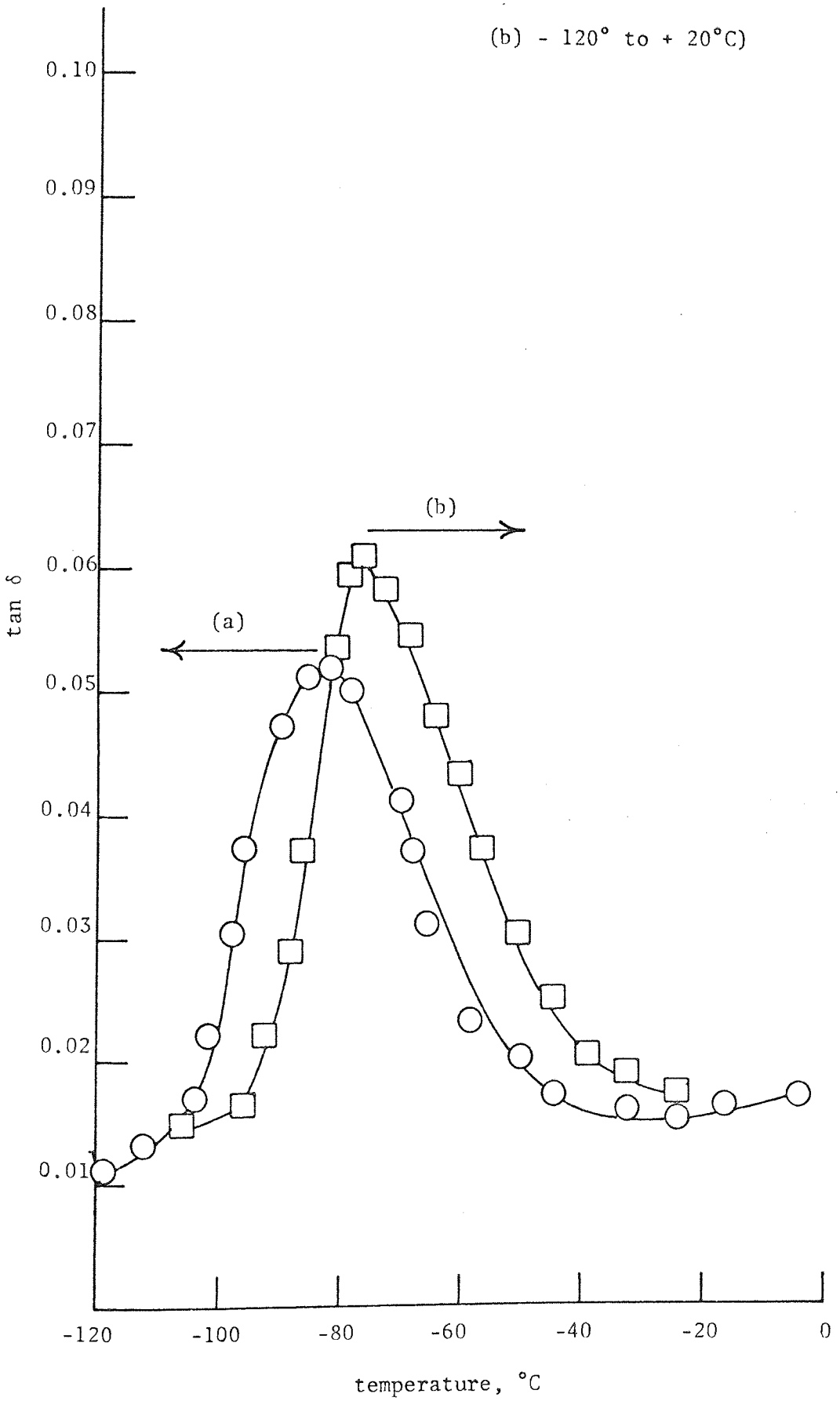

Figure 34.

Effect of experimental technique on height of the damping peak of unirradiated unstabilised HIPS extruded film (50 μm),(direction of orientation (a) transverse

(b) longitudinal

(temperature run from -130° to + 20°C)

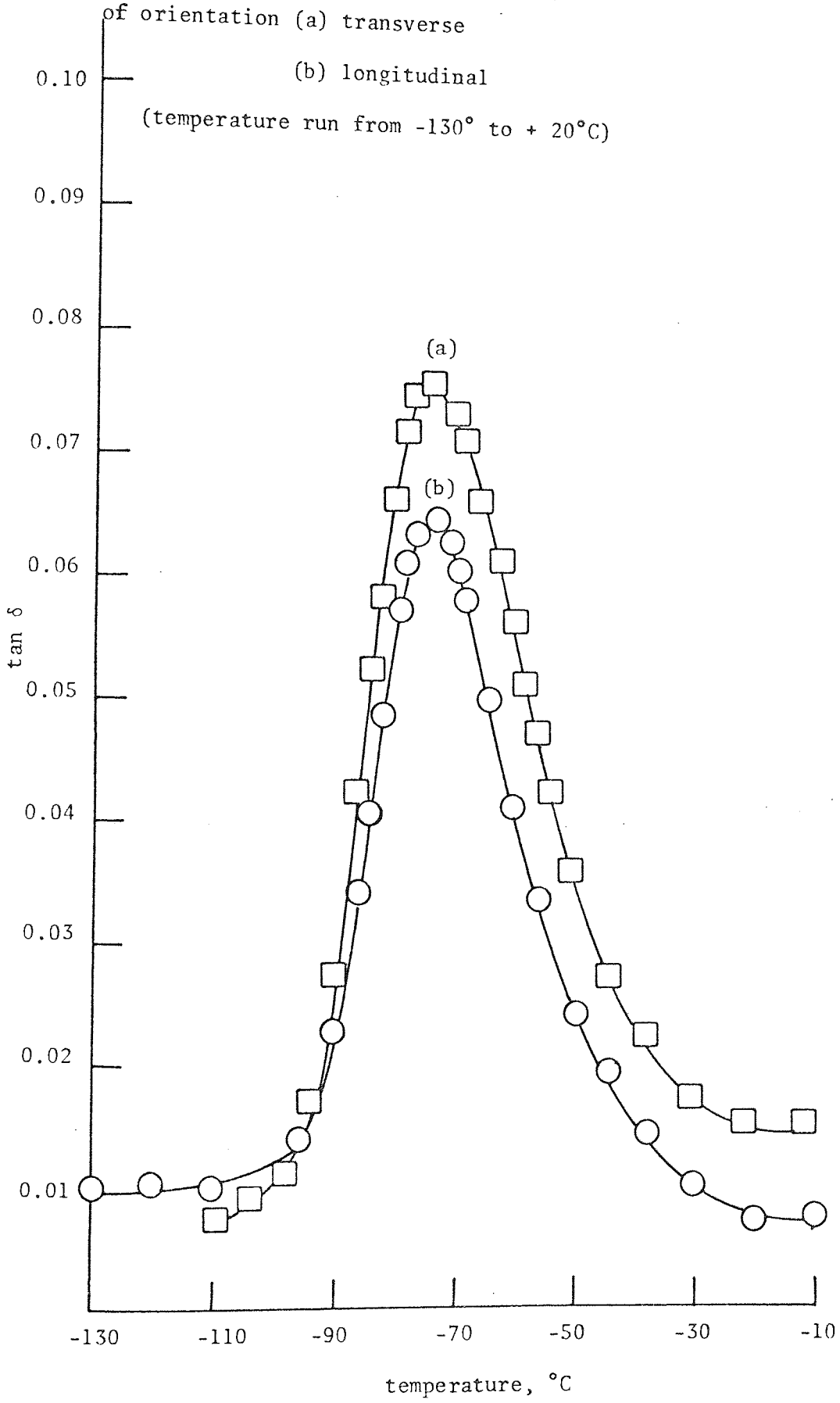

Figure 35

throughout the temperature range. Furthermore, the symmetry difference noted earlier was also a manifestation of experimental technique. The peak height of 0.062 for cast film was still less than that obtained for extruded film (0.064) measured under identical conditions. Also the peak occurred at a slightly lower temperature of -76.5°C and -75°C for cast and extruded film respectively. The peak height increased further in the case of a sample of extruded film made by cutting a specimen transverse to the direction of extrusion, figure 35. A tanδ of 0.074 is thus obtained, although the position of the apex occurs at the same temperature. Tanδ readings do not return to that obtained for the control sample cut in the longitudinal direction of extrusion but remain higher by an equivalent amount up to -10°C.

3.1.1.2 Polybutadiene

The dynamic-mechanical properties namely tanδ and complex modulus are shown for polybutadiene film, 450 μm, (see 1.2.2) over a temperature range of -120°C to +10°C in figures 36 and 37 respectively. Tanδ (figure 36) starts at approximately 0.02 for the control curve at -120°C and rises rapidly as the temperature is raised reaching a maximum of 1.66 at -83°C. Above this temperature the complex modulus (figure 37) approached zero, reaching the practical and indeed theoretical limitations of the Rheovibron, consequently no more readings were possible. However, during 55 hours exposure to UV, tanδ readings decreased and the shoulder shifted to higher temperatures. After 100 hours UV exposure the complete peak fell within the limitations of the Rheovibron, giving a maximum of about 0.2 at -82°C, and dropped to below 0.1 at -10°C, after which the complex modulus similarly

Development of a damping peak in compression moulded PBD film (450 μm) on photoxidation (temperature run from -120° to + 10°C)

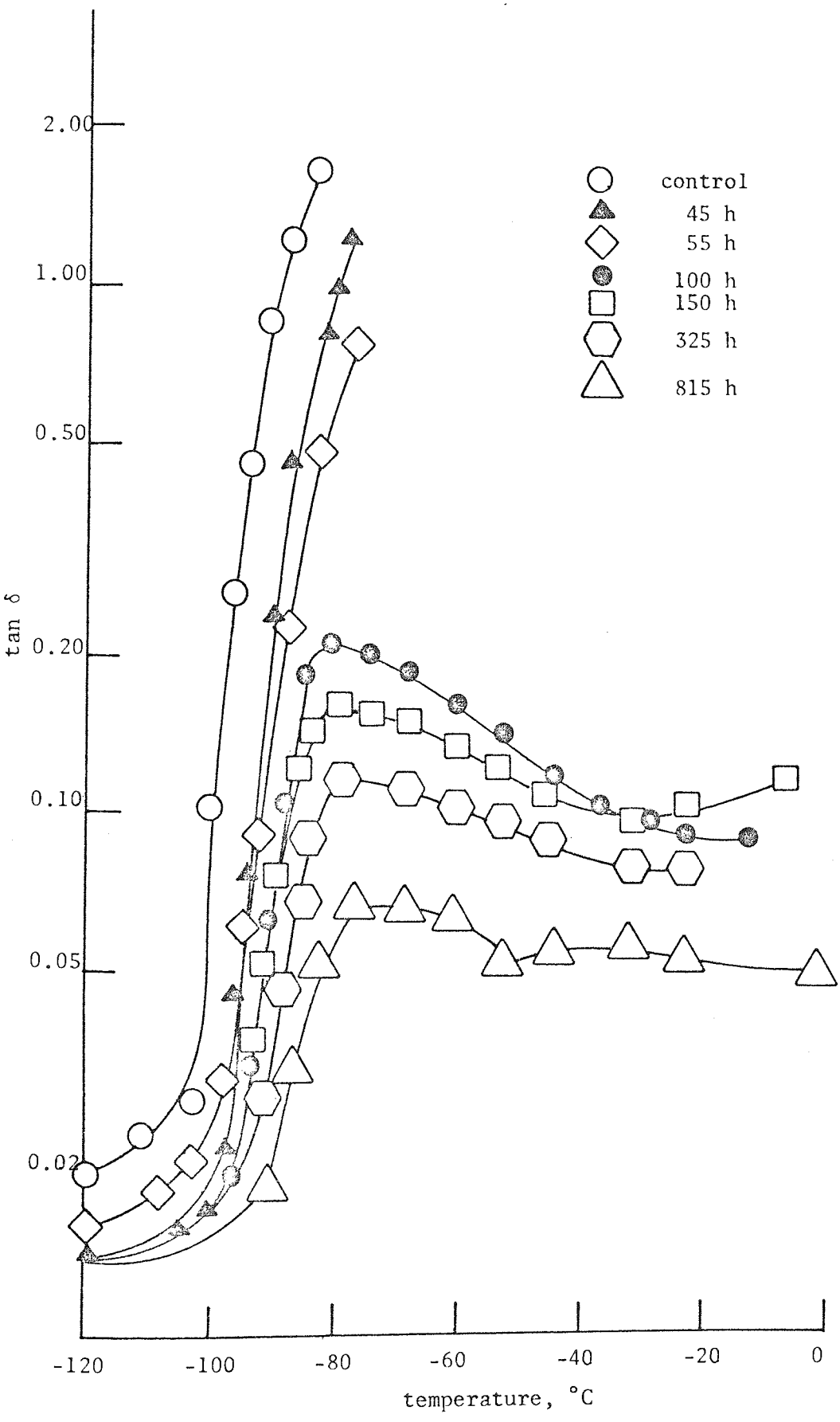

Figure 36.

approached zero and no further readings were possible. It is not apparent from figure 36, possibly because of the distorting effect of a logarithm-linear scale, that the decrease in tanδ from 55 hours to 100 hours UV exposure is very rapid. Many unsuccessful attempts were made to obtain an intermediate curve, even though 45 hours separate the two. With extensive UV irradiation the general behaviour is similar to HIPS (figure 29) the peak became depressed and shifted to higher temperatures up to -75°C after 815 hours of exposure to UV. The tanδ curves also become broader. Similarly around -10°C the phenomena of tanδ increasing then decreasing with longer periods of irradiation was apparent. The damping curve never became completely suppressed even after 815 hours of UV exposure whereas for HIPS 30 hours only were required for complete destruction of the low temperature peak (figure 29).

The values of all complex moduli curves for polybutadiene (figure 37) are less than those for HIPS, figure 30. However, the complex modulus increases with exposure to UV apart from an initial slight decrease below that of the control. The rapid drop for samples UV exposed up to 55 hours is superceded by a more gradual decline as the damping peak becomes measurable at higher temperatures (figure 36). The complex modulus continues to increase with UV irradiation time, extending further the limiting value of modulus to higher temperatures. Not all readings are displayed in figure 37 for lower temperatures owing to their coincident nature.

Changes in complex moduli of compression moulded PBD film (450 μm) during photoxidation (temperature run from - 120° to + 10°C)

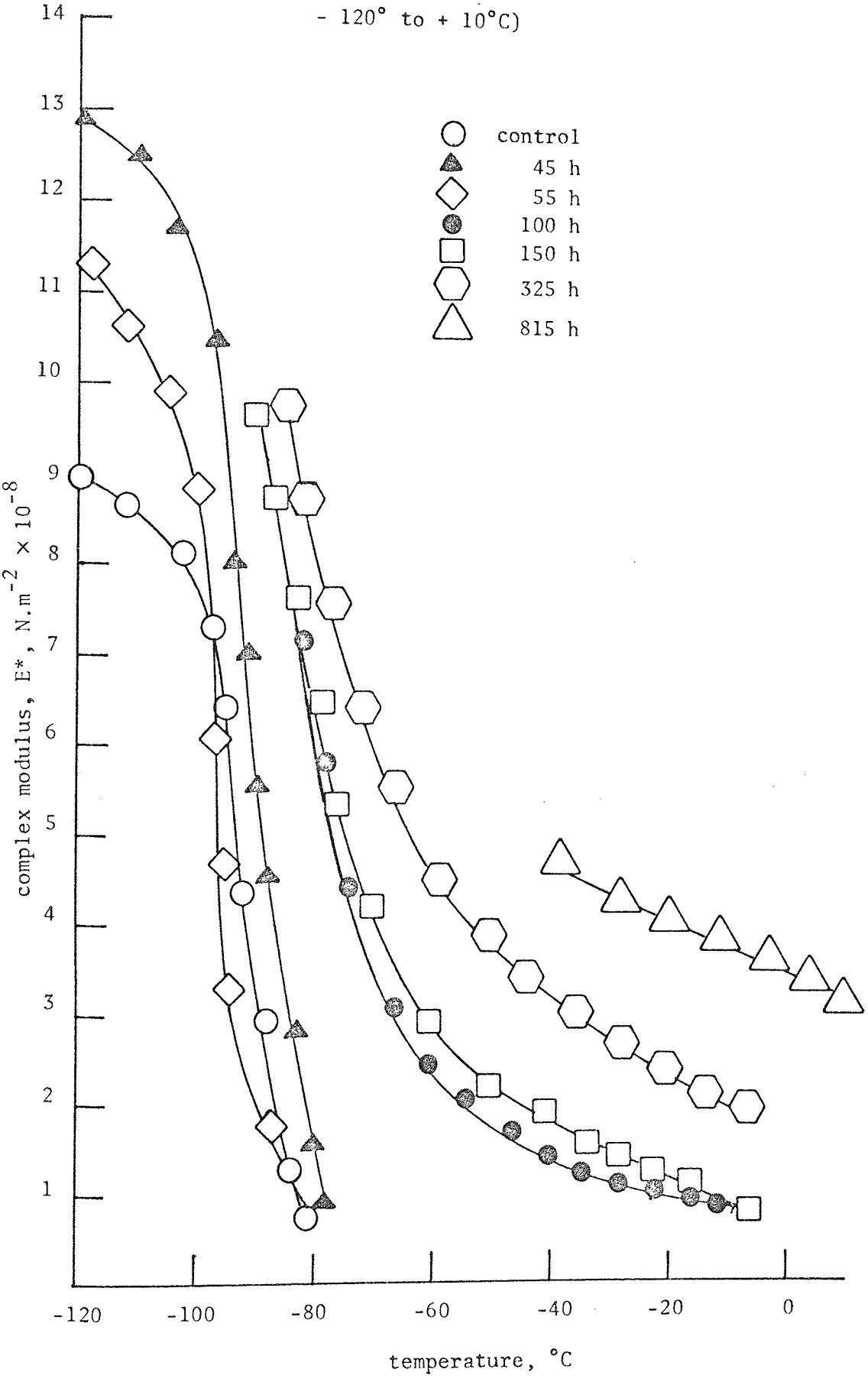

Figure 37.

3.1.1.3 Crystal polystyrene

The complete dynamic-mechanical spectra of "crystal" polystyrene extruded film (55 μm) are shown in figure 38. Readings were taken from -130°C up to +120°C. The behaviour of tanδ for "crystal" polystyrene during UV exposure is in complete contrast to that seen earlier for HIPS extruded film, figure 32. A small discrete damping peak is visible for unexposed "crystal" polystyrene at -85°C. This peak has a maximum of 0.011 which is considerably lower than that encountered for HIPS unexposed extruded film (0.064), figure 32. However, the base line for "crystal" polystyrene lies around 0.004 compared to 0.01 for HIPS. Crystal polystyrene is brittle even when unirradiated and thus prone to fracture during temperature runs. Consequently no further readings were obtained above -10°C for a control sample and -17°C for a UV exposed specimen having an extremely brittle nature. After the low temperature peak has been surmounted, tanδ rises in a similar manner to HIPS as the temperature is increased. However, the asympropic shoulder is inclined towards 110°C, although the final part of the tanδ range is not shown in figure 38. The effect of UV exposure on "crystal" polystyrene is to increase the peak height from 0.011 to 0.022 and to shift the apex by 5°C to -80°C. The peak also becomes broader and consequently the area increases. Tanδ is generally increased by at least 0.004 for the sample irradiated for 300 hours over the entire temperature range. Complex modulus of "crystal" polystyrene bears a similarity to HIPS, figure 33, although the control sample at -130°C has a value of 2.9×10^9 $N.m^{-2}$ compared to 2.6×10^9 $N.m^{-2}$ for HIPS. After 300 hours exposure to UV the complex modulus drops by about 0.5×10^9 $N.m^{-2}$ to approximately

Changes in dynamic-mechanical spectra (E*,tan δ) of "crystal" PS extruded film (50 μm) during photoxidation (temperature run from - 130° to + 120°C)

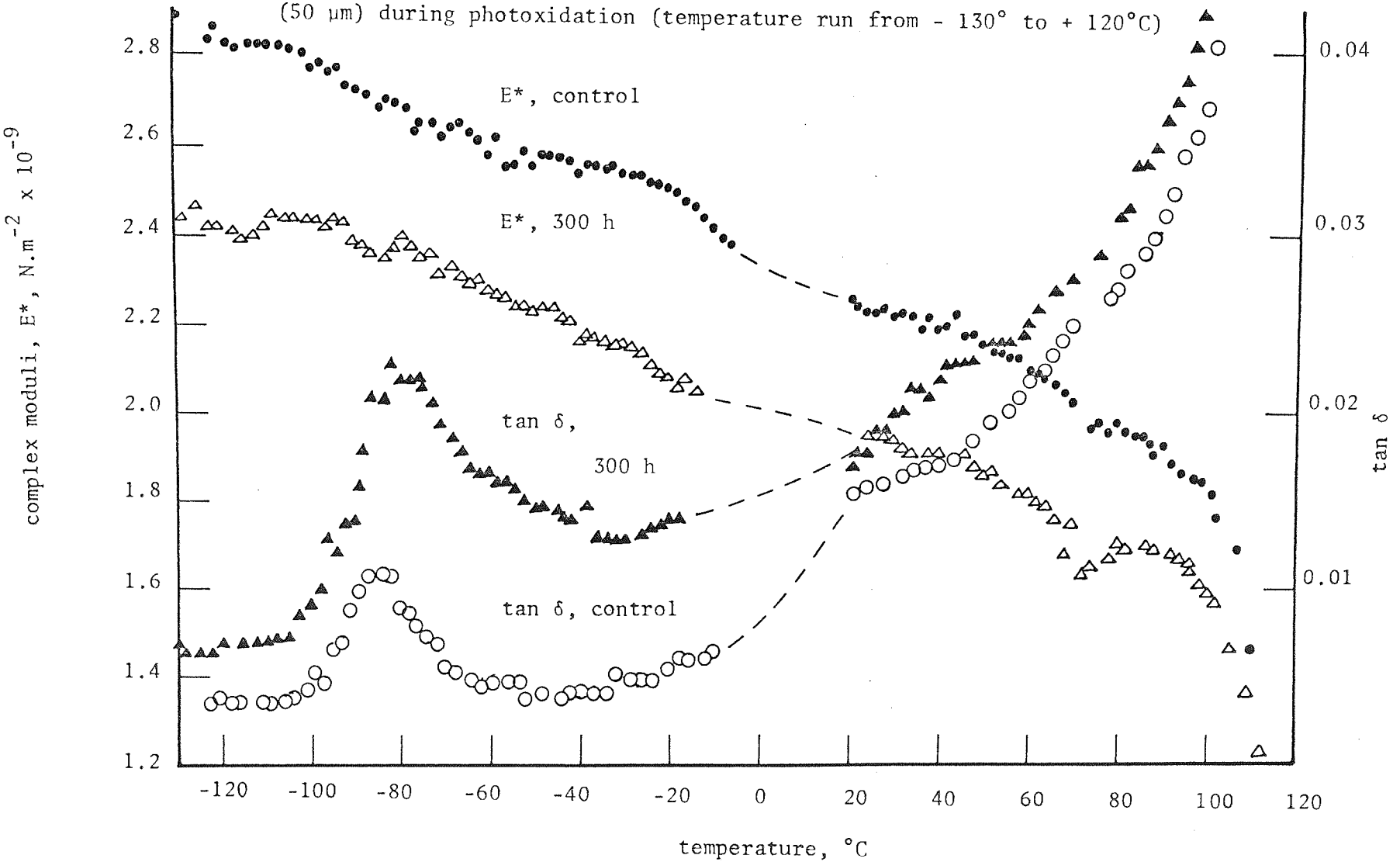

Figure 38.

2.5×10^9 $N.m^{-2}$ at -130°C, corresponding to 30 hours UV exposure for HIPS. The two complex moduli curves in figure 38 are almost parallel up to +110°C where they become coincident. No deflection around -80°C is apparent, within the accuracy of the Rheovibron, for either complex modulus curve and thus show a similar linear profile to a HIPS sample exposed for 30 hours. It must be appreciated that the larger low temperature peak shown in figure 38 for irradiated "crystal" polystyrene is still less than half that of the smallest displayed in figure 32 for HIPS film exposed to UV for 25 hours. Consequently, little response in complex modulus is to be expected. A small dip is, however, visible around 70°C for the UV exposed sample; this being observed for HIPS, figure 33.

3.1.2 Microscopy

Both stabilised and unstabilised HIPS have been examined by optical and electron microscopy. The effect of processing, UV ageing and solution casting from different solvents, on the detailed morphology of HIPS has been studied by a selection of pertinent experiments. Also UV degraded HIPS film was re-cast and examined by electron microscopy.

Plate one is a typical optical micrograph, phase contrast (see 1.7.2) of HIPS containing antioxidant (see 1.1). In this case the sample was processed in the closed chamber of the torque rheometer at 170°C for 10 minutes with a full charge of 35 g (see 1.2.1.2). The material was then pressed at 170°C and a film cast from toluene (see 1.2.3). The size and distribution of spherical particles is seen

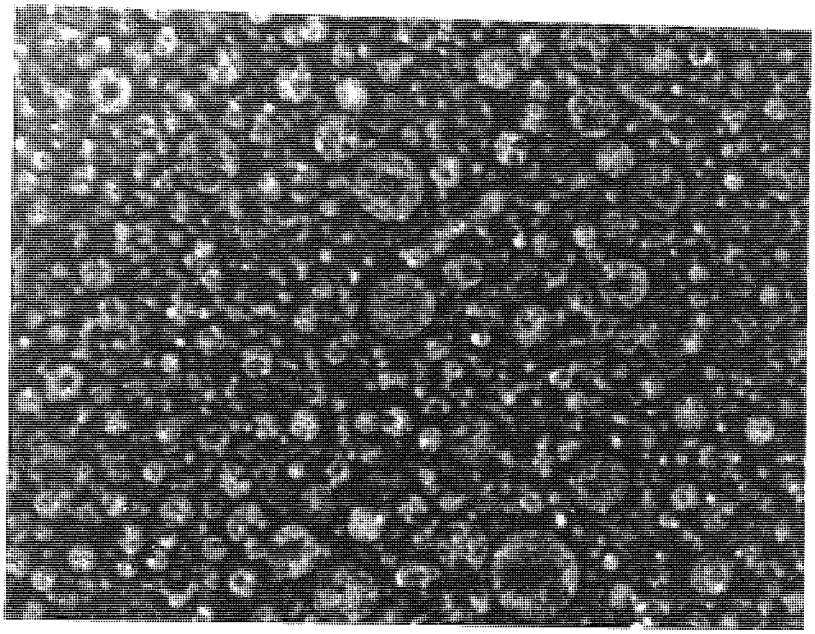

Plate one

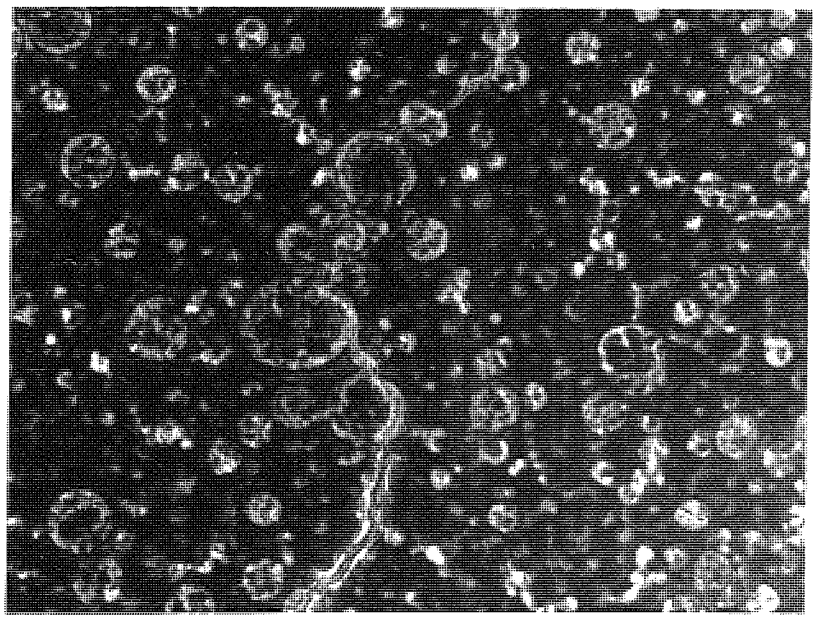

Plate two

clearly in plate one. The largest particles are approximately 5 μm in diameter, although these were not very numerous. No distortion of these particles was apparent.

Plate two is a phase contrast micrograph at identical magnification of a similar sample which has been exposed to UV for 70 hours and is thus rendered completely brittle. The contrast between the background (matrix) and the particles was more pronounced after UV irradiation. Inspection of the large particles in plate two reveals a continuous crack about 30 μm long and 0.2 - 0.5 μm wide joining these particles. The crack propagates through the matrix and along the inside of the particles at the interface[88]. Only a few cracks were visible even though the film was completely brittle.

Optical microscopy is ideal for examining the larger cracks and distribution of particles but it does not offer a viable means of viewing the detail morphology. In plate three the cellular structure of the particles is clearly distinguishable by electron microscopy (see 1.7.1). Plate three represents HIPS containing a phenolic antioxidant processed under the same conditions as described above but the solution casting stage was omitted. The microtomed sections are considerably thinner (0.06 μm) than samples used for optical microscopy. Consequently the remaining 6% of the spherical particle may be distorted by microtoming. A slight elongation is apparent transverse to the direction of microtoming; this being consistent in all micrographs. The omission of solution casting appears to have no marked effect on the cellular structure of the particles seen in plate three, although

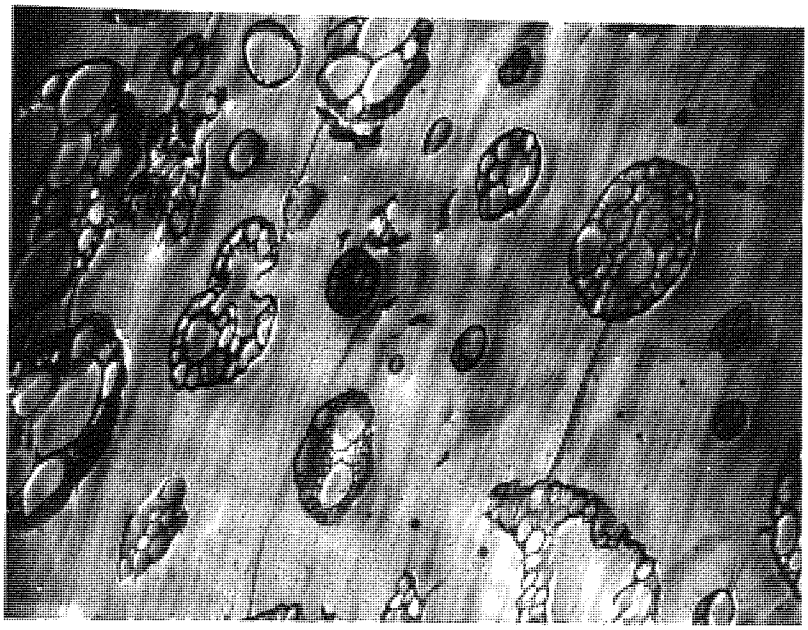

Plate three

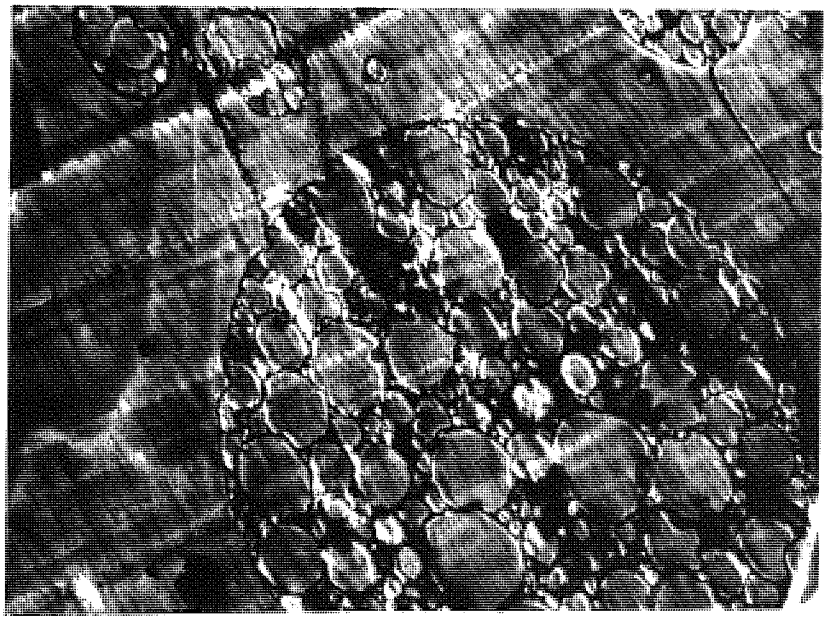

Plate four

a few broken fragments are present between larger structures. The cellular nature of the particles remains intact when the processing stage is omitted.

Plate four shows an EM of stabilised HIPS which has had no thermal processing whatsoever; the film being prepared by solution casting from toluene. The magnification was identical to plate three; the large well-preserved particle seen in plate four was atypical. This sample had been exposed to UV for 21 hours under ambient conditions and was partially brittle. No significant changes are visible in the area surrounding the particles. The parallel score marks running diagonally across plate four are caused by microscopic aberrations in the cutting edge of the glass microtome knife. The faint light lines randomly dispersed throughout the matrix arise from folding of the section on the grid. The lighter areas are caused by "etching" with the electron beam which volatilises the polymer. Small dark globules are sometimes seen, these are droplets of oil under high vacuum.

Plate five is a similar sample exposed to UV for 90 hours, by which time the film is completely brittle. The basic cellular structure of the particle remains intact, however, craze formation is clearly visible in the centre of plate five. These crazes propagate in a helixical manner through the matrix from the interfacial region of the particle and eventually join up neighbouring particles. This last observation is consistent with the larger crack described in plate two. No evidence was found for craze propagation through the internal interfacial regions of the particles.

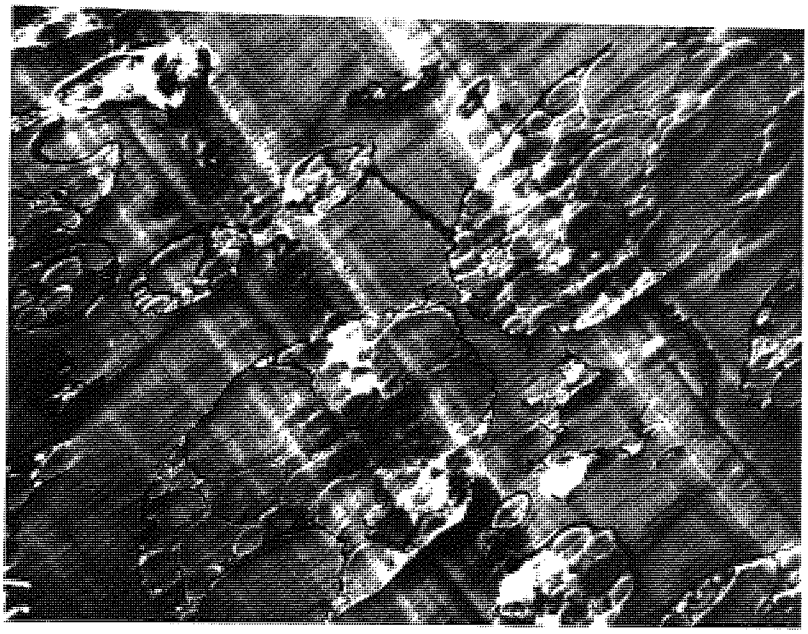

Plate five

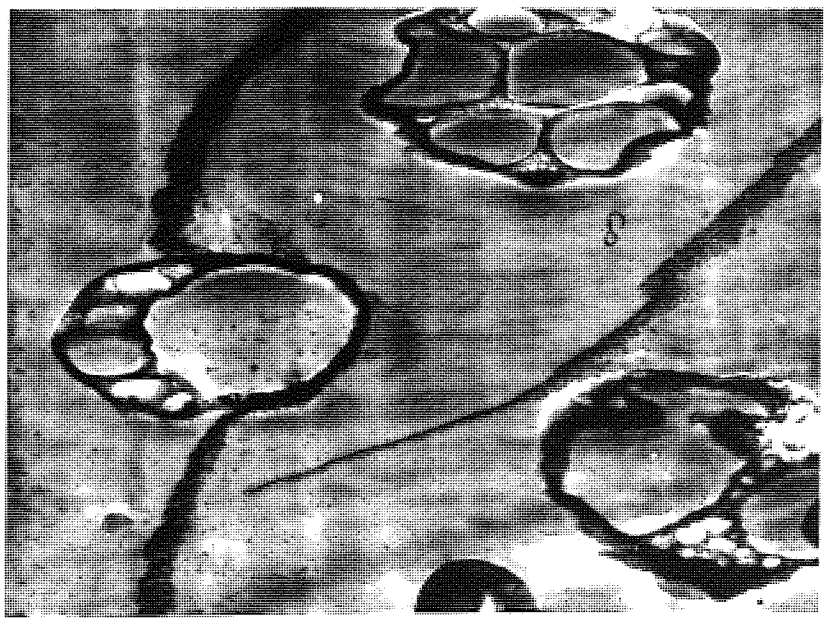

Plate six

Plate six shows a similar sample of stabilised HIPS cast from toluene and UV irradiated for 90 hours. The magnification is twice that for all other electron micrographs. The random direction of the craze is similarly observed, although the helixical propagation is not apparent here. The interfacial interaction may be interpreted as craze propagation through the boundary material of the particle. On close inspection of the craze it is possible to detect a fine grain structure. This is probably crystalline deposits of staining agent, osmium tetroxide, (see 1.7.1) in the crazes rather than chemical fixation.

Platesseven to ten are all electron micrographs of HIPS containing no antioxidant. HIPS was extruded (see 1.2.1.1) before casting into films. Plate seven illustrates HIPS cast from dichloromethane. It is clear that the same cellular structure of particles is present when either aromatic or chlorinated solvents are used. The faint craze lines visible are all transverse to the direction of microtoming and parallel with the long axis of the particles.

A similar sample was UV irradiated for approximately 70 hours thus rendering it brittle and then re-cast from a solution of dichloromethane. Plate eight is an EM of the microtomed, re-cast films after staining. Several striking features are apparent, notably, the contrast has greatly increased, indicating the ease of penetration of the osmium tetroxide into the particles. They display a disorientated and detached nature and appear to have collapsed or contracted. There also appears to be an increase in the number of broken fragments.

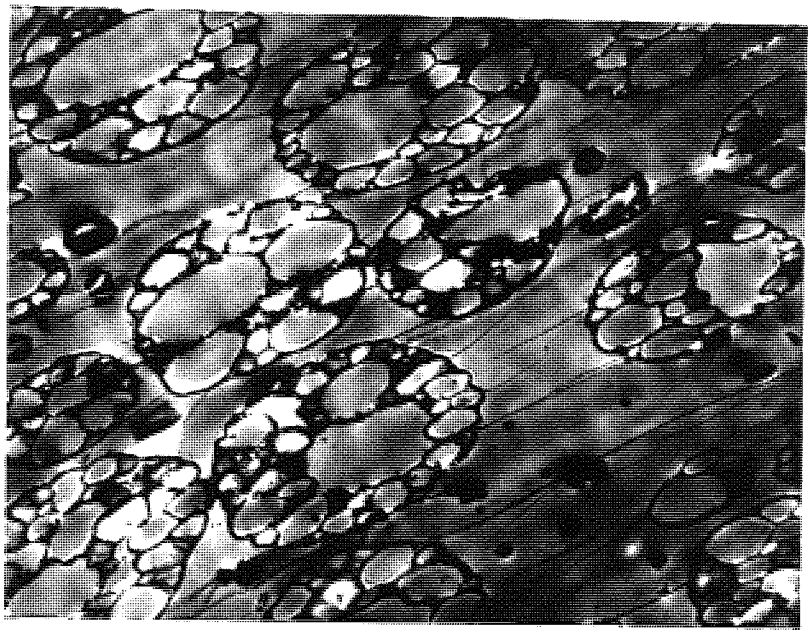

Plate seven

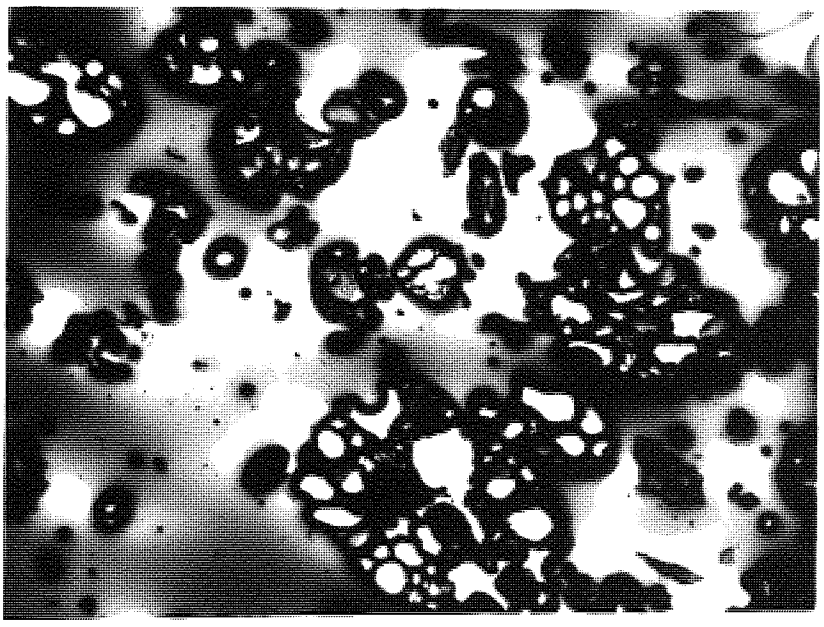

Plate eight

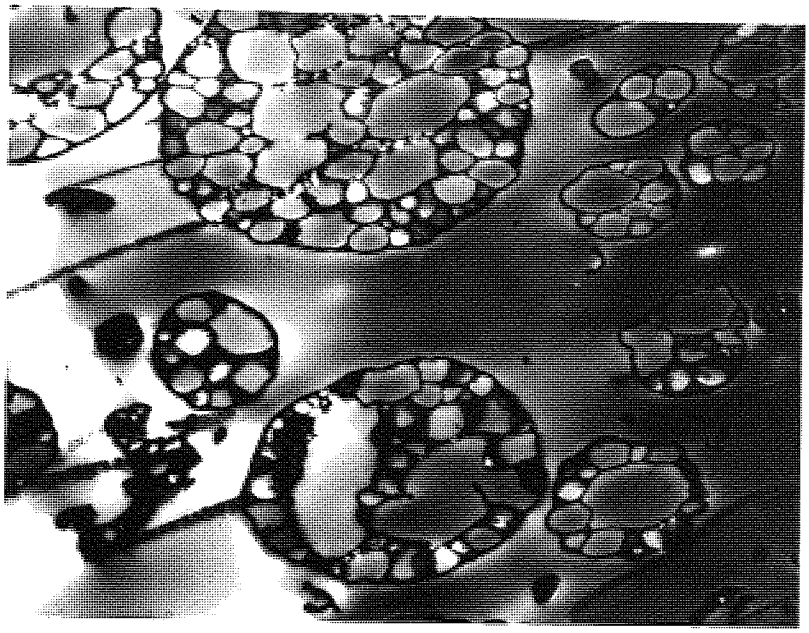

Plate nine

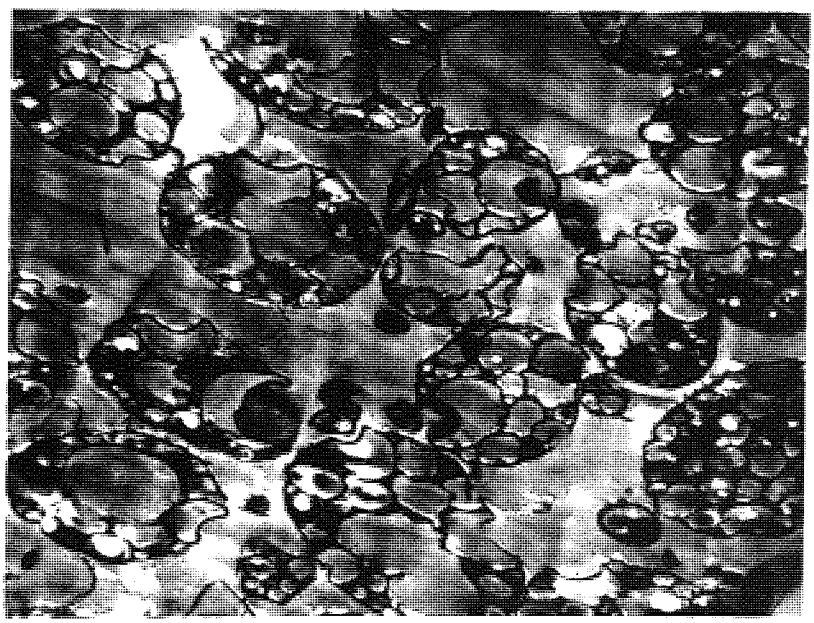

Plate ten

Plate nine represents an electron micrograph of the same unstabilised HIPS extruded film, but solution cast from toluene. The detailed structure and craze lines produced by microtoming resemble those described for HIPS cast from dichloromethane, plate seven. The clarity of plate nine is due to the extremely thin section produced by microtoming of this sample.

Part of this film was UV exposed and re-cast from toluene, under identical conditions to those used for the analogous experiment using dichloromethane. Similarly, the particles, although better defined have a disorientated and detached appearance. The internal cellular structure shows signs of breaking down.

3.1.3 I.R. spectroscopy

3.1.3.1 High impact polystyrene

The absorbance of photoxidation products of HIPS extruded film (50 μm) containing no antioxidant was measured by IR spectroscopy utilising the technique of difference spectroscopy (see 1.6.2). Spectra were taken every 2 hours exposure to UV. No absorbance was detected until 6 hours of UV exposure, figure 39. Afterwards a rapid increase in absorbance of two broad peaks centred at 3400 cm^{-1} and 1700 cm^{-1} were observed. The peak at 3450-3400 cm^{-1} has been assigned to inter-hydrogen bonded allylic alcohol[89]. The carbonyl region of 1700 cm^{-1} is considered to consist of a complement of different peaks of varying intensity and extinction coefficient. The apex of this broad band has two main peaks (1725 - 1700 cm^{-1} and 1725 - 1705 cm^{-1}) which have been attributed to saturated carboxylic

Development of functional groups in unstabilised HIPS extruded film (50 μm) on photoxidation (compensated IR spectra obtained in 1% w/v CH_2Cl_2 solution)

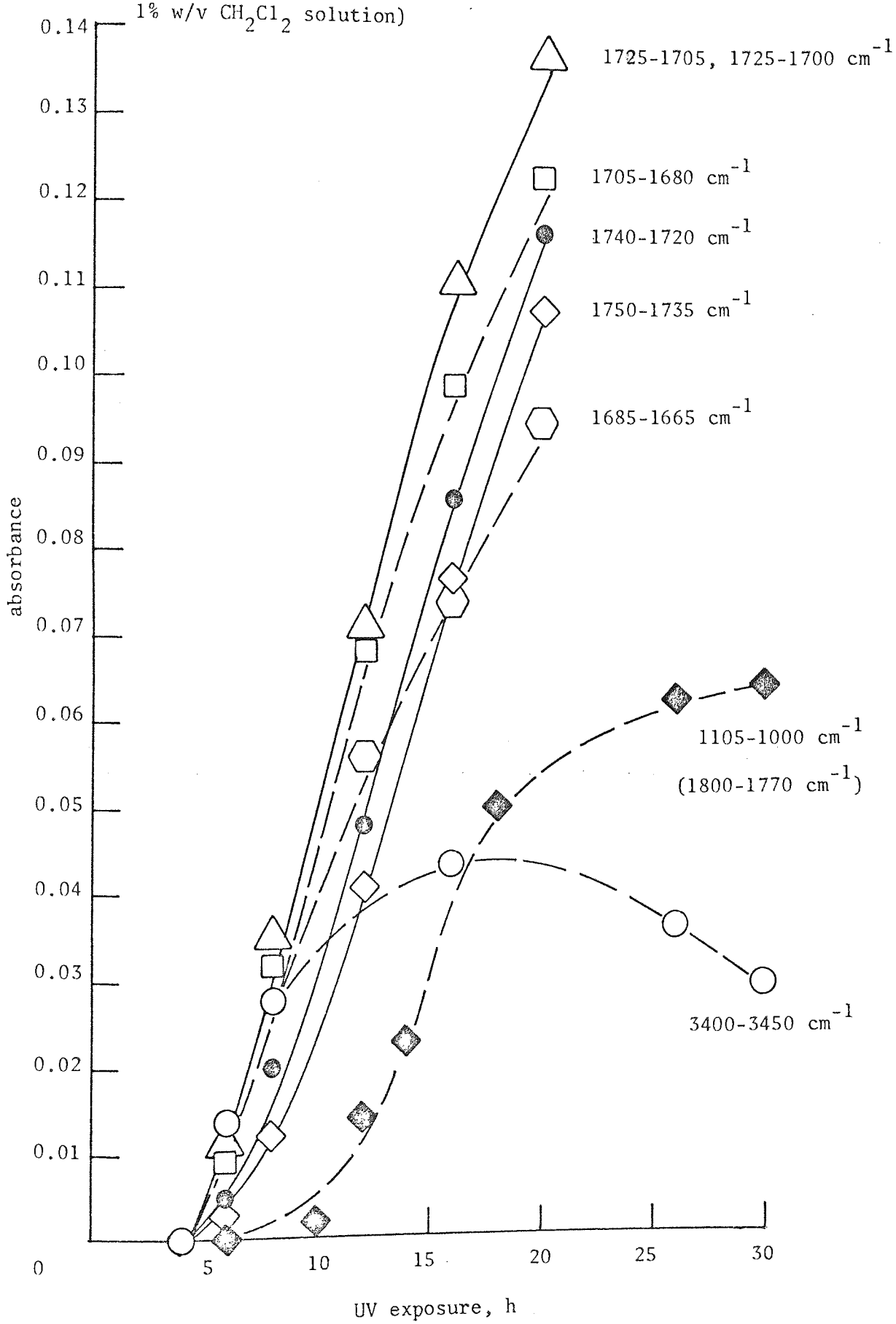

Figure 39.

acids and ketones[89]. In figure 39 these peaks may be seen to grow at the fastest rate in an auto-accelerating manner attaining linear kinetics after an induction period of 5 hours, found by extrapolation to the abscissa. The concentration of α,β-unsaturated aldehyde (1705 - 1690 cm^{-1}) increases at the same rate as for saturated acids and ketones, conferring the same induction period. However, it appears to deviate from the parent curve after 10 hours of exposure to UV resulting in an earlier retardation. Similarly, α,β-unsaturated ketone (1685 - 1665 cm^{-1}) initially follows the parent curve for saturated ketone, but after 10 hours of UV exposure falls off faster than α,β-unsaturated aldehyde. Allylic alcohol (3450 - 3400 cm^{-1}) also increases rapidly following the same curve as for ketone up to 10 hours exposure to UV even though the peaks are not in close proximity. After 10 hours UV exposure the concentration of allylic alcohol increases at a much slower rate than that of α,β-unsaturated ketone, reaching a maximum after 17 hours and possibly decreasing slightly with further UV irradiation. Both saturated aldehyde (1740 - 1720 cm^{-1}) and saturated ester (1750 - 1735 cm^{-1}) have longer induction periods of 7 and 8 hours of UV exposure, respectively. However, unlike the unsaturated groups which all retard at different rates, curves for saturated aldehyde, carboxylic acid, ester and ketone are all parallel up to 20 hours of UV exposure. In contrast to the two broad peaks described above a third broad band becomes of significance only after 10 hours of exposure to UV.

Absorbance in the region of 1105 - 1000 cm^{-1} has been assigned to carbon-oxygen (C-O) stretching of an unsaturated, branched aliphatic ether[90]. The rate of build-up of this group appears to be auto-accelerating and approximately follows the course of

Typical compensated IR spectrum obtained in 1% w/v CH_2Cl_2 solution of unstabilised HIPS extruded film (50 μm) UV irradiated for 26 hours.

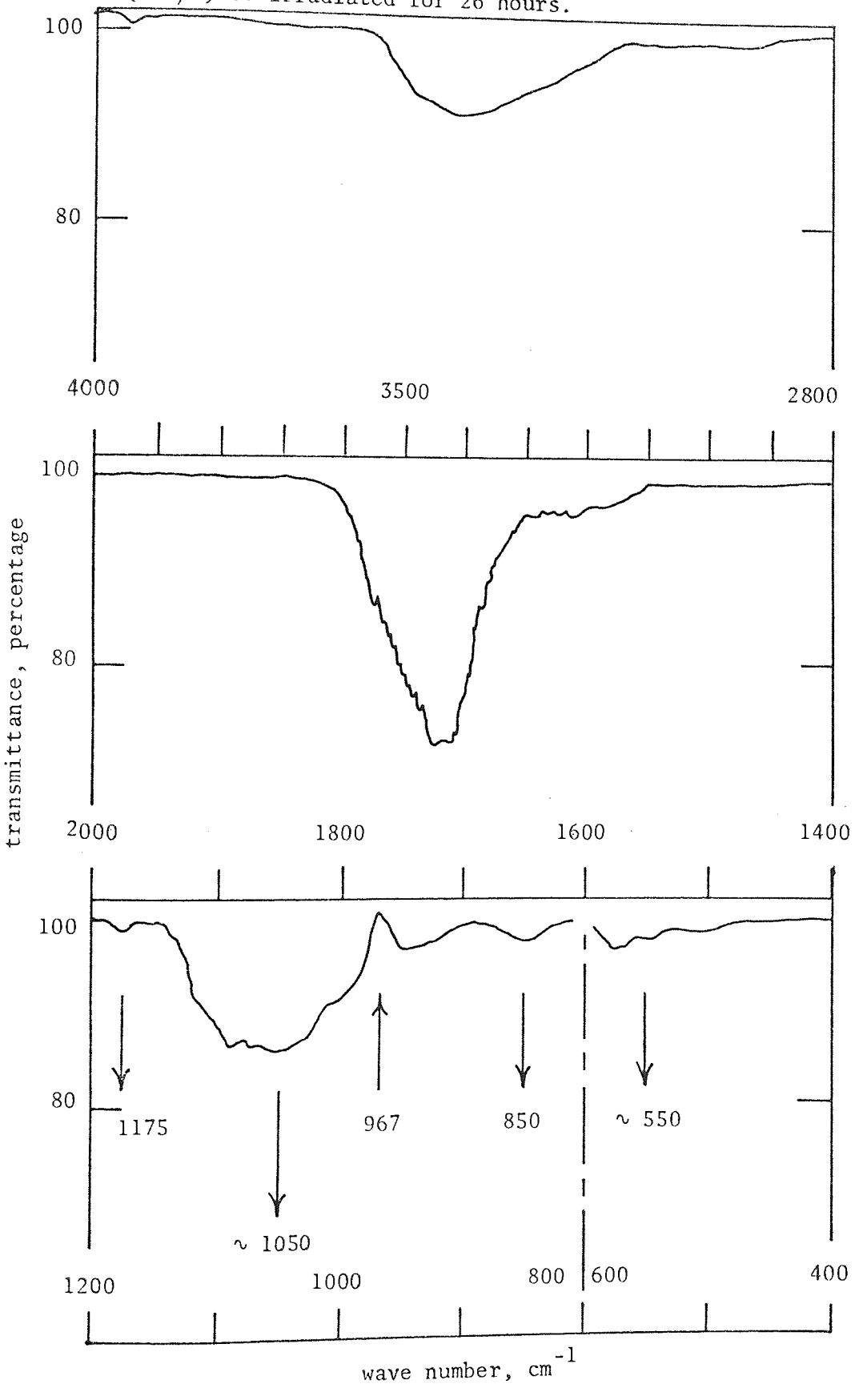

Figure 40.

carbonyl groups up to about 17 hours of UV exposure after which it retards but does not decrease up to 30 hours. A shoulder peak around 1800 - 1770 cm^{-1} attributed to peracid[89] follows an identical path as that described for the ether and is represented in figure 39 by the same curve.

A typical IR spectrum of a 1% solution in dichloromethane of unstabilised HIPS extruded film (50 μm) UV irradiated for 26 hours is shown in figure 40. The broad band assigned to the oxygen-hydrogen (O-H) stretching of allylic alcohol is seen clearly at 3400 cm^{-1}. Absorbance around 3280 cm^{-1} apparent towards the latter stages of degradation has been attributed carboxylic acids, including peracid[89] and is thus responsible for the asymmetric appearance of the band.

The complex spectrum in the carbonyl region assigned to carbon-oxygen stretching (C=O) is illustrated in figure 40. In addition to peaks displayed in figure 39, smaller shoulders were attributed to α,β-unsaturated and aryl ester (1730 - 1717 cm^{-1}), α,β-unsaturated carboxylic acid (1715 - 1690 cm^{-1}), aryl acid (1700 - 1680 cm^{-1}), aryl aldehyde (1715 - 1695 cm^{-1}), α,β,γ,δ-unsaturated aldehyde (1680 - 1660 cm^{-1}), α,β,γ,δ-unsaturated ketone (1670 - 1663 cm^{-1}), and carbon-carbon (C=C) conjugation (1645 - 1600 cm^{-1})[90].

The main absorbance around 1050 cm^{-1} (figure 40) has been attributed to aliphatic ether. Furthermore, a related peak designated as "medium" absorbance[90] (centred at 550 cm^{-1}) is visible after 26 hours of exposure to UV. The decay of trans-1,4-polybutadiene appears

Development of IR absorbance in stabilised HIPS cast film (75 μm) on photoxidation (numbers on spectra represent hours of exposure to UV)

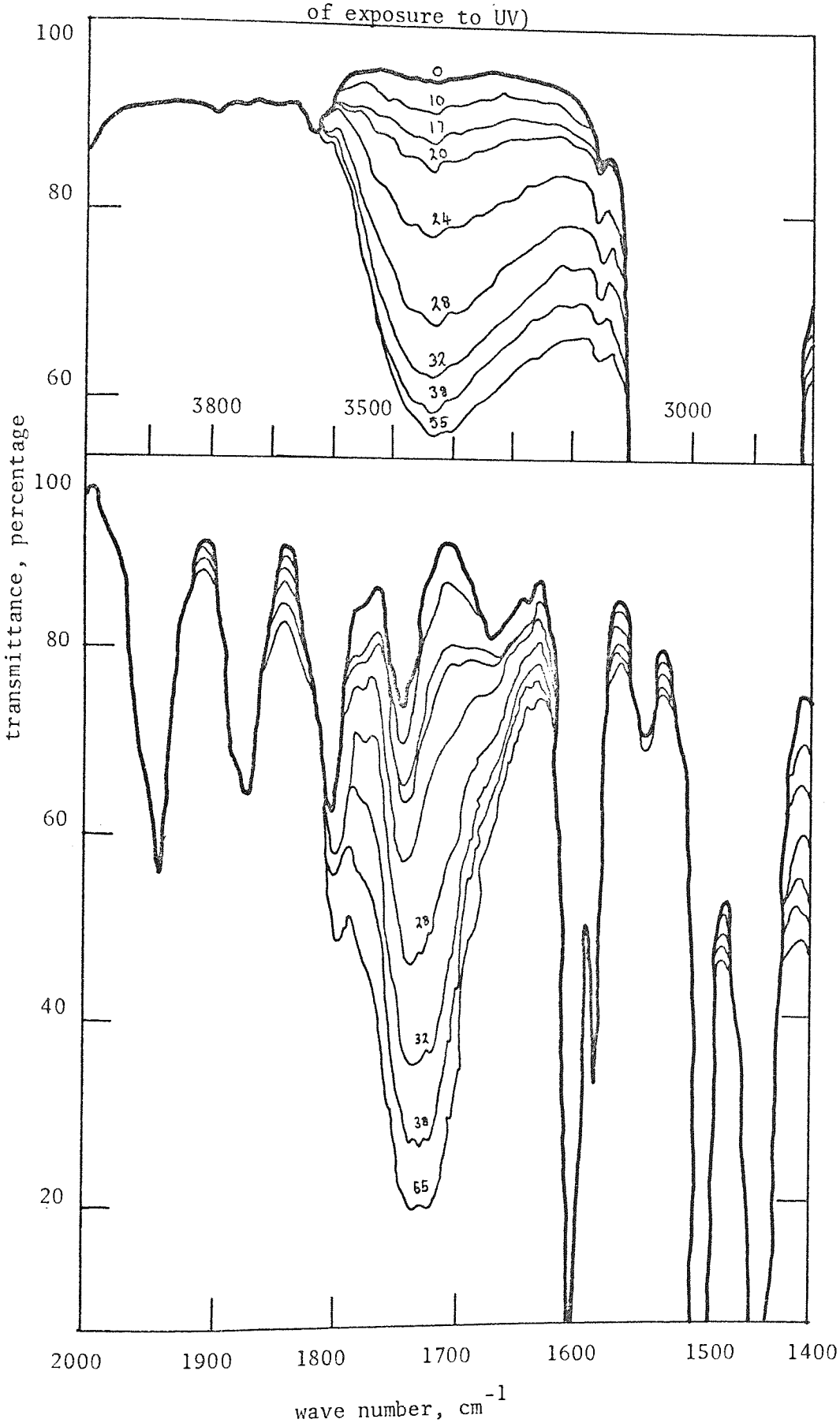

Figure 41.

as a sharp negative peak at 967 cm^{-1}. Two other minor peaks are seen at 850 cm^{-1} and one approaching 1200 cm^{-1} these may be attributed to epoxy ring formation[90].

3.1.3.2 Crystal polystyrene

In contrast to the broad featureless band around 3400 cm^{-1} assigned to oxygen-hydrogen stretching (O - H) for photoxidised HIPS (figure 41) "crystal" polystyrene displays two distinct peaks, figure 42. A broad peak at 3440 cm^{-1} and a slightly less intense but sharper peak at 3540 cm^{-1} have been attributed to tertiary benzylic alcohol and secondary methylenic alcohol (3440 cm^{-1}), and tertiary benzylic hydroperoxide (3540 cm^{-1}).

Inter-molecular hydrogen bonding of alcohol is also likely to predominate. Absorbances in the region of 3300 cm^{-1} to 3200 cm^{-1} and 2800 cm^{-1} to 2500 cm^{-1} have been attributed to inter-hydrogen bonded peracid and carboxylic acid[89]. These absorbances are more intense than in the case of HIPS, figure 41. The growth of hydroperoxide and alcohol with UV exposure is shown in figure 43. Both curves tend to be auto-accelerating reaching linear kinetics after approximately 40 hours of UV exposure. The rate of formation of benzylic hydroperoxide is faster than the corresponding alcohol. However, after 350 hours of photoxidation the rate of formation of benzylic alcohol supercedes that of benzylic hydroperoxide. The positive intersect on the ordinate at zero exposure indicates an initial low concentration of benzylic alcohol, figure 43.

Development of IR absorbance in "crystal" PS cast film (100 μm) on photoxidation (numbers on spectra represent hours of exposure to UV)

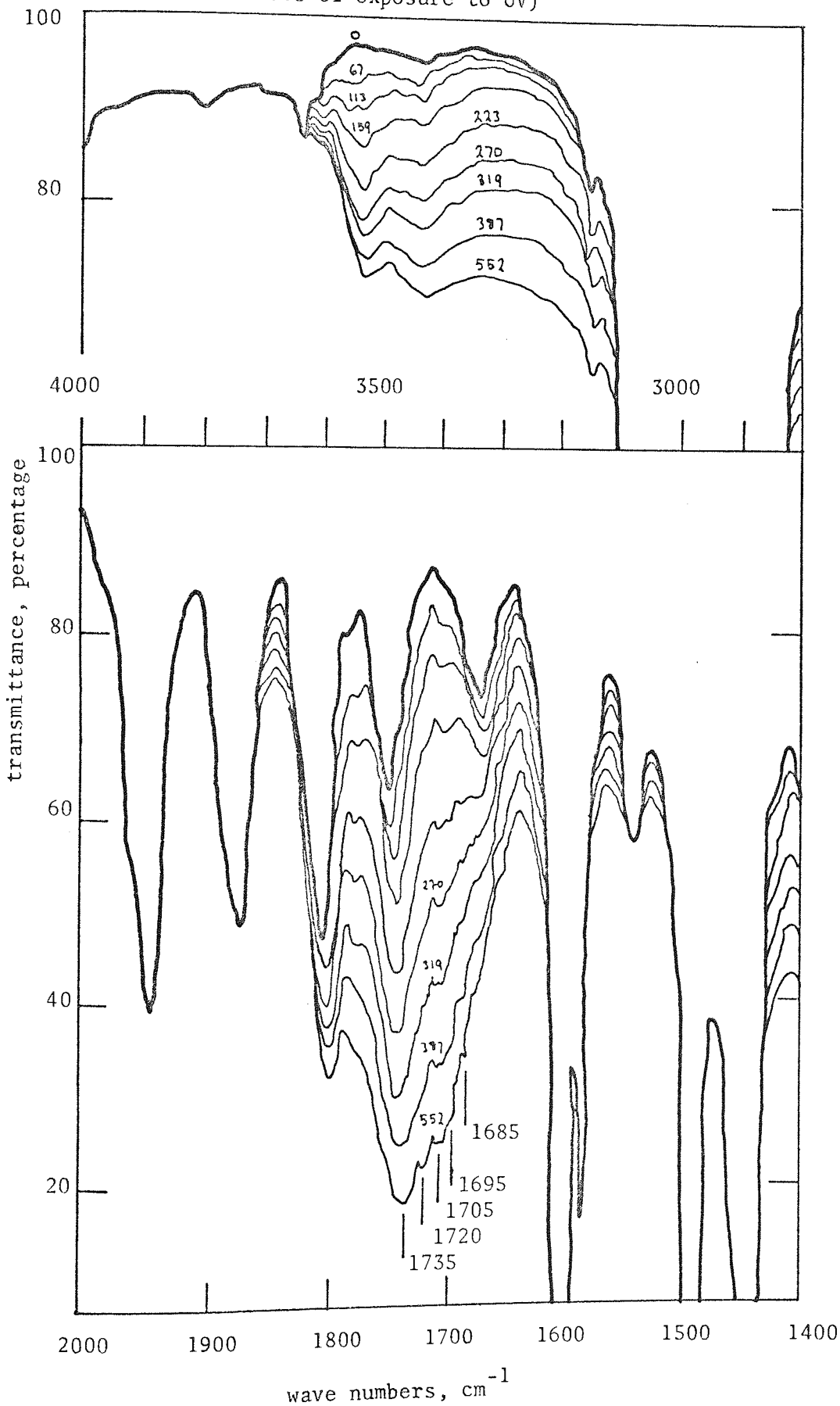

Figure 42.

Development of functional groups in "crystal" PS cast film (100 μm) on photoxidation

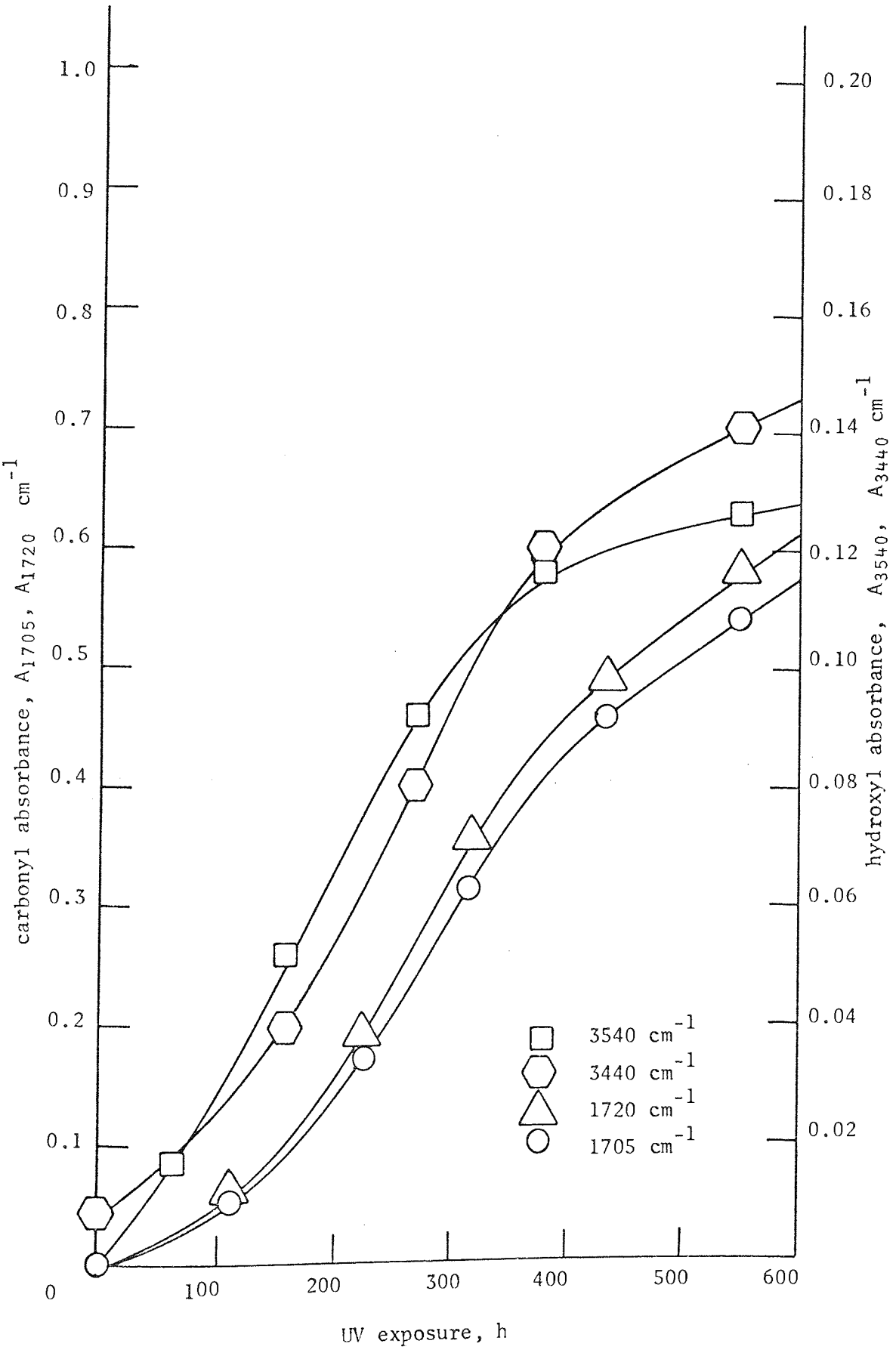

Figure 43.

The carbonyl region around 1700 cm^{-1} assigned carbon-oxygen stretching (C=O) was of similar complexity to HIPS. However, IR spectra obtained for "crystal" polystyrene films (figure 42) shows a small sharp peak at 1705 cm^{-1} attributed to carboxylic acid (1725 - 1700 cm^{-1})[89]. Another peak at 1720 cm^{-1} has been attributed to saturated aldehyde and ketone (1740 - 1720 cm^{-1}) and (1725 - 1705 cm^{-1}) respectively. The growth of these two peaks during UV exposure are shown in figure 43. Both curves start at the origin and increase in an auto-accelerating manner attaining linear kinetics after 120 hours of UV exposure. After 350 hours of exposure to UV the rate of formation of carbonyl departs from linearity, parallel to the curves representing alcohol. Apart from the groups displayed in figure 43, absorbance at 1735 cm^{-1}, although complemented by a background aromatic peak, has been attributed to saturated ester (1750 - 1735 cm^{-1}), and a small peak at 1685 cm^{-1} to aryl ketone (1700 - 1680 cm^{-1})[90]. A peak visible towards the latter stages of degradation at 1280 cm^{-1} has been attributed to carboxylic acid or aldehyde[90].

3.1.3.3 Polybutadiene

The spectral changes occurring during UV exposure of PBD film cast on a KBr disc from a 1% solution in dichloromethane were recorded up to 30 hours from 4000 cm^{-1} to 500 cm^{-1}, figures 44 and 45. In general the peaks described for degraded HIPS (see 3.1.3.1) are similarly observed for PBD. However, because no polystyrene is present the spectral changes arising solely from PBD are of greater relative intensity. Also important peaks which are masked by the absorbance of polystyrene in HIPS are clearly visible. The most

Spectral changes occurring during photoxidation of PBD on KBr cast from a 1% CH_2Cl_2 solution (numbers on curves represent hours of exposure to UV)

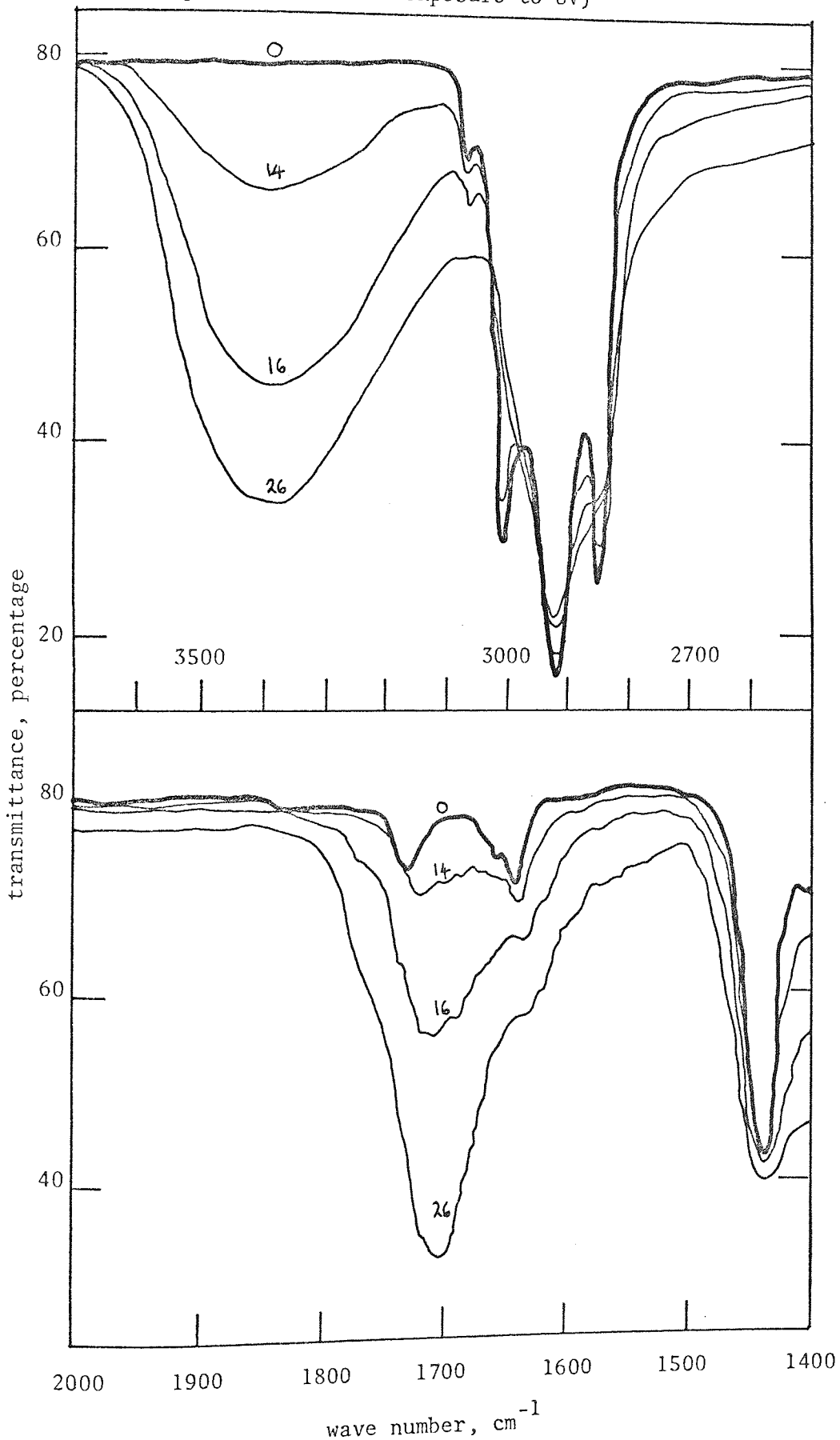

Figure 44.

Spectral changes occurring during photoxidation of PBD on KBr cast from a 1% CH_2Cl_2 solution (numbers on curves represent hours of exposure to UV)

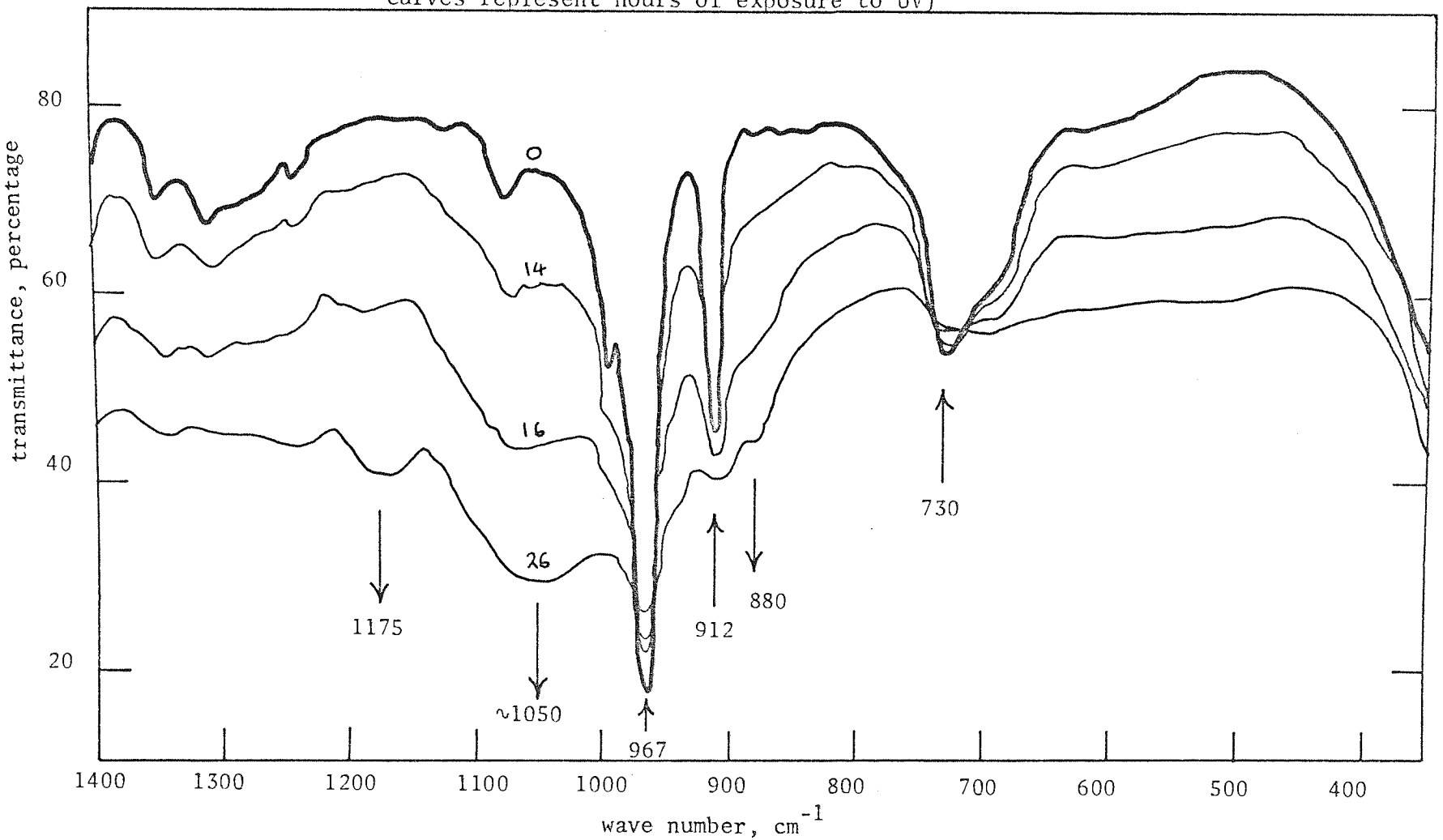

Figure 45.

important of these is 1,2-polybutadiene occurring as a sharp peak at 912 cm^{-1}, figure 45. Allylic hydroxyl (figure 44) is identified by a broad featureless band at 3400 cm^{-1}. The concentration of carbonyl around 1720 cm^{-1} to 1710 cm^{-1} together with allylic alcohol and 1,2-polybutadiene are plotted on figure 46 with respect to UV exposure up to 30 hours. All three curves are auto-accelerating and attain linear kinetics after an induction period, found by extrapolation to the abscissa. 1,2-polybutadiene gives the shortest induction period of 12 hours followed by hydroxyl and carbonyl with induction periods of 13 and 14 hours of UV exposure respectively. The destruction of 1,2-polybutadiene is almost complete after 28 hours UV exposure; an absorbance of 0.025 indicates zero concentration of 1,2-polybutadiene. Consequently the curve reaches a plateau towards 30 hours. Hydroxyl concentration increases at a slightly faster rate than carbonyl but slows down around 20 hours of UV exposure, although the growth of hydroxyl does not reach zero. Carbonyl on the other hand continues to increase in a linear manner at a slightly reduced rate up to 30 hours of exposure to UV.

In the case of HIPS it was possible only to measure trans-1,4-polybutadiene, however, the concentration of the other isomer cis-1,4-polybutadiene is readily determined when 100% polybutadiene is used. By knowing the relative percentage composition of each component of polybutadiene rubber (see 1.1) the absorbance during photoxidation of trans- and cis-1,4-polybutadiene and 1,2-polybutadiene may be converted to a percentage of each component, figure 47. All curves follow the same general pattern: auto-accelerating during the initial period, attaining maximum rate of decay after an identical induction period,

Development of functional groups in PBD (cast from 1% solution in CH_2Cl_2 onto KBr) on photoxidation.

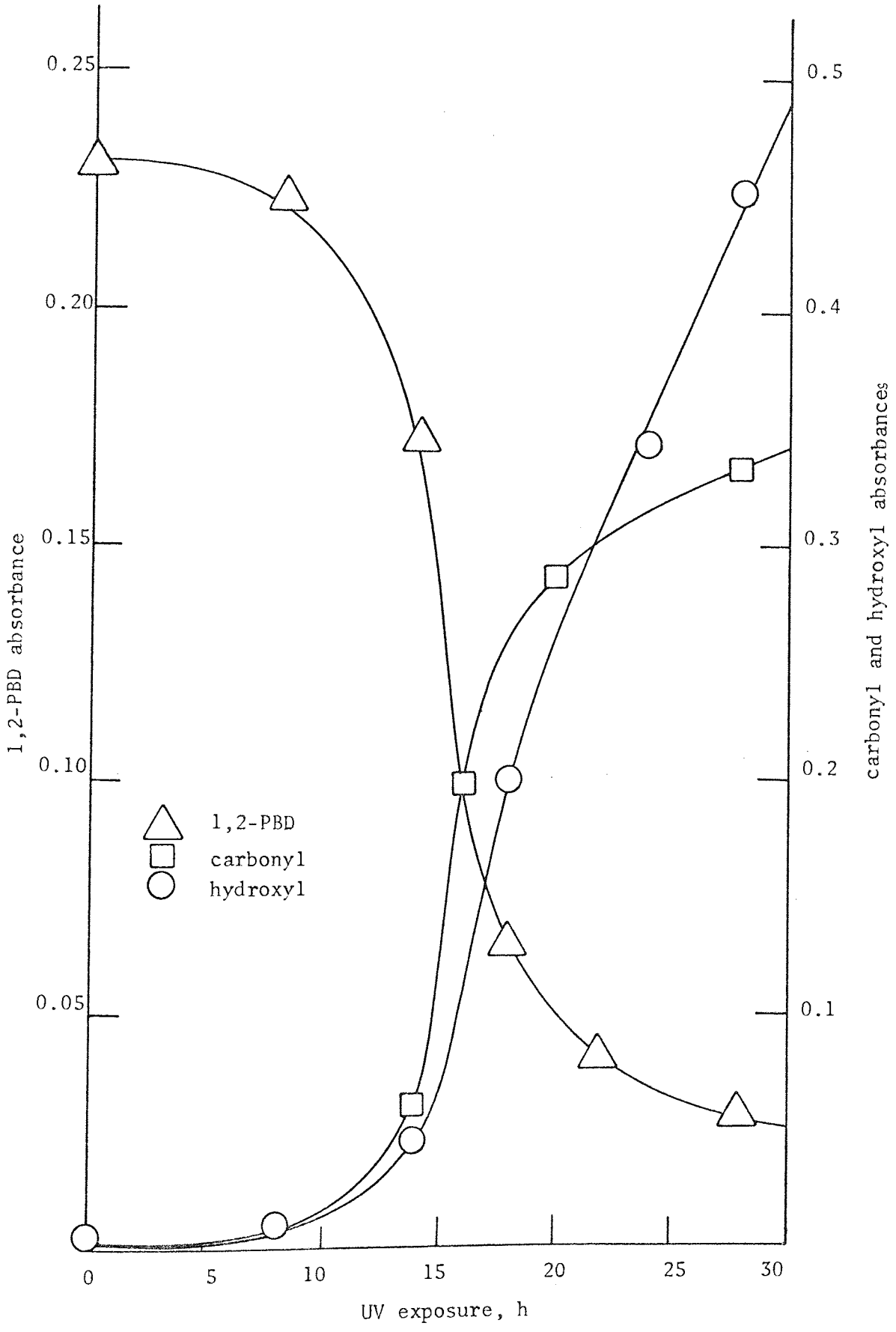

Figure 46.

Decay of unsaturation in PBD (cast from a 1% solution in CH_2Cl_2 onto KBr)on photoxidation

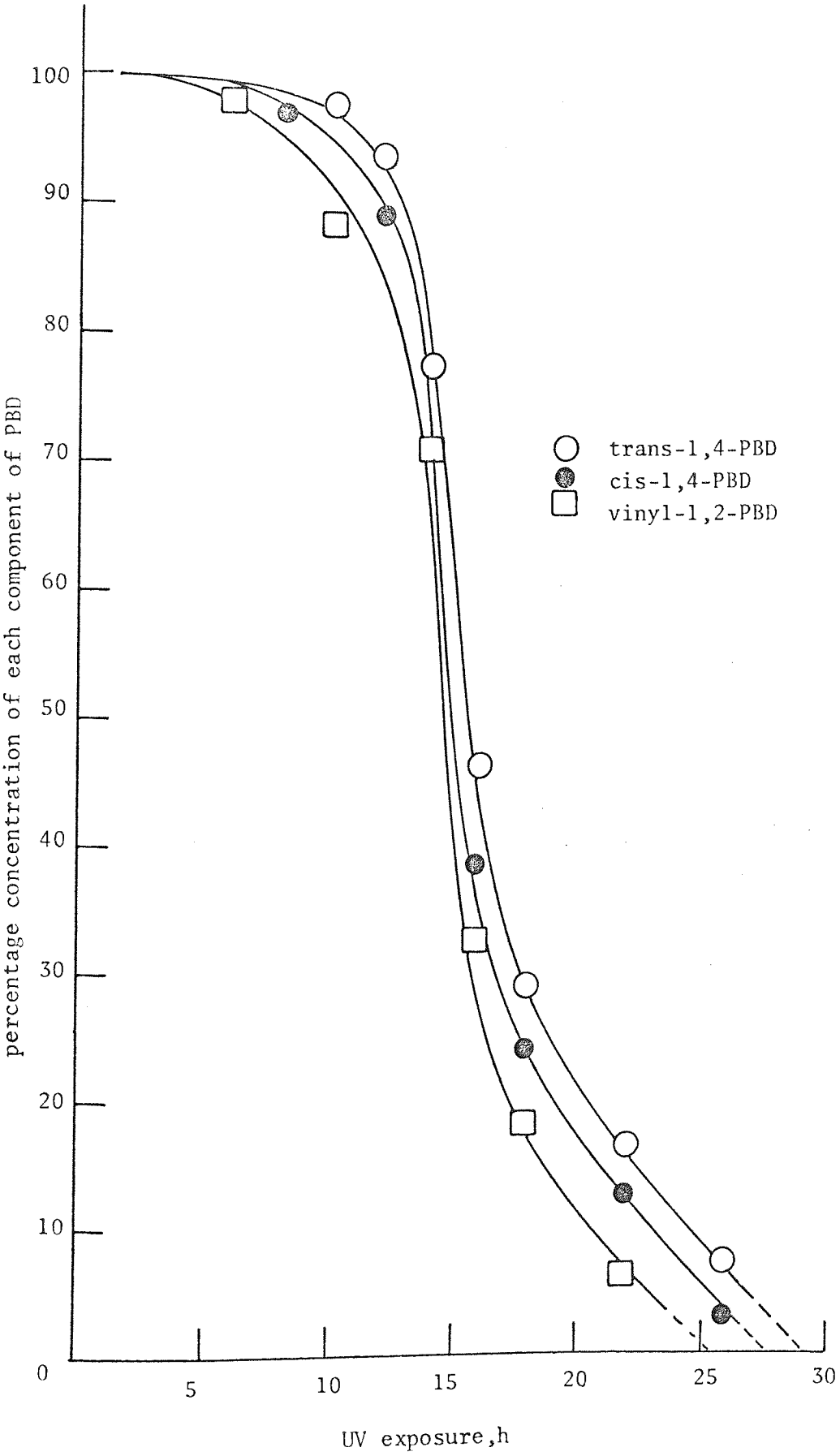

Figure 47.

(found by extrapolation to 100%) and finally falling to zero concentration with further UV irradiation. The difference lies mainly in the amount of each component of rubber consumed initially before linear kinetics are obtained and the maximum rate of decay. Figure 47 illustrates the order of consumption of the three components of polybutadiene rubber; 1,2-polybutadiene is initially consumed more readily than 1,4-polybutadiene.

The decay of PBD may be represented as a first order reaction. In figure 48 the first order kinetics with respect to the percentage concentration of cis- and trans-1,4-polybutadiene and 1,2-polybutadiene are depicted as three straight lines all of which extrapolate to the same point at zero on the ordinate, corresponding to 12 hours of exposure to UV, defined as the induction period. It is clear from figure 48 that 1,2-polybutadiene decays at a faster rate than trans-1,4-polybutadiene and that cis-1,4-polybutadiene decays at an intermediate rate [76]. However, from figure 48 it also appears that the rate of decay of cis-1,4-polybutadiene is marginally closer to that of its isomer trans-1,4-polybutadiene than to 1,2-polybutadiene. The rate constants for the decay of trans-1,4-polybutadiene, cis-1,4-polybutadiene and 1,2-polybutadiene are $5.22 \times 10^{-5}\ s^{-1}$, $6.14 \times 10^{-5}\ s^{-1}$ and $7.78 \times 10^{-5}\ s^{-1}$ respectively.

In addition to the spectral changes described above for photoxidised PBD several interesting features are apparent in the carbon-hydrogen (C-H) stretching region around 2900 cm^{-1}, figure 44.

First order plot for the decay of unsaturation in PBD (cast from a 1% solution of CH_2Cl_2 onto KBr) on photoxidation (numbers represent percentage of each isomer initially present)

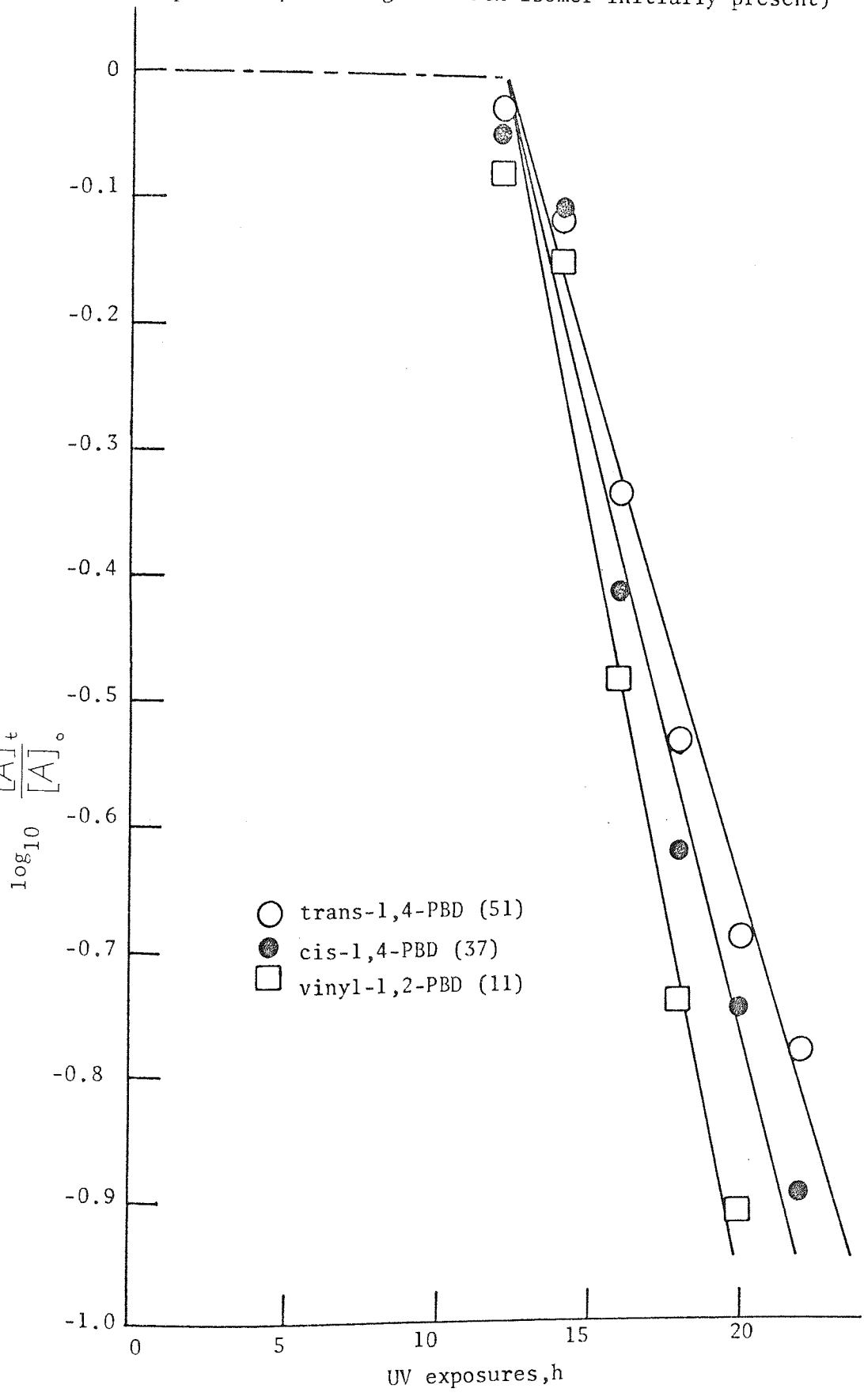

Figure 48.

Before UV irradiation a triple absorption band was visible centred at 2922 cm^{-1} with two sharp but less intense peaks at 3010 cm^{-1} and 2850 cm^{-1}. A small sharp peak at 3070 cm^{-1} was also present in the control spectrum. The peak at 3070 cm^{-1} has been assigned to the carbon-hydrogen (C-H) stretching of vinyl-1,2-polybutadiene[90]. Similarly the more intense peak at 3010 cm^{-1} has been attributed to 1,2-polybutadiene, but absorbance of both cis- and trans-1,4-polybutadiene also occur at 3010 cm^{-1}[90]. The peaks at 2922 cm^{-1} and 2850 cm^{-1} are characteristic of alkane and have been assigned to the carbon-hydrogen (C-H) stretching of the methylene (CH_2) group[90]. During UV exposure the sharp peaks at 3070 cm^{-1}, 3010 cm^{-1} and 2850 cm^{-1} all decrease very rapidly in a parallel manner to that described above (figure 46) for 1,2-polybutadiene absorption. The more intense peak at 2922 cm^{-1} decays similarly but not so drastically. After 28 hours of UV exposure only the peak at 2922 cm^{-1} was visible, although a slight shoulder at 2850 cm^{-1} could be identified.

A broad band develops during the UV ageing of PBD at 2800 cm^{-1} to 2500 cm^{-1} (figure 44) similar to that described for HIPS and is attributed to inter-hydrogen bonded carboxylic acid[89]. The carbonyl region around 1700 cm^{-1} is free of "interference" from aromatic peaks which are always present in HIPS and "crystal" polystyrene spectra (see 1.6.1), although the resolution of peaks occurring as shoulders is no easier. Apart from aryl substituted groups all the assignments described for HIPS (see 3.1.3.1) may be identified for PBD film exposed to UV. However, a slight shift in the apex of the carbonyl peak from 1715 cm^{-1} to 1710 cm^{-1} is apparent,

indicating a predominance of carboxylic acid over ketone during the latter stages of UV degradation.

After 14 hours exposure to UV a broad band around 1050 cm^{-1} (figure 45) develops identical to that described earlier for HIPS (see 3.1.3.1) and is likewise attributed to a branched, unsaturated aliphatic ether. A less intense but similarly broad peak is visible at 1175 cm^{-1} after 12 hours UV exposure and has been assigned to the carbon-oxygen (C-O) stretching characteristic of an ester. However, the band at 1175 cm^{-1} and another less intense peak at 880 cm^{-1} may also be attributed to epoxide formation (see 3.1.3.1)[90].

3.1.4 Correlation between gel content, cross-link density and peak height for polybutadiene

The maximum value of tanδ obtained during UV exposure of polybutadiene film (see 3.1.1.2, figure 36) has been plotted (figure 49) together with the weight percentage of gel (see 1.9) and the cross-link density (CLD), (see 1.10) of similar PBD film exposed to UV under identical conditions.

Tanδ decreases only slightly during the initial 25 hours of UV exposure, then drops sharply. After 100 to 150 hours of UV exposure tanδ decreases at a much slower linear rate up to 815 hours. Further UV irradiation resulted in a sample too brittle to be tested by the Rheovibron. A significant weight of gel (56%) was produced during the first 25 hours of UV exposure despite the relatively small decrease in tanδ. However, during the rapid drop of tanδ between

Correlation of physical changes occurring during the photoxidation of compression moulded PBD film (450 μm)

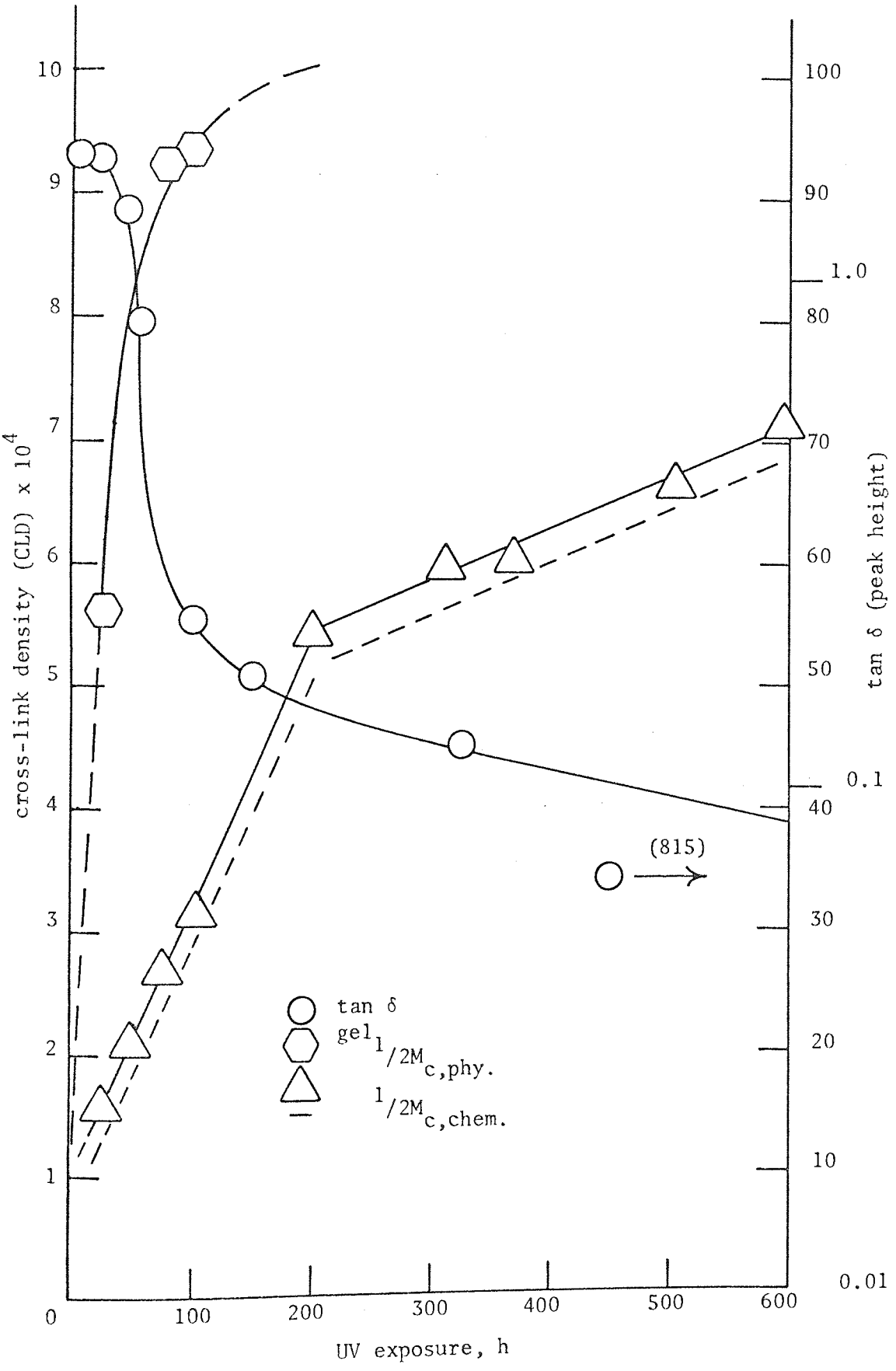

Figure 49

25 and 100 hours of UV exposure, the gel content rose to 94%. After 150 hours of exposure to UV no soluble phase could be isolated thus 100% gel content was recorded. Cross-link density (CLD) was determined during this rapid rise in gel content and was found to increase linearly from 25 to 200 hours of UV exposure. Afterwards CLD increased at about half the rate, also in a linear manner up to 600 hours. CLD determination on PBD UV irradiated for extensive periods became irreproducible because of the formation of large cracks in the relatively thick samples, 450 μm before swelling. CLD determined by swelling is an estimate of the physical cross-links present only and is defined as $1/2M_{c,phy.}$, where M_c is the inter cross-link molecular weight. This may be converted to chemical cross-links $1/2M_{c,chem.}$ (see 1.10) by use of the semi-empirical relationship derived for peroxide vulcanisates of natural rubber[65]. However, if the initial molecular weight of the unirradiated PBD is high then an estimate of the number of chemical cross-links may be obtained by subtracting 0.3×10^{-4} from the value found by swelling. This is shown in figure 49 as a dotted line parallel to the results obtained for physical cross-links. Between 25 and 200 hours of exposure to UV the corresponding inter cross-link molecular weight (M_c) fell from 3166 to 925 and down to 532 after 809 hours of UV irradiation.

3.1.5 Correlation between oxygen absorption, trans-1,4-polybutadiene and peak height for high impact polystyrene

The change in peak height, tanδ(-80°C) during UV exposure (see 3.1.1.1, figure 28) of stabilised HIPS cast film, annealed for 4 hours at 85 - 90°C, is shown in figure 50. Tanδ decreases from

Correlation of decay of peak height (tan δ) and unsaturation (trans-1,4-PBD) with oxygen absorption during the photoxidation of stabilised HIPS cast film (55 μm)

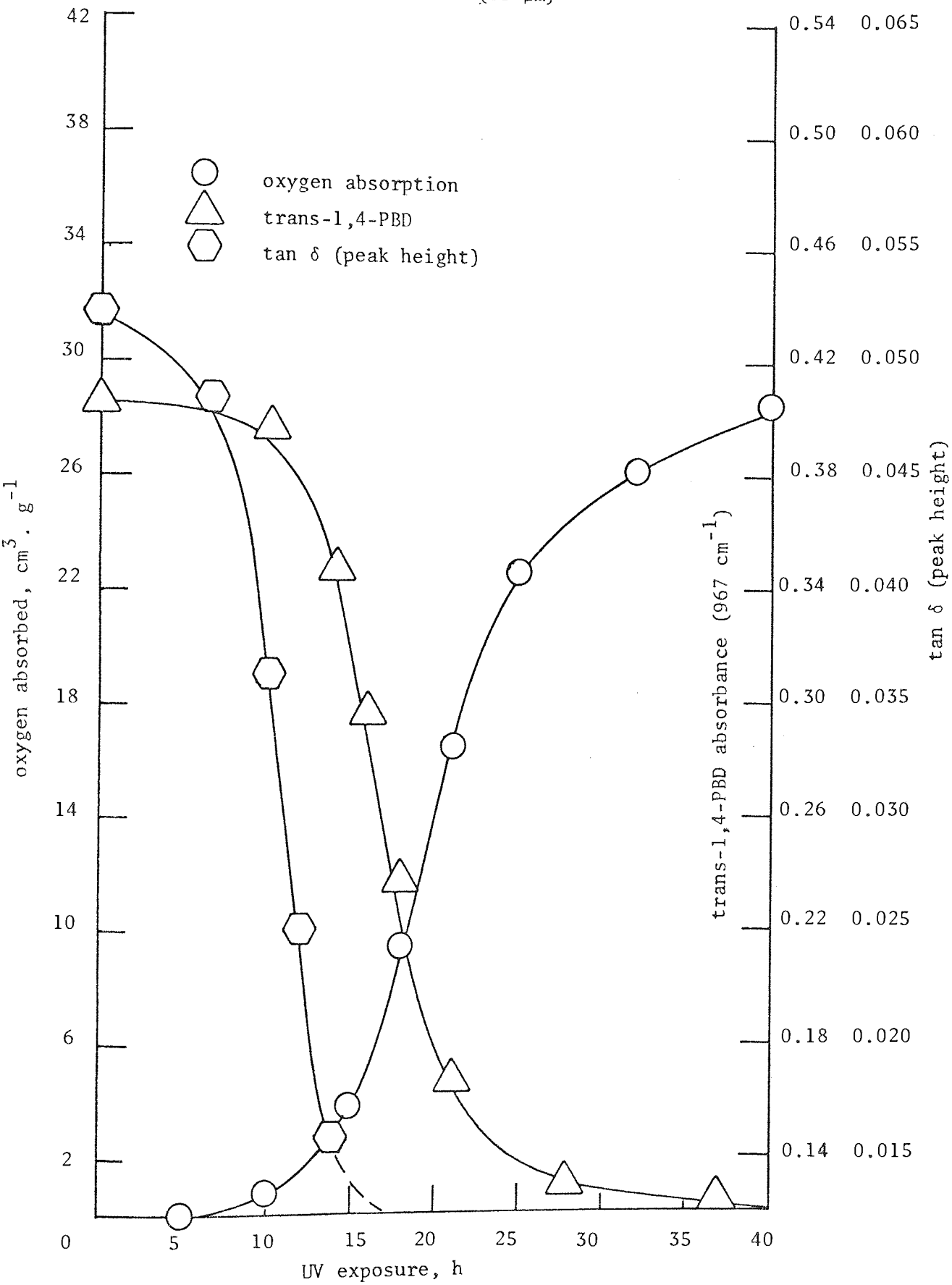

Figure 50.

the onset of exposure to UV and after 6 hours the linear rate of decay is very rapid up to 14 hours after which it levels out, but does not fall to zero. The decay of trans-1,4-polybutadiene measured by IR (see 1.6.1) during exposure to UV of the same cast film annealed under identical conditions and for the same time is also shown in figure 50. It is clear that initial rate of decay of trans-1,4-polybutadiene is slower than the disappearance of the peak height. Similarly the time required to attain the slightly slower linear rate of decay is longer. After 25 hours UV exposure trans-1,4-polybutadiene levels out and approaches zero concentration; an absorbance of 0.12 indicates no trans-1,4-polybutadiene remaining. IR spectra were also taken from actual Rheovibron samples used for the measurement of the low temperature peak. The induction period and maximum rate of decay of trans-1,4-polybutadiene were identical to that described in figure 50. Oxygen absorbance (see 1.4) mirrors the decay of trans-1, 4-polybutadiene, figure 50. However, the mid-point of the linear portion of the oxygen absorption curve is displaced to longer exposure times by approximately 3 hours relative to the corresponding mid-point of the decay for trans-1,4-polybutadiene, even though identical samples were used.

3.1.6 Correlation between damping and complex modulus at ambient temperature with peak height for high impact polystyrene

The peak height, tanδ (-80°C) for stabilised HIPS cast film shown in figure 50 has been superimposed on the changes in damping and complex modulus measured at ambient temperature on the same polymer

Correlation of dynamic-mechanical properties at ambient temperature with decay of peak height (-80°C) during the photoxidation of stabilised HIPS cast film (55 µm)

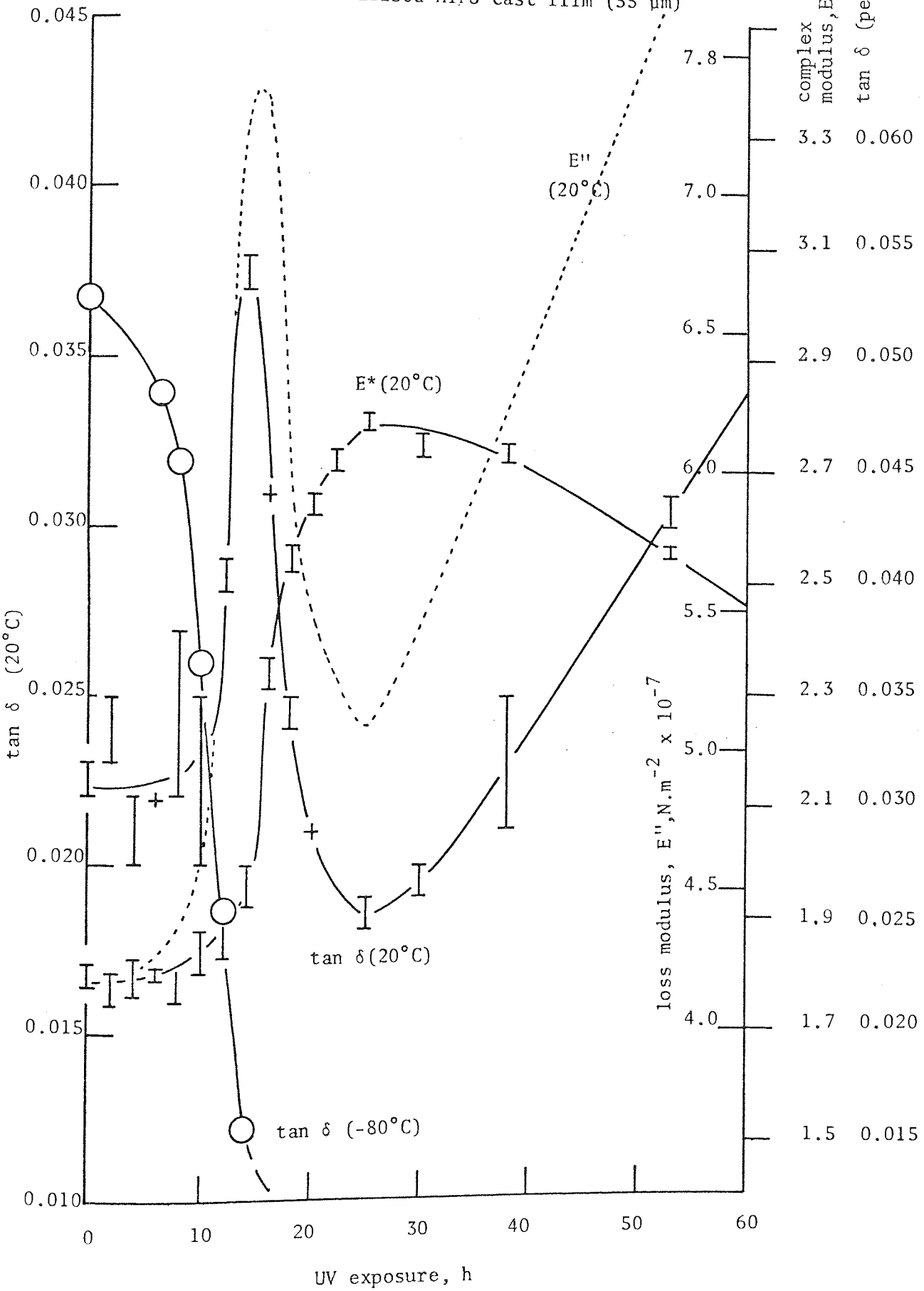

Figure 51

film which had been annealed under identical conditions for the same length of time, figure 51. However, the method of taking readings from the Rheovibron was different. For measurement of the low temperature peak only one reading was taken every 2°C change in temperature. The changes in tanδ, complex modulus,E*, and its viscous component, E'', occurring at ambient temperature (20°C) were recorded at least 5 times for each exposure to UV. The same sample was used throughout and the results are shown in figure 51 as vertical lines. More scatter was obtained for tanδ than complex modulus. Generally, the error was greater during the initial period of UV exposure. Tanδ measured at 20°C increased very slightly during the first 8 hours of UV exposure corresponding to the slow decrease in peak height, tanδ (-80°C). During the rapid, linear decay of tanδ at -80°C a similarly rapid increase in tanδ at +20°C is experienced culminating in a maximum of 0.0375 after 14 hours of exposure to UV, corresponding to the levelling out of the peak height at -80°C, (the temperature at which this peak occurs shifts during UV irradiation, however, it is the maximum value of tanδ for each curve that is referred to in figures 50 and 51). After 14 hours UV exposure tanδ at 20°C drops rapidly to a lower value than that of the control. With further UV irradiation tanδ increases again but at a much slower rate up to 53 hours, producing a minimum value in tanδ at 25 hours of exposure to UV. During the course of UV irradiation up to 53 hours, complex modulus measured at 20°C has an integral relationship with tanδ. The rapid linear rise in complex modulus corresponds to the maximum in tanδ (20°C) and the maximum in complex modulus of approximately $2.8 \times 10^{9} N.m^{-2}$ corresponds to the minimum value of tanδ (20°C) of

about 0.018 also at 25 hours of UV exposure. The value of complex modulus, E*, and its viscous, E'', and elastic components, E', were calculated by computer programme using a length correction factor (K) of 21 (see 1.5.2). Elastic modulus, E', followed the same path as complex modulus, E*, although at a slightly lower value but still within the scatter indicated for E*, figure 51. Conversely, the viscous component, E'', followed an intermediate path between tanδ and complex modulus, E*, or elastic modulus, E', according to the relationship: $E'' = E'\tan\delta$ (see 1.5.2).

3.2 DISCUSSION

The dynamic-mechanical properties of HIPS have been illustrated for cast film containing a phenolic antioxidant and an unstabilised extruded sample. Before discussing the relationship between peaks measured by dynamic-mechanical spectroscopy and chemical groups determined by IR and idiometry, reasons for the observed differences in tanδ and glass transition (Tg) for samples tested under different conditions or produced by casting or processing must be established. From figure 35 the effect of sample selection with respect to direction of extrusion on the magnitude of tanδ suggests that orientation of molecular chains is the sole contributing factor, as both specimens were cut from the same film and the experimental conditions of measurement were identical. During the extrusion of HIPS the extrudate (see 1.2.1.1) was quench-cooled from +220°C to +60°C. Under these conditions segments of chains aligned by drawing of the extrudate onto the rollers will become "frozen" in the direction of extrusion. Consequently samples cut in this direction will consist of a prepondance

of segments orientated parallel to the length of the sample. Conversely the segments of a specimen cut transverse to the direction of extrusion will be orientated at 90°. The transition from a rubber to a glass designated as Tg arises from segmental motion of molecular chains of PBD in HIPS; the magnitude of this glass transition will be dependent on the mobility of the rotating segments. The inter-molecular chain separation or "free-volume" will be identical for the above samples cut from the same extruded film. Furthermore, it is known that a lower level of stress is required to separate chains aligned 90° to the direction of stressing[91]. It is believed that the low level of stress associated with dynamic-mechanical testing is sufficient for partial separation with a corresponding increase in free-volume and mobility. Tanδ will, therefore, be slightly greater for a sample of extruded film cut transverse to the direction of orientation than for a specimen cut parallel to the direction of extrusion, figure 35.

In figure 34 damping characteristics of a solution cast film which had been annealed are shown. This sample, measured under identical conditions with those shown in figure 35 will be free from orientation and consequently tanδ falls from 0.065 to 0.061. But this drop was only half that experienced between the extruded samples discussed above (figure 35) demonstrating the importance of direction of orientation with respect to sinusoidal displacement (see 1.5.2). The small shift of 2°C of the Tg to lower temperatures (figures 34 and 35) for a cast film measured under identical conditions may be a consequence of the presence of residual casting solvent (toluene) or

the 3% paraffin oil (see 1.1) both of which will have a plasticisation effect on the polymer. The concentration of processing aid may be lowered during the extrusion process at 220°C by volatilisation. The inclusion of a plasticiser into a sample under dynamic-mechanical testing lowers the Tg[92] by reducing the inter-molecular forces thus permitting segmental motion at a lower temperature[93].

When readings from the Rheovibron are taken from +20°C down to -120°C tanδ is further reduced and the Tg occurs at a lower temperature, figure 34. This can not be accounted for by plasticisation because the samples were cut from the same cast film. The shift of 6.5°C in the glass transition suggests that an irreversable process is taking place when the sample is cooled to below the Tg[94] and that this process is time-dependent. Crystallisation of the PBD constituent of HIPS during the cooling of the sample before taking readings would conveniently explain the observed phenomena since it is known that crystallisation is a time-dependent process[95]. However, the presence of grafted chains of styrene-butadiene in HIPS will reduce the possibility of rearrangement of segments to form crystallites. Furthermore the bulky cis-1,4-polybutadiene present at a level of 37% in pure PBD (see 1.1) is unlikely to crystallise. Consequently crystallisation only of trans-1,4-polybutadiene in HIPS or PBD during cooling in the sample chamber of the Rheovibron may occur. During the cooling operation from +20°C down to -130°C a tension was maintained on the sample (see 1.5.1). This will inevitably result in a certain amount of molecular orientation being introduced into the sample parallel to the direction of loading.

This additional orientation of the PBD may increase the magnitude of tanδ observed in figure 34, although from the above discussion it was adduced that orientation in the direction of sinusoidal displacement was not significant. This secondary orientation which must also be present in samples shown in figure 35 did not destroy the original orientation induced by extrusion (otherwise the two curves would be congruent). This is because orientation takes place primarily in the PS matrix as the quenching passed through the Tg of PS around 100°C. Nevertheless this would necessitate orientation in the PBD phase because of the grafting of the two phases. It would appear that further explanation is necessary to account for the large difference in tanδ seen in figure 34. When a polymer is cooled it contracts and a decrease in the free-volume will follow. Moreover, if the polymer is quench-cooled through its glass transition the additional free-volume which is created by thermal expansion above its Tg may be frozen into the polymer. On warming up the sample from -130°C the segmental motion at the glass transition of PBD will be less restricted resulting in a higher tanδ value, figure 34. Therefore it is suggested that the anomalous behaviour observed during dynamic-mechanical testing of HIPS (or PBD) with respect to experimental technique (figure 34) is a combination of time-temperature dependance of crystallisation of PBD affecting the position of the Tg and the additional free-volume produced by quench-cooling affecting the value of tanδ.

The curves shown in figures 28 and 29 are therefore a representation of the same rubber peak that exists as a separate phase in HIPS;

the temperature is approximately the Tg of the PBD[96] which has been modified by grafting with styrene, this raises the Tg of the rubber towards that of the pure polystyrene[97]. The height of the loss peak is proportional to the amount of rubber present[96]. Exposure of HIPS films to UV has the effect of reducing the concentration of rubber to zero, figures 28 and 29. The shift of the rubber peak to higher temperatures and its broadening during UV exposure are consistent with extensive cross-linking in the PBD phase of HIPS, thus confirming the interpretation of data presented in Chapter Two. The broadening of the damping peak in figures 28 and 29 indicates an increase in the molecular weight distribution of the PBD as a result of cross-linking.

Destruction of the rubber peak in figure 28 for HIPS cast film stabilised with a phenolic antioxidant is complete within a shorter time than the analogous UV exposure of unstabilised HIPS extruded film, figure 29. This apparent contradiction may be resolved by considering that annealing the cast film for 4 hours in air at 85 - 90°C, even though it was stabilised, is more effective in producing hydroperoxides than extrusion at 220°C with a residence time of approximately 5 minutes.

It was established in Chapter Two that oxidation in the Wallace oven at 98°C produced a higher maximum concentration of hydroperoxide than processing at 200°C in the torque rheometer. Phenolic antioxidants do not destroy hydroperoxides formed during oxidation[98] so they will have little affect on the concentration of hydroperoxide formed during oven ageing of stabilised HIPS. The significance of

the phenolic antioxidant on the stability of HIPS after photolysis and during photoxidation will be discussed in Chapter Five.

The relaxation of PBD and styrene-butadiene graft co-polymer at a fixed frequency results in a maximum in the dynamic-mechanical loss ($\tan\delta$), figures 28 and 29 et seq., as the temperature is raised through the glass transition. Similarly the complex modulus, E* (figure 33) falls in a step-wise manner as the integral of the damping curve. The initial decline in complex modulus during photoxidation plotted in figure 30 for HIPS extruded film is similar to that found for low density polyethylene (LDPE) film exposed to UV and tested on the Rheovibron[87,99]. From figure 30 it may be calculated that the initial drop in complex modulus occurs after approximately 15% of the rubber has been destroyed by cross-linking. In Chapter Two (figure 27) it was shown that the initial peroxide gel formed during the photo-degradation of HIPS extruded film containing no antioxidant passed through a maximum after about 15% of the unsaturation (measured by IR) had been destroyed chemically. Consequently, the initial drop in complex modulus in figure 30 may be associated with the initial formation and decomposition of peroxide gel.

The marked absence of a distinctive β-peak, around 30°C, associated with polystyrene in figures 31 and 32 for cast and extruded HIPS and in figure 38 for "crystal" polystyrene is most likely a consequence of the relatively high frequency (110 Hz) selected as standard on the Rheovibron (see 1.5.1.) It is well known that an increase in frequency of dynamic-mechanical testing

results in a related shift of a transition to higher temperatures[100]. Therefore the β-peak of polystyrene will become engulfed in the glass transition of polystyrene thus precluding its measurement at 110 Hz by the Rheovibron[101]. Quench-cooling of a glassy polymer from the melt has been reported to enhance the β-transition[102]. However, no substantial improvement of the β-peak of polystyrene was detected for quench-cooled HIPS extruded film (figure 32) compared with cast HIPS film which has been annealed, figure 31. The β-transition of polystyrene reported by other workers has been attributed to the motion of phenyl side groups[103] but recent work[102] indicates that chain ends are responsible.

The glass transition of the polystyrene phase of HIPS film cast from toluene is seen as an asymptopic rise in tanδ at 95°C (figure 31) and was 5°C lower than the corresponding control sample for extruded HIPS film, figure 32. The plasticisation effect of the processing aid and residual solvent present in cast films may account for the shift in the Tg of polystyrene as described above for the rubber transition. During photoxidation of HIPS the Tg of polystyrene becomes broader shifting the shoulder observed in figures 31 and 32 to lower temperatures. This confirms that cross-linking is concomittient with photoxidation. However, the Tg of polystyrene did not become suppressed sufficiently so as to allow the tanδ peak to be measured by the Rheovibron. Extensive UV irradiation resulted in a brittle sample prone to fracture during testing on the Rheovibron. The above assumption that cross-linking in the PBD rubber phase which destroys the low-temperature mechanical loss peak also affects the Tg

of polystyrene is borne out in figure 33 showing the specific changes in complex modulus around -75 °C associated with the rubber peak together with the general increase in complex modulus up to +100°C. If photoxidation of HIPS destroyed the rubber phase without affecting the polystyrene then the complex modulus of a degraded HIPS film ought to return to that of the unirradiated "crystal" polystyrene. From figures 33 and 38 it is evident that the complex modulus of HIPS extruded film UV irradiated for 30 hours until brittle is identical to that for "crystal" polystyrene exposed to UV for 300 hours and rendered brittle, with respect to temperature rise from -130°C to +100°C. The extension of the asymptopic decline of complex modulus to +110°C for "crystal" polystyrene arises from the absence of grafted styrene-butadiene rubber which reduces the glass transition of polystyrene in HIPS by 8 - 10 °C, figure 38[97].

Similarly, the rubber peak (Tg) for pure PBD occurs at -80°C to -85°C figure 36; this was shifted by 8 - 10°C towards the Tg of polystyrene in HIPS, figure 32. Non cross-linked, pure PBD "rubber" was characterised by a very low elastic or storage modulus, E', and a relatively high viscous or loss modulus, E" . Consequently, no measurements on the Rheovibron were possible above the Tg of PBD. However, the formation of cross-links during photo-degradation increases the elastic component of PBD bestowing the properties of a elastomer thus permitting tanδ and complex modulus to be recorded at a higher temperature, above the Tg. Cross-linking of PBD was not uniform throughout the bulk of the polymer, although degradation appeared to commence at the same rate from the surface not exposed to

UV[81]. It is probable that the rate of photoxidation at the surface of PBD is controlled by oxygen diffusion into the polymer as a sample thickness of 450 μm was used as standard (nearly ten times greater than HIPS film). Consequently after the initial rapid cross-linking at the surface, extensive cross-linking of the bulk rubber requires increasingly longer times. As a result the bulk rubber still contains elastomeric properties arising from a low cross-link density while the outer layers are extensively cross-linked and rigid. This is illustrated in figure 36 by the presence of a damping peak (tanδ) after 815 hour of UV exposure corresponding to approximately 6% rubber remaining. The progressive increase in complex modulus (figure 37) of PBD during UV exposure confirms that cross-linking is prevalent in pure PBD and further supports the earlier postulate that cross-linking takes place predominantly in the rubber phase of HIPS.

Conversely in figure 38 the complex modulus of "crystal" polystyrene drops decisively after exposure to UV indicating that chain scission is more frequent than cross-linking. A mechanical loss peak (tanδ) for unirradiated "crystal" polystyrene (figure 38) occurs at -85°C similar to that for non cross-linked PBD, figure 36. However the tanδ peak in figure 38 for "crystal" polystyrene can not arise from the spurious presence of PBD or processing aid as exposure to UV increases the absorption by this structure contrary to the previous evidence for PBD. Therefore the structure involved in "crystal" polystyrene causing the observed relaxation at -80°C must be associated with a similar potential energy barrier to rotation as PBD. No transitions for atactic polystyrene have been reported in the literature

near-80°C[97] for dynamic-mechanical testing. It is postulated that because photoxidation increases the height and area of the low temperature peak (figure 38) the structure involved in the relaxation is an oxidation product involving chain scission. The height of this peak after extrusion corresponds to a concentration of "rubber" in HIPS of less than 1% and is increased to 1.5% after 300 hours exposure to UV.

In the above discussion on the dynamic-mechanical properties of HIPS cast or extruded film the results have been explained with reference to segmental motion of molecular chains only without reference to the morphology of the rubber particles. HIPS is a random graft co-polymer and may be considered to have three morphological regions or phases namely pure polystyrene, pure polybutadiene and an interfacial or intermixed region consisting of grafted segments of polystyrene and polybutadiene[104]. The glass transitions of the two homopolymers polybutadiene and polystyrene become closer when they are co-polymerised[93]. Therefore the Tg of the co-polymerised PBD appears at a higher temperature than the pure PBD depending on the amount of grafted styrene. By comparing figures 29 and 36, the Tg of the rubber is observed to be shifted by less than 10°C. This implies that the concentration of grafted material is low and that the degree of phase separation is high. It has been reported that systems that are purely phase separated are more prone to cross-linking and that some "blockiness" may exist in random co-polymers which would result in the casting solvent determining the detailed morphology of the co-polymer, although random systems do not exhibit a marked solvent

preference[104]. From the evidence presented in plates seven and nine for HIPS cast from dichloromethane and toluene respectively, no discernable morphological dependence on the casting solvent is visible. However, when the samples are UV irradiated and re-cast from their respective solvents the collapsed nature of the rubber particles was enhanced for the dichloromethane-cast film indicating the solvent preference for polystyrene. The collapsed appearance of these structures in plates eight and ten is postulated to be a result of preferential chain scission at graft points at the interfacial region of the rubber particle with the polystyrene matrix at both the exterior boundary region of the particle and at the interior cellular region. This effectively severs the PBD particle from the polystyrene matrix thus permitting "free" movement of the cellular structure resulting in contraction and disorientation. The above evidence directly supports the chemical mechanisms proposed in Chapter Two for the formation of a gel consisting of nearly 100% PBD by β-scission of the tie-bonds during photoxidation of HIPS film.

No orientation of the rubber particles, apart from the elongation introduced by microtoming, was observed in the relevant micrographs. Therefore, the orientation of HIPS (and "crystal" polystyrene) produced by extrusion discussed with respect to dynamic-mechanical properties must be restricted to alignment of molecular chains. Consequently possible morphological differences introduced by solution casting or extruding of HIPS film will have negligible effect on the dynamic-mechanical properties.

The changes in physical properties arising from cross-linking and chain scission of HIPS, "crystal" PS and PBD have been successfully monitored during photoxidation by dynamic-mechanical spectroscopy. Similarly the formation of chemical groups, some of which are involved in cross-linking reactions during photoxidation have been followed by IR spectroscopy, figures 40, 41, 42, 44 and 45. The most significant of the groups detected by IR, utilising the technique of difference spectroscopy (see 1.6.2) for HIPS (figure 40) and "crystal" PS (not shown) and solution casting for PBD (figure 45) is the formation of an ether linkage around 1050 cm^{-1} during photooxidation. In the case of HIPS film ether formation commenced after an induction period of 12 hours of exposure to UV (figure 39) while carbonyl compounds, both saturated and unsaturated, together with hydroxyl conferred an induction period of approximately 5 hours. It was postulated in Chapter Two that formation of an ether gel occurred as a secondary product after the breakdown of an initial peroxidic gel. Evidence from figure 27 (Chapter Two) showed that the initial rapid decomposition of peroxidic gel was superceded by the formation of a secondary gel after 10 to 15 hours of UV exposure of similar HIPS extruded film.

The decline in the concentration of hydroxyl group (3450 - 3400 cm^{-1}) shown in figure 39 confirms evidence presented in Chapter Two that the broad peak was complemented by hydrogen-bonded hydroperoxide; the reduction in hydroperoxide concentration during photoxidation of HIPS detracts from the absorbance in this region. An actual drop in hydroxyl during the photoxidation of HIPS was

observed only when measured by difference spectroscopy. It is probable that the dissolution of degraded HIPS in dichloromethane enhanced the sensitivity to measurement by IR of hydrogen-bonding by hydroperoxide.

From figure 39 it is evident that the formation of α,β-unsaturated carbonyl compounds retard to a greater extent than their saturated analogues during the photoxidation of HIPS. This is to be expected if the conjugating double bond is destroyed by addition of an alkoxy radical as postulated in Chapter Two for the destruction of conjugated aldehyde produced during processing in the torque rheometer.

During the photoxidation of "crystal" polystyrene a greater proportion of carboxylic acids (including peracid) were produced than for HIPS exposed to UV under the same conditions. This was indicated by the pronounced absorption towards lower wave numbers of the oxygen-hydrogen stretching frequency for "crystal" polystyrene (figure 42) compared with HIPS, figure 41. Carboxylic acid formation is concomittient with chain scission[105]. This implies that chain scission predominates over cross-linking during the photoxidation of "crystal" polystyrene contrary to HIPS. The reduction of complex modulus for degraded "crystal" polystyrene only (figure 38) confirms this. Cross-linking of polystyrene chains during photoxidation together with a rapid chain scission has also been reported by other workers[106]. A gel content of approximately 14% was found for "crystal" polystyrene exposed to UV for 308 hours under identical conditions to the samples used in dynamic-mechanical testing. It is

believed that hydrogen abstraction by an alkoxy radical derived from the decomposition of hydroperoxides produced during thermal processing may occur at either the benzylic or methylenic centre. The bond dissociation energy of a benzylic carbon-hydrogen bond is approximately 355 $k.J.mol^{-1}$ while that of a methylenic bond is about 397 $k.J.mol^{-1}$[1]. Consequently two principal mechanistic schemes 3 and 4 are proposed to account for the chemical groupings evidenced by IR spectroscopy. Hydrogen abstraction by an alkoxy (or peroxy) radical from the tertiary benzylic centre (see scheme 3) will predominate producing an alkyl radical whose stability may be increased by resonance with the aryl substituent[107]. Nevertheless combination with atmospheric oxygen will occur rapidly with the formation of a peroxy radical capable of hydrogen abstraction from another polystyrene chain to produce hydroperoxide. Homolysis of tertiary benzylic hydroperoxide will result in an alkoxy radical which will either undergo β-scission (b) with the production of radicals or abstract a hydrogen (a) to form benzylic alcohol (3440 cm^{-1}, figure 42). Acetophenone-type end group formed via β-scission may undergo Norrish type II photolysis with molecular product formation (acetophenone) and formation of an (unsaturated) styrene end group. Norrish type I photolysis of acetophenone-type end group (or acetophenone) will result in further chain cleavage with formation of alkyl and acyl radicals. The acyl radical will combine with (diradical) oxygen producing peracid via hydrogen abstraction from the polymer hydrocarbon (RH). Breakdown of the peracid may lead to benzoic acid with further hydrogen abstraction. An important termination reaction involving alkoxy and alkyl radicals derived in scheme 3 may be postulated to account for the gel formation

observed during the latter stages of photoxidation of "crystal" polystyrene analogous to that evidenced by IR for HIPS using the same technique of difference spectroscopy. This has been attributed to tertiary aryl ether (1105 - 1000 cm^{-1}) in the case of "crystal" polystyrene.

SCHEME 3

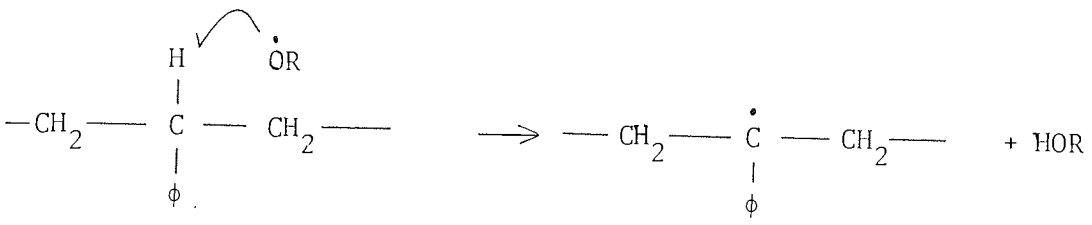

alkoxy radical abstraction of benzylic hydrogen

alkyl radical

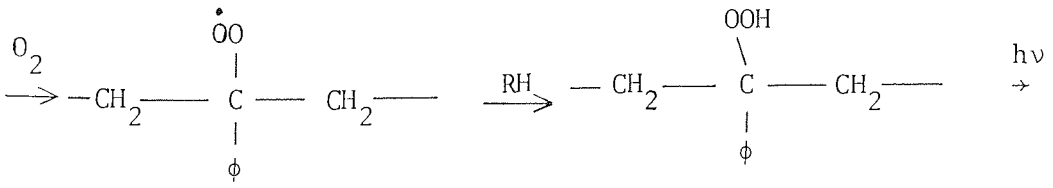

peroxy radical

benzylic hydroperoxide ($3540\ cm^{-1}$)

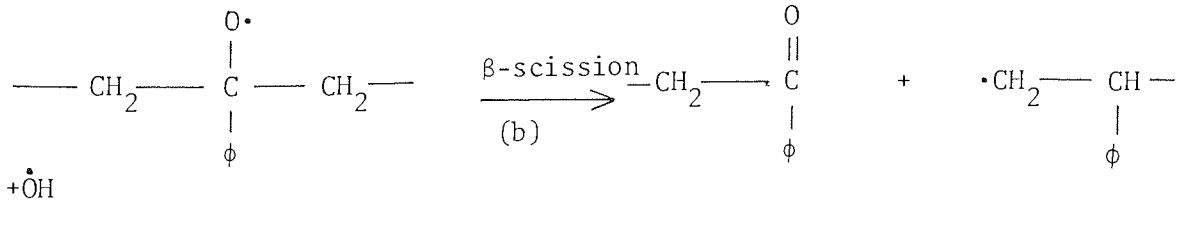

alkoxy radical

radical production accompanied by a reduction in molecular weight

(a) ↓ RH

↓

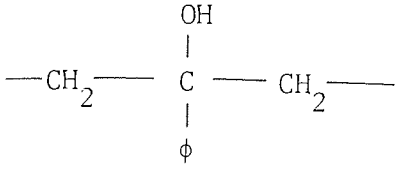

+ R·

tertiary benzylic alcohol (3440 cm^{-1})

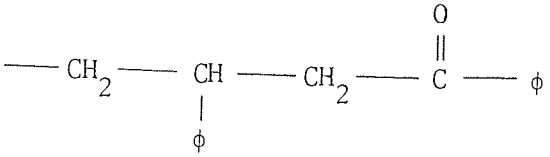

acetophenone end group (1685cm^{-1})

hν ↓ Norrish II

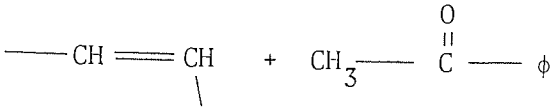

acetophenone + unsaturated chain end

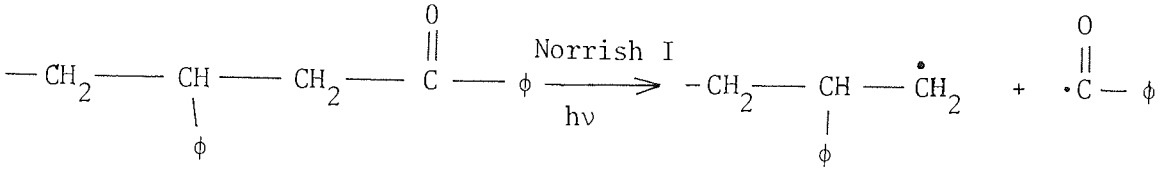

alkyl and acyl radicals

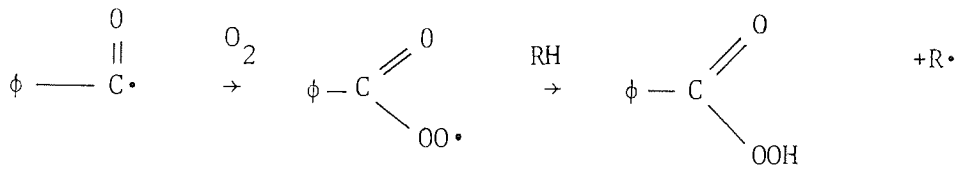

peracid

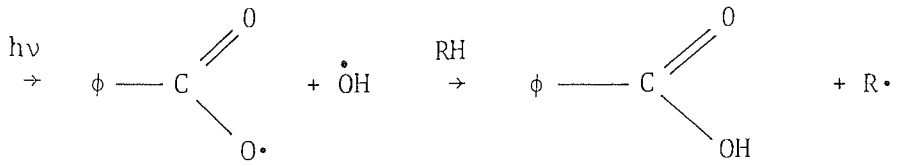

benzoic acid

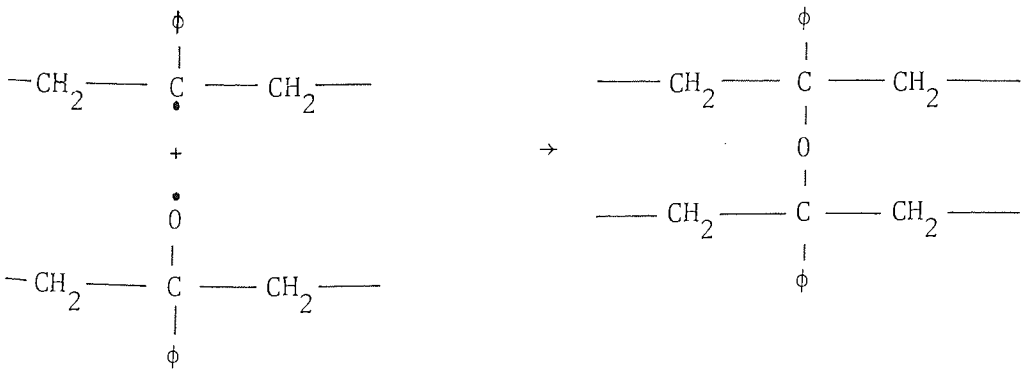

termination of alkyl and alkoxy radicals

ether linkage (1105 - 1000 cm^{-1})

Alkoxy (or peroxy) radical abstraction of the methylenic hydrogen in scheme 4 will similarly lead to formation of an alkyl radical followed by a peroxy radical. However, the hydroperoxide formed by hydrogen abstraction by the peroxy radical may either lose water to form main chain ketone (1720 cm^{-1}) or undergo homolysis resulting in an alkoxy radical. This will in turn hydrogen abstract (a) to form methylenic alcohol (3440 cm^{-1}, figure 42). Norrish-type I photolysis of β-aryl ketone (1685 cm^{-1}) will result in production of alkyl and acyl radicals accompanied by chain scission. The acyl radical will subsequently combine with (diradical) oxygen followed by hydrogen abstraction to form peracid (3280 cm^{-1}). Cleavage of the oxygen-oxygen bond of peracid will produce an alkoxy radical capable of either abstracting a hydrogen or combining with an alkyl radical to form carboxylic acid (1705 cm^{-1}) or ester (1735 cm^{-1}).

An alternative reaction to hydrogen abstraction by the methylenic alkoxy radical produced in scheme 4 is β-scission (b) resulting in formation of aldehyde (1720 cm^{-1}) and an alkyl radical accompanied by a reduction in molecular weight.

SCHEME 4

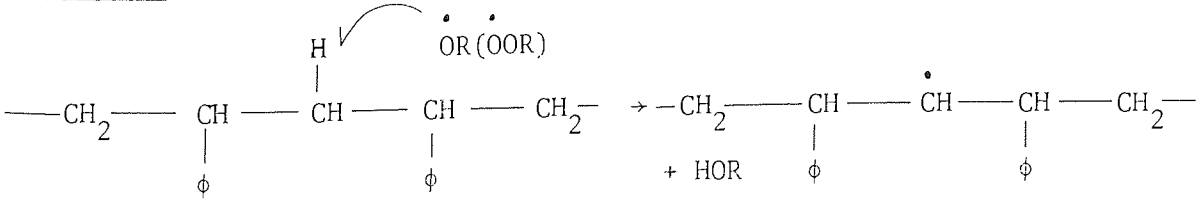

alkoxy radical abstraction of methylenic hydrogen

alkyl radical

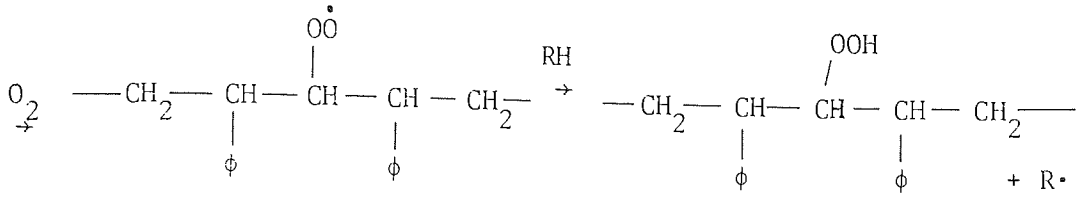

peroxy radical

methylenic hydroperoxide

hν ↓ (-H_2O)

+ •OH

alkoxy radical

β-aryl ketone (1720 cm^{-1})

(a) ↓ RH

hν ↓ Norrish I

+ •R

(methylenic alcohol (3440 cm^{-1})

production of alkyl and acyl radical, accompanied by chain scission

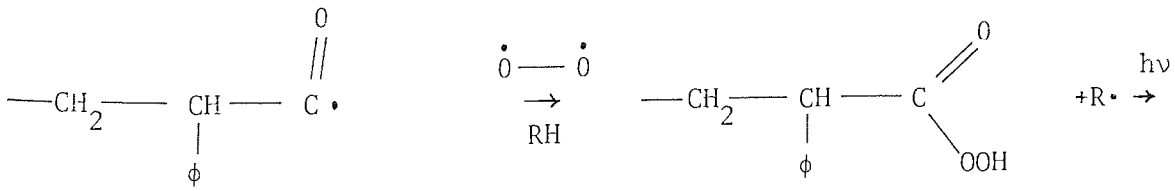

acyl radical

peracid (3280 cm^{-1})

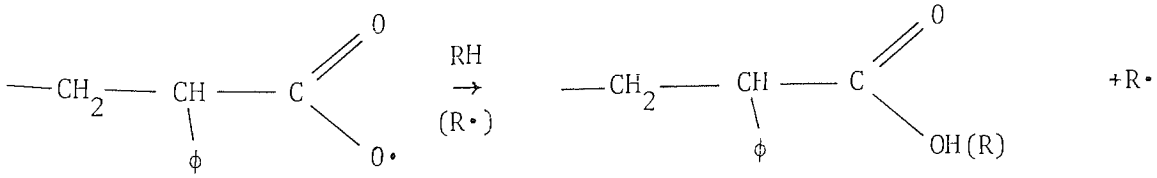

carboxylic acid (1705 cm^{-1}) or ester (1735 cm^{-1})

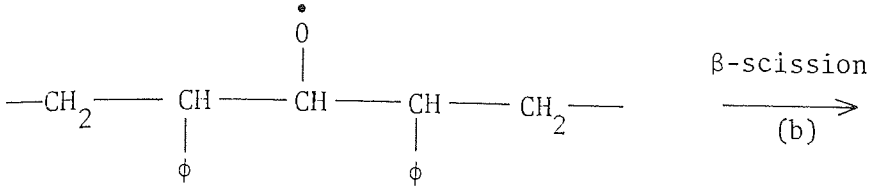

alkoxy radical

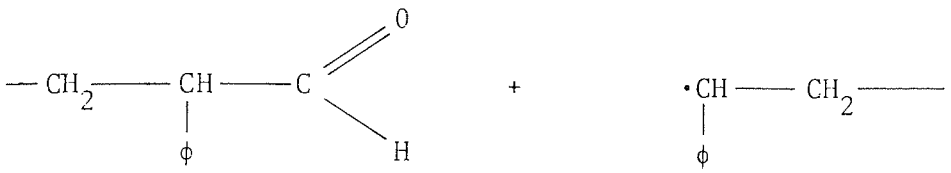

formation of aldehyde (1720 cm^{-1}) and alkyl radical accompanied by a reduction in molecular weight.

During the photoxidation of HIPS film it was not possible to observe the formation of hydroperoxide by IR. Inter-molecular hydrogen bonding will predominate in this case because of the close proximity of the allylic hydroperoxides derived from preferential oxidation of only 6.5% PBD in HIPS. Whereas photoxidation of pure polystyrene along the whole of the polymer chain will produce free hydroperoxide. In figures 15 and 27 et seq. (Chapter Two) the induction period for the decay of trans-1,4-polybutadiene during the photoxidation of HIPS extruded film containing no antioxidant was approximately 5 hours, while the induction period of trans-1,4-polybutadiene during the photoxidation of PBD cast film is about 12 hours, figure 47. However, HIPS cast film containing a commercial antioxidant (figure 50) showed an induction period of approximately 12 hours for trans-1,4-polybutadiene during photoxidation under similar conditions. Therefore it may be deduced that the presence of co-

polymerised polystyrene does not increase the stability of HIPS towards photoxidation. Furthermore the apparent instability of HIPS compared with PBD may be considered to arise from the additional labile carbon-hydrogen bonds of the tertiary allylic graft positions absent in PBD. A mechanistic scheme for the photo-degradation grafted styrene-butadiene segments was postulated in Chapter Two.

In the discussion so far the destruction of trans-1,4-polybutadiene during oxidative degradation only has been considered, although several important addition reactions involving 1,2-polybutadiene were shown in Chapter Two with respect to gel formation. It is well known that in both thermal and photoxidation the rate of destruction of the two isomers of 1,4-polybutadiene and 1,2-polybutadiene are not coincident[76] (figure 48) and that the order of reactivity is that shown in figure 47 for the photoxidation of PBD cast film. The rapid destruction of 1,2-polybutadiene may be explained by considering the formation of gel involving addition reactions to the pendant double bond to be more likely than the analogous addition of radicals to 1, 4-polybutadiene, and that the tertiary allylic carbon-hydrogen (C-H) bond of the 1,2-polybutadiene to be more labile than the secondary allylic C-H of 1,4-polybutadiene[1]. Hydrogen abstraction by an alkoxy (or peroxy) radical will result in an allylic alkyl radical which will react rapidly with oxygen to form an alkylperoxy radical capable of abstracting a hydrogen from the rubber hydrocarbon to produce allylic hydroperoxide (see scheme 5). This will be very unstable and will readily cleave under the action of UV producing a tertiary allylic alkoxy radical with the possibility of either

abstracting a hydrogen (a) resulting in allylic alcohol (3400 cm^{-1}) or undergoing β-scission with the formation of α,β-unsaturated ketone (1685 cm^{-1}) and another alkyl radical.

SCHEME 5

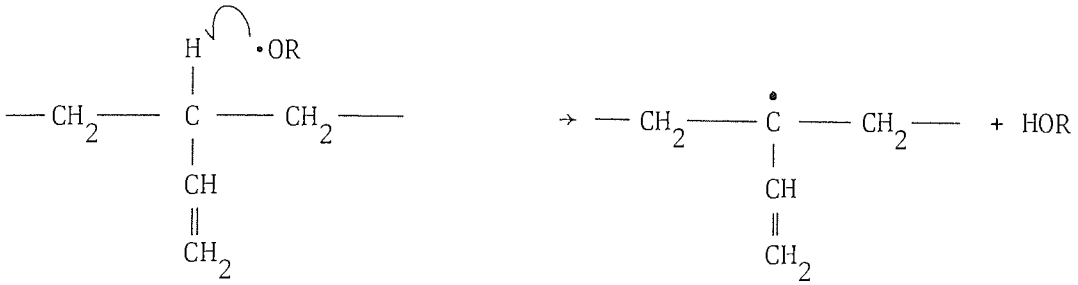

1,2-polybutadiene

(912 cm^{-1})

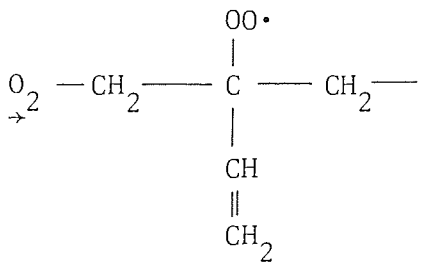

peroxy radical

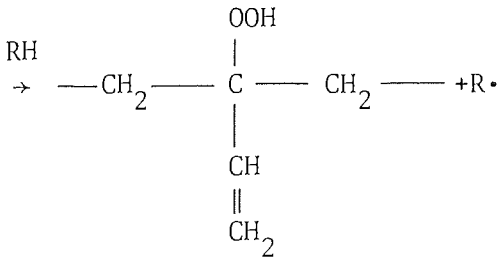

hydroperoxide (idiometry)

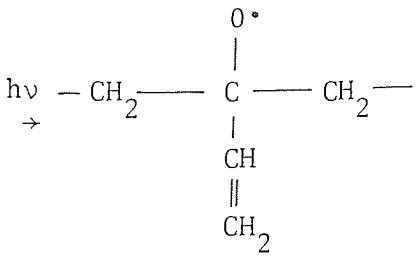

alkoxy radical

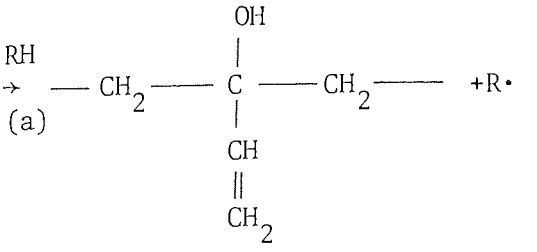

allylic alcohol (3400 cm^{-1})

(b) ↓ β-scission

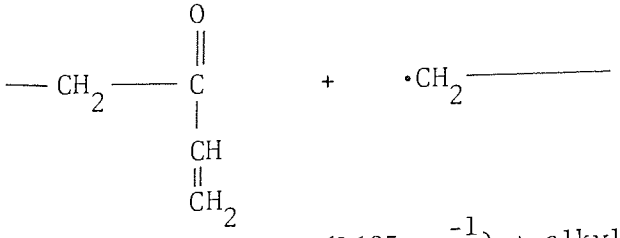

α,β-unsaturated ketone (1685 cm^{-1}) + alkyl radical

It is conceivable that the photochemical reactions postulated for trans-1,4-polybutadiene in Chapter Two may also apply to the destruction of cis-1,4-polybutadiene with the addition of cis- trans isomerism. The trans isomer will be more stable owing to the greater spatial freedom of neighbouring methylene hydrogens associated with the carbon-carbon double bond undergoing excitation and rotation[108]. Cis-trans isomerism may be invoked to explain the apparent increased susceptibility of the cis isomer relative to the trans[76]; isomerism of cis-1,4-polybutadiene during photoxidation would replenish the supply of the trans-1,4-polybutadiene. Alternatively the higher potential energy associated with the cis isomer may enhance the lability of the allylic hydrogen towards abstraction by a radical. In view of the fact that no evidence was obtained to support cis- trans isomerism as a means of depleting the concentration of the cis isomer it must be assumed that the cis isomer is more reactive.

In figure 49 an estimate of the number of cross-links produced by UV irradiation of PBD was illustrated by two linear relationships which intersected after 200 hours of exposure to UV. It is believed the rapid destruction of PBD rubber during the initial 200 hours of photoxidation shown in figure 49 as a substantial drop in tanδ measured at approximately -80°C is a result of a predominantly peroxidic gel formation, mechanistically indiscernable from the cross-linking discussed in Chapter Two for HIPS. The initial peroxidic cross-linking causes 100% gelation of the rubber making phase separation impossible after 100 to 200 hours UV exposure. After 200 hours of photoxidation further cross-linking commences at a slower rate (figure 49) this being

consistent with the formation of a more stable ether linkage. However, it must be appreciated that the thickness of the PBD film (450 μm) used for swelling, gel and Rheovibron measurements may impose a limitation on the rate of photoxidation by reducing the permeability of oxygen during increasing cross-linking. However, it is probable that oxygen-diffusion limitation serves only to extend the duration of photoxidation necessary to manifest the same physical changes as depicted in figure 49.

The destruction of the low temperature rubber peak during the photoxidation of HIPS has a profound affect on the dynamic-mechanical properties measured at ambient temperature (20°C), figure 51. The sharp peak in tanδ and loss modulus, E", occurring after 14 hours of UV exposure (figure 51) may be interpreted as a "transition" from a high damping rubbery polymer to a low damping glassy material, similar to the rubber-glass transition (Tg) encountered for HIPS (or PBD) as the temperature was lowered through -80°C. Inspection of the gel curve for HIPS extruded film shown in figure 27, (Chapter Two) revealed that the maximum weight of gel recovered occurred at about 2 hours after the sharp decrease in trans-1,4-polybutadiene absorbance. Similarly the change over to rapid decay of trans-1,4-polybutadiene absorbance shown in figure 50 for a solution cast HIPS film preceded the destruction of the low temperature peak by 2 hours. Therefore it is believed that the maximum weight of gel formed during the photoxidation of HIPS cast film occurs after 14 hours UV exposure and that changes in dynamic-mechanical damping namely loss modulus, E", and tanδ are related to gel formation. The maximum weight of gel, mainly peroxidic, is therefore coincident with the destruction

of the low temperature damping peak (tanδ) by cross-linking, figure 51. The rapid rise in complex modulus (figure 51) is consistent with a cumulative increase in cross-linking in the rubber phase confirming that the maximum weight of gel formation takes place during this period. After 25 to 30 hours UV exposure gel formation through a predominantly ether linkage is superceded by carbon-carbon chain scission causing the complex modulus to fall gradually, figure 51. It is apparent from figure 50 that the physical destruction of the rubber in HIPS film during photoxidation, monitored by the Rheovibron, is consummate before the chemical oxidation of the trans-1,4-polybutadiene. The greater reactivity of the cis isomer and 1,2-polybutadiene (figures 47 and 48) may partly account for these results. However, it is likely that a relatively small number of peroxidic and possibly ether linkages are required to alter the dynamic-mechanical properties of the rubber in HIPS.

CHAPTER 4

ACTIVATION AND STABILISATION IN MODEL SYSTEMS AND POLYMER SOLUTIONS

4.1 RESULTS

4.1.1 Effect of purification

The photoxidation of 1 ml of cumene (iso-propyl benzene) followed by oxygen absorption in an atmosphere of oxygen is shown in figure 52 with respect to purification (see 1.2.4.1). All reactions were stirred at a constant speed (see 1.4.3.3). The curves are characterised by their initial slow rate of oxygen absorption followed by a typical auto-accelerating stage leading to a linear rate. Purification appears to have no affect on the initial rate (figure 52); cumene used as supplied without purification follows initially the same course as a sample that has been re-distilled four times. However, the induction period (found by extrapolation of the linear stage to the abscissa) is markedly affected by purification. Repeated distillation of cumene under an atmosphere of argon increases the initial period of oxygen uptake before the onset of rapid auto-acceleration leading to linear kinetics, illustrated by parallel curves in figure 52. With further purification by distillation the initial stage of slow oxygen absorption could not be extended.

Effect of purification on the photoxidation of 1 ml of cumene (oxygen absorption in oxygen)

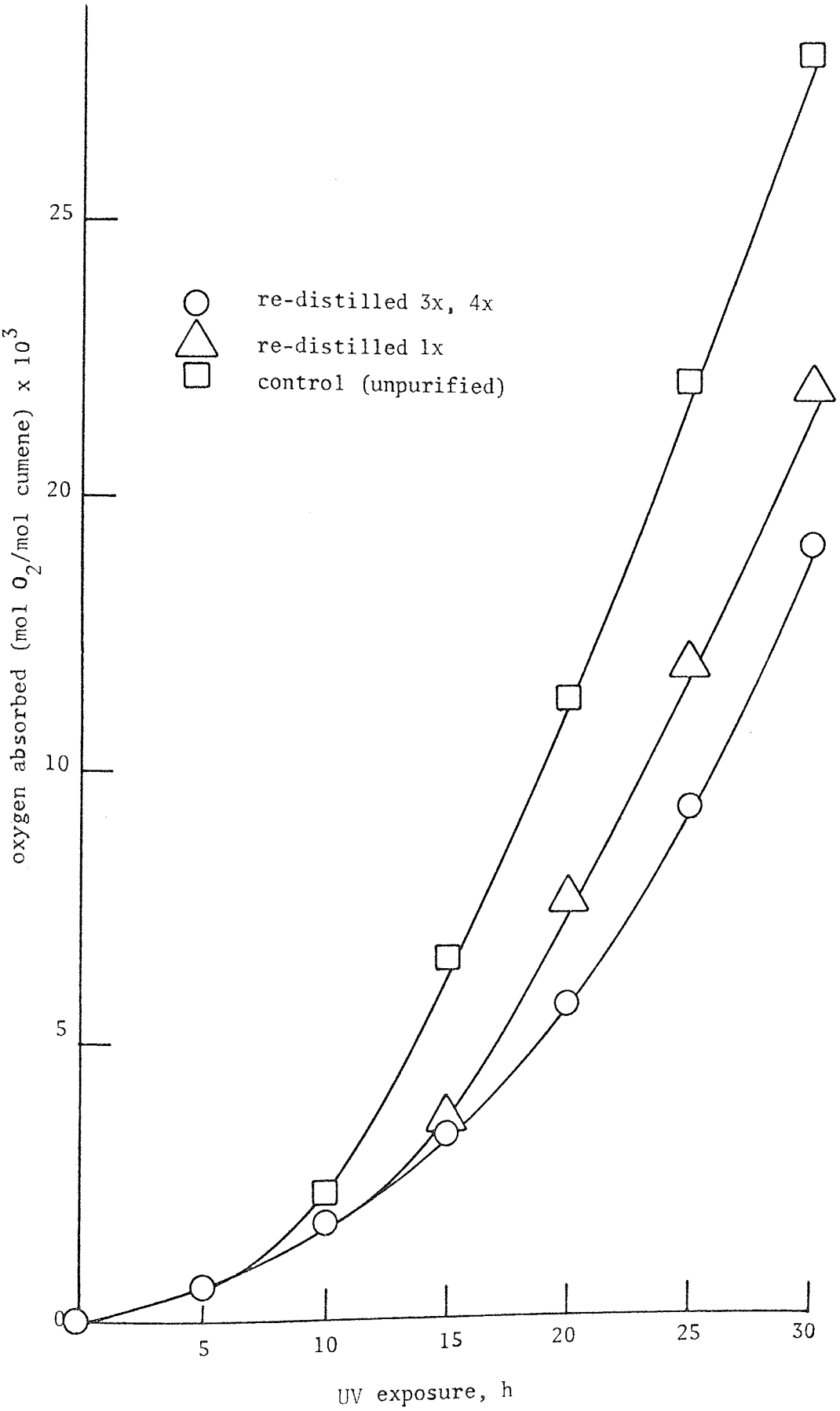

Figure 52.

4.1.2 Photoxidation of cumene by oxygen absorption

4.1.2.1 Cumene hydroperoxide

In figure 53 the effect of hydroperoxide-initiated photoxidation of pure cumene in oxygen is shown. 10 µℓ of pure cumene hydroperoxide (see 1.2.4.2), approximately 0.5×10^{-4} mols were added to 1 ml (ca. 7×10^{-3} mols) of cumene. 1% v/v cumene hydroperoxide (CHP) is sufficient to completely eliminate the auto-accelerating stage of the control giving rise to linear kinetics without induction period, figure 53. However, the hydroperoxide-initiated cumene curve is not parallel to the linear part of the control curve but proceeds at a slightly faster rate. Neither curves retard and continue to absorb oxygen at a steady rate until the hydrocarbon has been completely oxidised or possibly inhibited by oxidation products. This extreme situation is never reached in model studies portrayed in this work using cumene. Oxygen absorption was terminated after only 25×10^{-3} mols of oxygen had been absorbed by 1 mol of hydrocarbon, producing full scale deflection on the chart recorder.

4.1.2.2 Cumyl alcohol

The effects of addition of cumyl alcohol on the photoxidation of pure cumene and hydroperoxide-initiated cumene is shown in figure 54. 1% v/v cumyl alcohol (ca. 0.7×10^{-4} $mol.ml^{-1}$) reduced the induction period and increased the linear rate (after absorbing about 2×10^{-3} mols of oxygen) closer to that for 1% v/v CHP. Increasing the concentration of cumyl alcohol to 5% v/v (ca. 3×10^{-4} $mol.ml^{-1}$) does not eliminate the auto-accelerating stage of the curve

Effect of hydroperoxide on the photoxidation of 1 ml of cumene (oxygen absorption in oxygen)

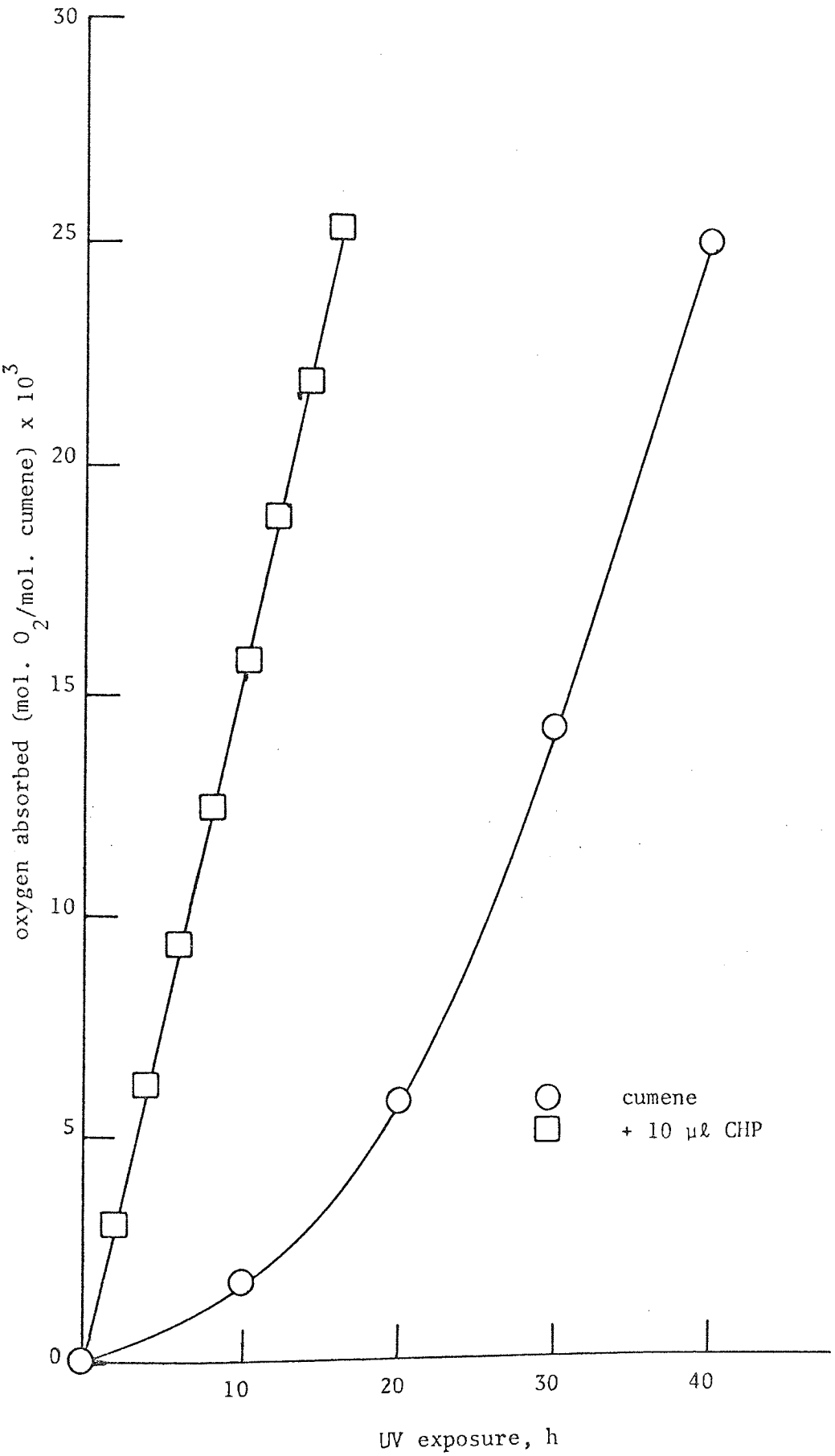

Figure 53.

Effect of cumyl alcohol on the photoxidation of 1 ml of cumene and hydroperoxide - initiated cumene (oxygen absorption in oxygen)

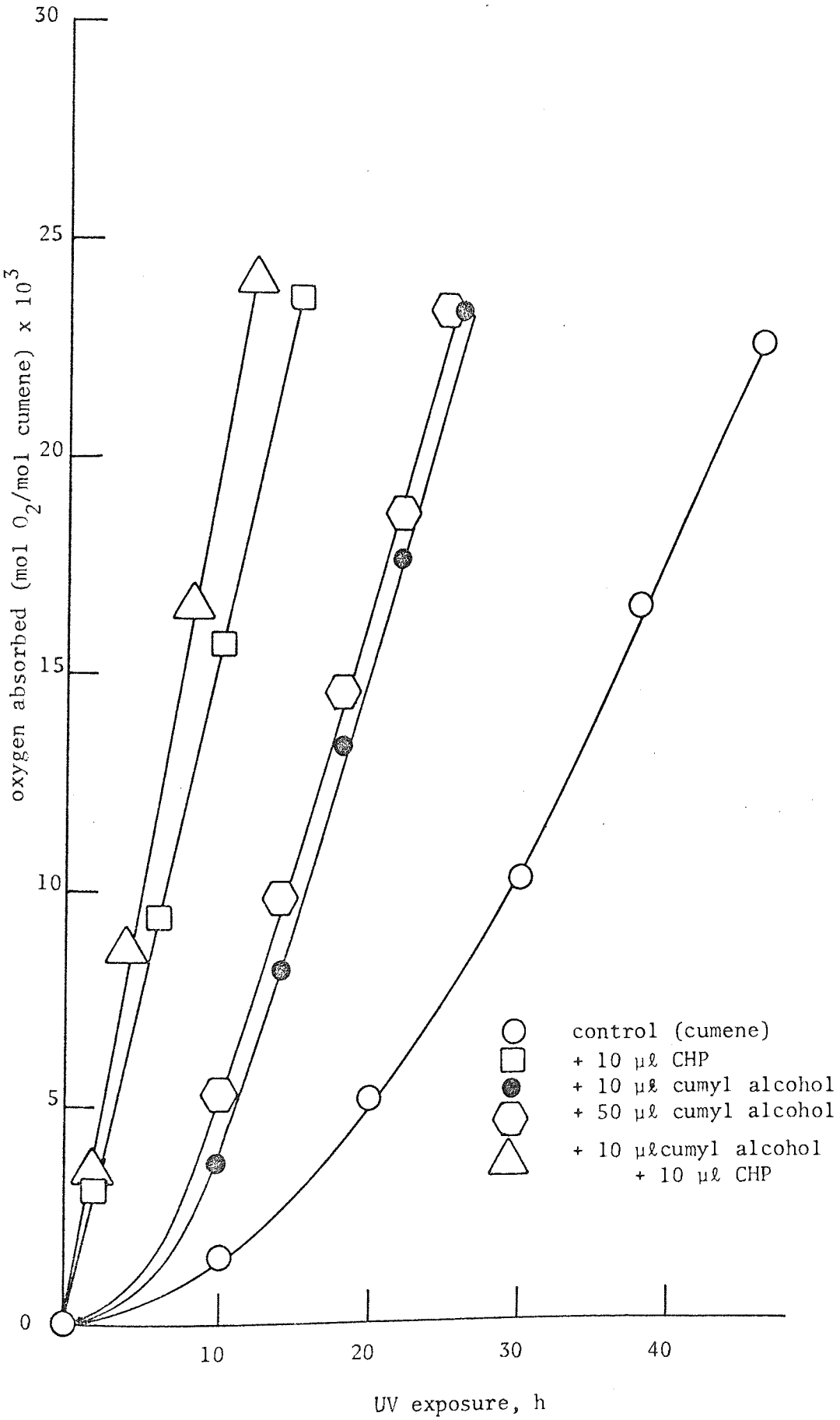

Figure 54

and only marginally reduced the induction period figure 54. However, a concentration of 1% v/v cumyl alcohol in 1 ml of cumene initiated by 1% v/v CHP increased the rate of oxygen absorption relative to the hydroperoxide-initiated "control", figure 54.

4.1.2.3 Dinonyl ketone

Addition of approximately 1×10^{-4} mols of dinonyl ketone (crystals) to 1 ml of cumene has a similar effect to 1% v/v cumyl alcohol. However, the curve does not attain linear kinetics until about 14×10^{-3} mols of oxygen have been absorbed, figure 55. Increasing the concentration of dinonyl ketone to approximately 5×10^{-4} $mol.ml^{-1}$ has no effect on the initial rate of oxygen absorption, but after about 5×10^{-3} mols of oxygen have been absorbed the sample containing 5×10^{-4} mols of dinonyl ketone became parallel to the control, figure 55. However, addition of 1×10^{-4} mols of dinonyl ketone to 1 ml of cumene initiated by 1% v/v CHP increases the rate of oxygen absorption relative to cumene initiated by hydroperoxide only, in a similar manner to that for cumyl alcohol, figure 54.

4.1.2.4 Mesityl oxide

Mesityl oxide (4-methyl-3-penten-2-one) has a more marked affect on the initial rate of oxygen absorption of cumene then dinonyl ketone. Addition of 10 µℓ (ca. 1×10^{-4} mols) of mesityl oxide to 1 ml of cumene increases the initial rate to such an extent that the auto-accelerating character of the curve tended towards linearity, figure 56. Increasing the concentration of mesityl oxide

Effect of dinonyl ketone on the photoxidation of 1 ml of cumene and hydroperoxide-initiated cumene (oxygen absorption in oxygen)

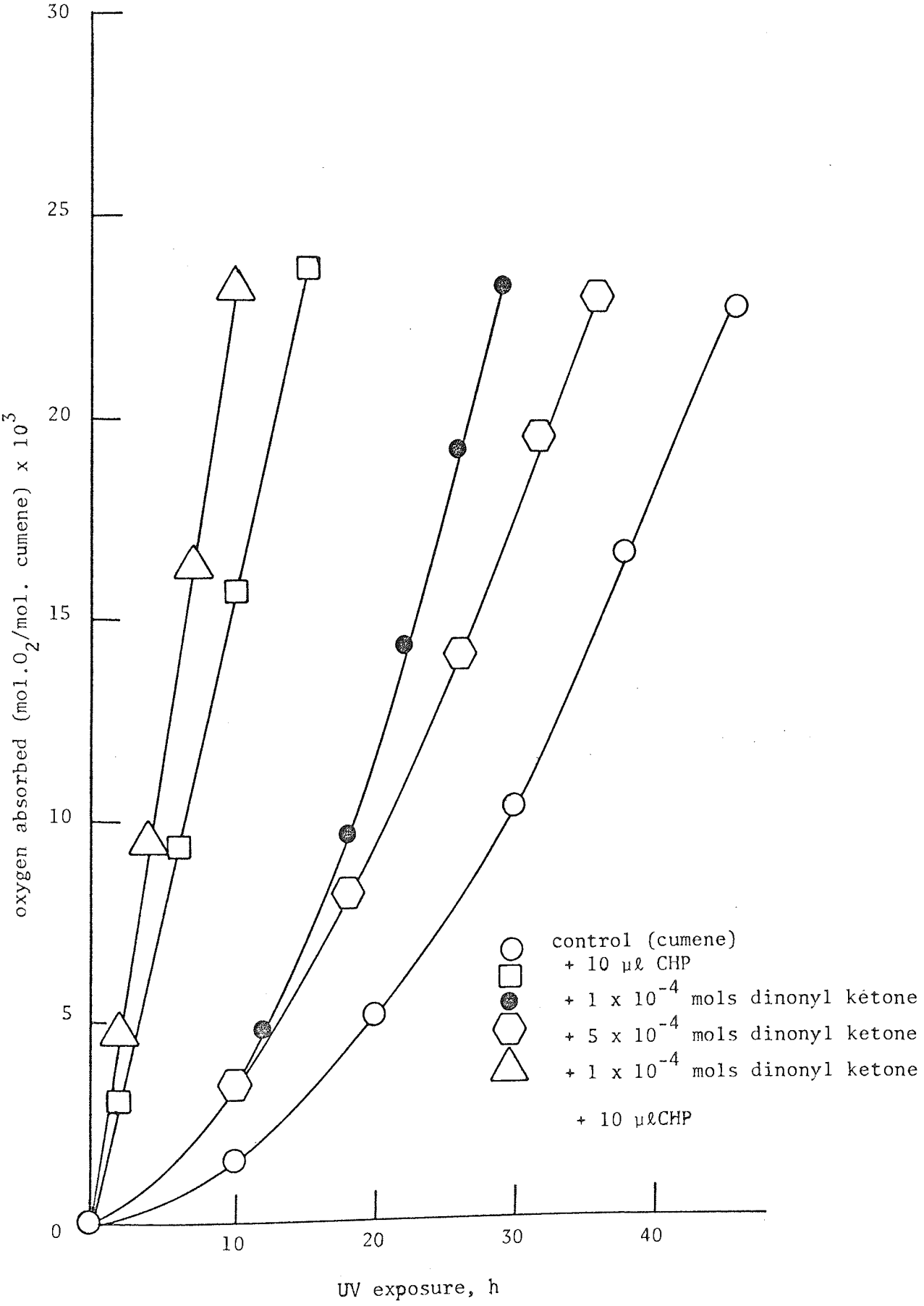

Figure 55

Effect of mesityl oxide on the photoxidation of 1 ml of cumene and hydroperoxide-initiated cumene (oxygen absorption in oxygen)

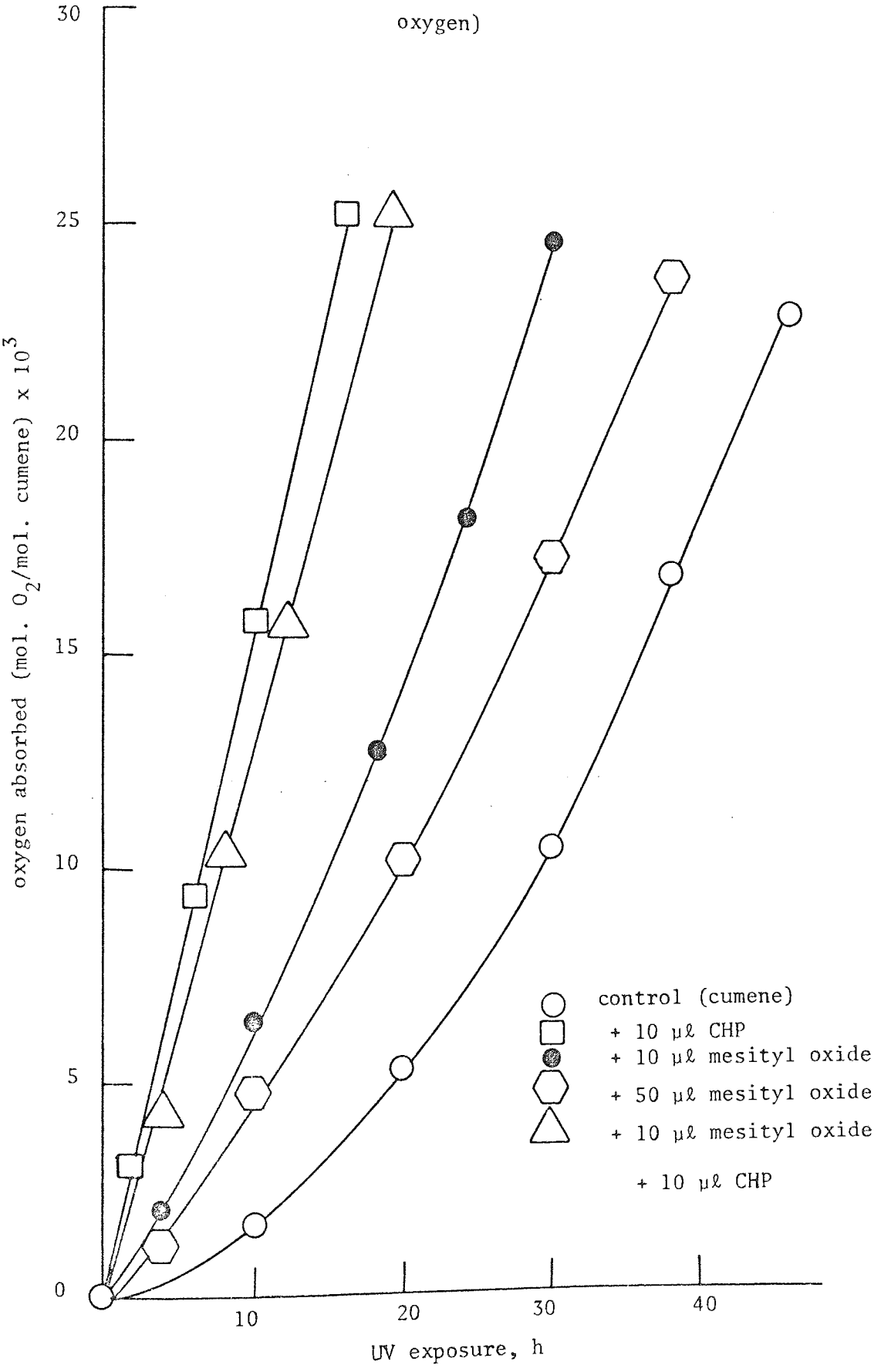

Figure 56.

to 5% v/v (ca. 5 x 10^{-4} mol. ml^{-1}) has an entirely analogous effect to dinonyl ketone (figure 55), the sample containing 5% v/v mesityl oxide became parallel to that of the control, figure 56. In contrast to dinonyl ketone, mesityl oxide retards the rate of oxygen absorption of cumene initiated by 1% CHP (figure 56) by an amount equivalent to its activation by dinonyl ketone or cumyl alcohol, figures 54 and 55.

4.1.2.5 Acetophenone

The effect of addition of acetophenone to cumene is shown in figure 57. Increasing the concentration of acetophenone from 1% v/v (ca. 0.8 x 10^{-4} mol. ml^{-1}) to 5% v/v (ca. 4 x 10^{-4} mol. ml^{-1}) raises the initial rate substantially and the linear rate marginally. This is in contrast with both dinonyl ketone (figure 55) and mesityl oxide (figure 56) which retarded the photoxidation of cumene at higher concentrations. In figure 57 the linear stage of the sample containing 1% v/v acetophenone is parallel to the hydroperoxide-initiated "control" curve, while at a concentration of 5% v/v the linear rate is greater, although the initial rate was slightly lower thus retaining its auto-catalytic nature. When 10 µℓ (ca.0.8 x 10^{-4} mols) acetophenone is added to 1 ml of cumene initiated by 1% CHP the linear rate surpasses that of the hydroperoxide-initiated "control" curve and became parallel to the curve representing 5% v/v acetophenone, figure 57.

4.1.2.6 Benzaldehyde

In marked contrast to the above carbonyl compounds 1% v/v (ca. 0.9 x 10^{-4} mol. ml^{-1}) benzaldehyde completely removes the

Effect of acetophenone on the photoxidation of 1 ml of cumene and hydroperoxide-initiated cumene (oxygen absorption in oxygen)

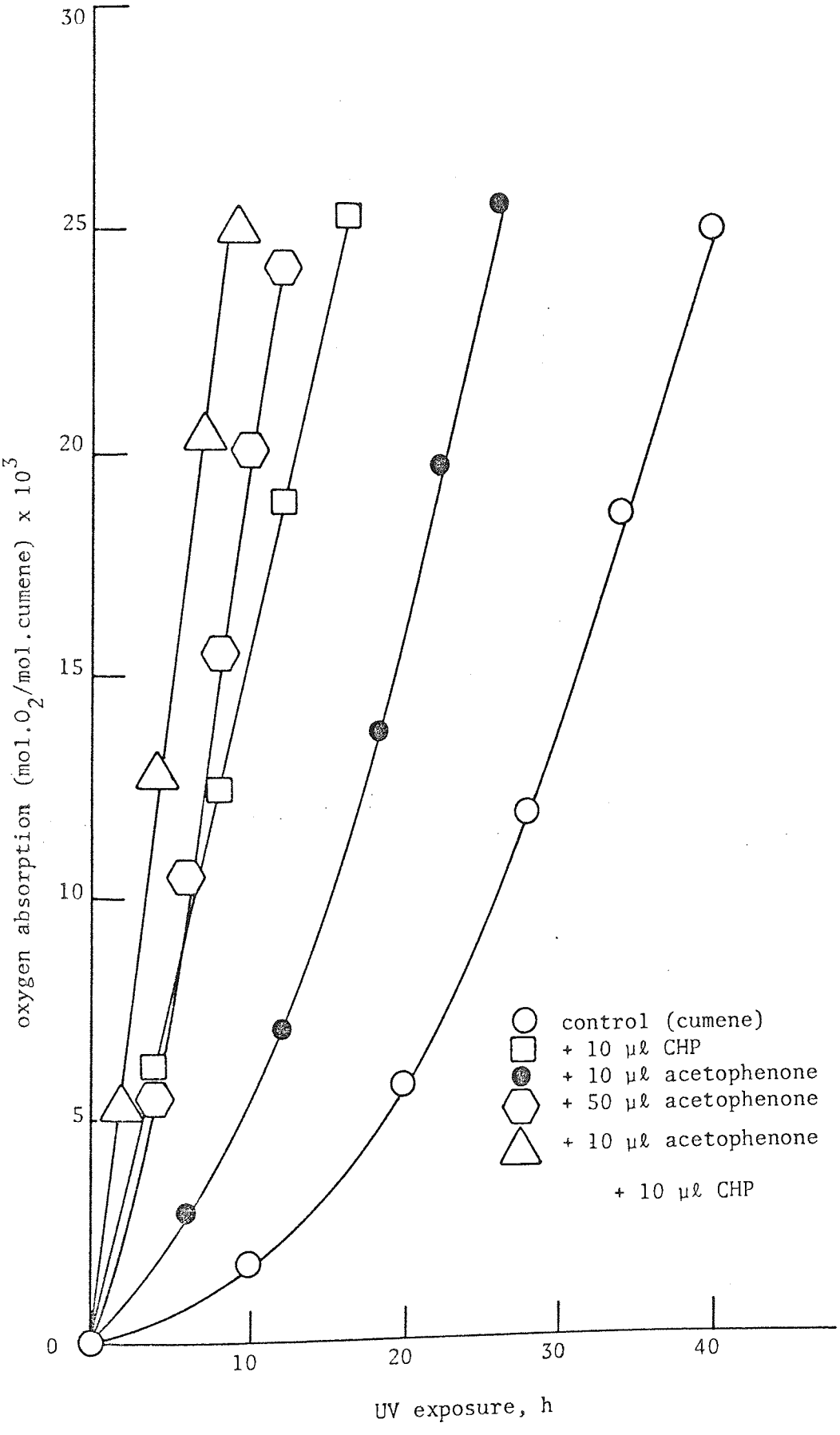

Figure 57.

Effect of benzaldehyde on the photoxidation of 1 ml of cumene and hydroperoxide-initiated cumene (oxygen absorption in oxygen)

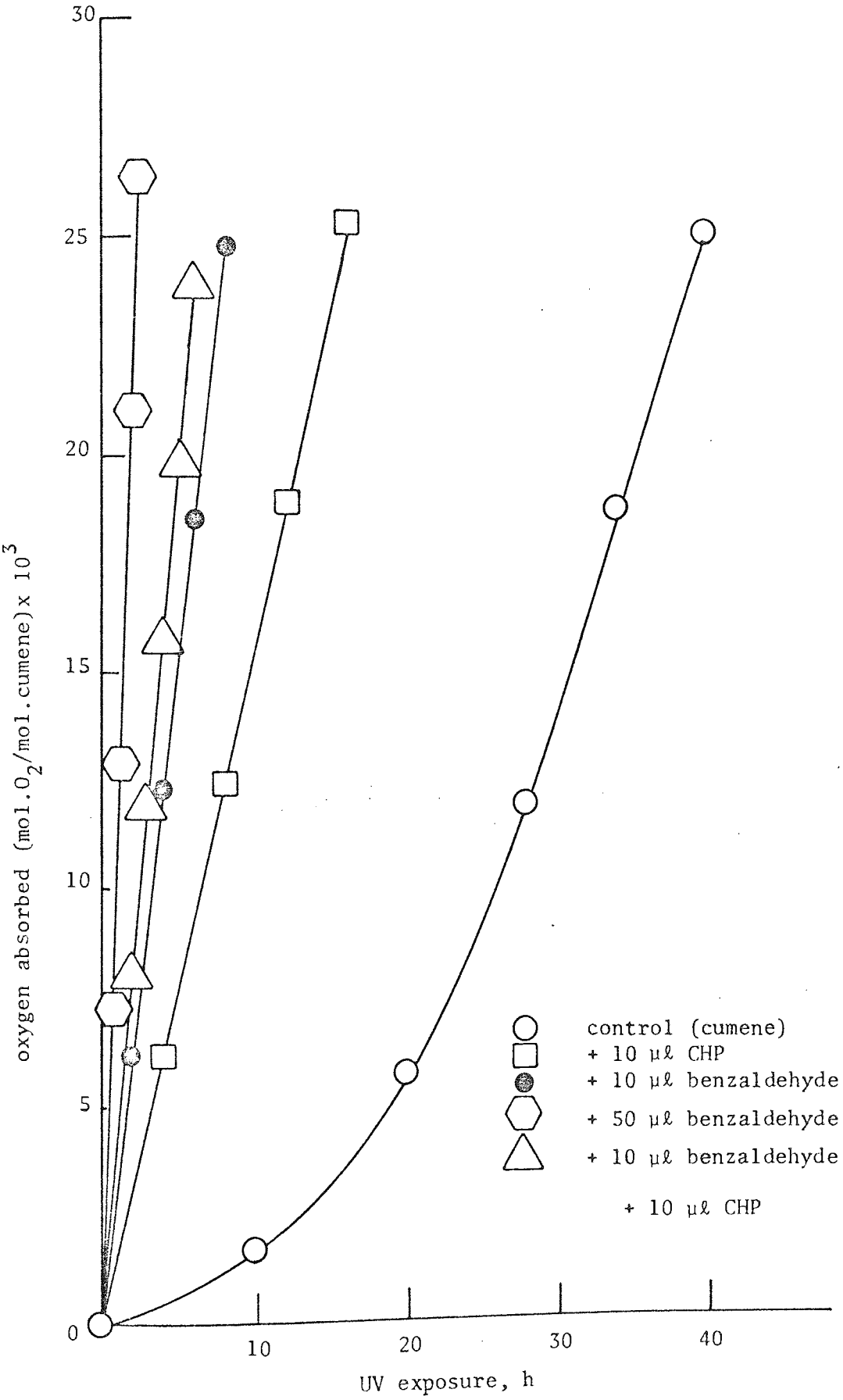

Figure 58.

auto-catalytic stage of the curve and proceeds at a faster rate than the hydroperoxide-initiated cumene "control" curve, figure 58. Increasing the concentration of benzaldehyde to 5% v/v (ca. 5×10^{-4} mol. ml^{-1}) activates the cumene towards rapid photoxidation with a substantial increase in rate, resulting in an absorption of 25×10^{-3} mols of oxygen after only 3 hours exposure to UV, figure 58. Cumene containing no additives absorbed only 0.34×10^{-3} mols of oxygen during the same period. Addition of 10 µl (ca.0.9×10^{-4} mols) of benzaldehyde to 1 ml of cumene initiated by 1% v/v CHP greatly increases the rate of oxygen absorption relative to the hydroperoxide-initiated "control" but was only marginally faster than the curve representing 1% v/v benzaldehyde, figure 58.

4.1.2.7 Benzoic acid

Addition of approximately 0.8×10^{-4} mols of benzoic acid (crystals) has little affect on the photoxidation of 1 ml of cumene, figure 59. However, the relatively low concentration of benzoic acid does reduce the induction period by a small amount; oxygen absorption parallels the control curve till about 14×10^{-3} mols of oxygen have been absorbed by 1 mol of cumene and then retards slightly but does not fall below that of the control within the time scale shown, figure 59. At a higher concentration of benzoic acid (ca. 4.0×10^{-4} mol. ml^{-1}) only a very small increase in initial rate is apparent, figure 59; the curve is almost coincident with the control but after 14×10^{-3} mols of oxygen have been absorbed it retards and falls below that of the control. The retarding influence

Effect of benzoic acid on the photoxidation of 1 ml of cumene and hydroperoxide-initiated cumene (oxygen absorption in oxygen)

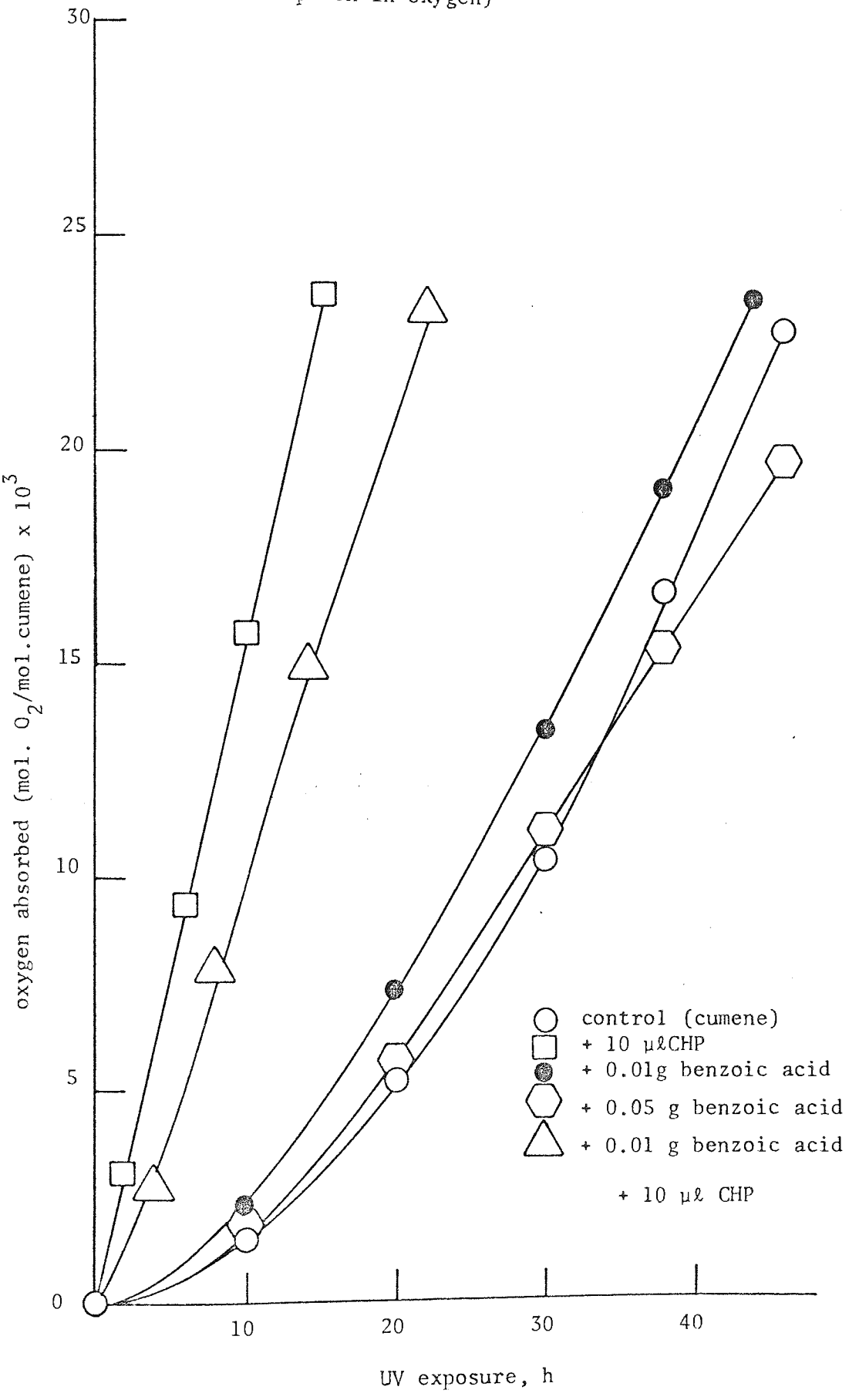

Figure 59.

of benzoic acid is also imparted on cumene initiated by 1% v/v, CHP, figure 59. The slight "inhibition" by approximately 0.8 x 10^{-4} mols of benzoic acid during the early stages of oxygen absorption by the hydroperoxide-initiated cumene produces a curve with a partial auto-accelerating character, figure 59.

4.1.2.8 Phenyl acetic acid

The effect of addition of phenyl acetic acid (crystals) on the photoxidation of cumene is shown in figure 60. Entirely analogous results are obtained to those depicted in figure 59 for benzoic acid. However, it appears that phenyl acetic acid is more effective than benzoic acid in its ability to retard the photoxidation of cumene. Addition of approximately 0.7 x 10^{-4} mols of phenyl acetic acid to 1 ml of cumene has only a marginal affect on the initial rate and induction period. Similarly, a higher concentration of phenyl acetic acid (ca. 4 x 10^{-4} mol. ml^{-1}) has no affect on the initial rate and retarded the photoxidation of cumene after only 1.4 x 10^{-3} mols of oxygen had been absorbed. A relatively low concentration of phenyl acetic acid (0.7 x 10^{-4} mol. ml^{-1}) in cumene initiated by 1% v/v CHP "inhibited" oxygen absorption to a greater extent than the equivalent molar concentration of benzoic acid.

4.1.2.9 β-carotene

The notable effect of β-carotene on the photoxidation of pure un-initiated cumene is shown in figure 61. Addition of approximately 0.2 x 10^{-4} mols (0.01 g) of β-carotene (powder) to 1 ml

Effect of phenyl acetic acid on the photoxidation of 1 ml of cumene and hydroperoxide-initiated cumene (oxygen absorption in oxygen)

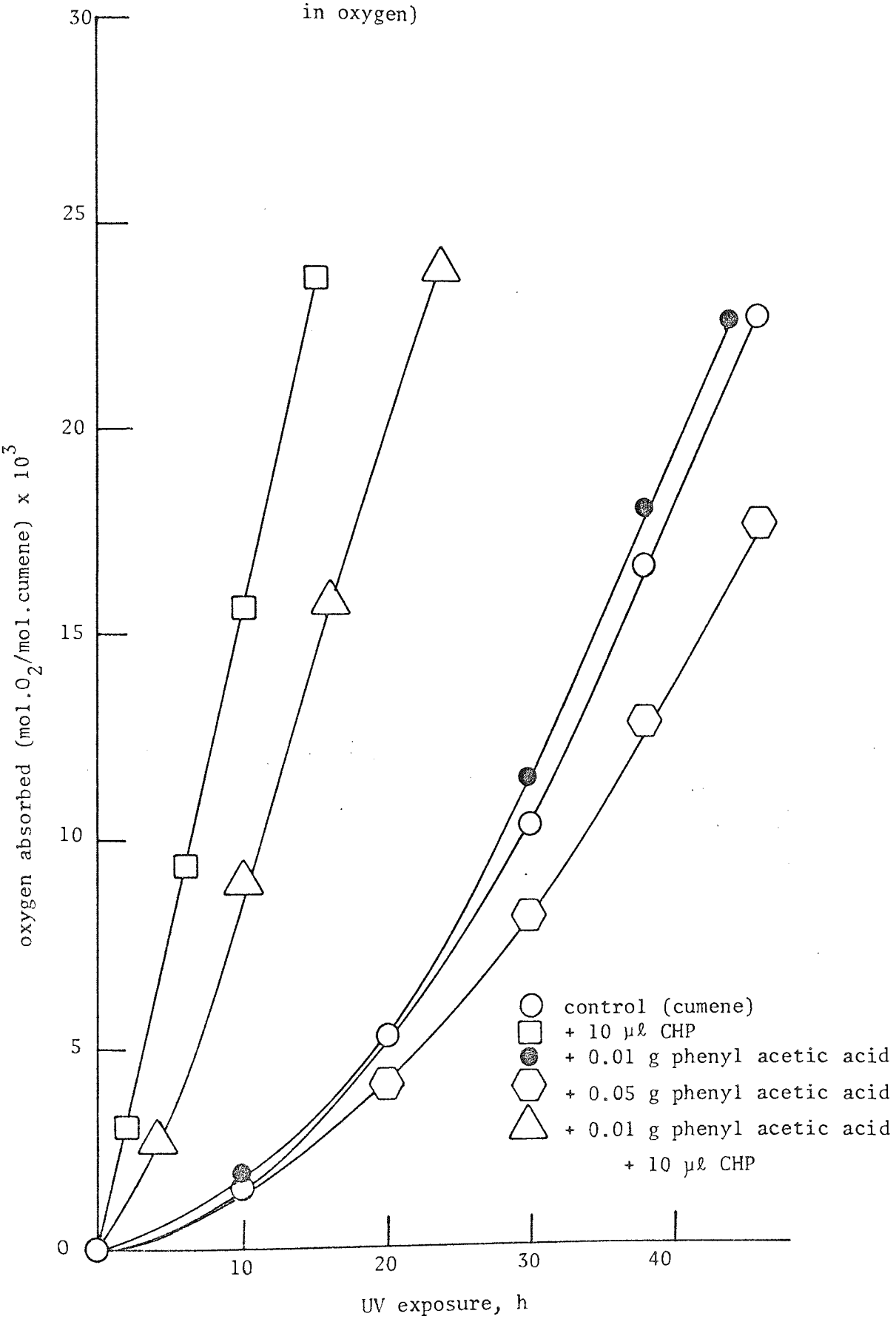

Figure 60.

Effect of β-carotene on the photoxidation of 1 ml of cumene and hydroperoxide-initiated cumene (oxygen absorption in oxygen)

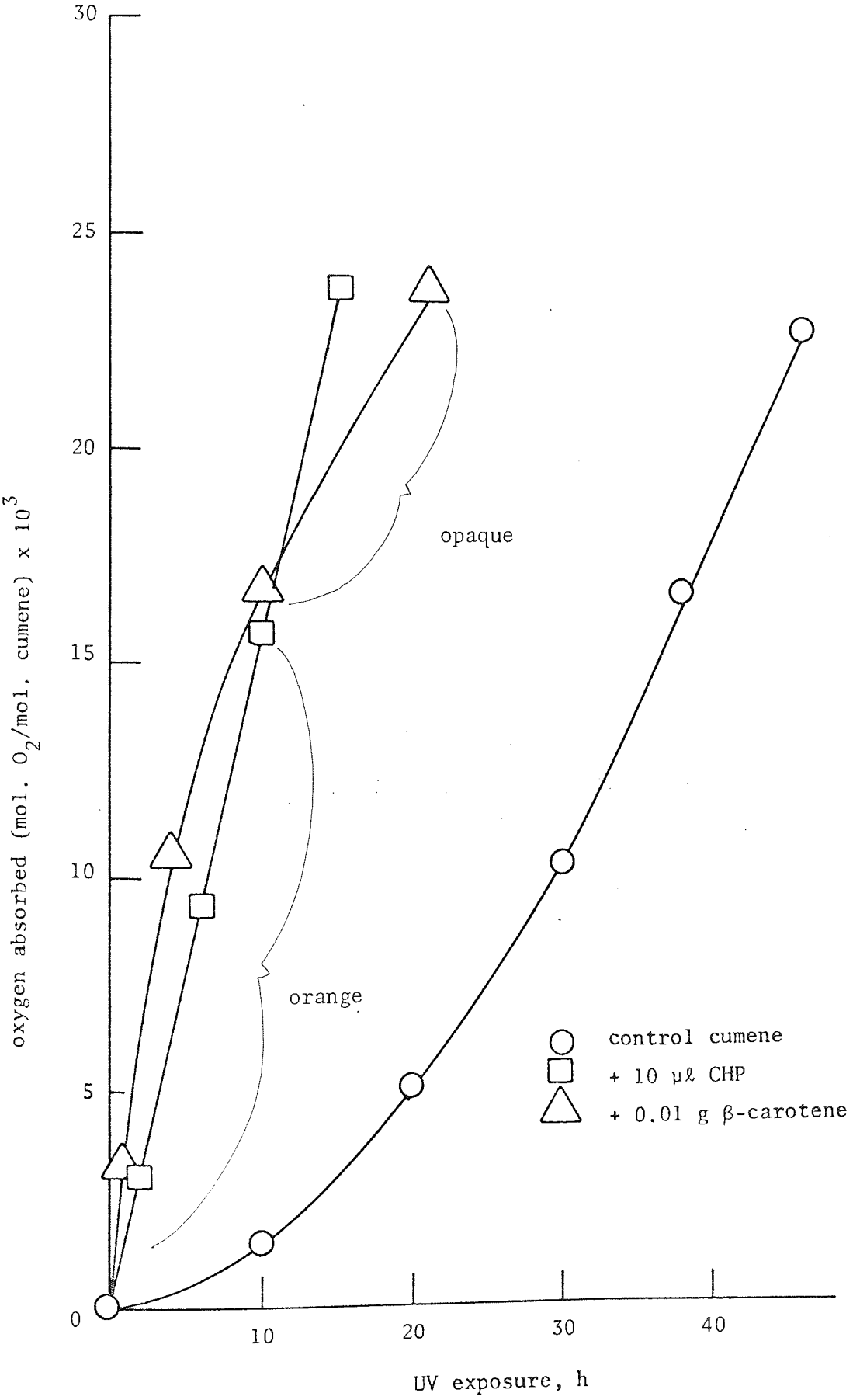

Figure 61.

of cumene activates the hydrocarbon to rapid photoxidation as indicated by the very fast initial rate of oxygen absorption, figure 61. After the sample containing β-carotene has absorbed about 10 x 10^{-3} mols of oxygen the rapid rate subsides and with further oxygen absorption (17 x 10^{-3} mols) crosses over the hydroperoxide-initiated "control" curve and returns to a rate of oxygen absorption parallel to the un-initiated cumene curve, figure 61. During this change-over period (after 10 hours exposure to UV) the characteristic bright red-orange of the β-carotene solution disappeared and was replaced by an off-white appearance.

4.1.2.10 3-methyl-1-butene

In contrast to the powerful activation bestowed by β-carotene, 3-methyl-1-butene has only a marginal affect on the photoxidation of initiated and un-initiated cumene, figure 62. A concentration of 5% v/v (ca. 5 x 10^{-4} mol. ml^{-1}) of 3-methyl-1-butene in cumene increases the initial rate slightly and the linear rate after approximately 10 x 10^{-3} mols of oxygen have been absorbed. A lower concentration (1% v/v) had no discernable affect on the rate of photoxidation of cumene. Similarly 5% v/v 3-methyl-1-butene in cumene initiated by 1% v/v CHP has practically no affect of the mode of oxygen absorption, figure 62. However, there appears to be a very slight "inhibition" introduced by addition of 3-methyl-1-butene in the early stages of oxygen absorption of hydroperoxide-initiated cumene, figure 62. This is followed by a marginally increased linear rate which retards slightly after about 17 x 10^{-3} mols of oxygen have been absorbed

Effect of 3-methyl-1-butene on the photoxidation of 1 ml of cumene and hydroperoxide-initiated cumene (oxygen absorption in oxygen)

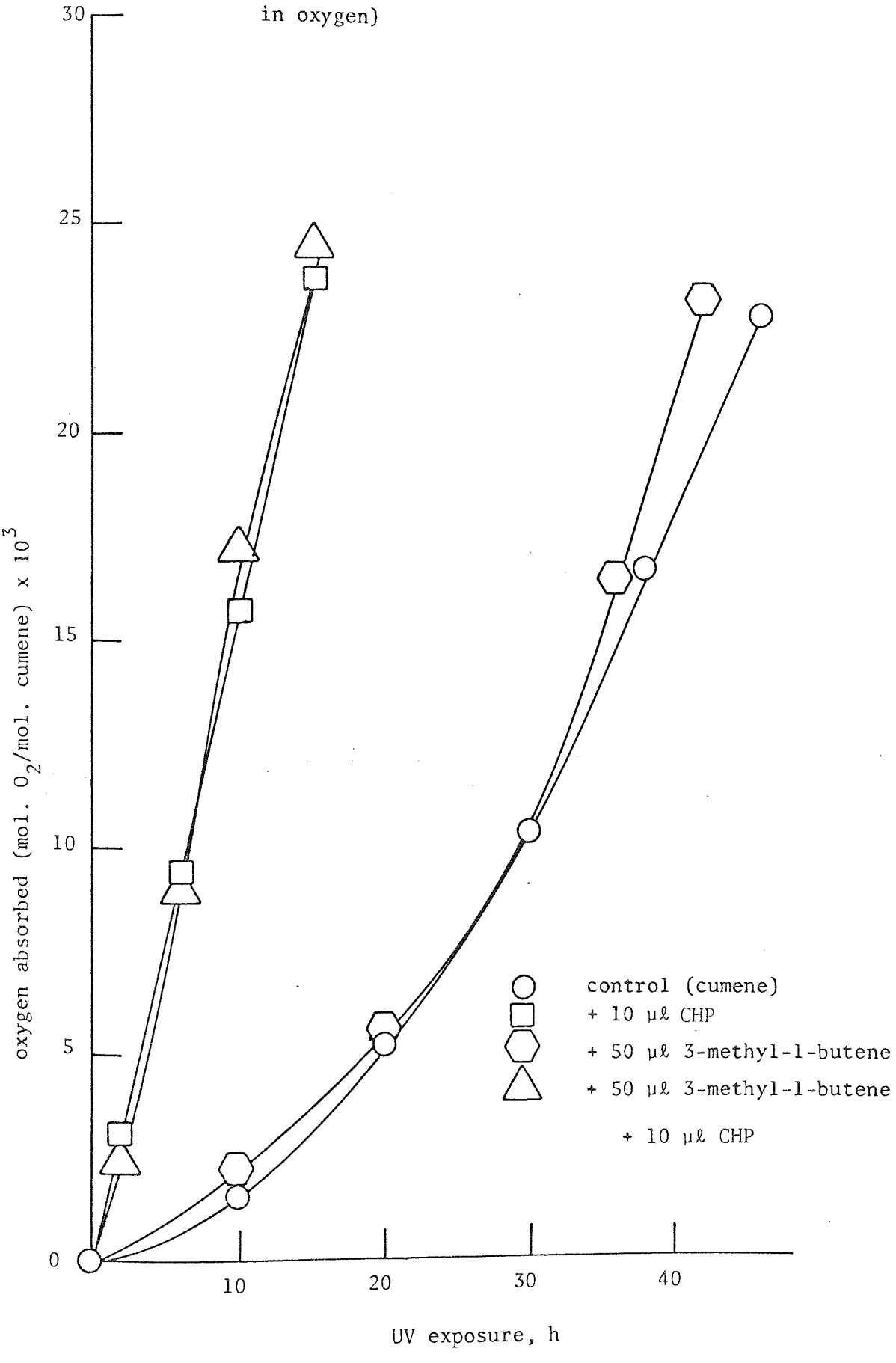

Figure 62.

and returns to a rate of oxygen absorption parallel to that representing 5% v/v 3-methyl-1-butene in cumene, figure 62.

4.1.3 Photoxidation of polybutadiene in chlorobenzene by oxygen absorption

4.1.3.1 Cumene hydroperoxide, cumyl alcohol and acetophenone

The effect of addition of CHP, cumyl alcohol and acetophenone on the photoxidation of a 1% w/v solution of PBD in chlorobenzene is shown in figure 63 (a 1% w/v solution was made by dissolving 1.0 g of polybutadiene rubber (see 1.1) in 100 ml of chlorobenzene under an atmosphere of argon, the solution was kept in a dark bottle below 0°C). All reactions were performed under identical conditions to those used for cumene (see 4.1.2) in quartz apparatus stirred at a constant speed under an atmosphere of oxygen. Addition of 100 µℓ of CHP to 1 ml of 1% w/v PBD solution (ca. 5×10^{-2} mol. g^{-1}) completely removes the auto-catalytic stage of the oxygen absorption curve representing the control, figure 63. The hydroperoxide-initiated curve proceeds with a linear rate for 10 hours and is parallel to that of the control up to 21 hours of exposure to UV, after which oxygen absorption drops sharply to the control curve, figure 63. Both the hydroperoxide-initiated PBD and the control curve retard after 10 hours UV exposure in contrast with cumene, figure 53. It will be appreciated that a higher concentration of hydroperoxide (CHP) is required to completely eliminate the induction period; a 10% v/v solution of CHP was used in this work. Similarly addition of 100 µℓ of acetophenone to 1 ml of 1% w/v PBD solution (ca. 8×10^{-2} mol. g^{-1})

Effect of cumene hydroperoxide, cumyl alcohol and acetophenone on the photoxidation of 1 ml of a 1% w/v solution of PBD in chlorobenzene (oxygen absorption in oxygen)

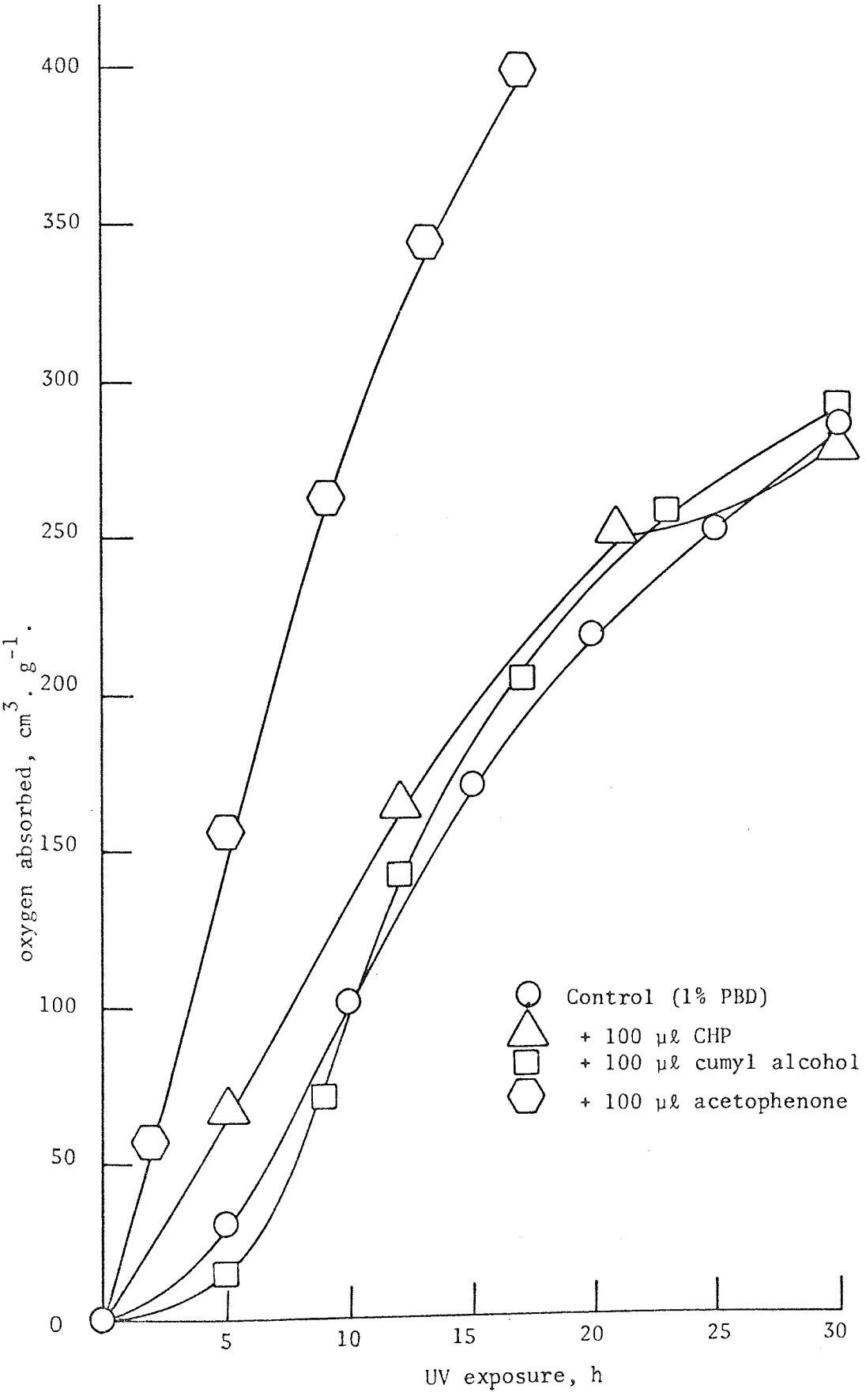

Figure 63.

greatly increases the initial rate of photoxidation (figure 63), the linear rate being considerably faster than hydroperoxide-initiated PBD solution. The latter observation was consistent with a concentration of 5% v/v acetophenone in cumene, figure 57. However, after about 10 hours UV exposure the rate of oxygen absorption of the PBD solution containing acetophenone retards slightly but retains a higher rate than that of the control, figure 63. Addition of 100 µℓ of cumyl alcohol to 1 ml of 1% w/v PBD in chlorobenzene (ca. 7×10^{-2} mol. g^{-1}) "inhibits" the photoxidation of the PBD solution shown by a decrease in the initial rate and an extension of the induction period, figure 63. After the auto-catalytic stage of oxygen absorption curve the linear rate of the 10% v/v cumyl alcohol sample increases faster than the control and the hydroperoxide-initiated PBD solution but is parallel to the curve representing 10% v/v acetophenone. However, after about 10 hours of exposure to UV the curve retards and proceeds parallel to the control, figure 63.

4.1.3.2 Dinonyl ketone

The effect of addition of dinonyl ketone on the photoxidation of 1% w/v PBD in chlorobenzene is shown in figure 64. At a relatively low concentration of approximately 5×10^{-2} mol. g^{-1} the photoxidation of PBD retards slightly, although both the initial and linear rates are not affected, figure 64. After 22 hours exposure to UV the rate of oxygen absorption drops sharply similar to that experienced for 10% v/v CHP in 1% w/v PBD solution figure 63. Increasing the concentration to approximately 10×10^{-2} mol. g^{-1} does not alter the initial rate of oxygen absorption, although

Effect of dinonyl ketone on the photoxidation of 1 ml of a 1% w/v solution of hydroperoxide-initiated and uninitiated PBD in chlorobenzene (oxygen absorption in oxygen)

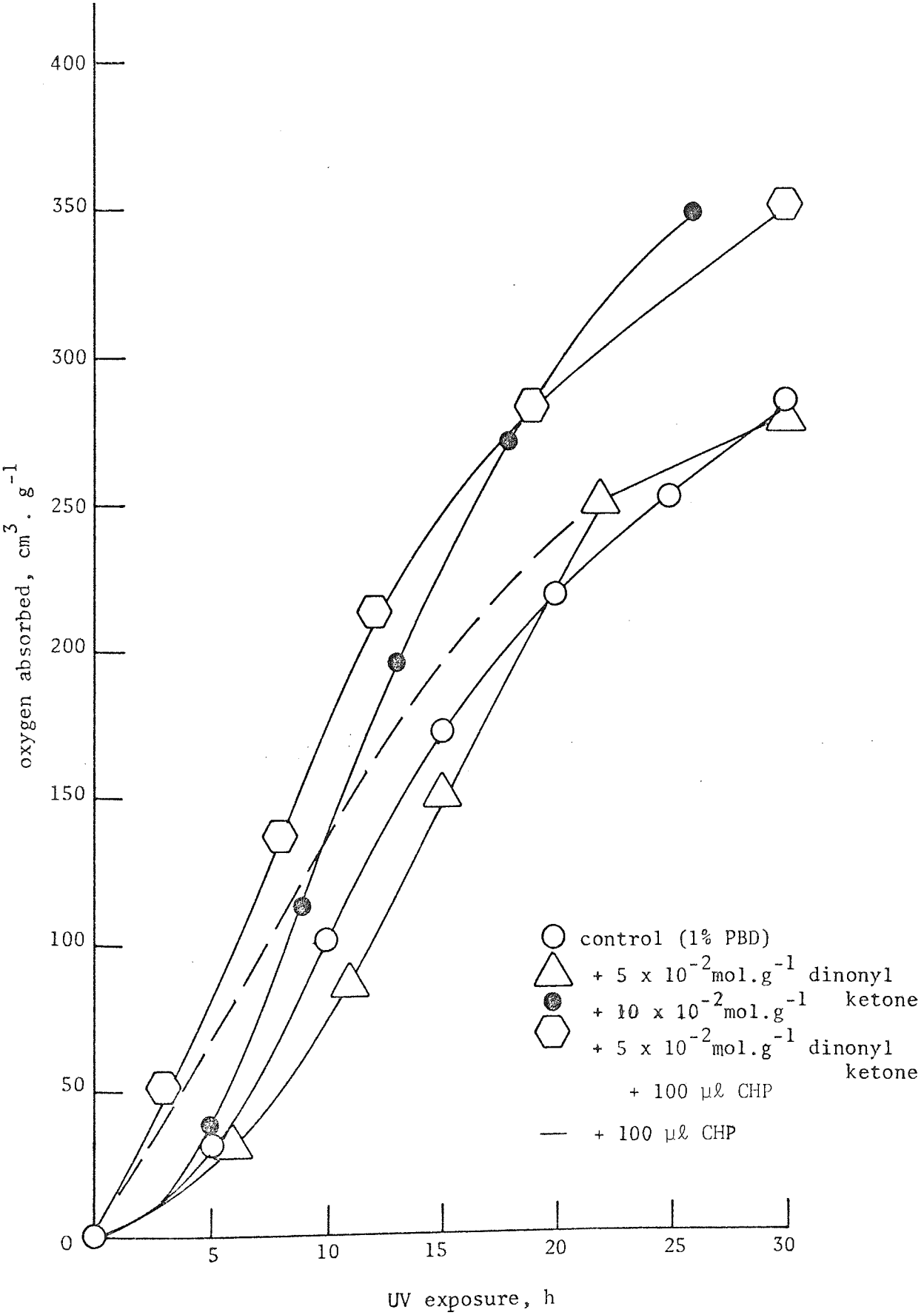

Figure 64.

the linear rate is substantially increased. Oxygen absorption by this sample proceeds to a greater extent than the control, figure 64. Addition of approximately 5 x 10^{-2} mols of dinonyl ketone to 1 ml of 1% PBD solution initiated by 50 µℓ of CHP completely removes the auto-catalytic stage of the oxygen absorption curve, figure 64. The initial rate (and the linear rate) are slightly greater than the curve representing 1% PBD in chlorobenzene initiated by 100 µℓ of CHP. The sample containing both dinonyl ketone and hydroperoxide continues to absorb oxygen parallel to that of the un-initiated control, figure 64. The activating effect of dinonyl ketone observed in hydroperoxide-initiated PBD solution is consistent with the analogous system using cumene shown in figure 55.

4.1.3.3 Mesityl oxide

The effect of addition of mesityl oxide on the photoxidation of initiated and un-initiated 1% PBD in chlorobenzene is illustrated in figure 65. In contrast to experiments concerning dinonyl ketone (figure 64), mesityl oxide "inhibits" the photoxidation of PBD at all concentrations studied illustrated in figure 65, showing a marked decrease in initial rate and a progressive increase in induction period. At a relatively high concentration of approximately 10 x 10^{-2} mol. g^{-1} the induction period (found by extrapolation of the linear portion of the curve to the abscissa) is lengthened by nearly 6 hours, figure 65. However, the linear rate increases slightly faster than that of the control but retards in a similar manner and remains below. At a concentration of approximately 5 x 10^{-2} mol. g^{-1} a parallel curve exactly half way between the control and the curve

Effect of mesityl oxide on the photoxidation of 1 ml of a 1% w/v solution of hydroperoxide-initiated and uninitiated PBD in chlorobenzene (oxygen absorption in oxygen)

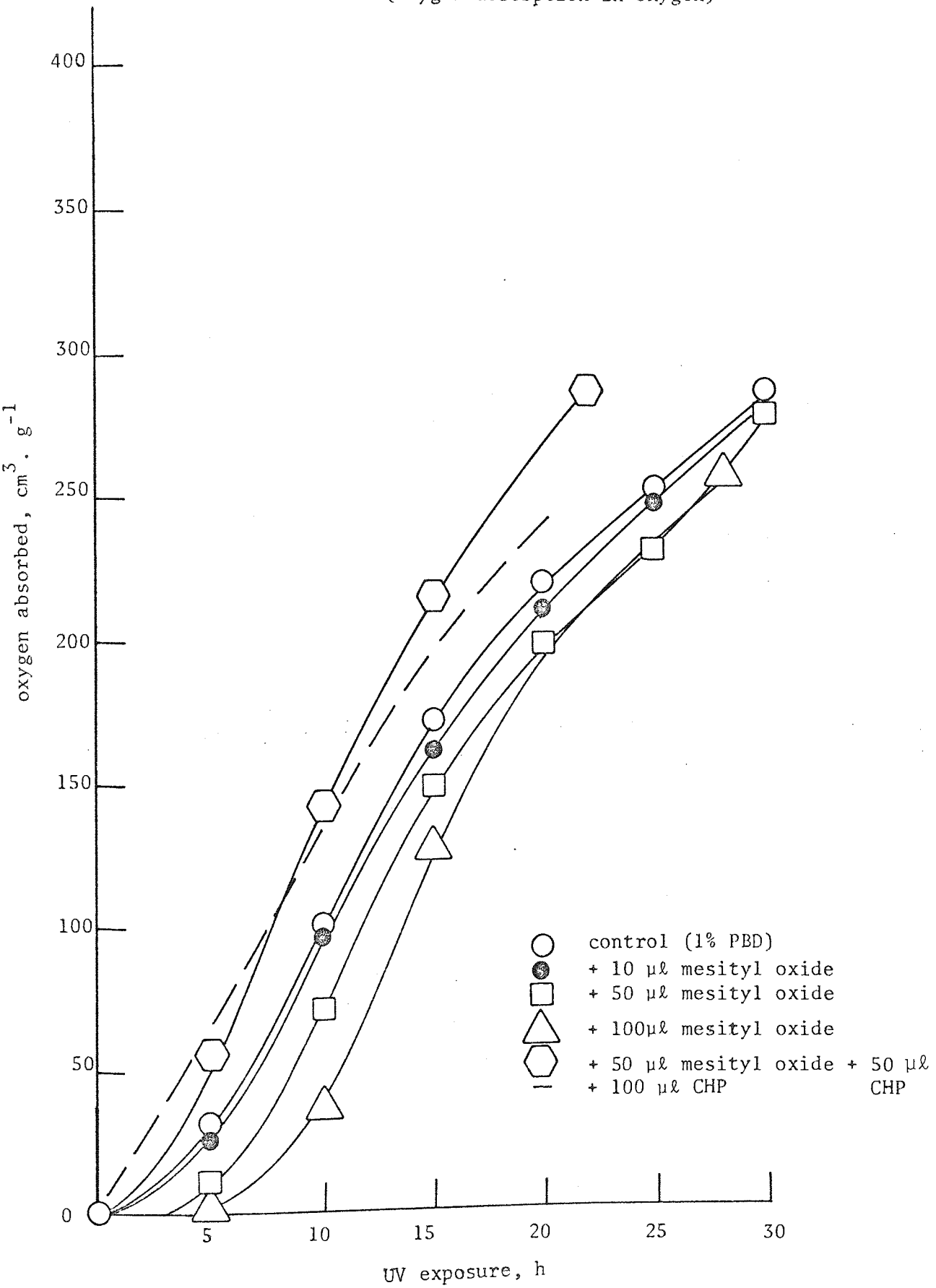

Figure 65.

representing 10 x 10^{-2} mol. g^{-1} is observed (figure 65) indicating that the extent of "inhibition" is directly proportional to the concentration of additive. Similarly at a relatively low concentration of approximately 1 x 10^{-2} mol. g^{-1} a parallel curve is obtained very close to that of the control, figure 65. Addition of approximately 5 x 10^{-2} mols of mesityl oxide to 1% PBD solution initiated by 50 µl of CHP failed to remove the auto-catalytic stage of the curve, nevertheless the linear rate is increased above that of the control curve; the sample continues to absorb oxygen at a rate parallel to the curve representing a concentration of 10 x 10^{-2} mol. g^{-1}. It will be appreciated that the initial rate of oxygen absorption of the sample containing both mesityl oxide and hydroperoxide is far less than 1% PBD initiated by hydroperoxide only; this "inhibition" of the hydroperoxide-initiated photoxidation of PBD is consistent with evidence obtained using cumene (figure 56) and is likewise contrary to dinonyl ketone, figures 64 and 55. In view of the experimental fact that "inhibition" of photoxidation of PBD in chlorobenzene by mesityl oxide was observed at all concentrations studied (figure 65) the above experiments were repeated using a different batch of mesityl oxide whose purity was confirmed by GLC, and a lower range of concentrations were examined. An entirely analogous set of results were obtained to those shown in figure 65. The "inhibition" at the higher concentration of mesityl oxide was even more marked with a corresponding linear rate of oxygen absorption parallel to that of the control. At concentrations down to approximately 10^{-7} mol.g^{-1} the oxygen absorption curve became congruent with the control.

4.2 DISCUSSION

To achieve a greater understanding of the photochemical mechanisms occurring during the initial photoxidative degradation of "crystal" polystyrene, polybutadiene and the graft copolymer HIPS, a low molecular weight hydrocarbon (cumene) was chosen as an analogue of "crystal" polystyrene and subjected to photo-oxygen absorption studies (see 1.4) in the presence of various oxidation products and other additives (see 4.1.2). The use of cumene as a model compound for oxidation chemistry is well established[109] and the decomposition reactions associated with cumene (CHP) are reported in the literature[43,110,111,112,113]. Cumene is also readily obtainable in the pure state (see 1.2.4.1) and relatively stable under ambient conditions. However, under the conditions used for accelerated testing of polymers (see 1.4) the rate of photoxidation of pure cumene is sufficiently rapid to allow experiments to be performed within a reasonable period.

A low molecular weight hydrocarbon was not commercially available to serve as an analogue of polybutadiene. The constituent structures of polybutadiene also provide additional problems. However, synthesis of a model compound 2,6-octadiene was attempted by known methods[114]. Low yields of 2,6-octadiene resulted in insufficient pure compound to be of practical value in photo-oxygen absorption studies. Therefore polybutadiene rubber was used in an "inert" solvent chlorobenzene as a "model" (see 4.1.3). The various carbonyl compounds,hydroperoxide and alcohol added to the polybutadiene solution were all readily soluble in chlorobenzene and homogenerity (with the PBD) was afforded by rapid stirring of the mixture.

Before discussing in detail the chemical reactions occurring during the photoxidation of cumene it is useful to establish the identity of the impurity present in commercial cumene which was removed by successive distillation, figure 52. It has been reported in the literature[12] that unpurified hydrocarbon photoxidises rapidly after a relatively short induction period (found by extrapolation to the abscissa) and that the induction period increases with purification until a limiting value is obtained which does not increase with further purification; this is consistent with results shown in figure 52 for cumene. Addition of "impurity" namely peroxide or carbonyl to the pure hydrocarbon decreased the induction period[12]. Similarly, addition of CHP to cumene (1% v/v) reduces the induction period to zero (figure 53) while a carbonyl impurity has a less dramatic effect, figure 57. However, in the present study it was also established that cumyl alcohol, another oxidation product of cumene, reduced the induction period, figure 54, and may therefore be included in the definition of "impurity".

The importance of hydroperoxide as an initiator in photoxidation has already been discussed in Chapter Two, consequently the chemistry of cumene photoxidation will be discussed with respect to the decomposition of cumene hydroperoxide (CHP) and cumene as the oxidisable hydrocarbon (RH), together with the interaction of other oxidation products and similar compounds presented in 4.1.2. There are two principal modes of decomposition of CHP namely an acid-catalysed, ionic mechanism, and decomposition involving free radicals[110]. The decomposition of CHP by a reagent that causes the evolution of oxygen

(e.g. transition metal ions) will not be discussed as it is believed that purification of CHP and cumene removes all trace elements, (see 1.2.4). The Lewis acid-catalysed, ionic rearrangement of CHP is well established[115] in the literature and involves an analogous carbonium ion rearrangement with the positive charge on oxygen instead of carbon (see Scheme 6). The products of the ionic rearrangement of CHP are always phenol and acetone, although the supervention of a free radical mechanism may occur under certain conditions[110] (for example, an ionic reaction performed at high temperature) with the formation of different products. Only phenyl appears to migrate to the positive oxygen in the ionic rearrangement of CHP, although in principle the methyl group could also be involved[115]. Under the conditions of photoxidation described in the present study of cumene/CHP and in the absence of a strong Lewis acid the decomposition of CHP is unlikely to follow an ionic mechanism.

SCHEME 6

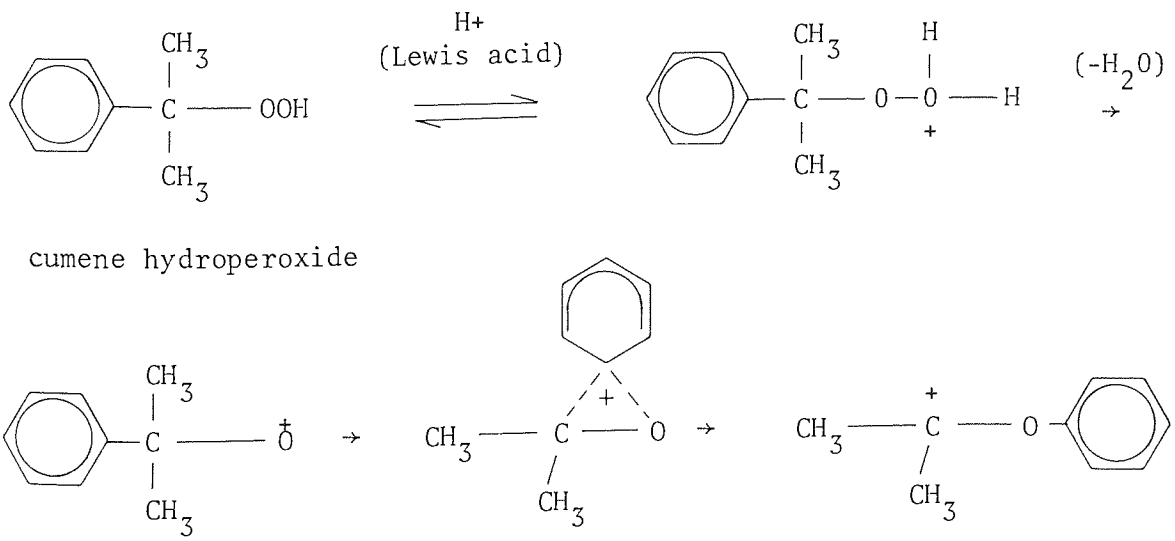

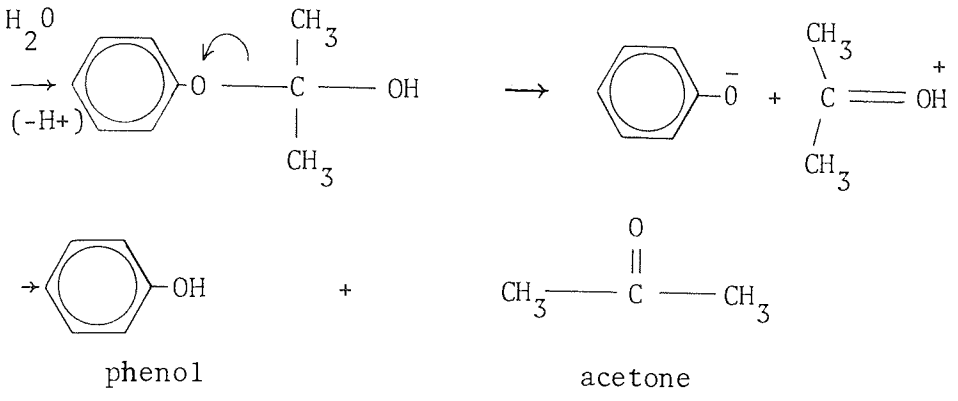

Photochemical decomposition of CHP will undoubtedly lead to production of free radicals namely cumyloxy and hydroxy radicals by homolytic scission of the oxygen-oxygen bond[113] (see Scheme 7). The cumyloxy radical, which is more stable than an analogous tertiary butoxy radical because of the stabilising effect of the phenyl group[113] will abstract a tertiary hydrogen from cumene to form cumyl alcohol and the corresponding cumyl radical, (a). In the presence of oxygen a cumylperoxy radical will be formed in preference to dimerisation of two cumyl radicals. The cumylperoxy radical may either abstract a hydrogen from the hydrocarbon solvent (cumene) to form cumene hydroperoxide and another cumyl radical or produce cumyloxy radicals plus oxygen via an intermediate tetroxide formed by the combination of two cumylperoxy radicals[116]. The hydroxy radical formed during the initial cleavage of CHP may also take part in the chain reaction discussed above by abstracting a tertiary hydrogen from cumene producing a cumyl radical. However, it is believed that the cumyloxy radical is the principal chain carrier in the photoxidation of cumene initiated by CHP. Under certain conditions, for example, in the presence of a Lewis acid dehydration of cumyl alcohol may occur with the formation of α-methyl styrene[117], although this is an unlikely

product under the conditions used in the photoxidation of cumene, (see 4.1.2.). When cumene is replaced by chlorobenzene as solvent the free radical decomposition of CHP proceeds by a different route, (b). This may be encountered during the photoxidation of a solution of PBD in chlorobenzene initiated by CHP, (see 4.1.3). Under this condition competitive hydrogen abstraction from the solvent (chlorobenzene) is not possible, although hydrogen abstraction from PBD is possible producing an allylic radical and will undergo similar reactions to those discussed above, (a). Nevertheless, migration of the methyl radical on the cumyloxy radical derived may take place[113] resulting in the formation of acetophenone and a free methyl radical, (i). Because the cumyloxy radical is relatively stable it may undergo primary recombination and rearrangement with a hydroxy radical to give phenol and acetone, (ii), analogous to the ionic rearrangement seen above, before it stabilises itself by ejection of a methyl radical[113].

SCHEME 7

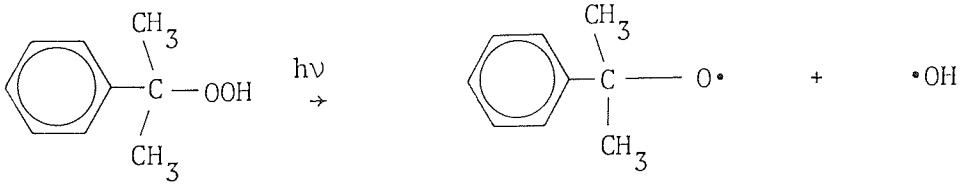

CHP

cumyloxy and hydroxy radicals.

(a) hydrocarbon solvent (cumene):

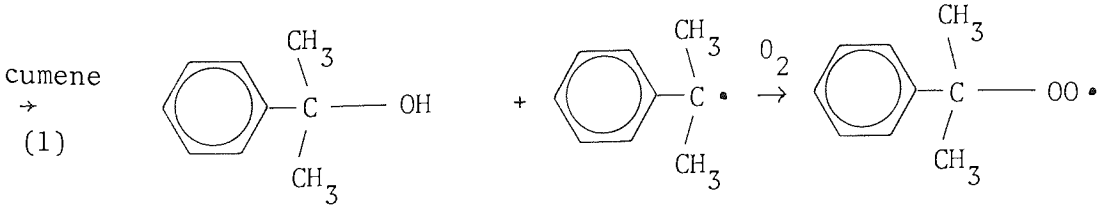

cumyl alcohol

cumyl radical

cumylperoxy radical

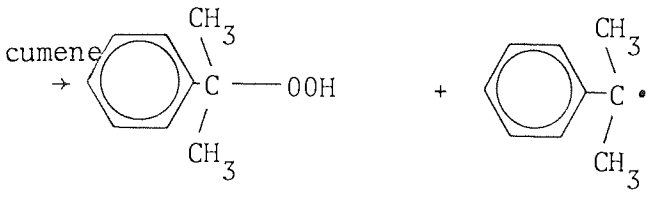

CHP cumyl radical

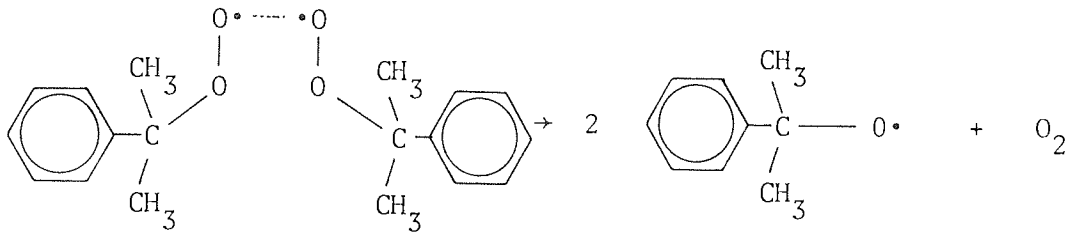

diradical intermediate cumyloxy radical

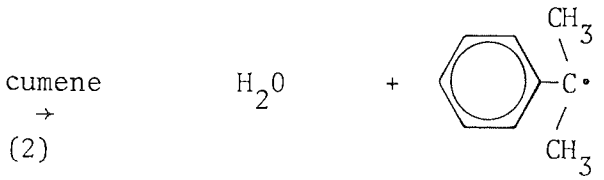

cumyl radical

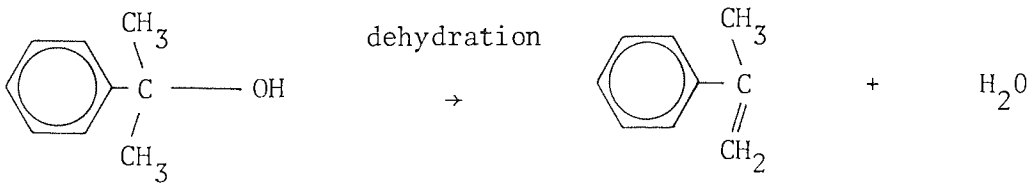

cumyl alcohol α-methyl styrene

(b) chlorinated solvents (chlorobenzene):

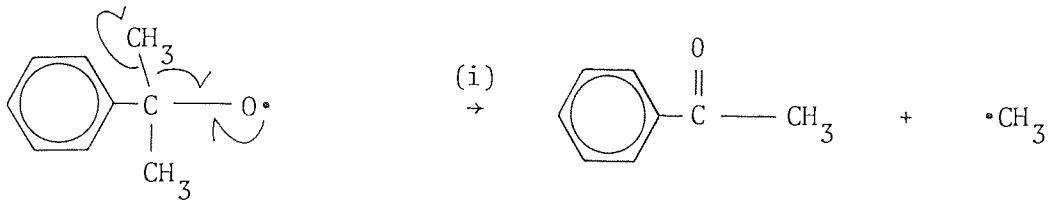

(i) migration of methyl radical. acetophenone

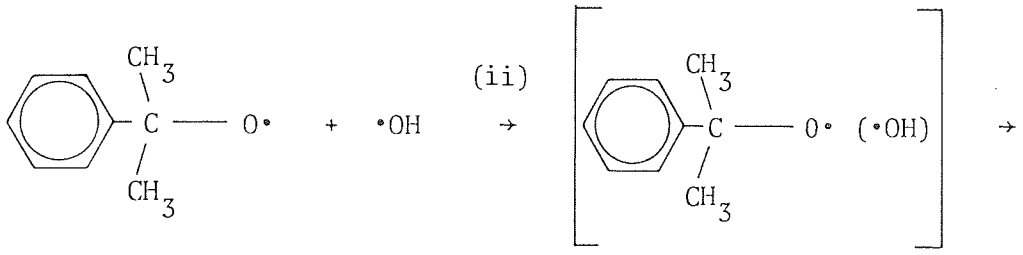

(ii) primary recombination of radicals.

phenol acetone

Another possible mechanism for the decomposition of CHP is by a free radical induced reaction similar to those proposed for thermal degradation[110, 118] of hydroperoxide (see Scheme 8). Hydroxy radicals produced during photolytic breakdown of hydroperoxide may combine with CHP to form cumylperoxy radicals via dehydration of the intermediate,(i). The above oxidative reaction does not involve solvent (cumyl) radicals and may occur during the photoxidation of a solution of PBD in chlorobenzene. Alternatively, (ii) radical induced decomposition of CHP by

solvent (cumyl) radicals may be important in the photoxidation of cumene initiated by CHP leading to cumyloxy radicals and cumyl alcohol. However, in the presence of oxygen competition for the cumyl radical will reduce the contribution of radical induced decomposition[118].

SCHEME 8

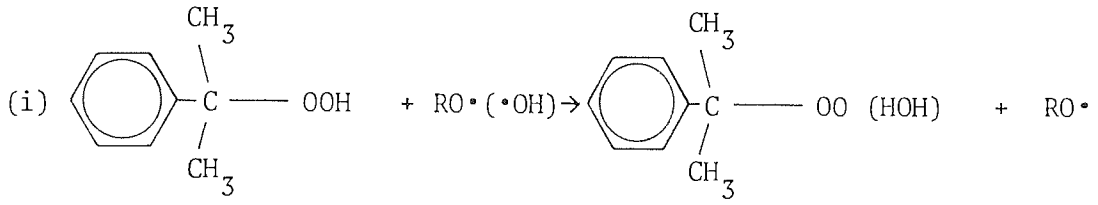

CHP

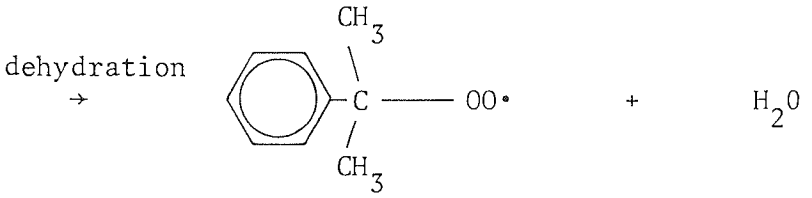

cumylperoxy radical

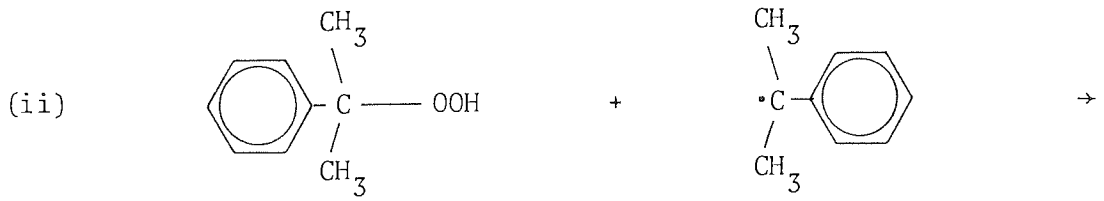

CHP

cumyl radical

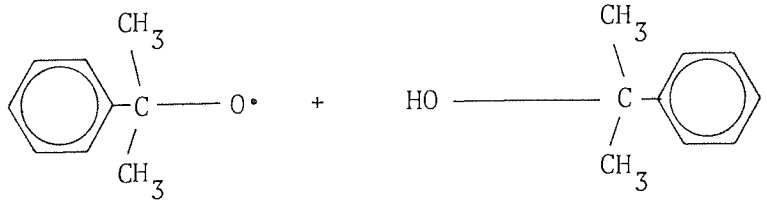

cumyloxy radical

cumyl alcohol

An interpretation of the various reactions incurred through addition of oxidation products and other compounds to cumene (see 4.1.2) may now be given with reference to the principal decomposition mechanisms discussed above. Cumyl alcohol behaves as an activator during the photoxidation of cumene (figure 54), although it is generally reported that alcohols inhibit the autoxidation of hydrocarbons[119]. Indeed this was found to be so for a solution of PBD in chlorobenzene; this will be discussed later. It is apparent therefore, that the anomalous effect of cumyl alcohol on the autoxidation arises from the nature of the hydrocarbon (cumene or PBD) ,whether or not the hydrocarbon is present as a "solvent", and the relative concentration of alcohol. It is believed that the case of cumene and cumene-initiated by CHP, induced hydroperoxide decomposition by alcohol is responsible for its activation (figure 54).

A similar activation observed (figure 55) in the cumene/CHP system when an aliphatic long chain ketone (dinonyl ketone) is present may be explained by considering the possible modes of dissociation of the additive during photoxidation (see Scheme 9). It must be appreciated that the lowest concentration of dinonyl ketone used in cumene (1×10^{-4} mol. ml^{-1}) corresponds to extensive oxidation; 1×10^{-4} mols of dinonyl ketone per g of HIPS (figure 89, Chapter Six) gives the same absorbance in the IR as a similar film of HIPS (containing no additives) heated in air at 98°C for 25 hours (figure 12, Chapter Two). Dinonyl ketone has a relatively weak absorption band around 285 nm with a tail extending beyond 300 nm and is therefore capable of absorbing UV when present in cumene which has a cut-off below 280 nm.

The absorption arises from a "forbidden" transition corresponding to the promotion of an electron from a non-bonding, n-orbital localised on the oxygen to a delocalised antibonding π^*-orbital[16]. Both excited singlet $^1(n\text{-}\pi^*)$ and triplet states $^3(n\text{-}\pi^*)$ of ketone may be involved in cleavage reactions[19], although the excited triplet state formed by intersystem crossing (ISC) has a longer lifetime. Intermolecular photoreduction of aliphatic ketones possessing an γ-hydrogen is unlikely[120] although both Norrish types I and II chain scission reactions occur; the relative quantum yields of the two processes will depend on the chain length[18, 21]. The quantum yield of the Norrish type II cleavage decreases in a regular manner for a series of di(n-alkyl) ketones reaching a value of 0.06 for tritetracontan-22-one, whereas the type I photolysis falls rapidly with increasing chain length to a limiting value of 0.012[18, 21]. An estimation of the quantum yields for Norrish types I and II chain scission reactions of dinonyl ketone and the subsequent lower molecular weight ketones may be deduced from the above data reported in the literature.

It would appear that Norrish type II cleavage of dinonyl ketone and methyl nonyl ketone is more important than type I photolysis producing radicals, until methyl nonyl ketone is cleaved resulting in formation of acetone which does not possess a γ-hydrogen and can only undergo chain scission by a Norrish type I mechanism. The excess energy carried off by the acyl radical produced by type I cleavage is non-thermally equilibriated and these "hot" radicals may break down further to form carbon monoxide and a methyl radical[121]. However, this reaction is unlikely to occur to an appreciable extent because the solvent (cumene) absorbs UV radiation below about 280 nm.

SCHEME 9

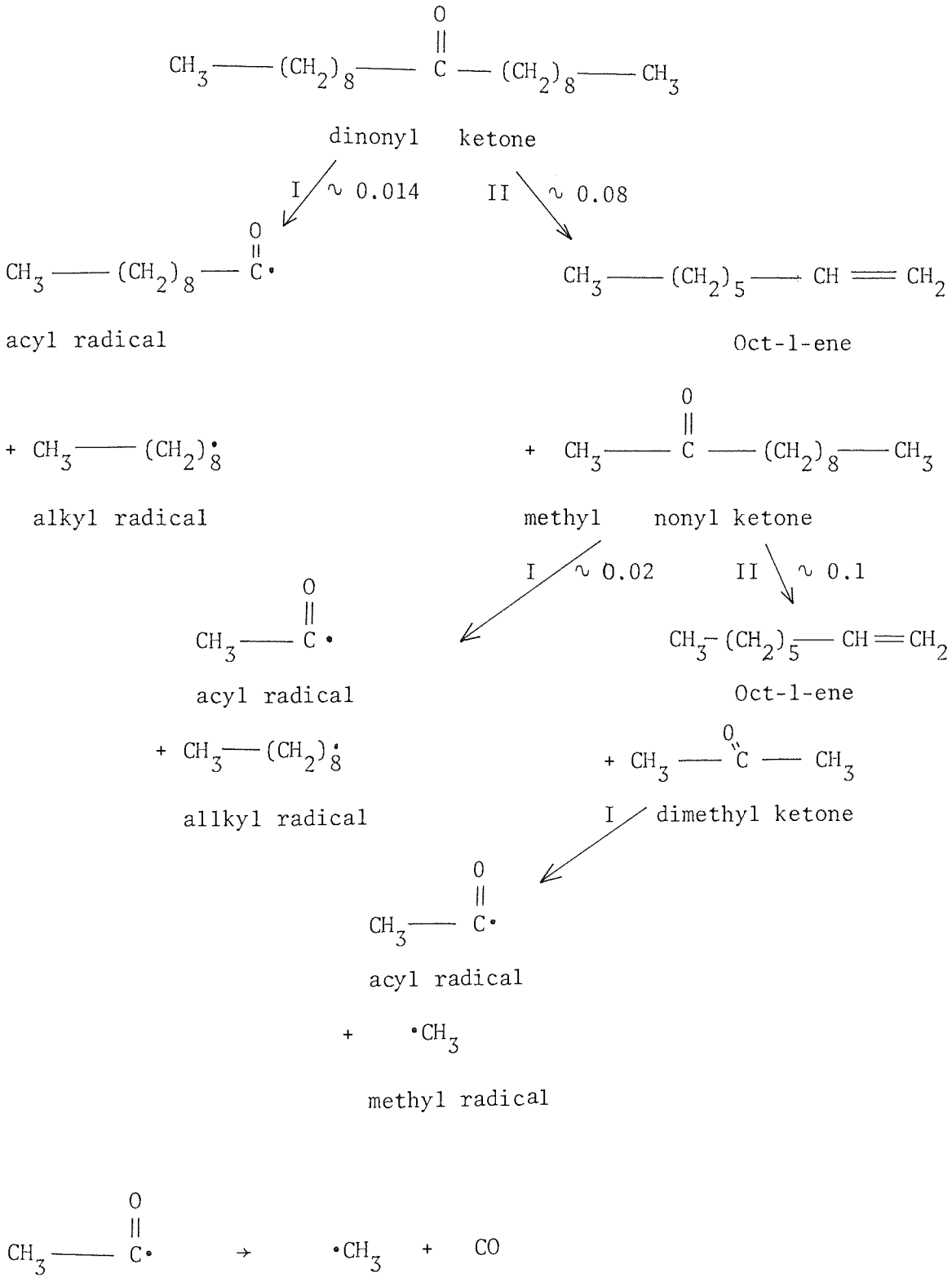

decomposition of acyl radical to carbon monoxide and methyl radical.

The extra supply of free radicals (acyl and alkyl) will contribute to the propagation and subsequent chain branching mechanisms during photoxidation of cumene, even though olefin production by Norrish type II cleavage is favoured. The effect of these radicals on the autoxidation of the cumene/CHP system is to reduce the time necessary to reach the critical concentration of hydroperoxide necessary to substain linear kinetics, figure 55[4]. In view of the fact that a high concentration of aliphatic ketone (1×10^{-4} mol. ml^{-1}) is required to produce a sufficient concentration of free radicals to affect the chain mechanisms occurring during autoxidation of cumene it is unlikely that the very low concentration of aliphatic ketone ($< 1 \times 10^{-6}$ mol. g^{-1} detectable by IR) presumably present at the start of the photoxidation of HIPS is involved in the initiation during the initial stages of oxidation. Further evidence supporting the above postulate will be presented in Chapter Six, concerning the addition of dinonyl ketone to HIPS by extrusion mixing. At a higher concentration of dinonyl ketone in cumene (5×10^{-4} mol. ml^{-1}) the linear rate was less than that observed for the lower concentration, figure 55. It is probable, at this artificially high concentration of aliphatic ketone the accelerating effect of the additional free radicals produced by Norrish type I photolysis is superceded by the dissipation of energy by photo-physical processes and non-radical mechanisms. This will result in internal UV screening of the cumene undergoing photoxidation. The reactions of alkyl and acyl radicals during autoxidation have already been discussed in Chapter Two with respect to the oxidation of HIPS. However the formation of a straight

chain vinyl compound (oct-1-ene) via Norrish type II photolysis of dinonyl ketone poses an interesting problem. It is unlikely that addition of alkoxy and alkylperoxy radicals to the double bond or hydrogen abstraction from the allylic position producing an alkyl radical which will combine rapidly with oxygen to form an alkylperoxy radical and subsequently to give hydroperoxide (analogous to the radical reaction cited in Chapter Two for hydroperoxide formation) contribute significantly to the initiation of pure cumene when the initial hydroperoxide concentration is exceedingly low. However, when cumene is initiated by addition of CHP (1% v/v) the plentiful supply of free radicals produced by photolytic decomposition of the hydroperoxide may undergo oxidative reactions with the olefin leading to further chain branching reactions and a subsequent acceleration of the rate of photoxidation of cumene, figure 55.

In the case of α,β-unsaturated ketones the presence of a double bond adjacent to a γ-hydrogen rules out the possibility of cleavage via a Norrish type II mechanism by preventing transference of the γ-hydrogen. It has been reported that irradiation of 4-methyl-3-hexen-2-one shows no change when UV of wavelengths above 300 nm are used[122]. Furthermore, Norrish type I cleavage of the methyl group of the above conjugated ketone may similarly be dismissed as energetically unfavourable when a UV filter is used[122]. The α,β-unsaturated ketone used in the present study was 4-methyl-3-penten-2-one (mesityl oxide). The presence of a γ-hydrogen in a methyl group does not invalidate mesityl oxide as model compound; it is reported that di(n-propyl) ketone irradiated with UV above 300 nm undergoes both Norrish types

I and II cleavage with quantum yields of 0.34 and 0.21 respectively[123]. Mesityl oxide has an absorbance maxima at 237 nm and 310 nm in alcohol solution with extinction coefficients of 11 700 and 57 respectively[124]. The presence of the conjugating double bond shifts the low intensity absorption band ($n \rightarrow \pi^*$) about 25 nm to longer wavelengths, than the saturated dinonyl ketone. The high intensity absorption band ($\pi \rightarrow \pi^*$ transition) is also shifted by 15 - 45 nm to longer wavelengths[125]. Therefore, UV absorption by the carbonyl group of mesityl oxide ($n \rightarrow \pi^*$transition) will readily occur when present in cumene which has a cut-off below 280 nm, leading to a diradical excited triplet state via intersystem crossing from the original excited singlet state of carbonyl. When the solvent has a labile hydrogen as is the case for cumene, intermolecular photoreduction by the excited triplet state carbonyl may occur producing a ketyl radical and a solvent (cumyl) radical (see Scheme 10). The cumyl radical will enter the chain propagation reactions of cumene with the formation of CHP (discussed earlier) leading to a reduction of the auto-accelerating stage of the control curve, figure 56. The ketyl radical produced may stabilise itself by termination by dimerisation or hydrogen abstraction from another solvent molecule or undergo disproportionation. The presence of unsaturation in this ketone suggests the possibility of addition reactions to the double bond (see Scheme 11). Addition of alkylperoxy radicals (ROO•) and alkoxy radicals (RO•) to the conjugating double bond of α,β-unsaturated carbonyl compounds formed during oxidative degradation of HIPS has been postulated in Chapter Two as a mechanism for the removal of conjugated carbonyl from the system. Addition of a cumylperoxy radical to the double bond of

mesityl oxide will be of importance when the concentration of peroxy radicals is relatively high and when the available hydrogen concentration is low as is the case for a 1% w/v solution of PBD (reactions of mesityl oxide in the presence of PBD in chlorobenzene will be discussed later). The removal of cumylperoxy radicals from the chain propagation reaction will retard the autoxidation of cumene, since the α-keto alkyl radical will be stabilised by resonance and will react with oxygen (and mesityl oxide) slowly with possible formation of polyperoxide[126]. However, polyperoxide of the above conjugated ketone will not be stable owing to the lack of a stabilising group (methyl) in the α-keto position[126]. Breakdown of polyperoxides will produce a supply of alkoxy radicals which will enter the chain branching reactions discussed previously, thus allowing the auto-oxidising media to attain the critical (maximum) concentration of hydroperoxide necessary to sustain linear kinetics[4].

SCHEME 10

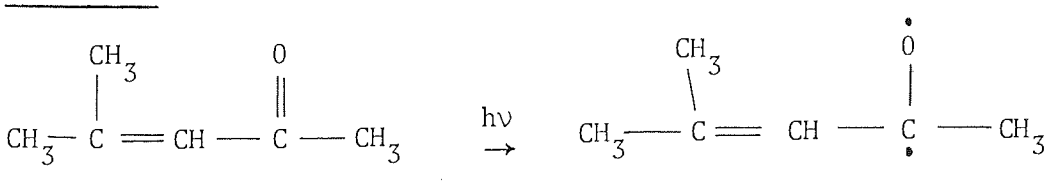

mesityl oxide — excited triplet state

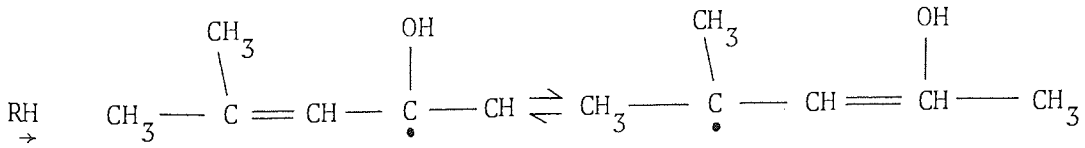

resonance stabilisation of ketyl radical

(i) hydrogen abstraction

(or disproportionation) →

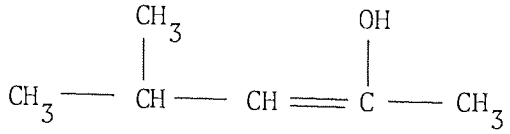

(ii) dimerisation →

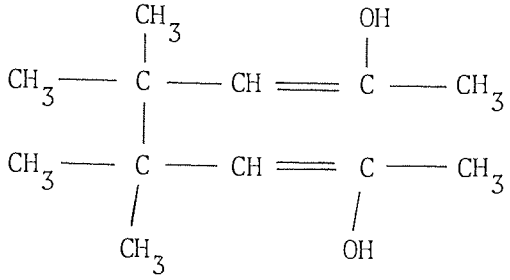

SCHEME 11

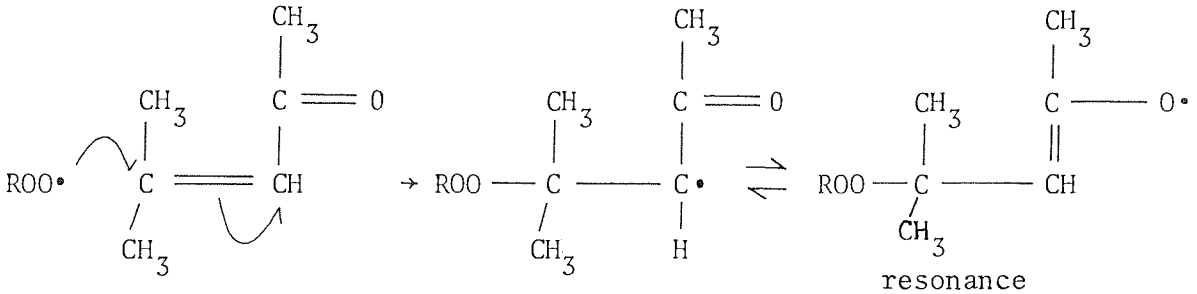

mesityl oxide

resonance stabilisation

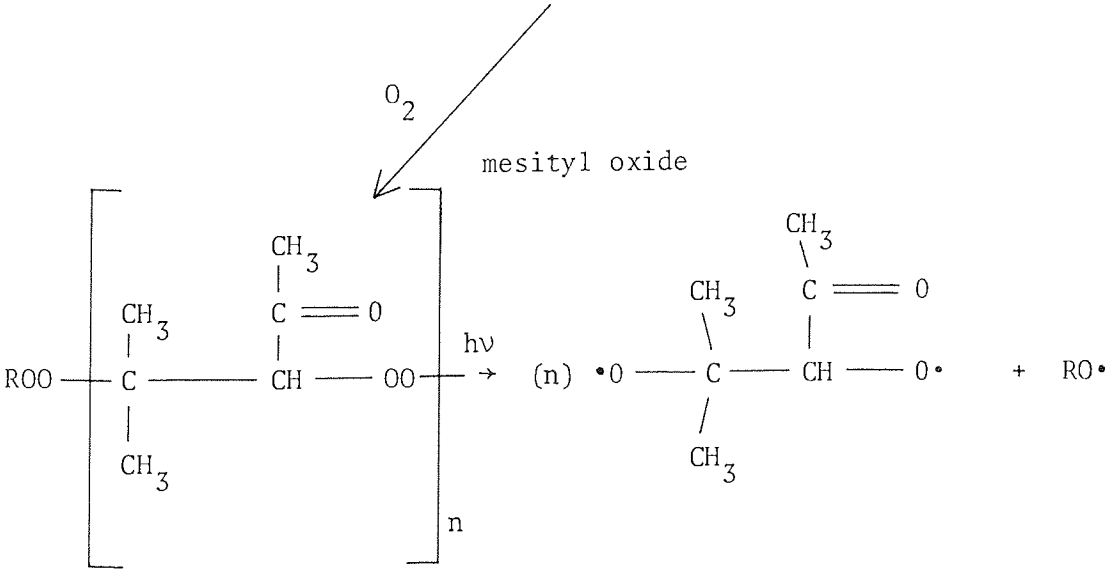

mesityl oxide

polyperoxide

alkoxy radicals

In contrast to mesityl oxide, dinonyl ketone increased the initial rate of photoxidation (figure 55) of cumene-initiated by CHP. At high concentration of mesityl oxide in cumene (ca.5 x 10^{-4} $mol.ml^{-1}$) retardation was observed, this may be a result of absorption by the tail of the high intensity band ($\pi \rightarrow \pi^*$ transition) which is not involved in photoreduction, acting as an internal screen.

Substitution of one of the alkyl groups in dialkyl ketone by an aryl does not prevent Norrish type II cleavage, for example, butyrophenone undergoes type II photolysis efficiently[127]. Unfortunately the model compound chosen as an analogue of the aryl-alkyl ketone formed in the oxidation of polystyrene (acetophenone) has no γ-hydrogen to be transferred in the Norrish type II rearrangement. Similarly Norrish type I cleavage of acetophenone releasing a methyl radical is not very likely in a hydrogen-donor solvent (cumene). The presence of an aryl substituent shifts the low intensity absorption band ($n - \pi^*$ transition) of the carbonyl group in acetophenone to higher wavelengths even more so than the conjugating double bond in mesityl oxide. The extinction coefficients for the high intensity absorption band at 237 nm ($\pi - \pi^*$ transition) and the low intensity absorption band at 320 nm in cyclohexane are approximately 13 000 and 50 respectively[128]. Consequently absorption of UV energy by the $n - \pi^*$ transition will occur readily in cumene leading to an excited triplet state of carbonyl via intersystem crossing from the original excited singlet state. Aromatic ketones undergo photoreduction reactions with high quantum efficiency in suitable solvents[129]. Excited acetophenone is, therefore more likely to abstract a hydrogen from cumene

forming an aromatic ketyl radical and a cumyl radical (see Scheme 12) than the corresponding photoreduction of α,β-unsaturated ketone discussed above. The accelerating effect of these radicals on the photoxidation of cumene is shown in figure 57. At higher concentrations of acetophenone in cumene the rate of oxidation was accelerated further, in contrast to addition of mesityl oxide, figure 56. The absence of unsaturation in acetophenone rules out the possibility of addition reactions discussed above for α,β-unsaturated ketone. The lack of an "inhibitory" mechanism was confirmed in the CHP/cumene system in which addition of acetophenone accelerates the photoxidation of cumene (figure 57) similar to that found for aliphatic ketone (figure 55) albeit by a predominantly dissociative mechanism. The possibility of acetophenone-type end groups acting as initiators for the photoxidation of polystyrene has been reported in the literature[28, 130]. Luminescence spectroscopy was used by the same workers to confirm the presence of low concentrations of acetophenone-type end groups in carefully prepared polystyrene and were suggested to arise from the breakdown of peroxides formed during polymerisation[130]. The above mechanism necessitates the formation of a terminal alcohol for which no evidence is available. In view of the overwhelming evidence presented in Chapter Two for the importance of hydroperoxide as a photo-initiator for HIPS it seems more likely that acetophenone-type end groups are produced via the decomposition of hydroperoxide formed during the photoxidation of polystyrene. This alternative mechanism is supported by other workers[29]. In Chapter Three (figures 42 and 43) the rate of formation of aryl-alkyl ketone (1685 cm^{-1}) was found to be auto-accelerating which is consistent with a hydroperoxide

autoxidation mechanism in which the breakdown products are carbonyl and alcohol. Therefore, possible acceleration of the photoxidation of "crystal" polystyrene by photoreduction of excited triplet states of either terminal aryl ketone or acetophenone (see Scheme 12) will be of significance only after a considerable concentration of carbonyl has built up in the polymer. The equivalent molar concentration of ketone (acetophenone) necessary to obtain an activation in cumene (ca. 1×10^{-4} $mol.ml^{-1}$), figure 57, will not be reached until after the auto-accelerating period of polystyrene photoxidation (figure 43, Chapter Three).

SCHEME 12

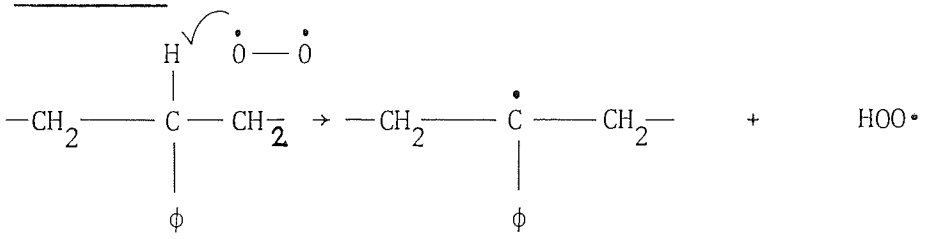

hydrogen abstraction by diradical oxygen leading to formation of alkyl and hydroperoxy radicals

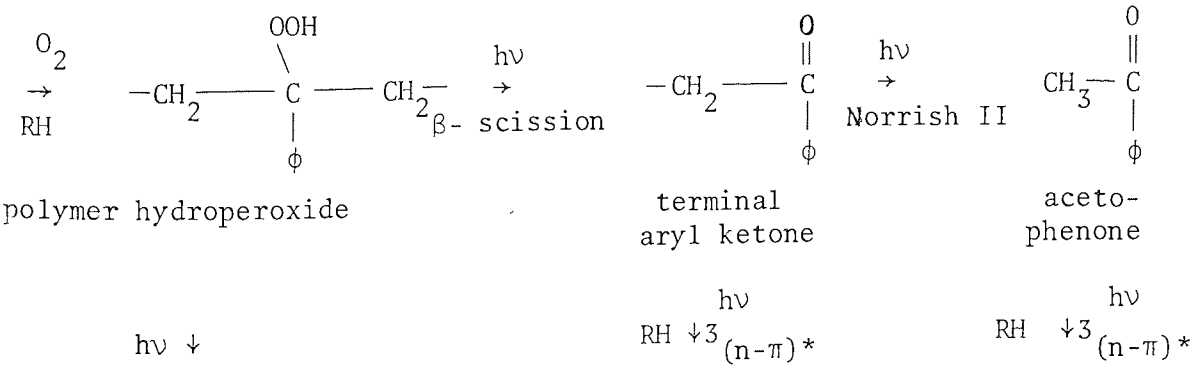

polymer hydroperoxide

terminal aryl ketone

acetophenone

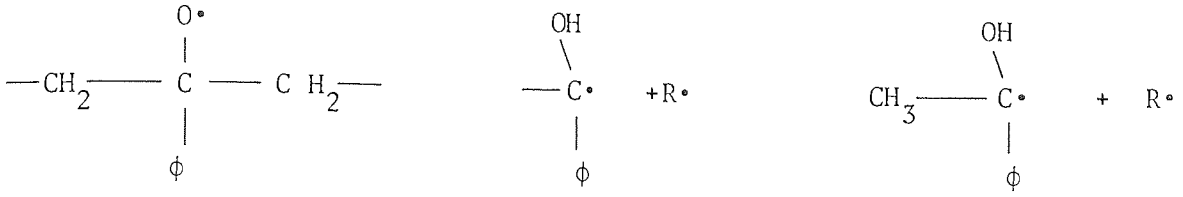

polymer alkoxy radical ketyl and alkyl radicals

The replacement of the methyl group in the above aryl-alkyl ketone (acetophenone) by a hydrogen (benzaldehyde) provides an opportunity for additional reactions of the aldehydic hydrogen. The high intensity absorption band (π - π^* transition) of benzaldehyde appears at longer wavelengths (282 nm, extinction coefficient of 1600 in hexane[131]) than acetophenone. Similarly the low intensity absorption band (n - π^* transition) lies between 310 and 380 nm. Therefore absorption of UV energy in this region is probable in cumene which does not absorb above 280 nm. Photoreduction (see Scheme 13) of the diradical triplet state of carbonyl of benzaldehyde may proceed via hydrogen abstraction from the donor solvent (cumene) with the formation of a cumyl radical (the reactions of which have been discussed earlier) or from the aldehyde leading to an acyl radical. The ketyl radical may dimerise or undergo further reactions. Abstraction of the aldehydic hydrogen may occur via a peroxy (or alkyl) radical (B) producing an acyl radical and hydroperoxide (or hydrocarbon, RH). Acyl radicals may also be formed by direct photolytic cleavage of the aldehydic carbon-hydrogen bond (C) ($\Delta H \sim 335$ k.J. mol^{-1}), although the quantum yield at 25°C using light of 313 nm is reported to be low[131]. Nevertheless, the acyl radicals produced via Schemes A, B and C will react with oxygen

to form a peroxy radical capable of abstracting an aldehydic or cumyl hydrogen resulting in perbenzoic acid. Aryl peracid is a relatively stable hydroperoxide[132] although it may be cleaved photolytically (a) forming a reactive hydroxy radical which will enter the chain branching reactions discussed earlier for cumene autoxidation. The aryl-alkoxy radical may abstract a hydrogen producing benzoic acid. Aryl carboxylic acid may also be formed by reaction of perbenzoic acid with benzaldehyde[133] (b).

SCHEME 13

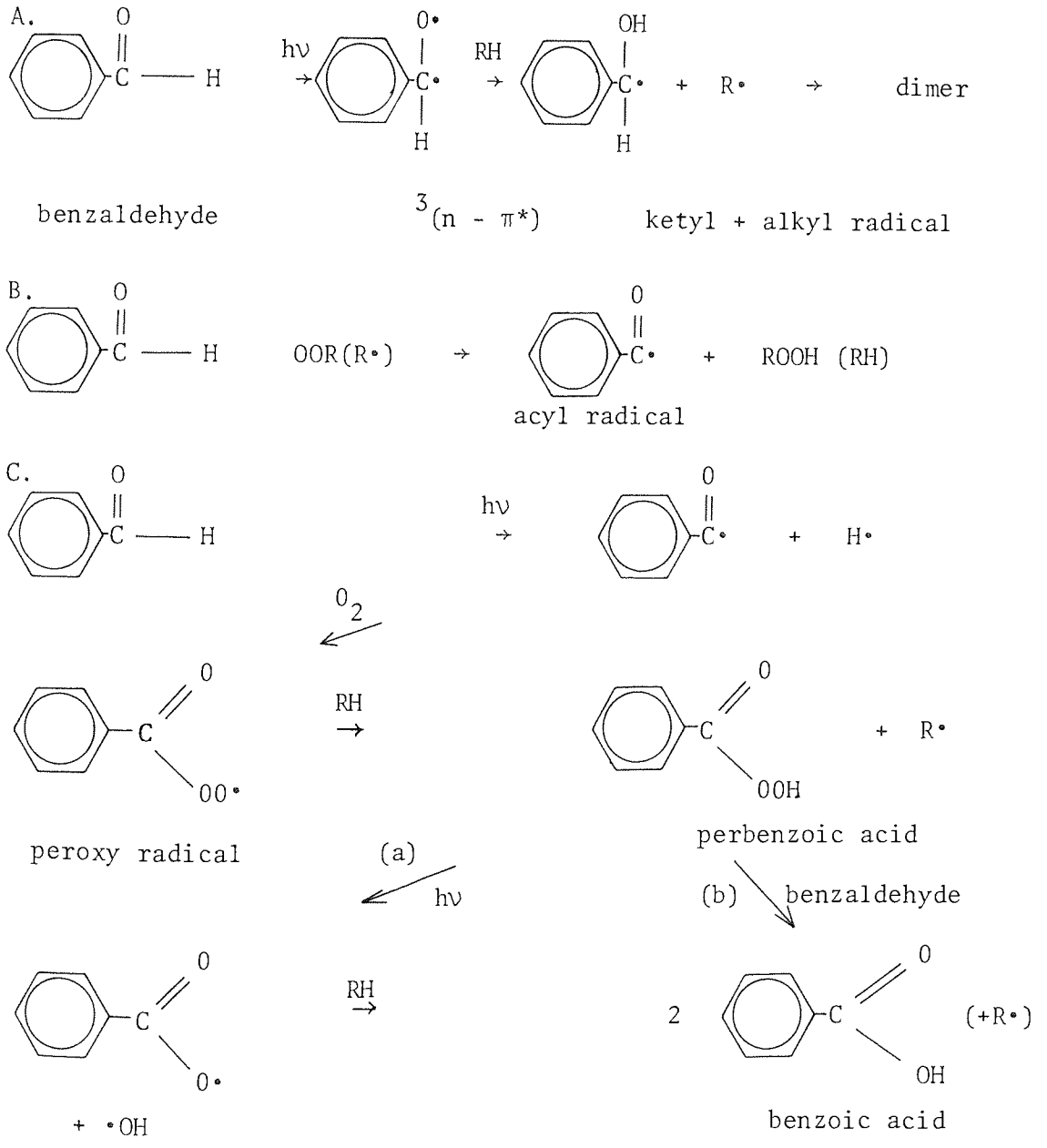

The consequences of the above free radical reactions derived from the aldehydichydrogen of benzaldehyde was seen in figure 58 as an extremely rapid photoxidation of cumene. The linear rate (figure 58) is typical of addition of a hydroperoxide (perbenzoic acid). However, the rate of oxygen absorption of cumene containing benzaldehyde was significantly higher than the equivalent molar concentration of CHP, figure 58; this suggests that photoreduction (Scheme A) may be of importance. Phosphoresence from commercial polystyrene has also been attributed to benzaldehyde[134]. However, its formation during oxidative degradation of "crystal" polystyrene is unlikely to be of importance compared with the sunstantial amount of aryl ketone formed even though benzaldehyde was found to be more reactive than acetophenone in cumene. The absence of retardation of photoxidation of benzaldehyde-accelerated cumene (figure 58) indicates that benzoic acid is formed only during the latter stages as this would retard the oxidation of benzaldehyde[135].

At lower concentrations of benzoic acid in cumene an activation was observed (figure 59). This is probably due to a rapid chain-transfer reaction (see Scheme 14) between the cumylperoxy radical formed during the photoxidation of cumene and benzoic acid resulting in CHP and a carboxyl radical. The CHP will be cleaved photolytically producing radicals in accordance with the chain branching mechanism. The carboxy radical may abstract a hydrogen from the solvent (cumene) regenerating the acid and forming a cumyl radical which will combine readily with oxygen producing another cumyloxy radical. When the concentration of benzoic acid is very high (ca. 4×10^{-4} mol. ml^{-1})

or an initial quantity of hydroperoxide has been added (figure 59) the rate of photoxidation of cumene was retarded. It is likely that additional hydroperoxide decomposition occurs via a hydrogen bonding CHP - benzoic acid complex formation[77] (B) analogous to hydroperoxide bimolecular decomposition[80] producing a cumyloxy radical and an acyl radical.

SCHEME 14

A.

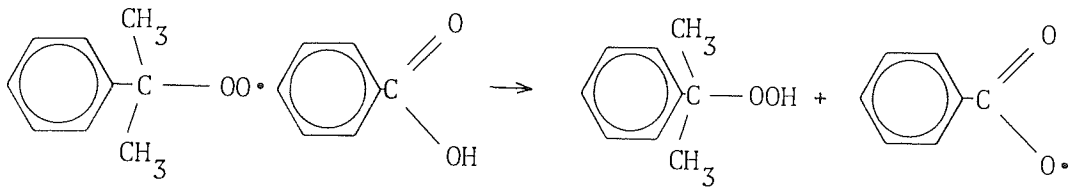

cumylperoxy radical benzoic acid CHP carboxy radical

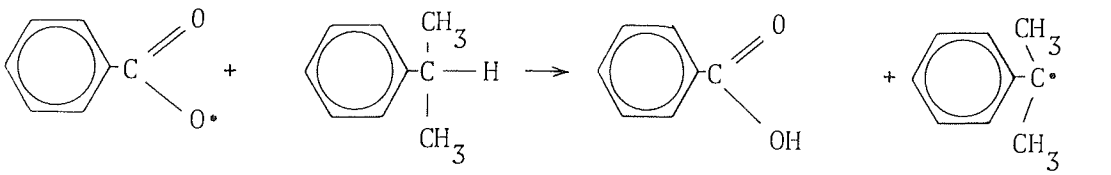

carboxy radical cumene benzoic acid cumyl radical

B.

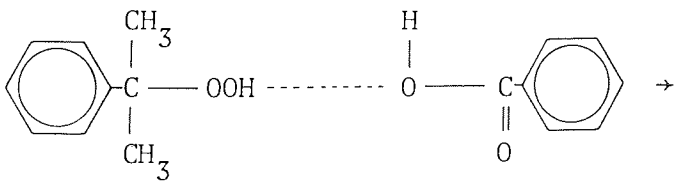

hydroperoxide - acid complex

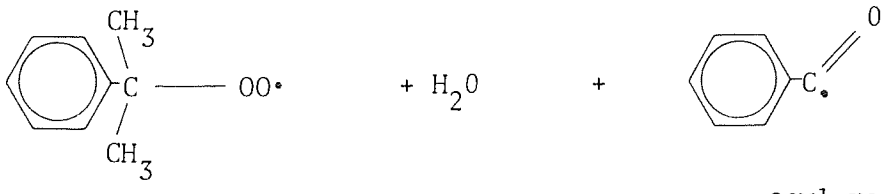

cumylperoxy radical acyl radical

The possibility of carboxylic acid- induced decomposition of polymer hydroperoxide occurring during the photoxidation of HIPS has already been discussed in Chapter Two. Phenyl acetic acid is believed to behave in an entirely analogous manner to benzoic acid[136] discussed above, figure 60. The difference in reactivity of the two carboxylic acids is probably due to the relative stability of the carboxy radical[137].

An alternative initiation step for the photoxidation of polystyrene has been suggested[30] to occur via reaction with singlet oxygen. If this mechanism is of importance then addition of an efficient quencher of singlet oxygen (β-carotene)[30] should inhibit the photoxidation of cumene. Evidence from figure 61 shows that βcarotene activates cumene towards rapid photoxidation. The rate of oxygen absorption after 15 hours UV exposure for the sample containing β-carotene was greater than that of the control curve after the same period, figure 16. The initial rapid oxygen absorption of the sample containing β-carotene, which is faster than the CHP-initiated "control", is believed to be a result of preferential oxidation of β-carotene. β-carotene absorbs strongly in the UV and visible region of the spectrum (maximum absorption at 450 nm; extinction coefficient 140 000[138]) by virtue of its conjugated structure. Addition of cumyloxy or peroxy radical to a conjugating double bond will destroy the conjugation of that bond producing an adjacent alkyl radical which may react with oxygen forming a (β-carotene) peroxy radical capable of hydrogen abstraction from the solvent. The number of mols of oxygen absorbed by 0.2×10^{-4} mols of β-carotene after 10 hours exposure to UV was approximately 0.8×10^{-4}, calculated from

figure 61 (see 1.4.5). This implies that 4 mols of oxygen are absorbed by every mol of β-carotene (assuming that all the oxygen reacts with β-carotene). The oxidation of β-carotene and subsequent destruction of conjugation was seen as a loss of colouration after 10 hours UV exposure.

The apparent lack of photo-activation of cumene and hydroperoxide-initiated cumene by 3-methyl-1-butene (figure 62) confirms that it is the allylic hydroperoxide derived from the olefin that is involved in the initiation step. 3-methyl-1-butene absorbs below 260 nm and is therefore not capable of being excited in cumene which has a cut-off below 280 nm. The tertiary allylic hydrogen of 3-methyl-1-butene is unlikely to be substantially more active than the tertiary benzylic hydrogen of cumene similarly possessing two methyl substituents. Consequently, addition of 3-methyl-1-butene to cumene would not be expected to increase the rate of photoxidation by an appreciable amount. The unalteration of the rate of photoxidation of the CHP-initiated cumene by addition of 3-methyl-1-butene (figure 62) may similarly be explained by considering the derived hydroperoxide from 3-methyl-1-butene to be only marginally more reactive than the initial CHP. However, in Chapter Three the rate of photoxidation of vinyl-1,2-polybutadiene in PBD, of which 3-methyl-1-butene is a model, was shown to be substantially faster than polystyrene. It may, therefore, be concluded that the reactivity of the hydrogen in cumene is greater than the benzylic hydrogen of polystyrene. The oxidative reactions of 3-methyl-1-butene are believed to be similar to those discussed previously in Chapter Three for 1,2-polybutadiene including addition reactions to the vinyl double bond.

The problem of relative reactivity of model compounds as compared with that of the polymer does not arise when PBD is used as a "model". However, the induction period during photoxidation (found by extrapolation of the linear portion of the curve to the abscissa) of 1% PBD solution was approximately 4 hours (figure 63) compared with 12 hours for a solution cast film (Chapter Three, figure 48). This would suggest that the freedom of the PBD from oxygen diffusion limitation implemented by rapid stirring of the solution is more significant than the screening of wavelengths below 286 nm by the chlorobenzene. It is likely that the diluent effect of chlorobenzene in this system necessitates the incorporation of a higher concentration of additive to have a similar effect on the course of photoxidation of PBD than cumene, discussed earlier. This was typified in figure 63 by the addition of CHP at a concentration of approximately 5×10^{-2} mol. g^{-1}. CHP absorbs below 270 nm but the tail extends beyond 300 nm, therefore, in chlorobenzene a small portion of the tail will be available for excitation. Nevertheless, scission of the oxygen-oxygen bond will still take place with a high quantum efficiency producing cumyloxy and hydroxy radicals. The cumyloxy radical may either hydrogen abstract from PBD forming cumyl alcohol or eject a methyl radical producing acetophenone. The hydroxy radical may also abstract a hydrogen from PBD. The oxidative reactions of PBD have already been discussed at length in Chapters Two and Three. It is believed that the radicals derived from PBD are involved in the propagation reactions and not those associated with CHP which serves only to initiate the photoxidation of PBD in this system, figure 63. This was confirmed by the parallel rate of oxygen absorption for the control and the hydroperoxide-initiated PBD (figure 63) even though

acetophenone may be produced via the decomposition of CHP. Acetophenone exhibits a marked activation in the PBD/chlorobenzene system. This is because the low intensity band occurs at 320 nm and is therefore not screened by clorobenzene. The significant acceleration of the rate of photoxidation of PBD by acetophenone implies that photoreduction by intermolecular hydrogen abstraction from allylic positions ofPBD takes place in solution. It would appear that quenching of the excited triplet $^{3}(n - \pi^*)$ state of acetophenone by the solvent (chlorobenzene) is unlikely, although quenching of the excited singlet $^{1}(n - \pi^*)$ state is a possibility but no evidence has been found to show that this is of importance in the above system. The triplet energy of acetophenone is 308 $k.J.mol^{-1}$ in hydrocarbon solvent[139] while the $n - \pi^*$ transition corresponds to a maximum at 320 nm. The secondary band of chlorobenzene has a peak at 264 nm and will therefore have a triplet energy in excess of 308 $k.J.mol^{-1}$. For energy transfer to occur readily the donor (acetophenone) must have a triplet energy greater than the accepter (chlorobenzene).

The "inhibition" of photoxidation of PBD in chlorobenzene (figure 63) by addition of cumyl alcohol is believed to arise from a chain transfer reaction with a hydroxy radical[119]. This may be represented by the following equilibrium:

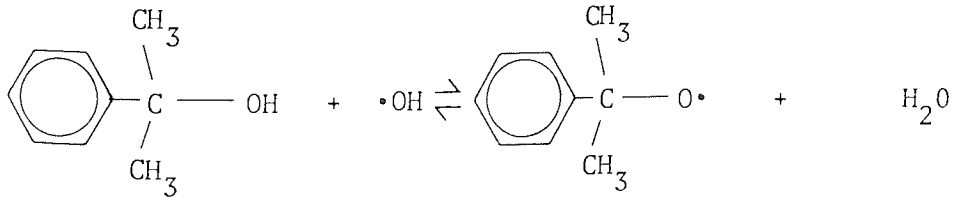

Cumyl alcohol is oxidised to cumyloxy radical which is likely to be more stable (because of the presence of the benzene ring) than the original hydroxy radical. When a large quantity of alcohol is present, as in the above case, the formation of a more stable radical will be an effective "inhibitor" during the early stages of photoxidation of PBD in chlorobenzene when the concentration of hydroxy radicals is low. After the auto-accelerating stage has been surmounted cumyl alcohol is no longer effective in removing the high concentration of hydroxy radicals and explains why no retardation of the linear (maximum) rate was observed, figure 63.

The slight retardation of photoxidation observed when an aliphatic ketone (dinonyl ketone) was added to a solution of PBD in chlorobenzene (figure 64) may be explained by internal UV screening of the PBD by the chromophore. This is apparent in the above system because of the high concentration of ketone present. Also the rate of oxidation of the PBD in solution is much faster than that of cumene (figure 55). The breakdown products of dinonyl ketone, namely free radical and olefinic are not effective as photo-initiators in the concentration range experienced during the photoxidation of PBD cast film (figure 46, Chapter Three). An activation of unitiated PBD in chlorobenzene was achieved only when an excess of aliphatic ketone was present, figure 64. The inability of dinonyl ketone to photo-sensitise the PBD of HIPS is confirmed in figure 89, Chapter Six. However, when aliphatic ketone (at a concentration similar to that which would be formed after extensive oxidation of the polymer) was added to a hydroperoxide-initiated system an increase in the initial linear rate was found (figure 64).

This may be a consequence of an accelerated breakdown of the initial concentration of hydroperoxide by an energy transfer process from the photo-excited ketone. This mechanism is unlikely to be of significance during photo-degradation of uninitiated polymer film as a sufficiently high concentration of carbonyl is built up in the polymer only after a maximum concentration of hydroperoxide has been reached (figure 15, Chapter Two).

The "inhibition" and lack of photo-activation of a solution of PBD by addition of an α,β-unsaturated ketone (mesityl oxide) over a wide range of concentrations (figure 65) is most likely due to a predominance of addition reactions to the double bond (Scheme 11) over photoreduction of the carbonyl (Scheme 10). Internal UV screening of the PBD by the conjugated ketone may be of importance at high concentration, although this is more likely to retard the linear rate of photoxidation (the retardation by UV screening mechanisms will be discussed in Chapter Six). The radical scavenging reaction (Scheme 10) discussed earlier is supported by the "inhibition" of the hydroperoxide-initiated photoxidation of PBD in chlorobenzene (figure 64) contrary to the activation observed for aliphatic ketone (figure 65) under identical conditions. Photoreduction of mesityl oxide in a hydrogen-donor solvent (cumene) has been inferred from the increase in initial rate of photoxidation (figure 56). However, in an inert solvent (chlorobenzene), hydrogen abstraction can take place only from the PBD. This will occur only if the lifetime of the excited triplet $^3(n - \pi^*)$ state of carbonyl is long enough to react with the low concentration of PBD (1% w/v). In the case of the acylic

α,β-unsaturated ketone used in the present study rotation about the double bond is possible during photo-excitation with a subsequent shortening of the lifetime of the triplet state. In a rigid polymer matrix rotation about the conjugating double bond should be restricted increasing the lifetime of the excited triplet state of carbonyl but the consequences of this on the reactivity of diradical carbonyl in photoxidised polymer are not known. However, it will be demonstrated in Chapter Six that addition of a sensible amount of saturated ketone to HIPS has a negligible effect on the photoxidation.

CHAPTER 5

INITIATION OF PHOTOXIDATION OF HIGH IMPACT POLYSTYRENE AND ACTIVATION OF POLYSTYRENE BY POLYBUTADIENE

5.1 RESULTS

5.1.2 Activation of high impact polystyrene by photolysis

5.1.2.1 Unstabilised

Figure 66 depicts the photoxidation of HIPS extruded films (50 μm) which have been UV irradiated in argon through a quartz cell for various times prior to oxygen absorption in oxygen after exposure to air for two hours in the dark (see 1.11). It is clear that pre-irradiation of the polymer film removes the auto-accelerating stage of the curve in a regular manner. The linear rate of all the curves is unaffected by pre-irradiation in argon, although the initial rate increases dramatically, figure 66.

The above-mentioned experimental procedure was repeated with the substitution of pyrex (borosilicate glass) for the quartz cell. This technique filters out wavelengths below 290 nm. By comparison of figures 66 and 67 it is evident that the screening of the shorter wavelengths does not alter the general pattern. However, the length of the pre-irradiation time necessary to produce a similar response to

Effect of prior UV irradiation in argon through quartz on the photoxidation of unstabilised HIPS extruded film (50 μm) after 2 hours exposure to air in the dark (oxygen absorption in oxygen)

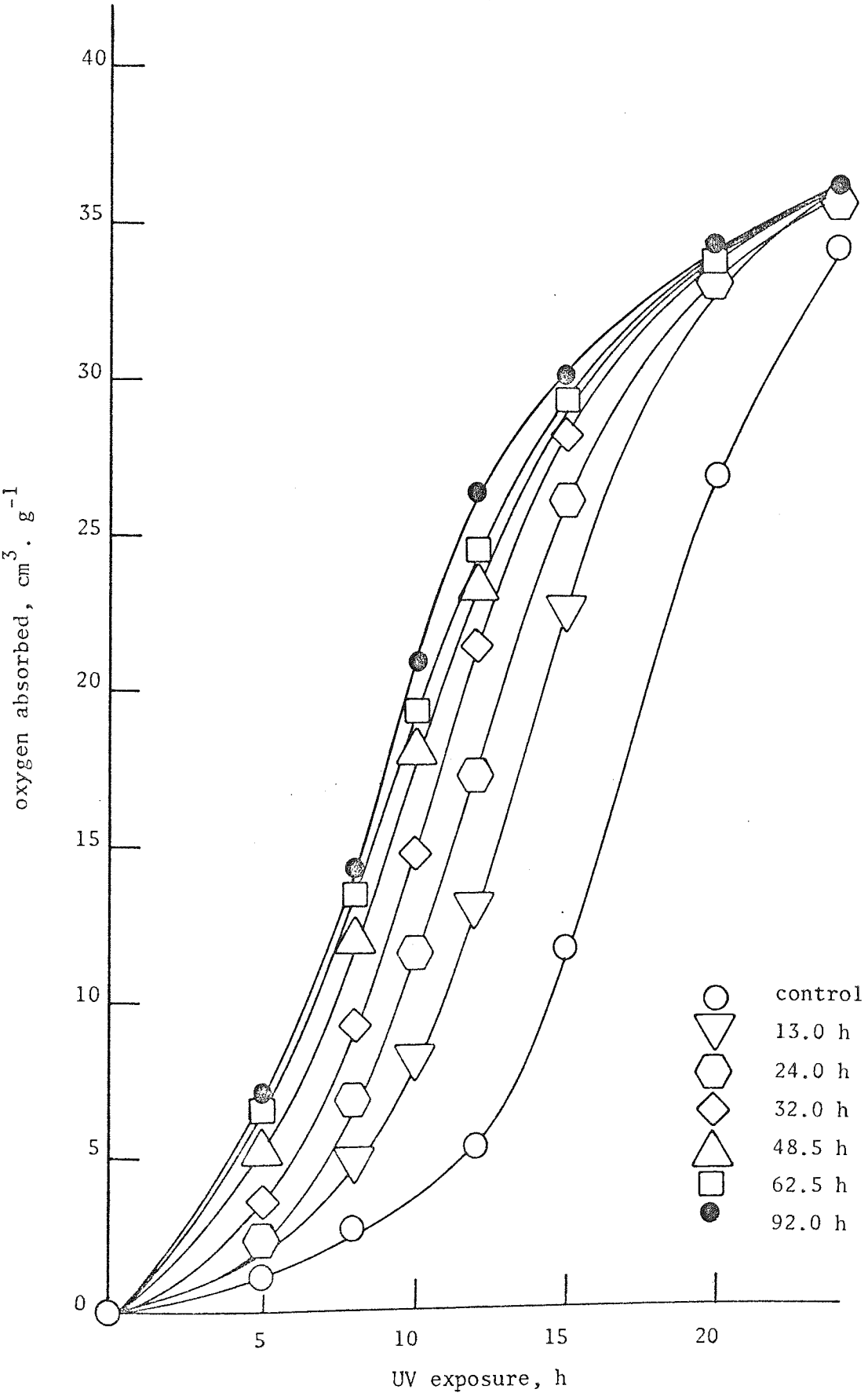

Figure 66.

Effect of prior UV irradiation in argon through pyrex on the photoxidation of unstabilised HIPS extruded film (50 μm) after 2 hours exposure to air in the dark (oxygen absorption in oxygen)

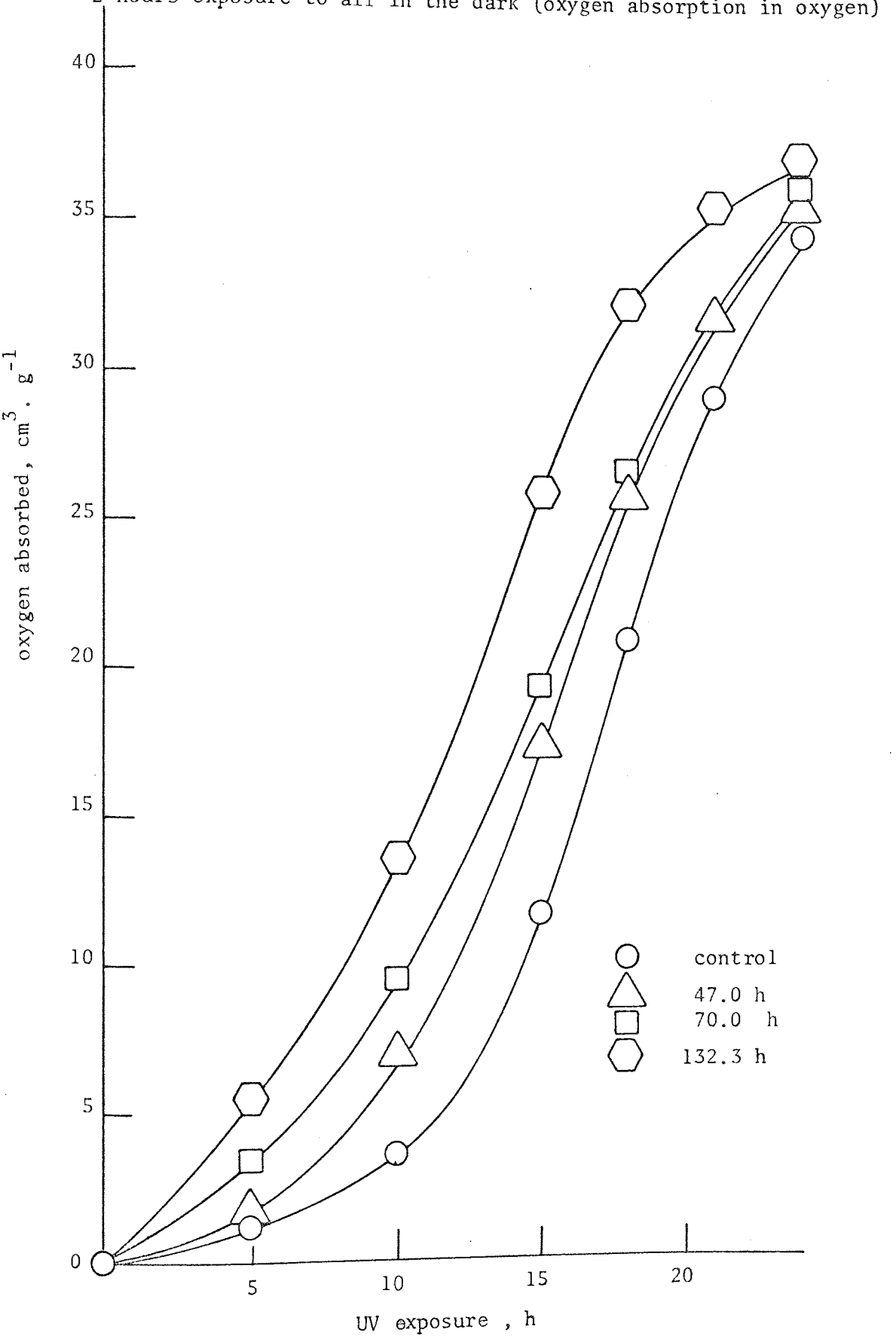

Figure 67.

photoxidation is extended by an appreciable amount. The linear (maximum) rate of photoxidation of the samples of HIPS film pre-irradiated through pyrex (figure 67) is less than those which have been pre-irradiated with unscreened UV (figure 66) although both sets of curves converge on the same point after 25 hours of UV exposure.

Figure 68 shows the changes in the initial rate of photoxidation (defined as the secant to the oxygen absorption curve from the origin up to 2 hours exposure to UV) for HIPS film pre-irradiated in argon through quartz and pyrex, calculated from figures 66 and 67 respectively. The small difference in initial rate of photoxidation measured from the control curve (pre-irradiation time of 0 hours) plotted on figures 66 and 67 was an error in measurement ; nevertheless, it is believed to be consistent for all points shown in figure 68. Both curves follow the same general pattern: an initial slow rise in initial rate followed by a rapid increase which levels out and does not increase with further pre-irradiation. HIPS film pre-irradiated in argon through quartz requires only about 25 hours of photolysis before the onset of the rapid increase in initial rate. Whereas samples of an identical batch of film pre-irradiated through pyrex required approximately 50 hours of photolysis to achieve a similar effect. Similarly the rapid increase in initial rate subsides after about 50 hours for the HIPS films pre-irradiated through quartz and after approximately 100 hours for the samples pre-irradiated through pyrex, figure 68.

5.1.2.2 Stabilised

Figure 69 depicts the photoxidation of HIPS extruded films (50 μm) containing 0.1% w/w phenolic antioxidant

Initial rate of photoxidation of unstabilised HIPS extruded film (50 μm) as a function of UV irradiation in argon (oxygen absorption in oxygen)

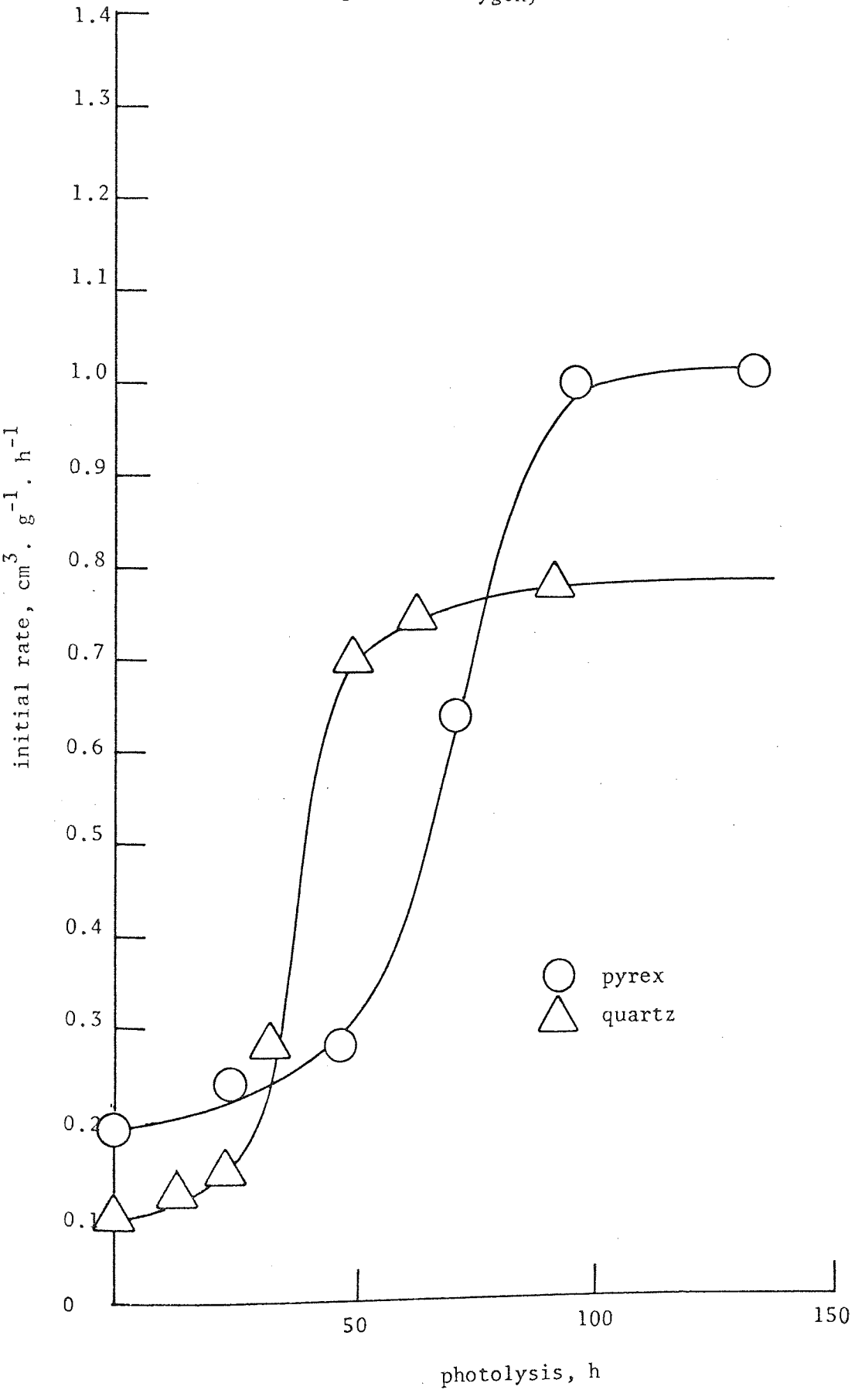

Figure 68.

Effect of prior UV irradiation in argon through quartz on the photoxidation of stabilised HIPS extruded film (50 μm) after 2 hours exposure to air in the dark (oxygen absorption in oxygen)

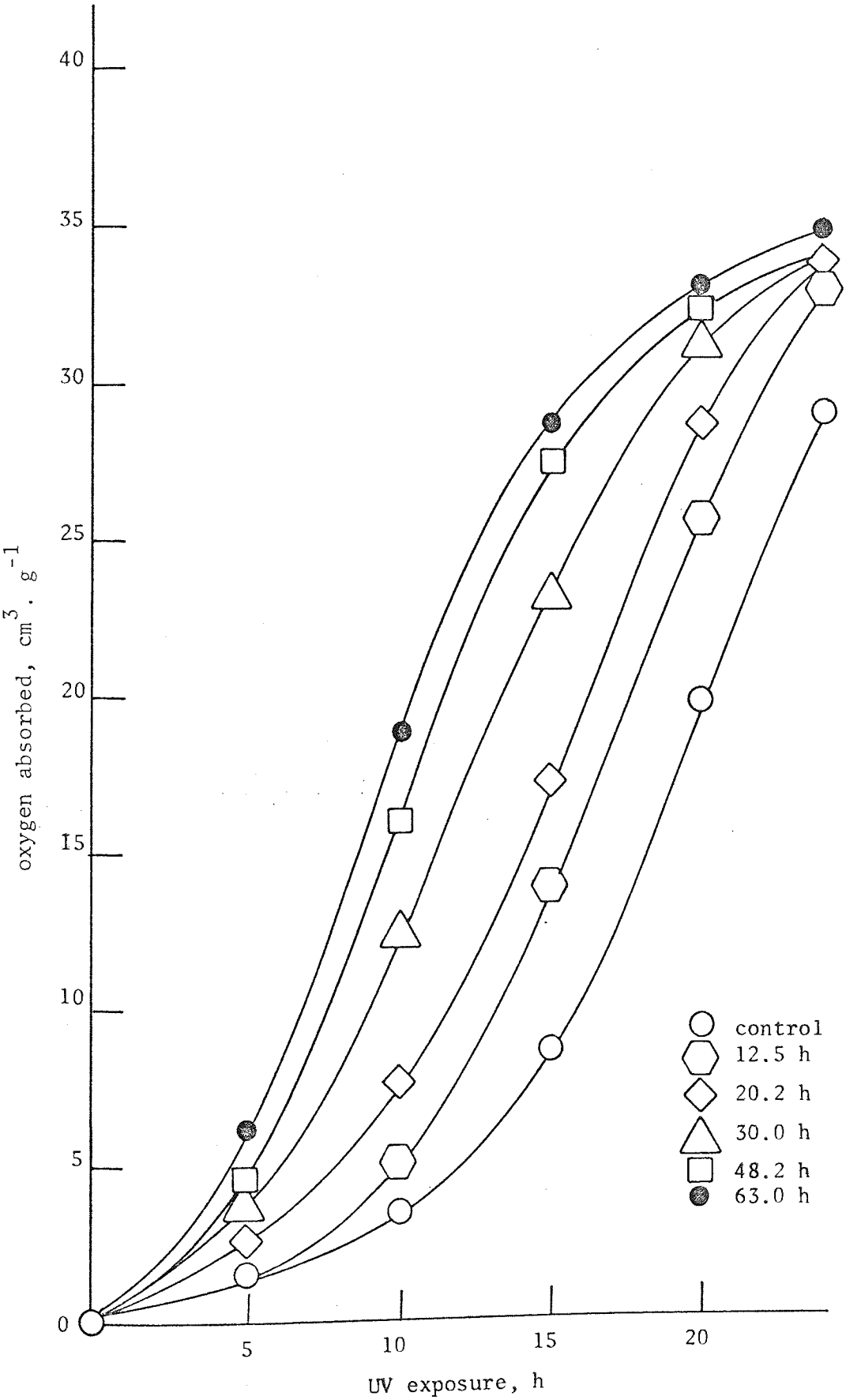

Figure 69.

(see 1.1) which have been pre-irradiated through quartz under identical conditions to the results shown in figure 66. By comparison of figures 66 and 69 it would appear that the presence of the commercial stabiliser has little affect on the response of pre-irradiated HIPS films to photoxidation; the linear (maximum) rate remains parallel to its respective control with increasing photolysis time. However, when the control curves from figures 66 and 69, together with samples which have had a similar pre-irradiation time (ca. 30 hours) are superimposed (figure 70) several important features are apparent. The initial rate of both samples containing a phenolic antioxidant is higher than the unstabilised polymer (figure 70) and the difference is more marked between the pre-irradiated films. This increase in oxygen absorption is maintained up to 6 hours of exposure to UV, thereafter both the control and the pre-irradiated film containing a phenolic antioxidant fall below the unstabilised samples, figure 70. It will be appreciated that the separation between the stabilised and unstabilised samples is almost identical for both the control and pre-irradiated films. Similarly the induction period during photoxidation (found by extrapolation of the linear part of the curve to the abscissa) is approximately the same for stabilised and unstabilised HIPS extruded film. This is because of the retardation of the linear stage of the oxygen absorption curve by the phenolic antioxidant. This is confirmed in figure 71 in which the induction period during photoxidation for stabilised and unstabilised HIPS film is plotted with respect to duration of photolysis. The data from figures 66 and 69 are represented in figure 71 by a single curve which drops in a linear manner for the first 30 hours of photolysis and then levels out after 50 hours.

Effect of phenolic antioxidant on the photoxidation of HIPS extruded film (50 μm) previously UV irradiated in argon through quartz (oxygen absorption in oxygen)

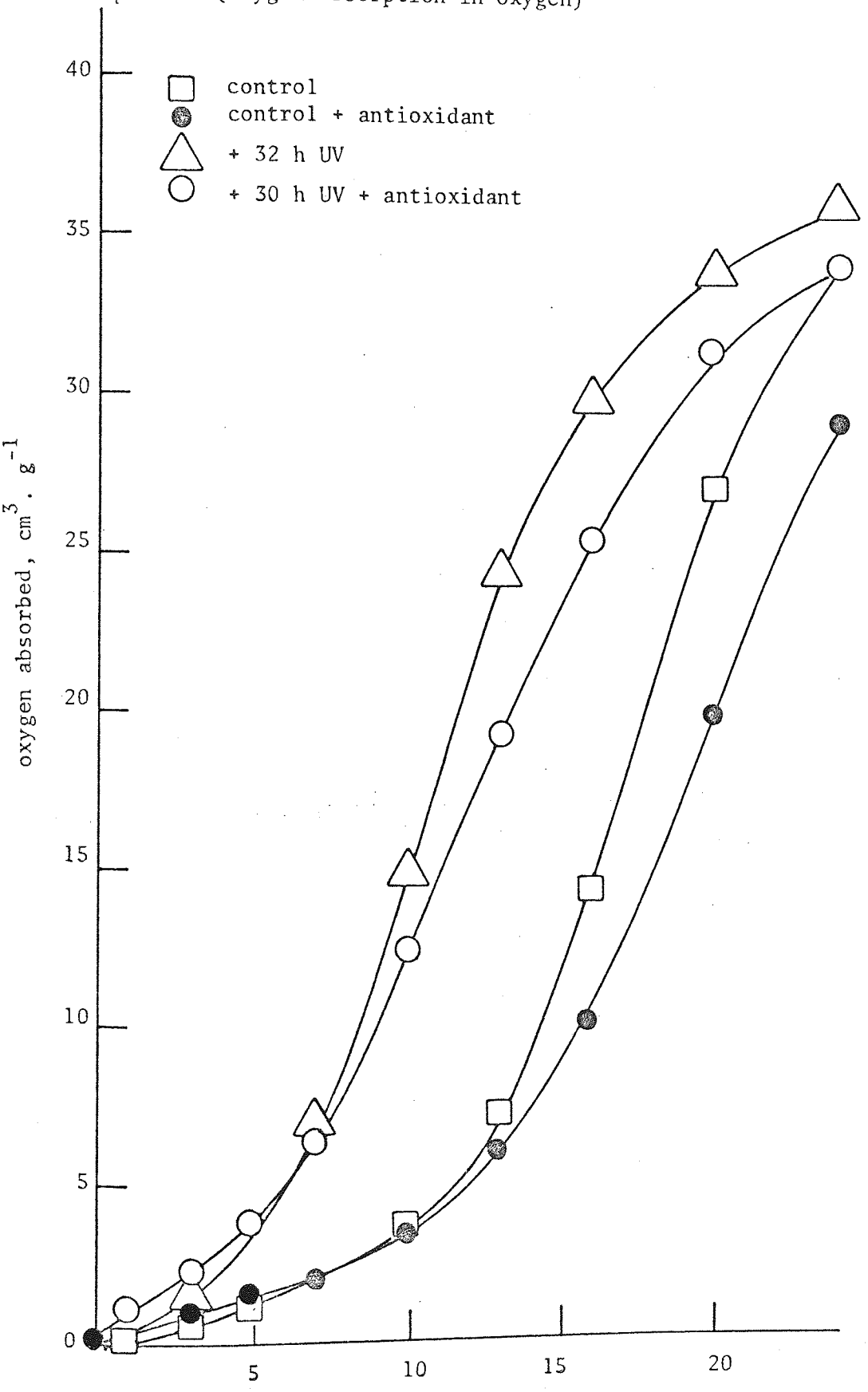

Figure 70.

Variation in induction period to rapid photoxidation of stabilised and unstabilised HIPS extruded film (50 μm) as a function of UV irradiation in argon through quartz (oxygen absorption in (a) air and (b) oxygen).

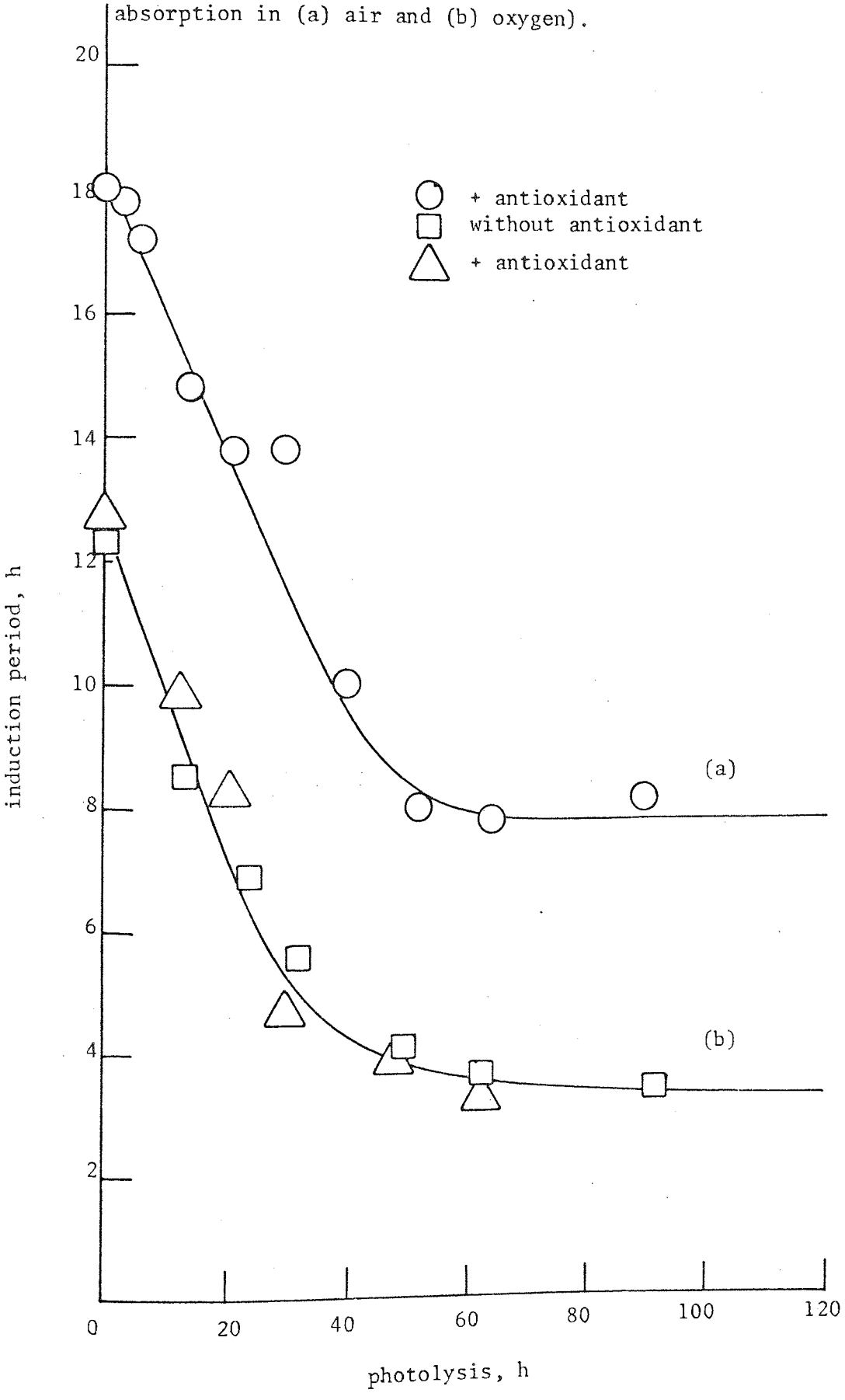

Figure 71.

The auto-catalytic character of the oxygen absorption curves (figures 66 and 69) was not eliminated with extensive pre-irradiation and this is seen in figure 71 by the curve representing induction period reaching a constant value. The parallel curve shown in figure 71 represents data obtained from the photo-oxygen absorption in air of stabilised HIPS extruded film (50 μm) pre-irradiated in argon through quartz. The longer induction period exhibited (figure 71) by HIPS photoxidised in air has already been illustrated in Chapter One (see 1.4.4). The levelling out of the induction period similarly occurs after 50 hours of photolysis (figure 71) demonstrating that the conditions of photo-oxygen absorption do not affect this value. The initial rate of photoxidation of samples also pre-irradiated through quartz (figure 68) plateaus out after the same duration of photolysis. The IR spectrum of a sample that had been pre-irradiated for 64 hours through quartz revealed that the trans-1,4-polybutadiene had been depleted by about 2.4%. This corresponds to a concentration of hydroperoxide of approximately 2×10^{-6} mol.g^{-1} of HIPS that would have been formed during photoxidation, calculated from figure 27, Chapter Two for similar HIPS extruded film (50 μm). Furthermore, the concentration of hydroperoxide formed after pre-irradiation of HIPS extruded film (50 μm) for 64 hours under identical conditions was found to be in excess of 2×10^{-6} mol. g^{-1} (figure 18, Chapter Two).

If a pre-irradiated sample of HIPS is transferred immediately to the oxygen absorption vessel without the usual exposure to air for 2 hours in the dark a rapid, initial absorption of oxygen is observed. Figure 72 depicts the course of oxygen absorption at 25°C in the dark for a HIPS extruded film, containing a phenolic antioxidant, which has

Activation of stabilised HIPS extruded film (55 μm) by UV irradiation in argon through quartz for 16 hours prior to oxygen absorption in air in the dark at 25°C.

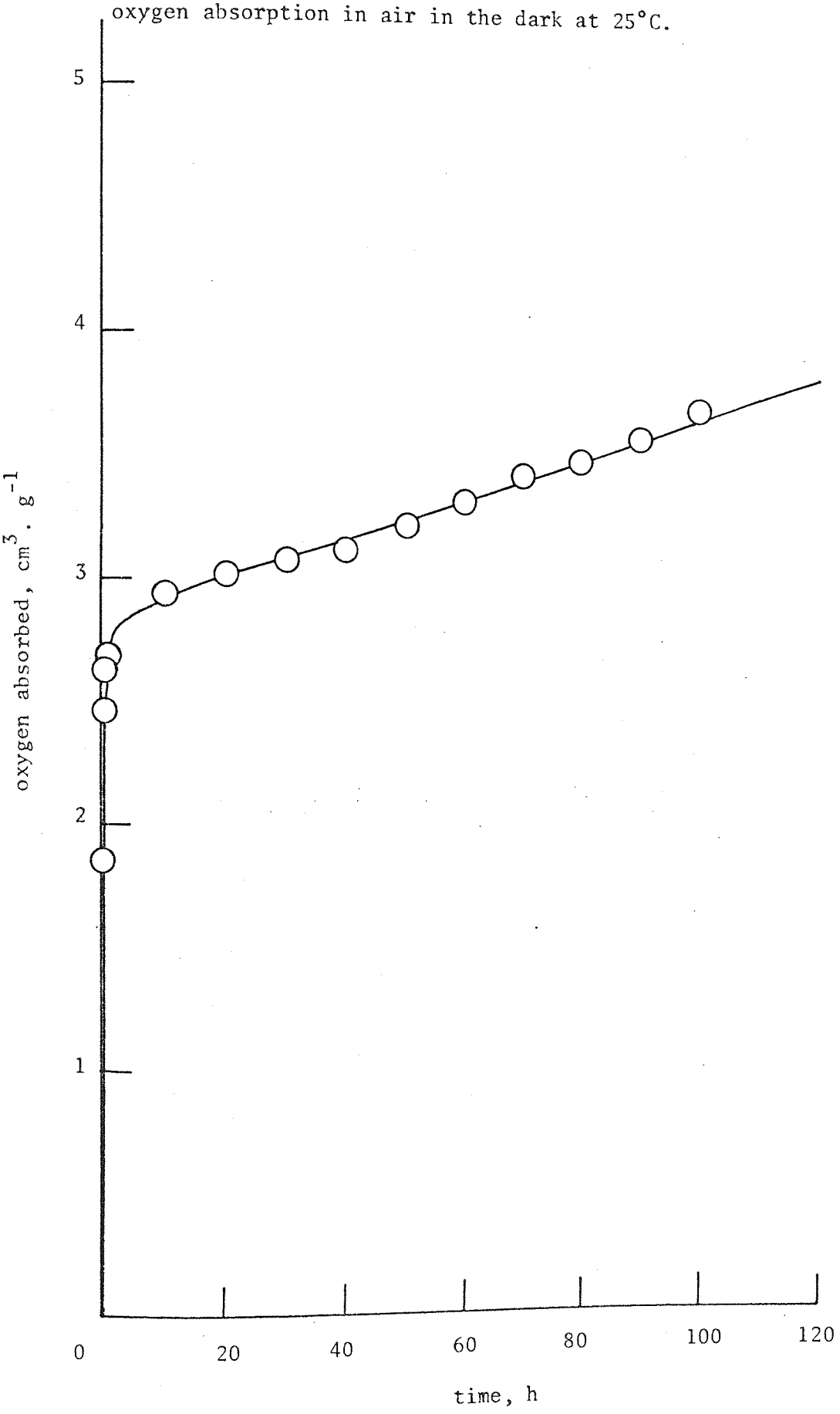

Figure 72.

been pre-irradiated in argon through quartz for 16 hours under identical condition used for the previous experiments. This rapid absorption of oxygen subsides after 2 hours but continues to rise at a very slow linear rate for another 100 hours at 25°C in the dark, figure 72.

The dynamic-mechanical properties of HIPS film (50 μm), containing a phenolic antioxidant, were measured at ambient temperature on the Rheovibron (see 1.5.1) after pre-irradiation in argon through quartz under identical conditions to those used for samples shown in figure 66 et seq. Figure 73 contrasts the changes in complex modulus, E*, between samples which have been photoxidised and the above-mentioned photolysed specimens. The effect of photoxidation on the dynamic-mechanical properties of stabilised HIPS film measured at ambient temperature (20 °C) has already been discussed in Chapter Three (figure 51). It is clear from figure 73 that the dynamic-mechanical properties of pre-irradiated HIPS film undergo similar overall changes to those observed during photoxidation. The principal difference between photoxidised and photolysed HIPS film is the duration of UV irradiation necessary to impart similar dynamic-mechanical properties. A maximum value of complex modulus was attained during photoxidation in air after only 25 hours while 175 hours of UV irradiation in argon are required to reach a maximum. Furthermore, the numerical value of complex modulus for photolysed specimens is markedly lower than for photoxidised samples, figure 73. It was deduced in Chapter Three that the maximum concentration of hydroperoxide obtained during photoxidation corresponded to the mid-point of linear rise in complex modulus. The maximum concentration of hydroperoxide formed after photolysis of unstabilised HIPS film and

Changes in complex moduli during (a) photoxidation of stabilised HIPS cast film (55 μm), (b) photolysis of unstabilised HIPS extruded film (50 μm)

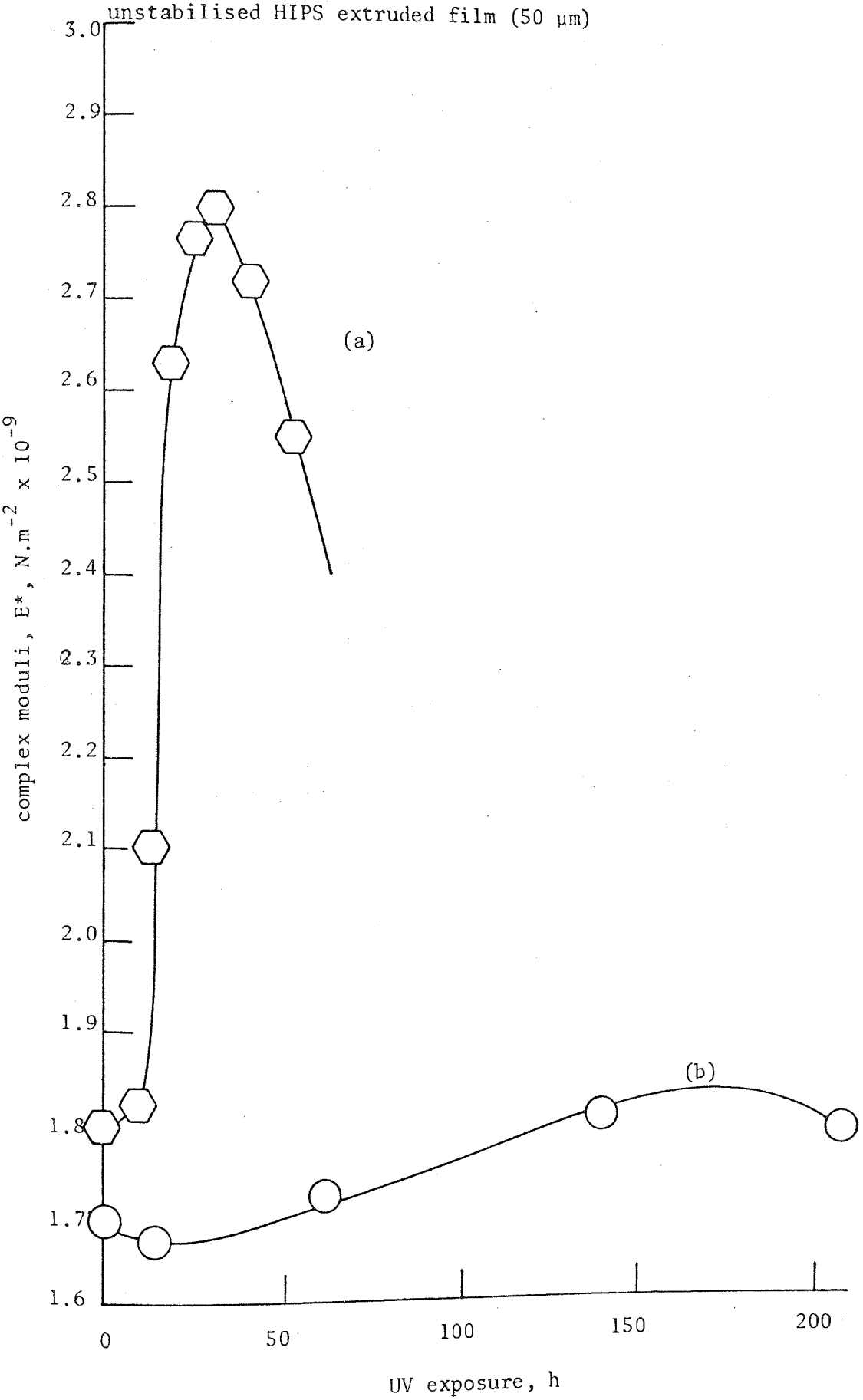

Figure 73.

exposure to air for 2 hours in the dark (figure 18, Chapter Two) occurred after approximately 90 hours and similarly corresponds to the mid-point of the complex modulus curve, figure 73. Embrittlement of HIPS film took only 50 hours of photoxidation compared to over 200 hours of photolysis. In both cases embrittlement occurs on the decline of complex modulus after the maximum, figure 73.

5.1.3 Activation of polystyrene by polybutadiene

5.1.3.1 High impact polystyrene film

Figure 74 depicts the photo-oxygen absorption in oxygen of HIPS and "crystal" polystyrene extruded films, over 2 g of molecular sieves. HIPS film has been photoxidised beyond the familiar auto-accelerating curve which retards after 20 hours of exposure to UV. However, oxygen continues to be absorbed for another 300 hours in a much slower auto-accelerating manner. Re-purging of the oxygen absorption vessel after 200 hours of UV exposure had no effect on the course of photoxidation. Crystal polystyrene also absorbs oxygen during the same period of extended photoxidation (figure 74) although at a slightly lower auto-accelerating rate. This is confirmed by measuring the rate of oxygen absorption of HIPS and "crystal" polystyrene of similar thickness (either 15 or 20 μm) after the same duration of photoxidation. At both thicknesses of polymer the rate of oxygen absorption of HIPS after 25 hours of UV exposure is considerably greater than the corresponding rate for "crystal" polystyrene, figure 74. It was established in Chapter One (see 1.4.3) that the rate of photoxidation of HIPS film was not limited by diffusion of oxygen into the polymer when the thickness was less than 55 μm. However, for "crystal" polystyrene it was deduced that the limiting

Photoxidation of HIPS and "crystal" PS, extruded film

(oxygen absorption in oxygen)

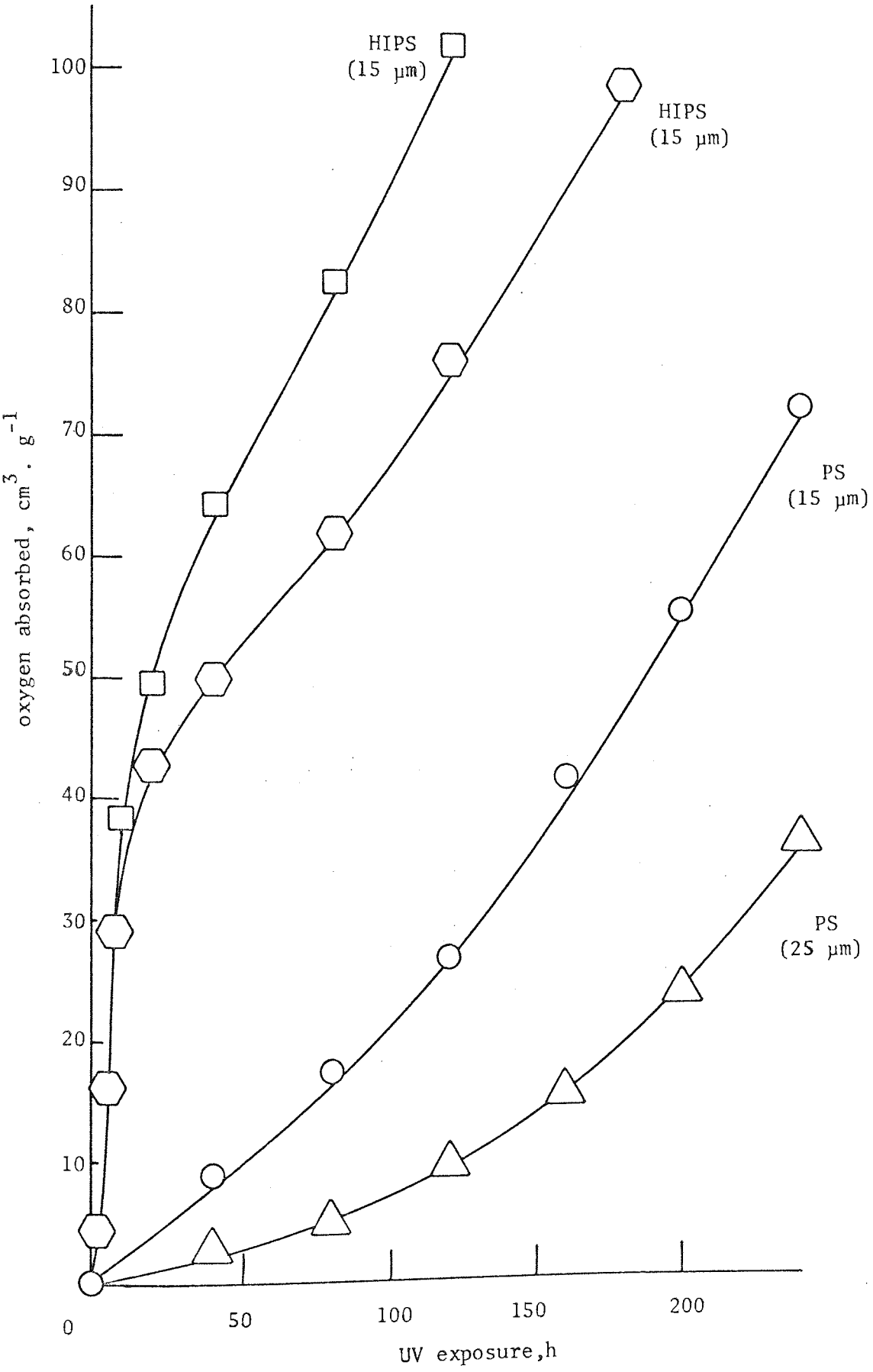

Figure 74.

thickness was less than 15 μm. The increase in rate of oxygen absorption after 20 hours with decreasing thickness of HIPS film is analogous to the corresponding increase in rate for "crystal" polystyrene, figure 74.

5.1.3.2 Polybutadiene/polystyrene solution

The concentration of PBD in HIPS used was 6.5% (see 1.1). Nevertheless it is possible to observe the effect of increasing the concentration of PBD relative to polystyrene by mixing appropriate quantities of 1% w/v chlorobenzene solutions of PBD and polystyrene together prior to photo-oxygen absorption in oxygen under identical conditions to those used for model compound studies (see 4.1.3). Figure 75 illustrates the effect of addition of PBD to polystyrene at concentrations of 0%, 5%, 10%, 25% and 100%. In all cases 1 ml of solution was photoxidised. Consequently the weight of PBD undergoing photoxidation ranged from 0 to 0.01 g. Pure "crystal" polystyrene exhibits a definite auto-accelerating mode of photoxidation in solution (figure 75) similar to that already described for extruded film, figure 74. With increasing concentration of PBD the initial rate of oxygen absorption increases dramatically but the secondary, linear rate remains parallel to the curve representing 100% polystyrene, figure 75. The rate of photoxidation after 25 hours increases with increasing concentration of PBD compared with that of pure polystyrene, confirming evidence presented in figure 74. The amount of oxygen absorbed after 20 hours of exposure to UV for a 10% solution of PBD in polystyrene (figure 75) (ca. 40 $cm^3 . g^{-1}$) is similar in magnitude to that found for HIPS, figure 74.

Photoxidation of 1 ml of a 1% w/v solution of PBD and "crystal" PS in chlorobenzene and mixtures of intermediate composition (oxygen absorption in oxygen)

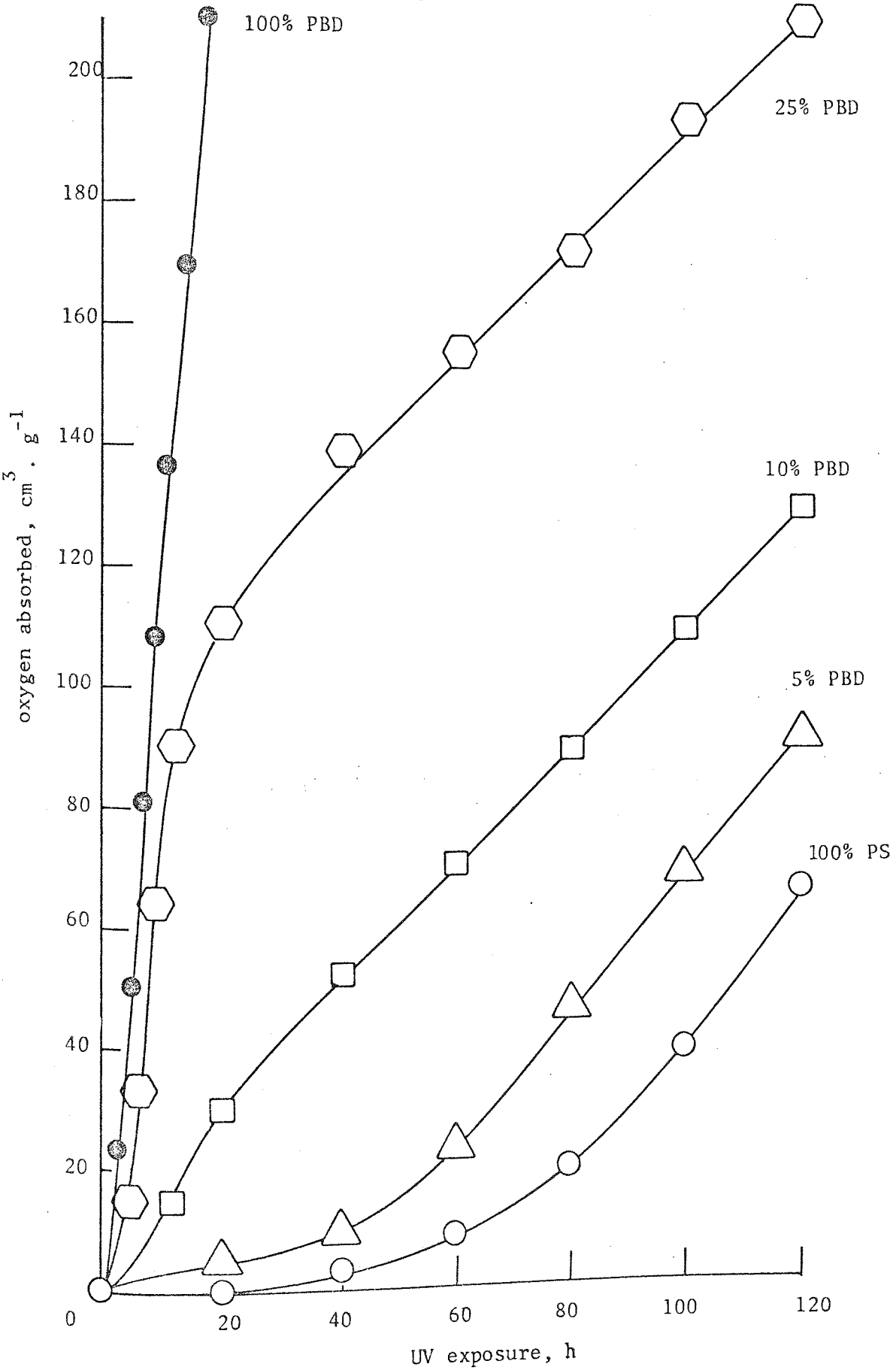

Figure 75.

5.1.4 Exposure of high impact polystyrene to ozone

The peroxide concentration determined by iodimetry (see 1.8) of unstabilised HIPS extruded film (50 μm) which has been exposed to an ozone concentration of 25 ppm at 25°C (see 1.13) for various times is shown in figure 76. The initial concentration of peroxidic oxygen observed for the unexposed polymer is the same as that determined for similar unstabilised HIPS extruded film (50 μm) before photoxidation (see figure 27, Chapter Two) and is likewise attributed to hydroperoxide formation during processing. During exposure to ozone peroxide concentration increases rapidly at first after which the rate if build-up diminishes in a regular manner (figure 76) although it does not reach a plateau up to 160 hours of exposure. The concentration of peroxide generated by ozonisation is of the same order as the concentration of hydroperoxide formed during thermal oxidation of similar unstabilised HIPS extruded film (50 μm) (figure 12, Chapter Two). However, in the latter case oxidation products, namely carbonyl and hydroxyl were observed to increase dramatically while unsaturation was destroyed (figure 12, Chapter Two). No carbonyl (or hydroxyl) could be detected during ozonisation of HIPS film even after 160 hours of exposure to ozone with a corresponding peroxide concentration of 12×10^{-6} mol. g^{-1}. Similarly no apparent decrease in the concentration of unsaturation (trans-1,4-polybutadiene) could be observed by IR spectroscopy. Samples which have been exposed to ozone under identical conditions were photoxidised in oxygen. Figure 77 shows the effect of ozonisation on oxygen absorption of HIPS film. Only the initial 8 hours of photoxidation are presented in figure 77. Consequently, the typical auto-accelerating mode of the

Development of peroxides in unstabilised HIPS extruded film (50 μm) on exposure to ozone at a concentration of 25 ppm at 25°C

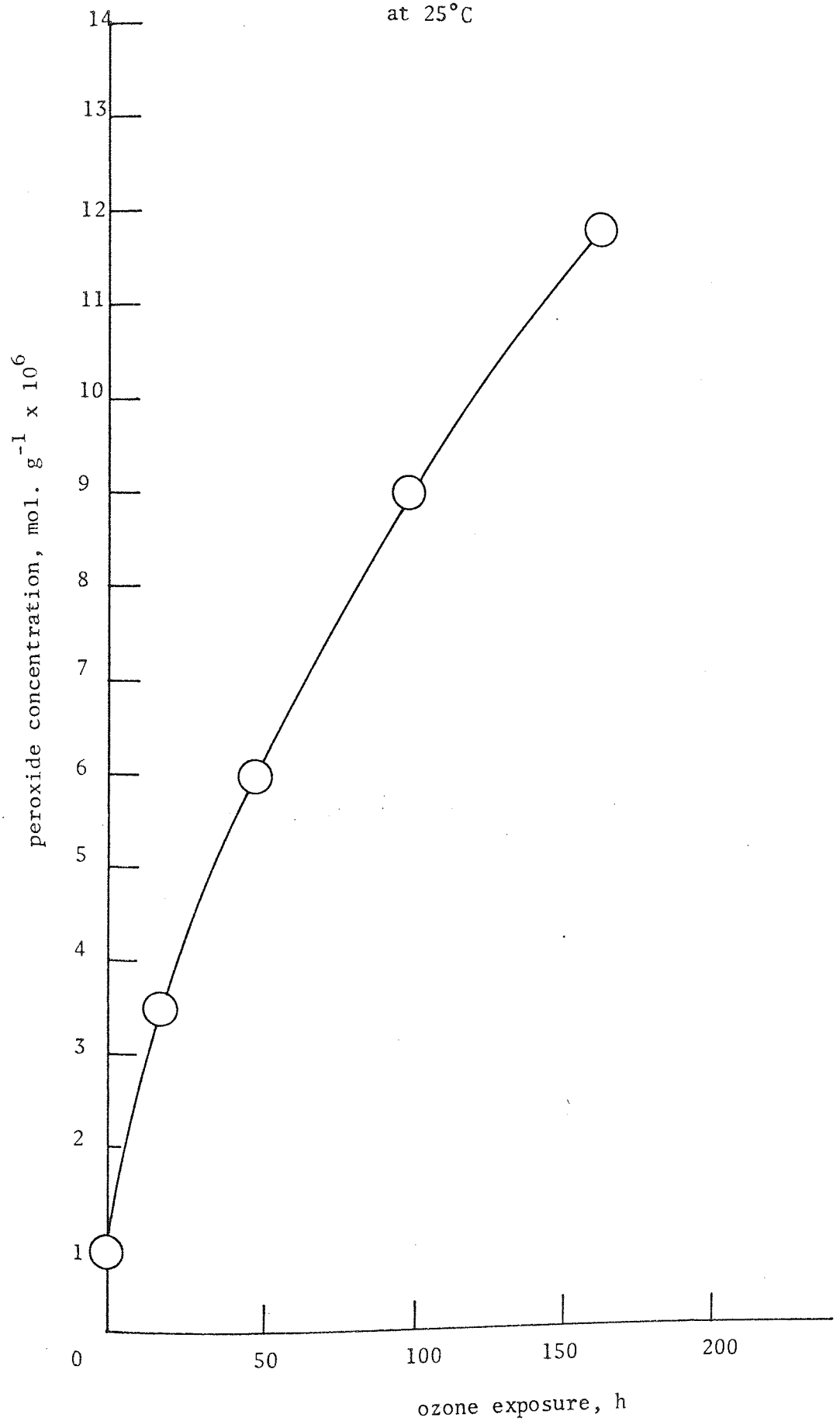

Figure 76.

Effect of ozonisation (25 ppm) on the photoxidation of unstabilised HIPS extruded film (50 µm) (oxygen absorption in oxygen)

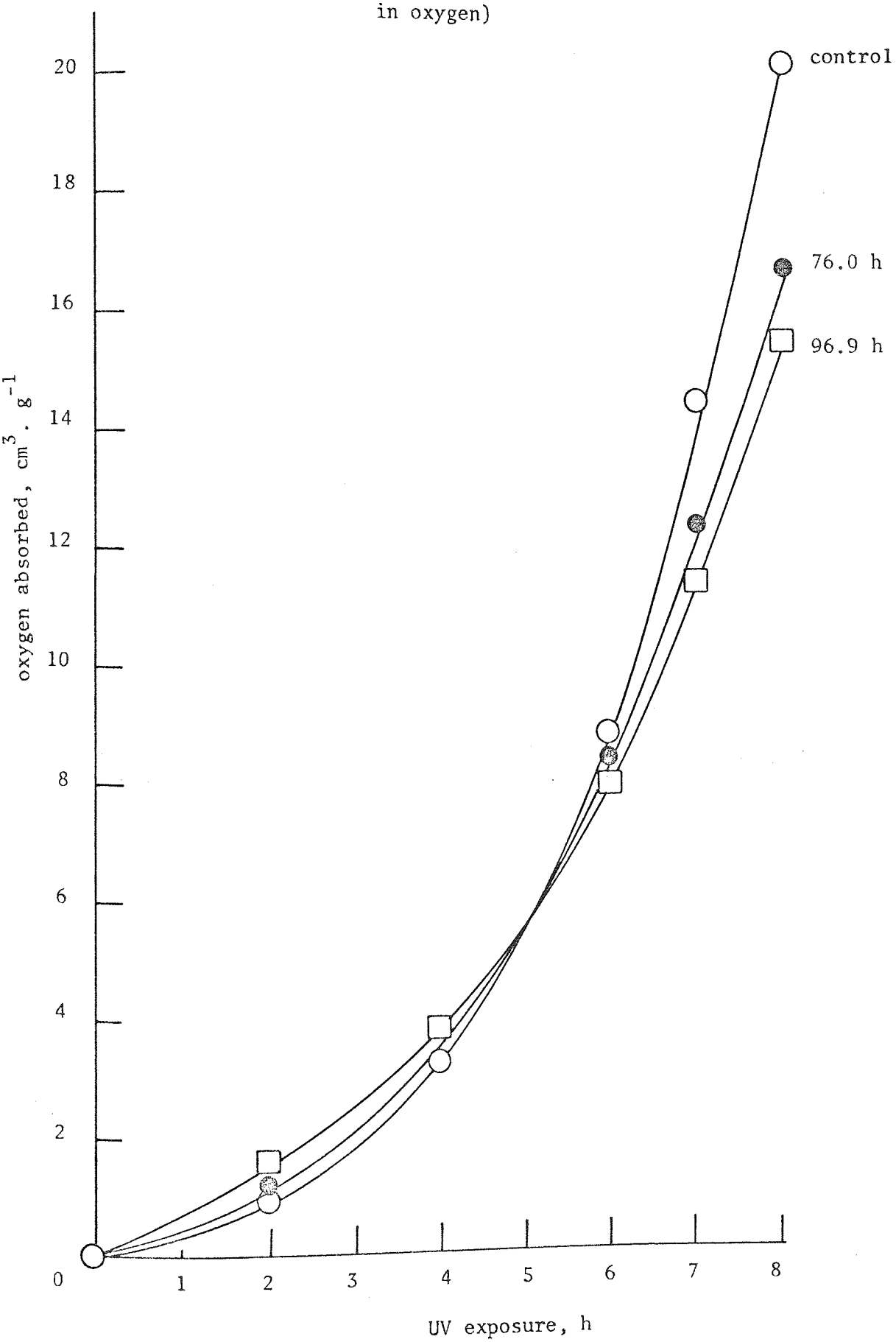

Figure 77.

Initial rate of photoxidation of unstabilised HIPS extruded film (50 μm) as a function of peroxide concentration

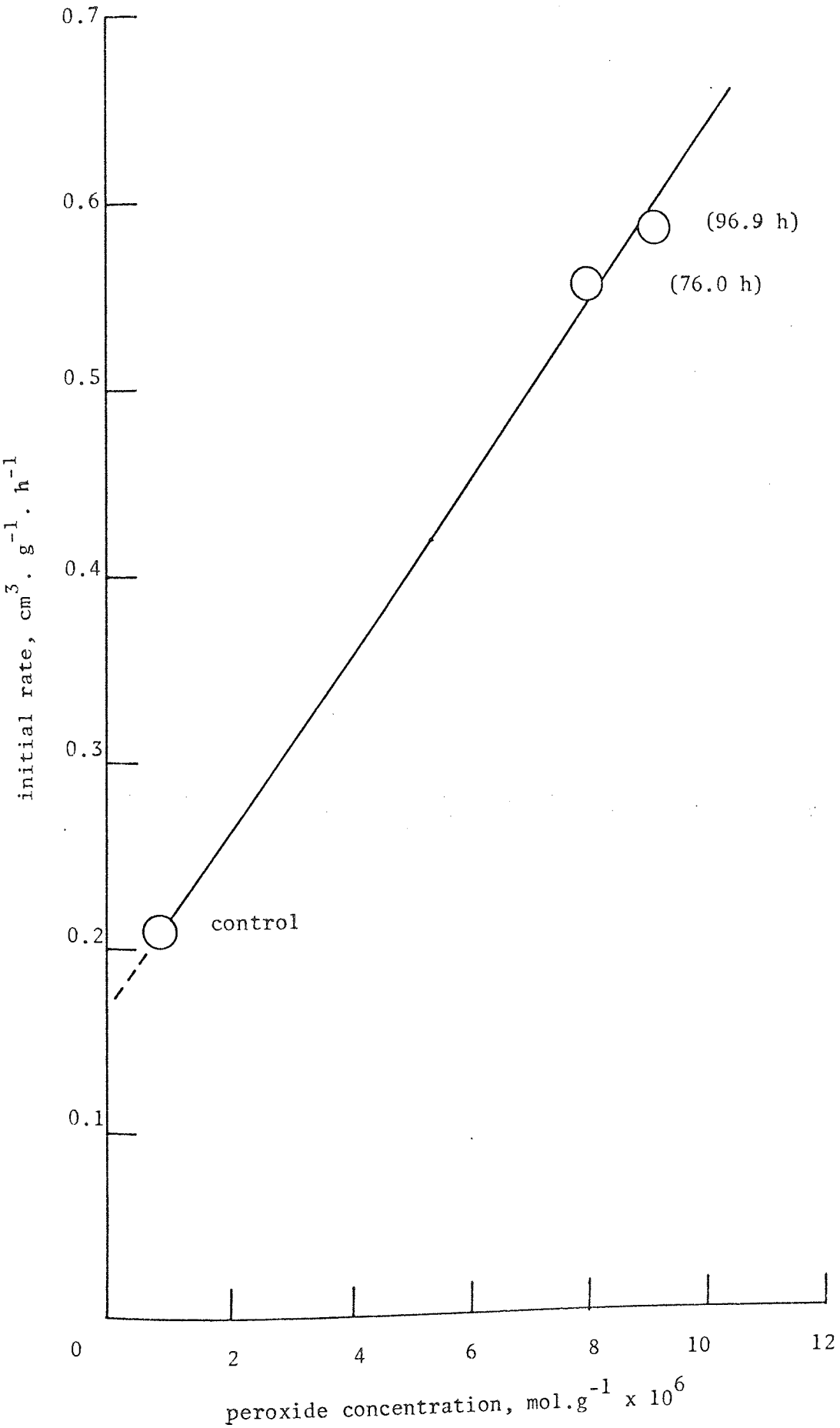

control curve is seen clearly. With increasing exposure to ozone the initial rate increases slightly and the linear (maximum) rate drops by a corresponding amount. Nevertheless, ozonisation does not eliminate the auto-accelerating character of the curves during photoxidation. Figure 78 illustrates the relationship between initial rate of photoxidation and concentration of peroxidic oxygen. It would appear that a positive correlation holds between initial rate of photoxidation and concentration of peroxidic oxygen.

5.1.5 Exposure of high impact polystyrene and polybutadiene to singlet oxygen.

Singlet oxygen was generated in a quartz gas discharge tube by microwave excitation of ground state triplet oxygen (see 1.14). Unstabilised HIPS extruded film (50 μm) was placed in the reaction vessel 30 cm downstream from the discharge glow and examined for hydroperoxide formation by iodiometry and IR after exposure to singlet oxygen for up to 10 hours. Also, the photostability of HIPS film exposed to singlet oxygen was determined by oxygen absorption. No additional hydroperoxide, above that already present in the control, could be detected by iodiometry or IR in films exposed to singlet oxygen. Similarly the oxygen absorption of HIPS film exposed to singlet oxygen was identical to that of the control. Polybutadiene, cast from a solution of dichloromethane on a KBr disc under nitrogen, was also exposed to singlet oxygen for up to 10 hours (imput power to microwave generator of 50 w). No absorbance in the oxygen-hydrogen (O-H) stretching frequency could be detected by transmission IR spectroscopy after exposure to singlet oxygen. Similarly no depletion of unsaturation was observed.

5.2 DISCUSSION

The effect of thermally-produced hydroperoxide introduced into HIPS by melt processing in the torque rheometer, film extrusion and oven ageing of extruded film, on photoxidation has already been discussed in Chapter Two. However it is believed that a direct activation of the unsaturation in HIPS prior to hydroperoxidation is possible in the absence of oxygen.

Under the experimental conditions used for the pre-irradiation (in argon) of HIPS extruded film (see 1.11), photolytic cleavage of the peroxidic bond, with a quantum efficiency approaching unity[15], will preclude the build-up of a stationary concentration of hydroperoxide. Moreover the initial very low concentration of hydroperoxide, below 0.5×10^{-6} mol.g^{-1} (see figures 15 and 27, Chapter Two) present in extruded film will be photolysed in an argon atmosphere within the first few hours[140]. The highest concentration of hydroperoxide that is likely to be present at the start of photolysis is 0.5×10^{-6} mol.g^{-1} and the maximum concentration of hydroperoxide obtained after pre-irradiation and exposure to air was in excess of 2×10^{-6} mol.g^{-1} (figure 18, Chapter Two). However, one mol of hydroperoxide may either break down giving two mols of alkoxy and hydroxy radicals or dehydrate forming carbonyl and no other radicals. The alkoxy radical will produce an alkyl radical via β-scission, addition to a double bond or hydrogen abstraction. The hydroxy radical will undoubtedly hydrogen abstract from the polymer resulting in an alkyl radical. The maximum concentration of hydroperoxide derived from initial hydroperoxide in HIPS extruded film via production of alkyl radicals which

will combine very rapidly with oxygen during the two hours preceding iodiometry to form hydroperoxide (via hydrogen abstraction by the derived alkylperoxy radical) will thus be less than 1×10^{-6} $mol.g^{-1}$.

Furthermore, the instability of the allylic radical (at ambient temperature) formed during the above mechanism will detract further from this maximum hydroperoxide concentration through dimerisation during photolysis in argon. Perhaps more conclusive evidence against the above mechanism is that during the subsequent photoxidation of pre-irradiated HIPS film (see 5.1.2) the maximum concentration of hydroperoxide (determined after exposure of photolysed polymer films to air in the dark for two hours) occurred after nearly 100 hours of pre-irradiation (figure 18, Chapter Two).

An alternative mechanism for the subsequent formation of hydroperoxide after exposure to air of pre-irradiated HIPS extruded film is required. A direct activation of the PBD moiety in HIPS during photolysis leading to radical formation would account for the higher concentration of hydroperoxide observed after extensive pre-irradiation in argon (figure 18, Chapter Two). Furthermore, it is believed that direct activation is primarily responsible for the progressive reduction of the auto-accelerating stage of the photo-oxygen absorption curves shown in the present chapter (see 5.1.2.). Morand has shown[141] that the unsaturation of cis-rubbers (1,5-dienes) can undergo direct activation by exposure to UV light above 290 nm. Discrete wavelengths of maximum activity were found by stress photo-relaxation of vulcanised rubber[141]. Similar stress photo-relaxation spectra were found for both UV irradiation in air and in vacuum, although the maxima were

slightly further apart in the latter. The above stress photo-relaxation spectra were also found to be associated with UV absorption maxima[141]. The separation of the maxima in the UV corresponded to 1500 cm^{-1} which is similar to that for polyenes[142]. However, the separation of stress photo-relaxation maxima was found to correspond to 950 cm^{-1}[141]. It was concluded[141] that the associated UV absorbance maxima resulted from oxygen-perturbed triplet state ($S_o \rightarrow T_1$ transition) of conjugated polyenes which has a vibrational separation of 1500 cm^{-1} in the first triplet state[143]. Similarly the oxygen-perturbed triplet state of isolated double bonds has a vibrational structure of 950 cm^{-1}[141].

In the present study of HIPS it is postulated that a red-shift in the UV spectrum arises via formation of extended conjugation (polyene) during photolysis in argon. Absorption of UV by this chromophore may lead to radical formation during photolysis. On exposure to oxygen hydroperoxide will be formed via hydrogen abstraction by the peroxy radical. Allylic radicals may also be formed during photolysis of HIPS by cleavage of the methylene-methylene bond of 1,4-polybutadiene[144]. However, simple 1,5-dienes (PBD) have an absorption maximum around 200 nm ($S_o \rightarrow S_1$ transition)[145,146] which does not extend much beyond 240 nm. Therefore, it is unlikely that carbon-carbon scission of non-conjugated 1,4-polybutadiene will be of significance under the conditions used in the present study (UV > 280 nm quartz and UV > 290 nm, pyrex). Indeed no allylic radical formation in PBD was reported[144] when a pyrex filter was used even though allylic radicals could be identified by ESR using shorter wavelengths, (254 nm)[144].

Cis-trans isomerisation of cis-polybutadiene has been reported[147] to occur during vacuum irradiation with UV light of wavelength 254 nm, even though 1,5-dienes are transparent above 240 nm. It was concluded[147] that direct excitation of the π-electrons of the double bonds of cis-polybutadiene to the anti-bonding (π*) state permitting free rotation to the more thermodynamically stable trans isomer did not take place directly at this wavelength but occurred via an energy transfer process from chromophoric impurities namely catalyst residues and insignificant amounts of carbonyl. Indeed, PBD used in the present study does show an absorption tail extending beyond 290 nm. Therefore absorption of UV by PBD (HIPS) through a pyrex filter (> 290 nm) with a subsequent energy transfer to the π-electrons of the double bond of cis-polybutadiene will lead to excitation and eventual isomerisation. Only 309 $k.J.mol^{-1}$ are required for cis-trans isomerisation via triplet excitation[148] which is equivalent to 400 nm. Therefore sufficient energy is available (via energy transfer) for photoisomerisation of cis-polybutadiene in HIPS under the condition used in the present study (see 5.1.2). However, it is postulated that hydrogenation (see Scheme 15) of the excited cis-polybutadiene takes place in preference to isomerisation to the trans-isomer. Transference of hydrogen from a saturated unit of another cis-isomer to an excited double bond via a six-membered intermediate will be favoured energetically by the lowering of π-bond energy of the resulting conjugated system. The above dis-proportionation reaction will result in loss of unsaturation (cis-polybutadiene) and indeed this has been reported[147] to be associated with cis-trans isomerisation during UV irradiation of cis-polybutadiene with UV of shorter wavelengths (254 nm). Similarly a weak ESR spectrum of UV irradiated cis-polybutadiene has been attributed[144]

to polyenyl radicals, although reported to arise from carbon-hydrogen scission from α-methylene groups of polymer radicals with a possible production of hydrogen[144]. No hydrogen could be detected in the present study after extensive photolysis (in argon through quartz) of HIPS or PBD by mass spectroscopy (AEI,MS9). Therefore it seems more likely that polyenyl radicals are produced by carbon-carbon scission of the methylene-methylene bond adjacent to a conjugated system. Absorption of UV above 290 nm by the π-electrons delocalised over an extended sequence of conjugated double bonds is possible under these conditions resulting in cleavage of the weakest bond along the polymer chain which is the methylene-methylene bond (160 $k.J.mol^{-1}$)[149]. The derived polyenyl and alkyl (allylic) radicals will be stabilised by resonance, although the polyenyl radical is likely to be more stable, and may possibly hydrogen abstract from an α-methylenic centre of another polyene. The polyenyl radical will also be stabilised by resonance. When a critical concentration of polyenyl radicals has built up during photolysis of HIPS they may either terminate by dimerisation or more likely add to the double bond of an extended conjugated system. This cross-linking mechanism is analogous to the oxidative reactions discussed in Chapters Two and Three for gel formation. Further evidence to support the formation of polyenes during pre-irradiation stems from the fact that a yellowing of HIPS film was observed after extensive photolysis even though no conjugated carbonyl could be detected by IR. Similar results have been reported for UV irradiated cis-polybutadiene[144].

SCHEME 15

(1) hydrogen/isomerisation :

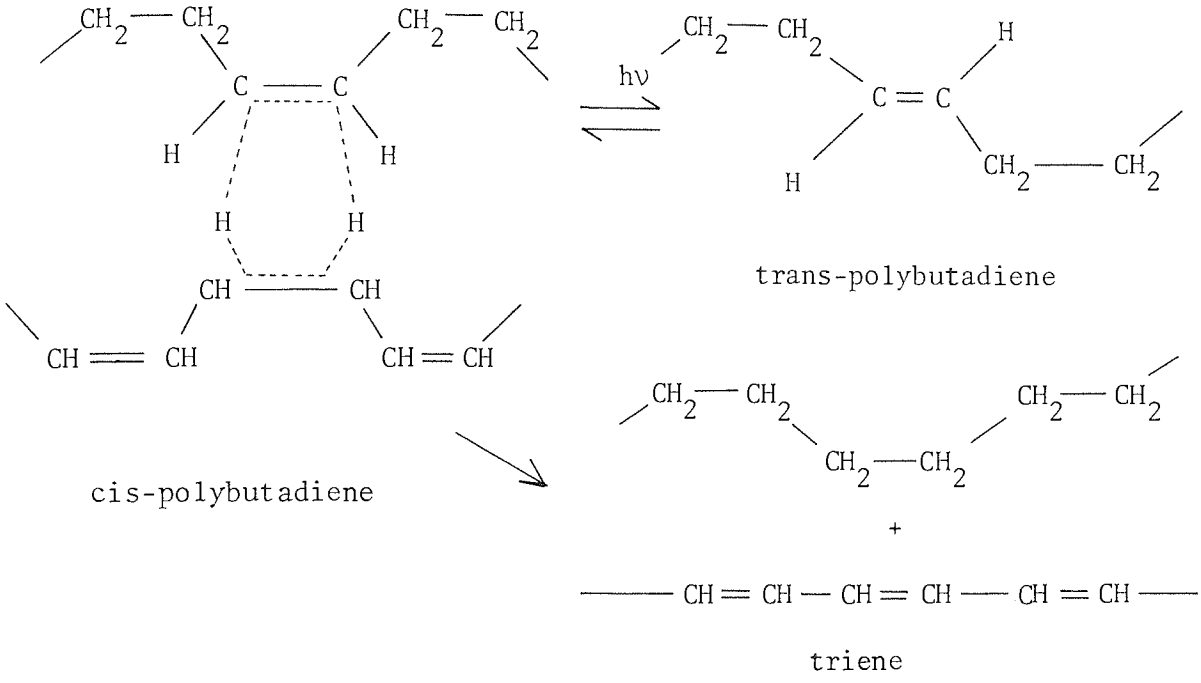

(2) photolysis:

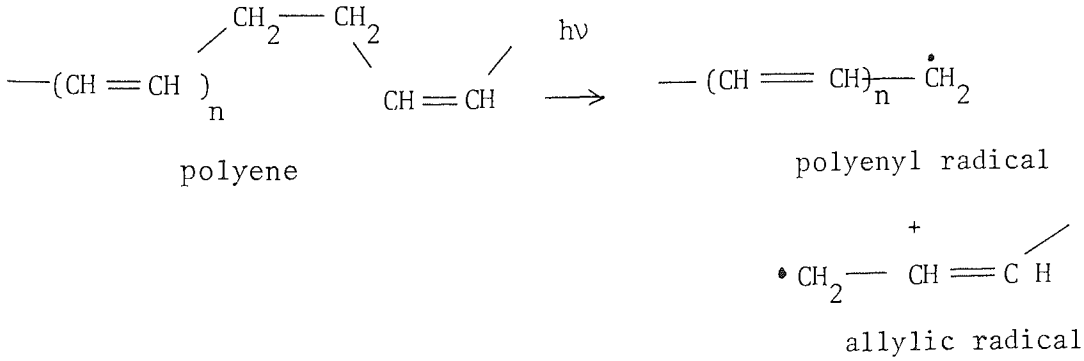

(3) resonance stabilisation:

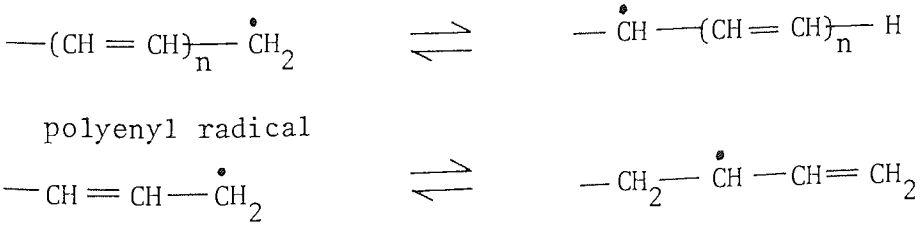

(4) cross-linking:

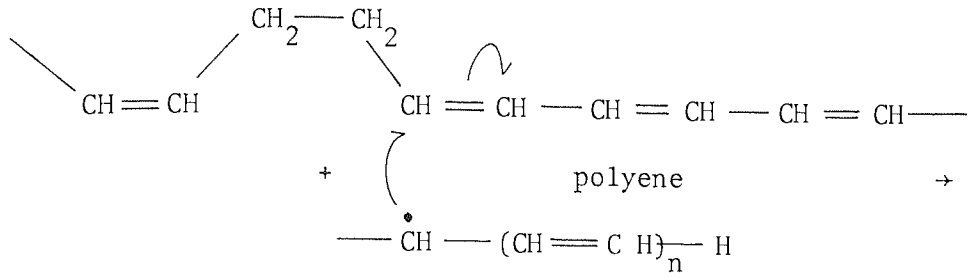

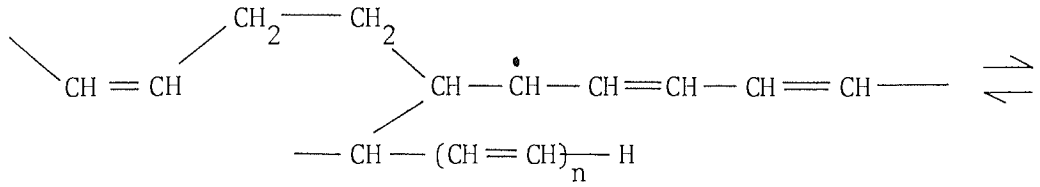

(5) resonance stabilisation:

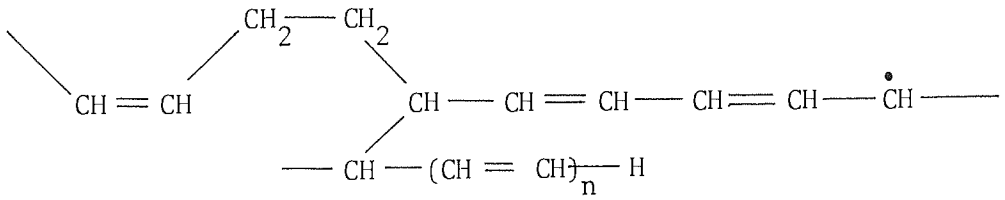

(6) hydrogen abstraction:

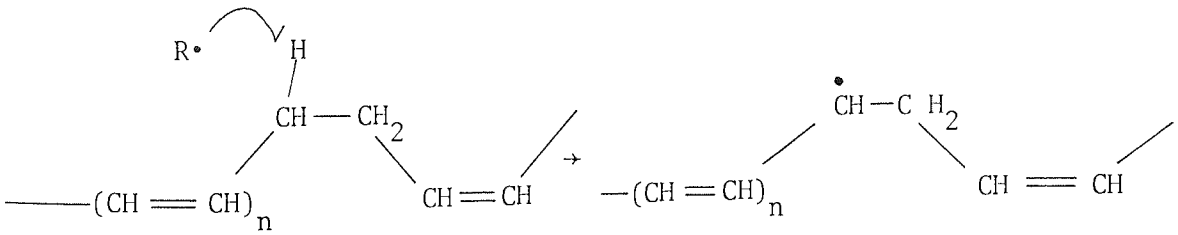

(7) resonance stabilisation:

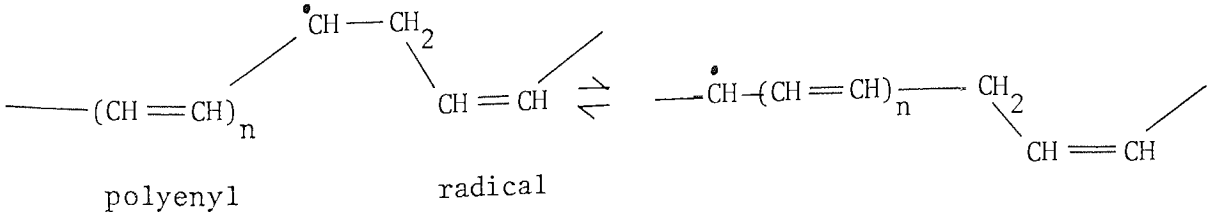

The "induction period" observed during photolysis of HIPS, seen in figure 68 as a slow increase in initial rate prior to a rapid rise, may be interpreted as the time required to build up a sufficient concentration of photo-sensitive species necessary for the removal of the auto-accelerating stage of the oxygen absorption curves, figures 66 and 67. This is because it is necessary to form an extended conjugated system (polyene) of sufficient length to absorb in the UV at the appropriate wavelength. The longer "induction period" observed for HIPS film pre-irradiated through pyrex which removes the shorter wavelengths substantiates this, figure 68. The concentration of photo-sensitiser (polyene and derived polyenyl radical) will never be high enough to form sufficient hydroperoxide to completely eliminate the auto-accelerating portion of the photoxidation curves (figures 66, 67 and 69) because of competing termination reactions of polyenyl radicals, notably dimerisation. However, the polyenyl radicals that survive dimerisation will combine rapidly with oxygen on exposure and this is demonstrated in figure 72 by a rapid absorption of oxygen. Quantitative information can not be deduced from the oxygen absorption curve during the initial rapid rise because of thermal non-equilibility of apparatus over the same period. The slow, linear rate of absorption of oxygen that follows is undoubtedly due to the same chain mechanisms discussed in Chapters Two and Three resulting, in this case, from the thermal breakdown of initially formed hydroperoxide.

Cross-linking during photolysis will have a profound affect on the dynamic-mechanical properties (figure 73), but it will also affect the oxidisability of the polymer during photoxidation. A polymer which is

extensively cross-linked will be more stable towards oxidative attack for several reasons. Primarily the number of labile sites for hydrogen abstraction will have been depleted by formation of cross-links and also oxygen permeability may be reduced. This is evident from figures 66 and 67 in which the linear (maximum) rate of oxygen absorption of pre-irradiated HIPS films was slightly retarded in the case of samples which had been photolysed through pyrex (figure 67). It is reasonable to believe that because twice the duration of pre-irradiation in argon is required when using a pyrex filter, to remove the auto-acceleration stage of the curves by the same amount, more polyenyl radicals will be involved in cross-linking (and dimerisation) reactions. Unequivocal evidence to show that cross-linking of HIPS film is a salient feature of photolysis is seen in figure 73, in which entirely analogous changes in complex modulus, E*, occur during photolysis and photoxidation. This is to be expected in view of the analogous cross-linking mechanism proposed to account for pre-irradiated HIPS film (addition of polyenyl radicals to an extended conjugated system). Cross-linking (and dimerisation) may also provide an explanation for the maximum in radical concentration produced during photolysis; termination reactions will prevail after a critical (limiting) concentration of radicals have been formed. This was illustrated by a maximum concentration of hydroperoxide (figure 18, Chapter Two). In contrast to photolysis, a maximum concentration of hydroperoxide formed during thermal or photoxidation of HIPS appeared as the differential of decay of unsaturation and formation of carboxylic acid (figures 12 and 15, Chapter Two). Moreover, an insignificant amount of unsaturation (trans-1,4-polybutadiene) was destroyed during

photolysis of HIPS film and no carboxylic acid could be detected by IR. Confirmation that a structural modification of the rubber component of HIPS takes place during photolysis was illustrated by the experimental fact that a sample pre-irradiated for over 200 hours was extremely brittle even though the usual total destruction of PBD observed during oxidative degradation had not occurred.

It is evident (figure 70) that the formation of a photo-sensitive species during photolysis of HIPS occurs independently of and is unaffected by the presence of a commercial phenolic anti-oxidant. The lack of retardation by a phenolic antioxidant (probably a substituted bis-phenol, although alcoholic extraction of stabilised HIPS and examination by IR failed to confirm this) during pre-irradiation is not unexpected in view of the above mentioned mechanism for sensitisation (Scheme 15). The principal mode of operation of hindered phenolic antioxidants is to undergo a chain transfer reaction with a propagating alkylperoxy radical by donating a hydrogen (Scheme 16) forming hydroperoxide plus a relatively stable phenoxy radical[150]. Termination of the phenoxy radical by reaction with another alkylperoxy radical producing a peroxy dienone[150] or by dimerisation will reduce the kinetic chain length. The consequences of this are seen clearly during photoxidation of HIPS (figure 70) as a retardation of the linear (maximum) rate after the auto-accelerating stage of the oxygen absorption curves for both the pre-irradiated and control samples. However, during the "induction period" the initial pro-oxidant effect observed (figure 70) is believed to be due to photolytic breakdown of peroxy dienone producing initiating alkoxy radicals (see Scheme 16). The

pro-oxidant effect is likely to be greater when the initial supply of alkylperoxy radicals is higher as in the case of a pre-irradiated sample on exposure to air (figure 70).

SCHEME 16

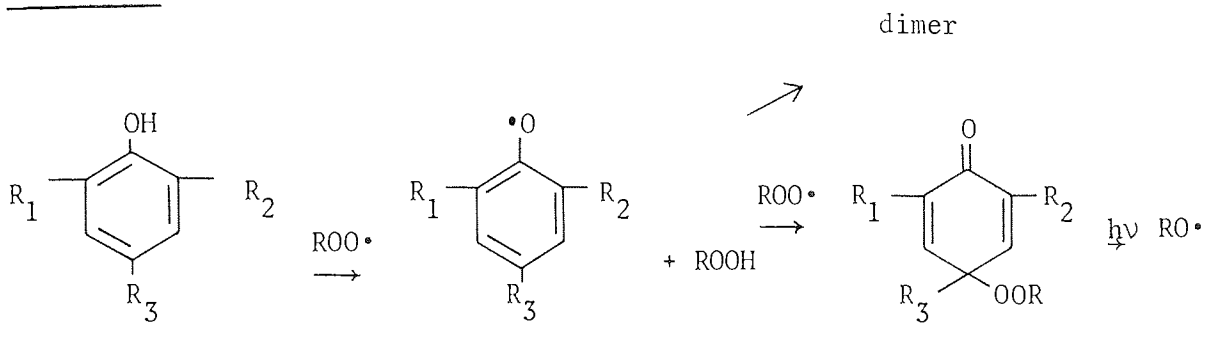

phenol phenoxy radical peroxy dienone

It was shown in figure 71 that the induction period of HIPS film with and without a phenolic antioxidant followed the same curve and reached a constant value after extensive pre-irradiation. It is believed that this is a result of the removal of the initial stage of the photoxidation curve which precedes auto-acceleration and not a reflection of the radical concentration as was the case for the measurement of initial rate (figure 68).

The importance of PBD as an oxidisable component of HIPS during oxidative degradation has been discussed fully in Chapter Two and Three. Also the possible photo-sensitisation of PBD by UV irradiation prior to photoxidation has been postulated in the present chapter. However, the question now arises whether or not PBD behaves as a pro-oxidant for the photoxidation of the polystyrene component of HIPS. It is evident from figures 74 and 75 that PBD does act as a photo-pro-oxidant

for the photoxidation of PS. After the destruction of the PBD the concentration of allylic hydroperoxide derived from its oxidation does not fall to zero (figure 15, Chapter Two) but remains at a finite level. It is this hydroperoxide that removes the auto-accelerating stage of the polystyrene photoxidation curve which is required for the build-up of hydroperoxide in the absence of PBD. It is apparent, therefore, that the photoxidising polystyrene containing the oxidation products of PBD has already reached the stationary hydroperoxide concentration (after 25 hours of UV exposure, figure 74) that is necessary for linear kinetics[4]. The apparent auto-accelerating character of the HIPS curves (after 25 hours) is interesting in view of the experimental fact that the rate of oxidation after 25 hours is already similar to that of "crystal" polystyrene after its auto-accelerating period of approximately 150 hours. It may be deduced, therefore, that although the allylic hydroperoxide derived from PBD initiates the photoxidation of the PS phase it is primarily the radical products of the photolytic cleavage of benzylic hydroperoxide that continue the chain branching reactions. It is likely that the initial allylic hydroperoxide is consumed and replaced by benzylic hydroperoxide which may continue to increase slightly for another 300-400 hours of UV exposure (not shown). The photo-pro-oxidant effect of PBD on the polystyrene component is confirmed in figure 75. Furthermore, because an activation of the "crystal" polystyrene is observed by addition of PBD in solution as a separate phase it may be concluded that a chemical bonding (grafting) of the PBD/polystyrene phases is not a pre-requisite of activation. However, it would appear that more PBD (10%) is required to achieve a similar pro-oxidant effect to that observed for

a graft co-polymer of PBD and polystyrene (6.5%). It is probable that the absence of tertiary allylic graft centres (see Chapter Three) in the admixture reduces its reactivity.

Another possible method of photo-sensitisation of HIPS to photoxidation involves reaction with ozone. This is of some practical significance since ozone is a normal constituent of the atmosphere. The concentration of which varies considerably over the earth's surface and normally ranges from 0 - 10 pphm[151]. To assess the effect of "ageing" of HIPS by ozone, ozonolysis was accelerated by using a concentration 25 times greater than the most polluted atmosphere (100 pphm)[152]. Ozone readily undergoes a cis-cycloaddition reaction with an olefinic double bond[153] to produce an unstable intermediate (molozonide, see Scheme 17). The molozonide rearranges with destruction (chain scission) of the original double bond forming a relatively stable zwitterion and a carbonyl product[154]. Recombination of these dissociation species leads to the ozonide[154]. However, the zwitterion may also combine with a similar product to form the cyclic, diperoxide or higher polyperoxide[154]. If stress is applied to the polymer film during ozonisation the zwitterionic and carbonyl products produced will be unable to recombine as the chain ends separate.

SCHEME 17

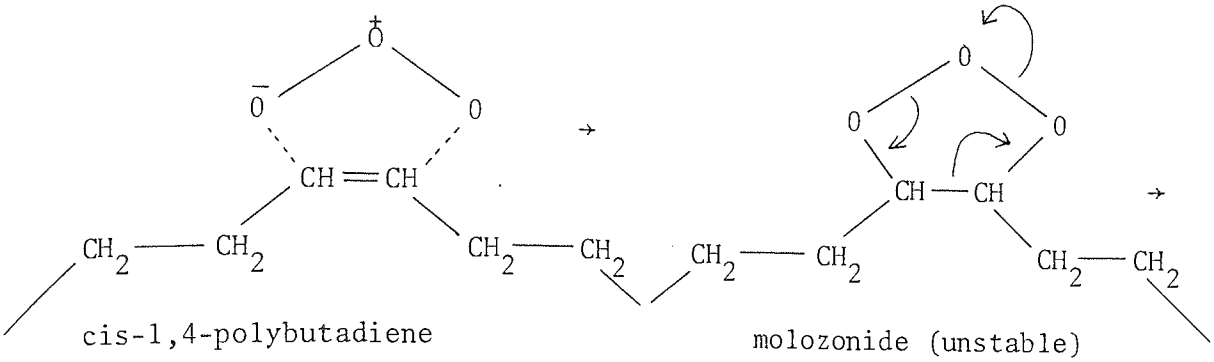

cis-1,4-polybutadiene — molozonide (unstable)

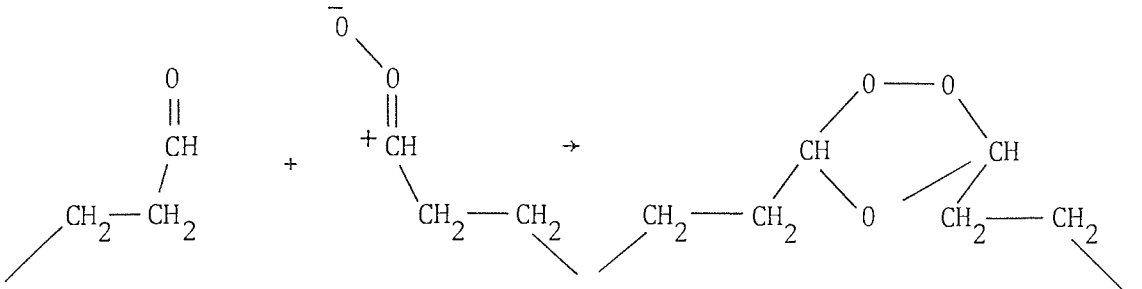

carbonyl — zwitterion — ozonide

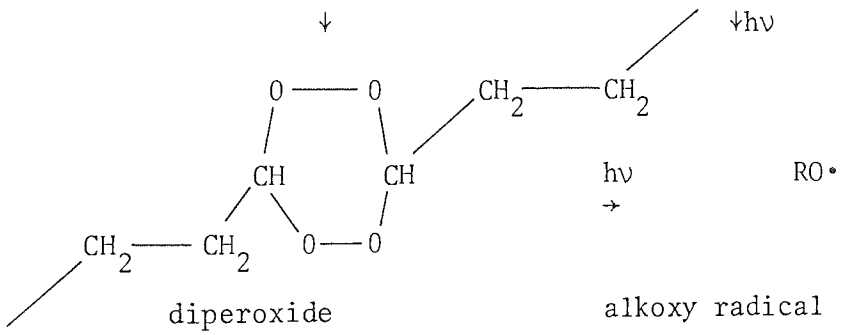

diperoxide — alkoxy radical

SCHEME 18

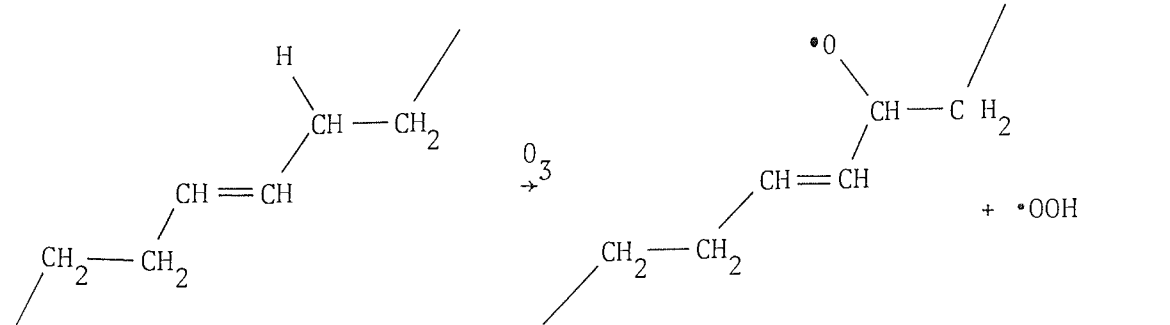

trans-1,4-polybutadiene — alkoxy and peroxy radicals

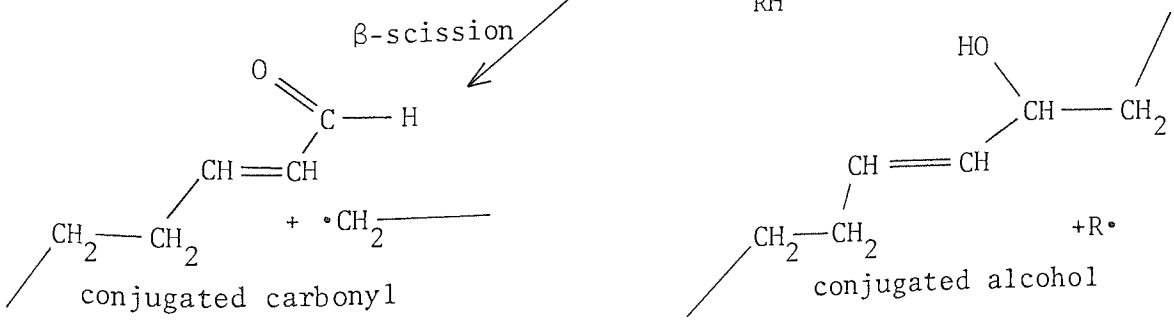

conjugated carbonyl — conjugated alcohol

In the present study on HIPS the strips of polymer films were suspended in the ozone atmosphere without applied stress. Under these conditions recombination of the dissociation products will take place readily with the formation of an impermeable surface layer without the usual crack formation[155]. This provides a satisfactory explanation for the observed decrease in the rate of peroxide formation during exposure to ozone (figure 76) even though no significant decrease in trans-1,4-polybutadiene could be detected by transmission IR spectroscopy, although cis-1,4-polybutadiene may be more reactive towards ozone. Furthermore, no loss of mechanical properties was apparent after 160 hours of exposure to ozone, which suggests that addition of ozone to the unsaturation of HIPS and subsequent destruction of the double bond by chain scission occurs at a very low level. However, the concentration of peroxides formed on the surface of the HIPS film is comparable with those produced during prior thermal treatment. In Chapter Two it was demonstrated that the presence of allylic hydroperoxides produced by thermal oxidation completely eliminated the auto-accelerating stage of the photoxidation curve. Whereas the presence of ozonides (and diperoxides) at equivalent concentration, on the surface of the film, failed to photo-sensitise the polymer to any appreciable extent, figure 77. This further supports the mechanism of photo-initiation by thermally-produced allylic hydroperoxides. The hydroxy radical derived from the photolytic cleavage of hydroperoxide will not undergo termination reactions so readily as the alkoxy radicals derived from the breakdown of ozonide and diperoxide (see Scheme 17) and may account for the lack of reactivity of ozone-photo-sensitised samples. Nevertheless, photo-sensitisation by ozonolysis

does appear to be directly proportional to the concentration of peroxides present, figure 78. In addition to the above mentioned ionic mechanism for ozonisation, a radical reaction involving triplet ozone and α-methylenic hydrogen has been suggested[156] (see Scheme 18). This mechanism will also photo-sensitise HIPS to photoxidation. However, no carbonyl or alcohol could be detected by IR and therefore the superimposition of a free radical mechanism on ozonisation is not believed to be of importance under the conditions described here (see 1.13). In conclusion, it may be stated that ozonisation does provide a viable means of photo-sensitisation of HIPS film to photoxidation through formation of peroxidic structures, although their reactivity is less than that of allylic hydroperoxides and formation of ozonides is restricted to the surface of the polymer film. However, under the influence of dynamic stress, diperoxide formation may be greatly enhanced.

Many workers have invoked a singlet oxygen ($^1O_2$) intermediate for the photo-initiation of polymers[30]. Unlike ozone, singlet oxygen is not a normal constituent of the atmosphere, although it has been suggested that polycyclic aromatic compounds known to be present in the atmosphere as pollutants may produce singlet oxygen through a sensitisation reaction[157]. Therefore, if singlet oxygen is involved in the photo-initiation process of polymers it must be generated in situ[23]; the lifetime of singlet oxygen in the gas phase is 45 minutes[158], although its diffusion through the polymer is limited[159]. Carbonyl chromophores have been cited as sensitisers for the formation singlet oxygen[23] and indeed plausible reaction

schemes have been reported in the literature[23]. However, to date no evidence has been presented to demonstrate the presence of singlet oxygen during photoxidation of polymers not containing added sensitisers, even though the chemical reactivity of externally-produced singlet oxygen has been shown to occur with unsaturated rubbers[26]. In the present study on HIPS and PBD no hydroperoxide could be detected by transmission IR spectroscopy after exposure to singlet oxygen (see 5.1.5). It is likely that the limitation imposed by diffusion of singlet oxygen into PBD excludes the detection of hydroperoxides formed on the surface by any other technique except for ATR.

CHAPTER 6

INITIATION AND STABILISATION OF HIGH IMPACT POLYSTYRENE WITH METAL COMPLEXES AND OTHER ADDITIVES

6.1 RESULTS

6.1.1 Metal complexes of thiocarbamic acid

6.1.1.1 Nickel

Figure 79 shows the effect of incorporation of nickel dibutyldithiocarbamate (Ni^{II}D4DC) (see 1.15) by extrusion mixing (see 1.2.1.1) into HIPS containing no other additives. Photoxidation of HIPS film (50 μm) was followed by oxygen absorption in oxygen. Increasing the concentration of Ni^{II}D4DC in HIPS from 0.1×10^{-3} mol/100 g to 1.5×10^{-3} mol/100 g (ca.0.7% w/w) progressively retards the rate of photoxidation. Both the initial rate and the linear (maximum) rate of photoxidation decrease dramatically with increasing concentration of Ni^{II}D4DC in HIPS. Similarly the auto-accelerating part of the oxygen absorption curve was lengthened. However, the increased stability observed (figure 79) by addition of Ni^{II}D4DC to HIPS is accompanied by a green colouration which is typical of this transition metal complex and is comparatively dark at higher concentration (1.5×10^{-3} mol/100 g). The colour fades slightly during photoxidation of HIPS film, but embrittlement occurs before a significant loss of colour.

Photoxidation of HIPS extruded film (50 μm) containing Ni^{II}_{D4DC} only (oxygen absorption in oxygen)

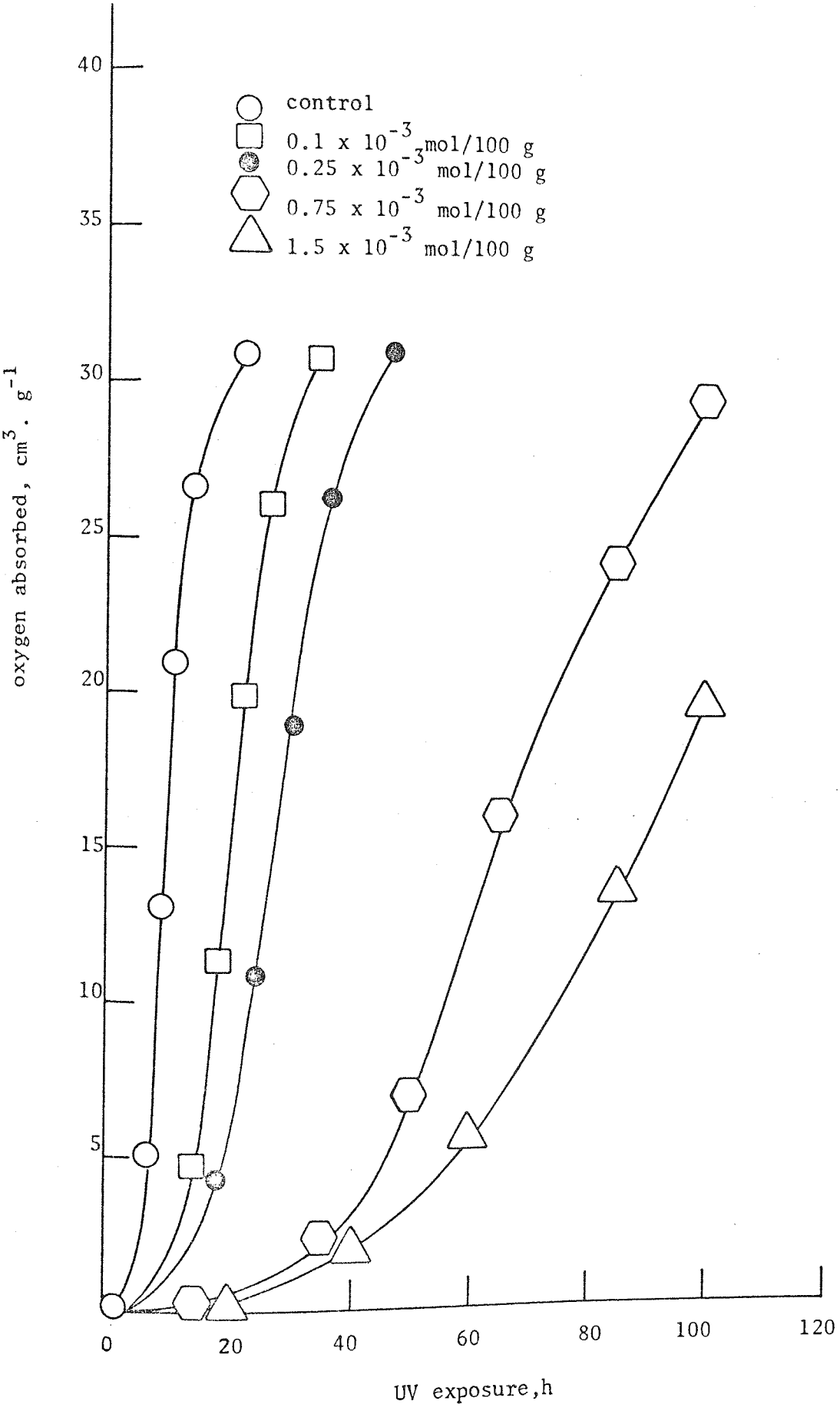

Figure 79.

6.1.1.2 Cobalt

Addition of cobalt dibutyldithiocarbamate (Co^{III}D4DC) to HIPS by extrusion mixing resulted in an entirely analogous behaviour towards photoxidation. Figure 80 shows the effect of increasing concentration of Co^{III}D4DC in HIPS (50 μm) from 0.05 x 10^{-3} mol/100 g to 1.5 x 10^{-3} mol/100 g (ca. 1% w/w), followed by oxygen absorption in oxygen. Co^{III}D4DC was slightly less effective than Ni^{II}D4DC in stabilising HIPS; the same "control" curve is plotted all figures shown in section 6.1.1. HIPS films containing Co^{III}D4DC were also green; the colour is more pronounced than for Ni^{III}D4DC at similar molar concentration. Similarly embrittlement occurred prior to substantial loss of colour.

6.1.1.3 Copper

Addition of copper dibutyldithiocarbamate (Cu^{II}D4DC) to unstabilised HIPS under identical conditions of melt-processing also stabilised the polymer to UV degradation over the range of concentration used (0.05 x 10^{-3} mol/100 g to 1.5 x 10^{-3} mol/100 g, ca. 0.7% w/w). However, Cu^{II}D4DC is not so effective as either Co^{III}D4DC or Ni^{II}D4DC in stabilising HIPS (50 μm) to photoxidation (figure 81) in oxygen, followed by oxygen absorption under identical conditions. Moreover, the yellowish-brown imparted by the Cu^{II}D4DC in HIPS at high concentration does not appear to fade during photoxidation within the time scale shown in figure 81.

6.1.1.4 Zinc

The incorporation of zinc dibutyldithiocarbamate (Zn^{II}D4DC into HIPS by a similar melt-processing operation resulted in only marginally improved photo-stability. Figure 82 shows the effect increasing the concentration of Zn^{II}D4DC in HIPS (50 μm) from 0.75 x 10^{-3}mol/100g to 1.5 x 10^{-3} mol/100 g (ca. 0.7% w/w) on the rate of photoxidation.

Photoxidation of HIPS extruded film (50 μm) containing Co^{III}D4DC only (oxygen absorption in oxygen)

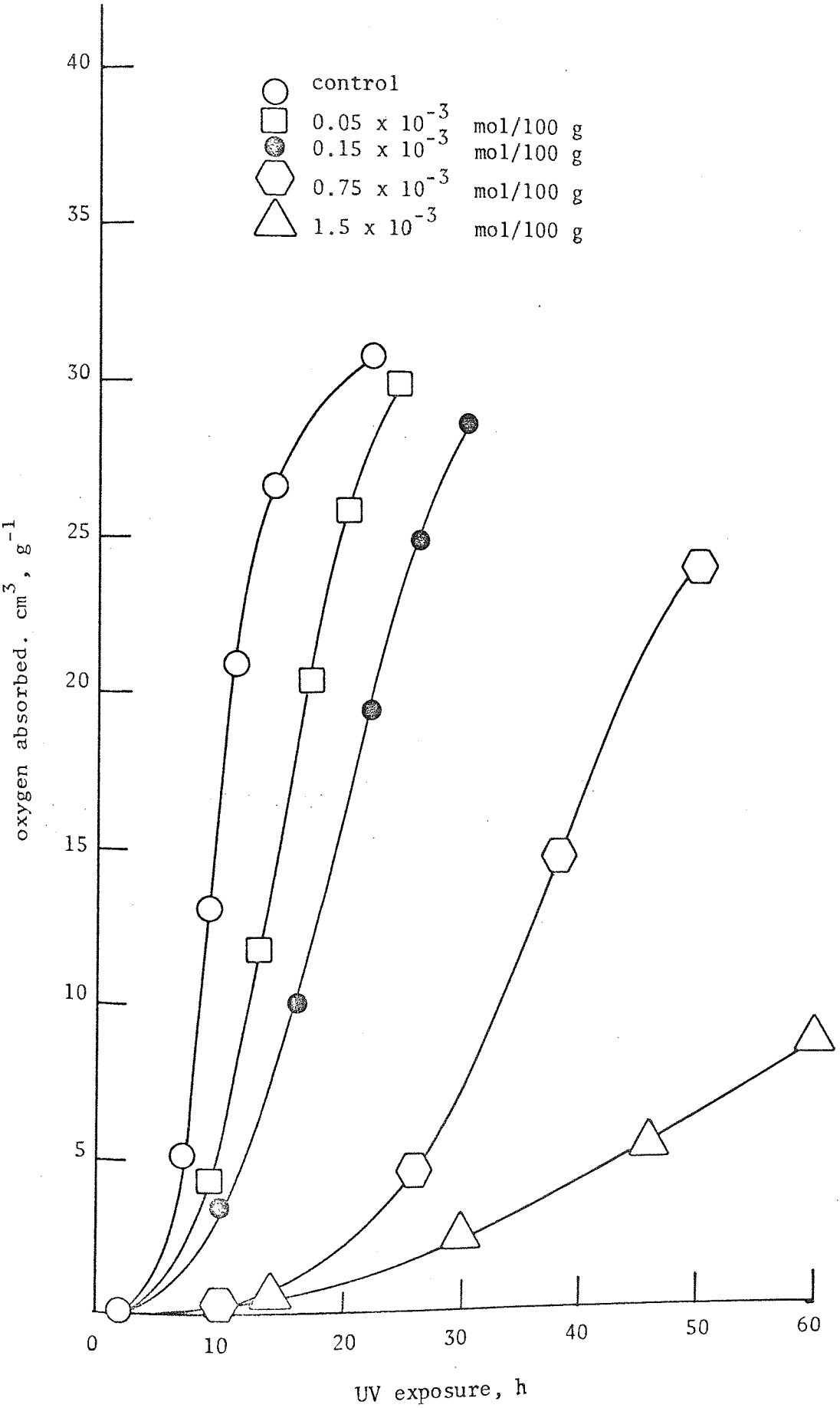

Figure 80.

Photoxidation of HIPS extruded film (50 μm) containing Cu^{II}D4DC only (oxygen absorption in oxygen)

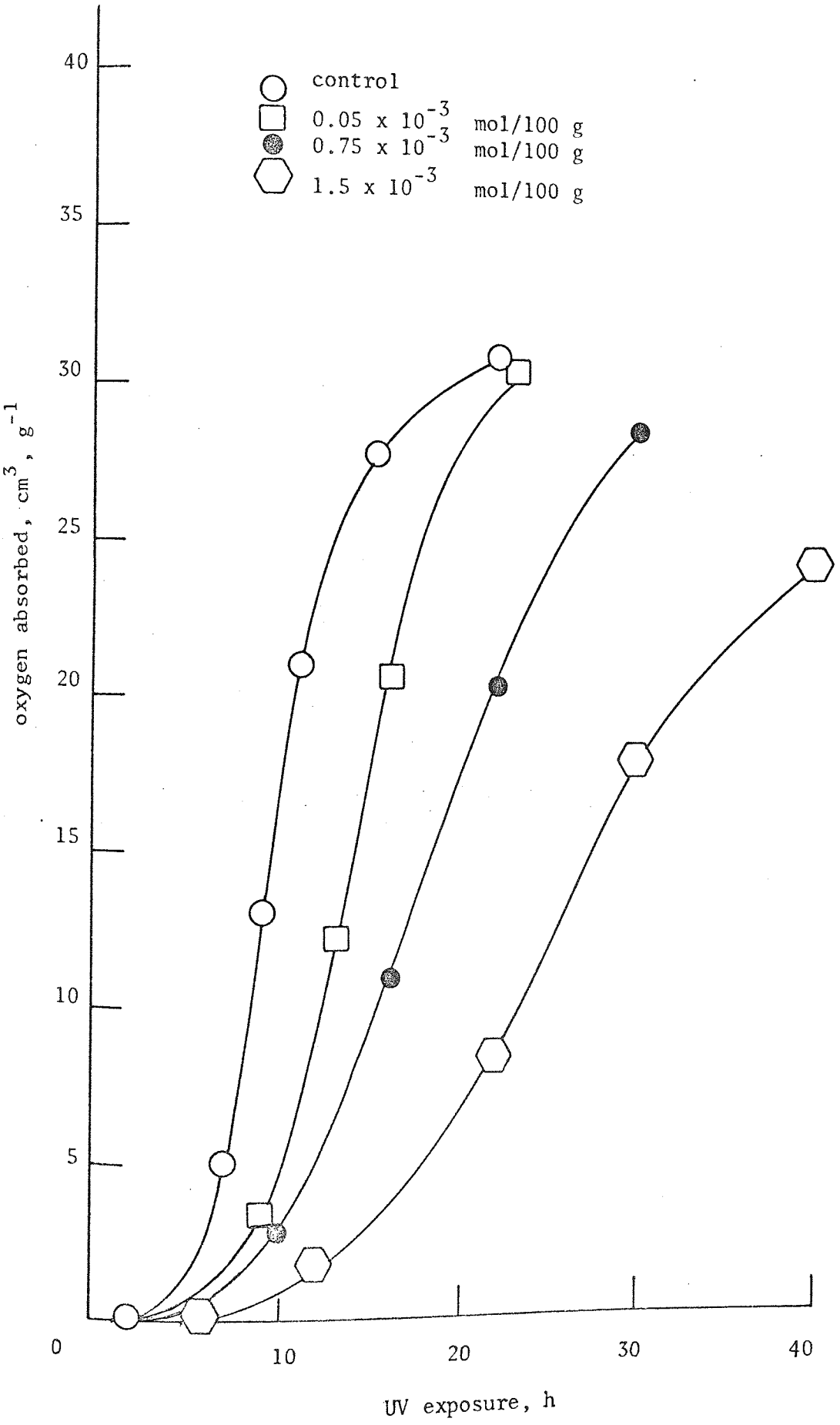

Photoxidation of HIPS extruded film (50 µm) containing Zn^{II}D4DC only (oxygen absorption in oxygen)

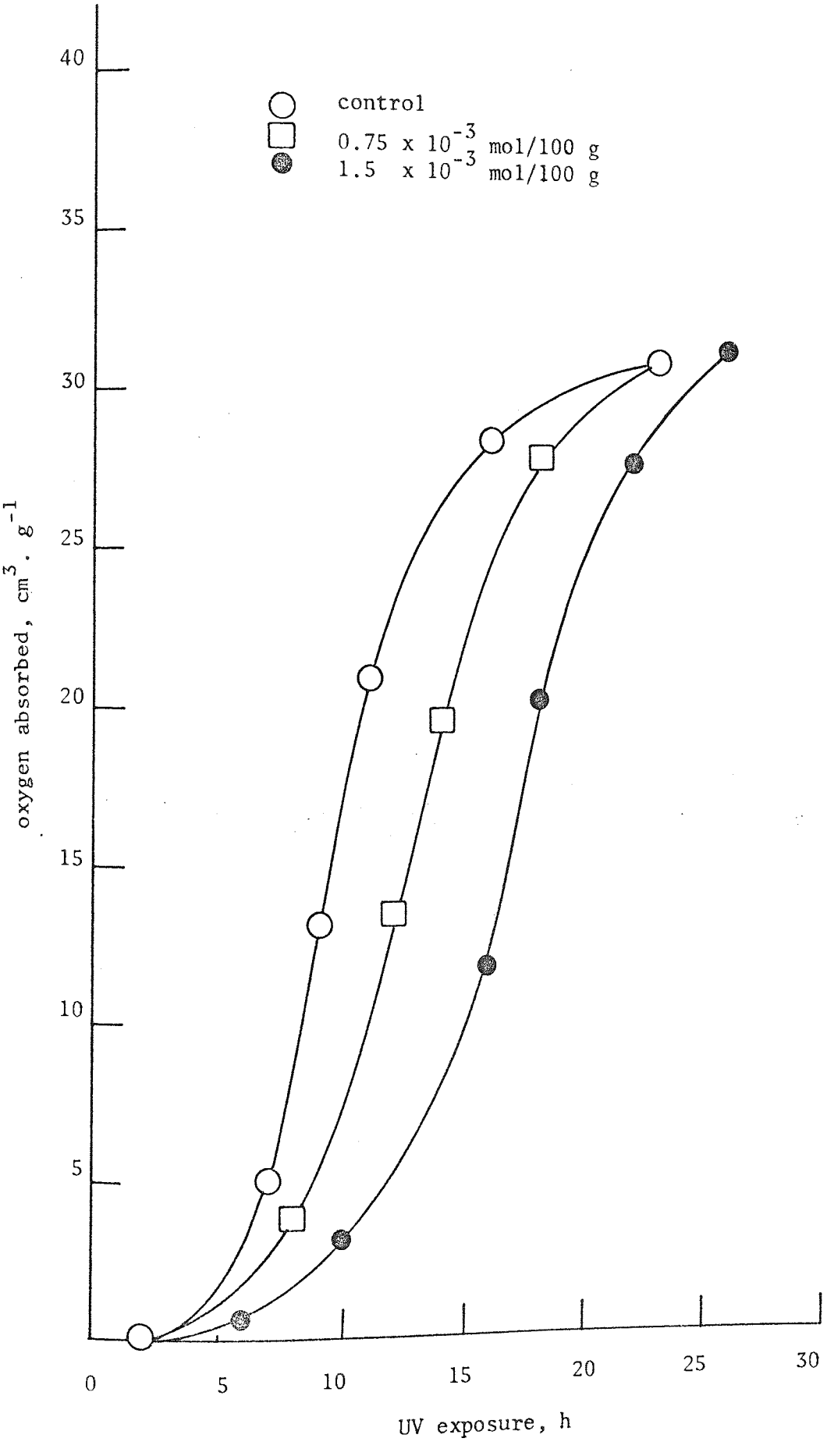

In contrast to Ni^{II}, Co^{III} and Cu^{II}D4DC, the linear (maximum) rate of oxygen absorption of HIPS containing Zn^{II}D4DC does not retard significantly with respect to that of the control. Furthermore, addition of Zn^{II}D4DC to HIPS does not change the original colour of HIPS.

6.1.1.5 Iron

Figure 83 illustrates the pro-oxidant effect observed when ferric dibutyldithiocarbamate (Fe^{III}D4DC) is added to unstabilised HIPS by extrusion mixing under similar conditions to those used for the other metal complexes. Photoxidation of HIPS (50 μm) containing Fe^{III}D4DC) was followed by oxygen absorption in oxygen under identical conditions to those used for the stabilisers. At all concentrations used (0.05×10^{-3} mol/100 g to 1.5×10^{-3} mol/100 g, ca. 1% w/w) the initial rate of photoxidation is greater than that of the control (figure 83), although the linear (maximum) rate retards with increasing concentration of Fe^{III}D4DC in HIPS. The latter observation being consistent with the above-mentioned metal complexes. HIPS films containing Fe^{III}D4DC are dark grey at high concentration, similar to samples containing Cu^{II}D4DC. Furthermore, the colour does not fade during photoxidation within the comparatively short time scale (figure 83).

To compare the effectiveness of metal complexes of thiocarbamic acid as stabilisers (and activator) in HIPS during photoxidation the induction period (defined as the value obtained on the abscissa by extrapolation of the linear, maximum rate) was calculated for various concentrations of additive. Figure 84 displays the marked variation in ability of the metal complexes to retard the photoxidation of HIPS at equivalent molar concentration. It is evident that a linear

Photoxidation of HIPS extruded film (50 μm) containing Fe^{III}D4DC only (oxygen absorption in oxygen)

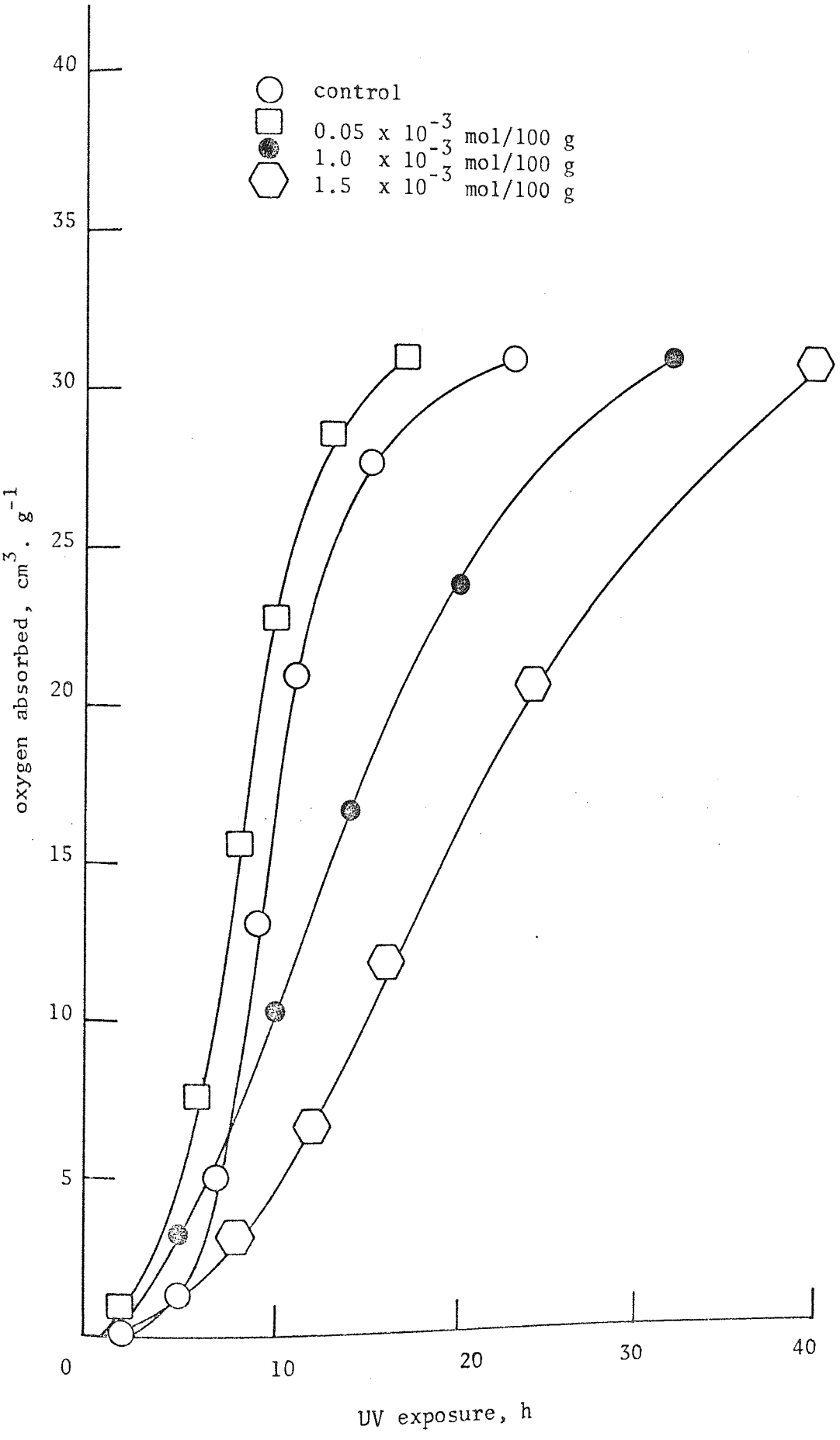

Variation in induction period to rapid photoxidation of HIPS extruded film (50 μm) containing a peroxide decomposer only as a function of additive concentration

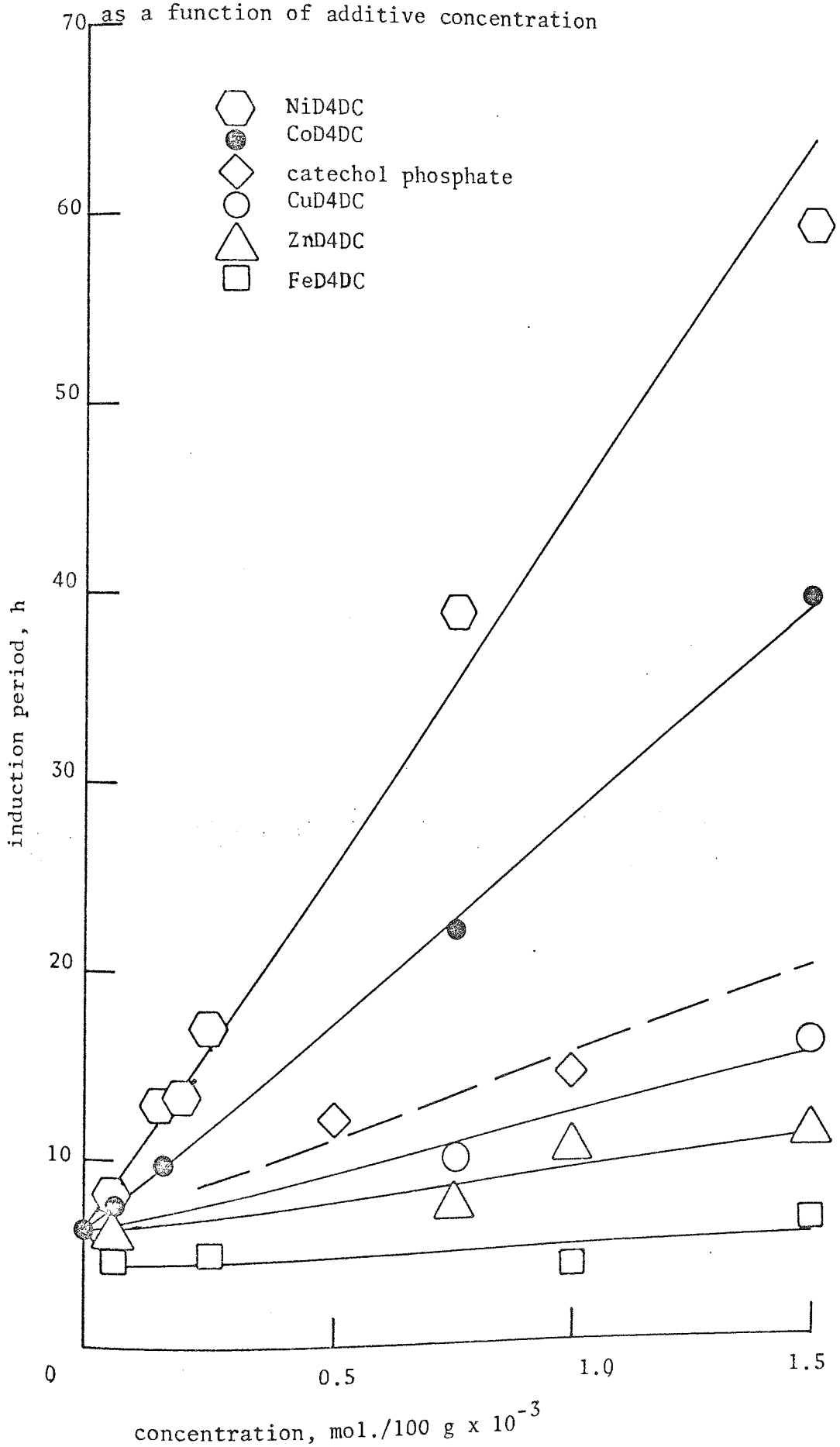

Variation in maximum rate of photoxidation of HIPS extruded film (50 μm) containing additional stabiliser only as a function of additive concentration

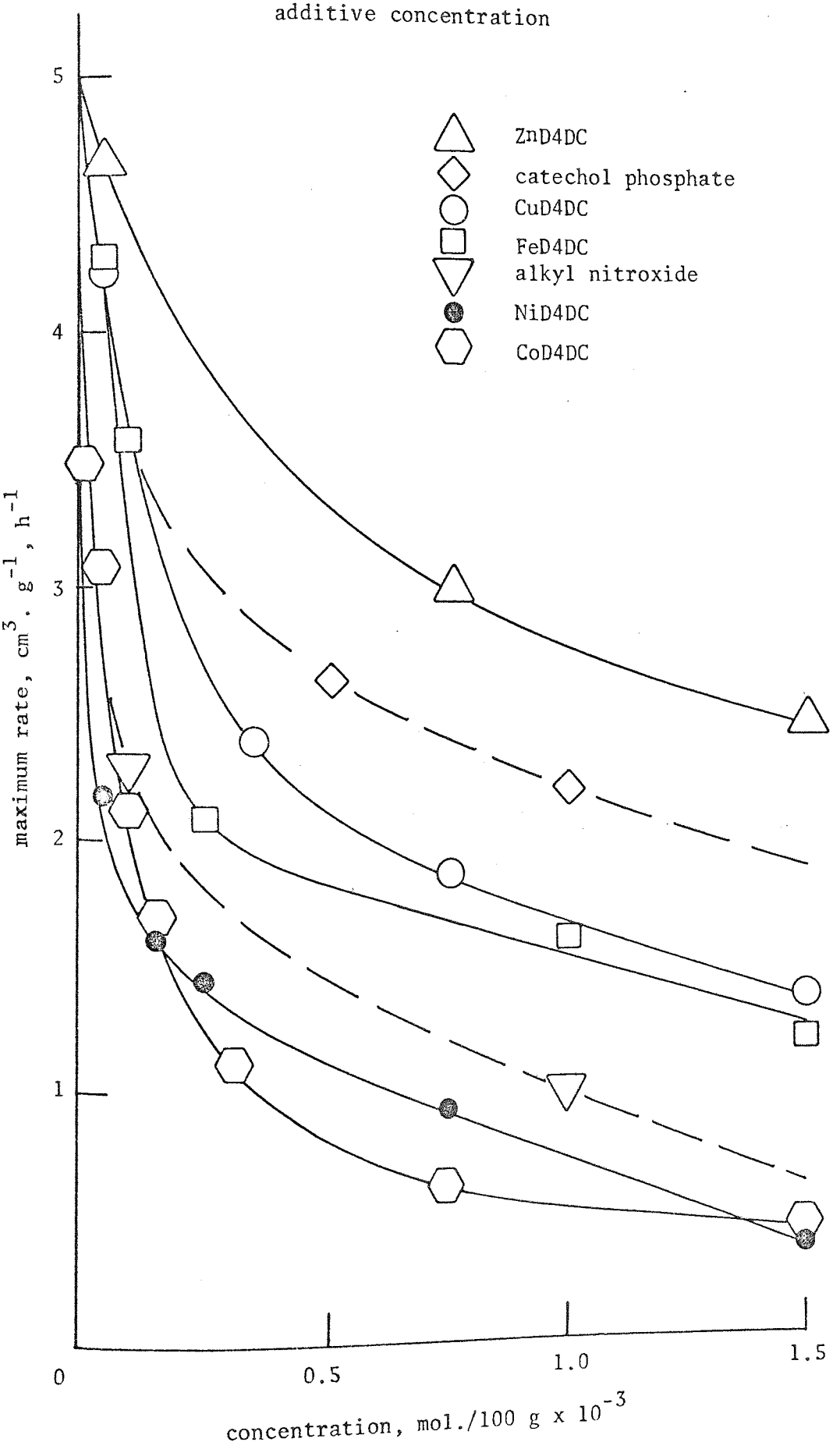

relationship holds for the induction period and concentration for all metal complexes. Ni^{II}D4DC is clearly the most effective stabiliser, followed by Co^{III}, Cu^{II} and Zn^{II} complexes. The pro-oxidant effect of Fe^{III}D4DC is depicted in figure 84 as an initial drop in the induction period around 0.05×10^{-3} mol/100 g, after which the induction period returns slowly to that of the control with increasing concentration and unlike the stabilisers does not rise above.

Figure 85 shows the fall in maximum rate of photoxidation with increasing concentration of metal complex in HIPS extruded film. In contrast to the changes in induction period (figure 84) all metal complexes exhibit an initial rapid drop in rate followed by a more gradual decline towards higher concentrations. Ni^{II}D4DC is similarly the most effective retarder (figure 85) of photoxidation and the order of effectiveness is preserved except for Fe^{III}D4DC which is an effective retarder and lies between Cu^{II} and Co^{III}D4DC.

6.1.2 Alkyl nitroxide

Figure 86 shows the effect of incorporation of an alkyl nitroxide (2,2,6,6-tetramethyl-piperid-4-one-N-oxyl) into unstabilised HIPS by extrusion mixing under similar conditions to those used for metal complexes. Photoxidation of HIPS film (50 μm) was followed by oxygen absorption in oxygen. Increasing the concentration of nitroxide from 0.1×10^{-3} mol/100 g to 10×10^{-3} mol/100 g (ca. 1.7% w/w) retards the photoxidation of HIPS effectively although nickel and cobalt complexes (figure 85) were more efficient stabilisers. Moreover, the alkyl nitroxide does not suppress the initial period

Photoxidation of HIPS extruded film (50 μm) containing alkyl nitroxide only (oxygen absorption in oxygen)

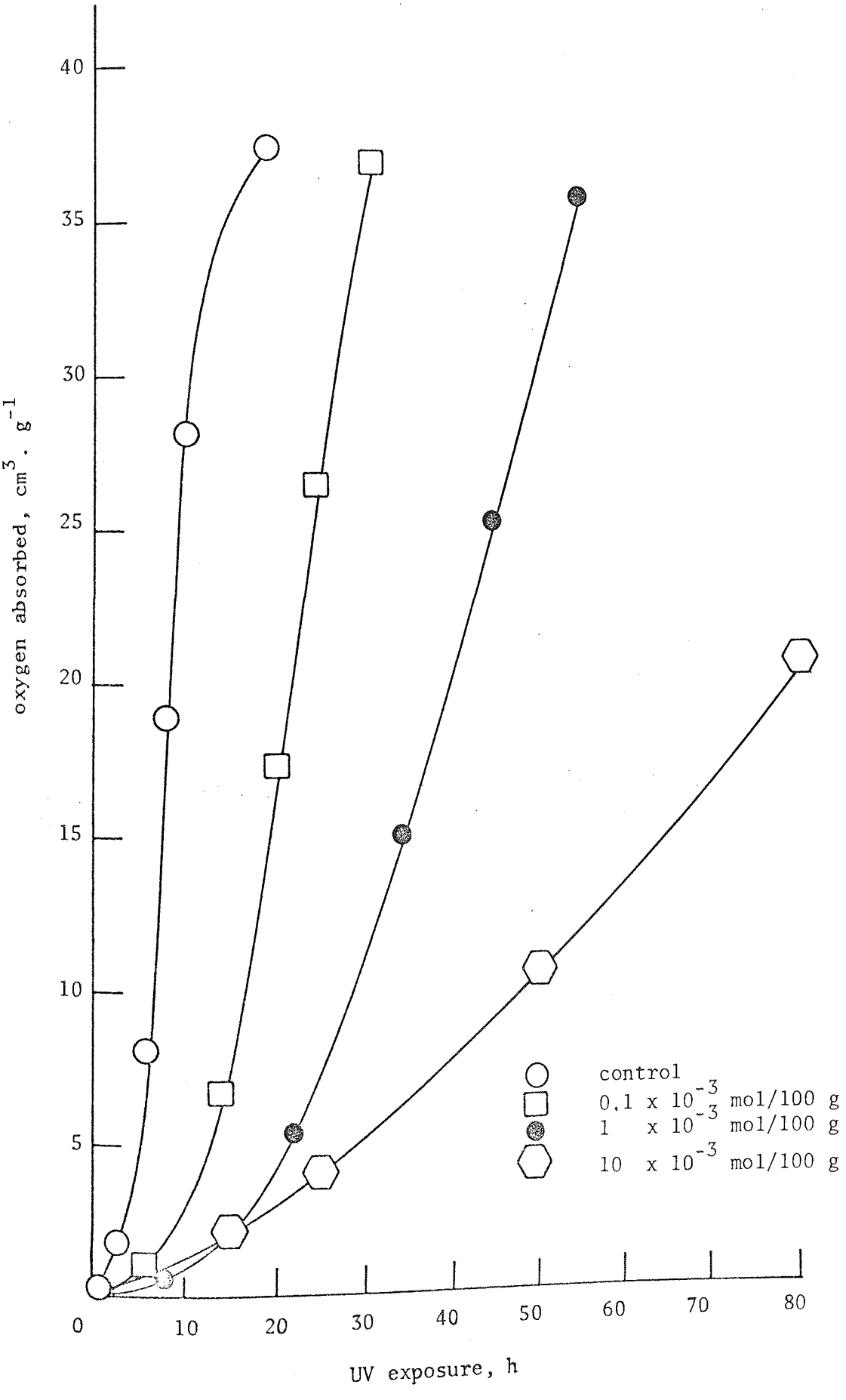

of photoxidation (figure 86) to the same extent as the metal complexes (except for Fe^{III}D4DC) and indeed at a high concentration (10^{-2} mol/100 g) an initial "pro-oxidant" effect is observed even though the rate is greatly retarded. However, similar to the transition metal complexes, HIPS extruded films containing the above alkyl nitroxide are coloured. Furthermore, no fading of the light brown films was observed during photoxidation.

6.1.3 Mono-(o-hydroxy-phenyl)phosphoric acid

Addition of mono-(o-hydroxy-phenyl)phosphoric acid to unstabilised HIPS by extrusion mixing stabilised the polymer towards photoxidation. Figure 87 shows the effect by increasing the concentration of mono-(o-hydroxy-phenyl)phosphoric acid in HIPS (50 μm) from 0.5×10^{-3} mol/100 g to 4.0×10^{-3} mol/100 g (ca. 0.8% w/w). In contrast to nitroxide (figure 86) addition of mono-(o-hydroxy-phenyl) phosphoric acid to HIPS extends the initial period of slow absorption of oxygen. Consequently at high concentration of additive (4.0×10^{-3} mol/100 g) a slow, linear rate of oxygen absorption is observed prior to the usual linear (maximum) rate of photoxidation that follows the auto-accelerating stage. Furthermore, the retardation of the maximum rate is insignificant (figure 85) compared to that observed for the alkyl nitroxide and all the metal complexes, except for Zn^{II}D4DC. Similarly HIPS containing mono-(o-hydroxy-phenyl)phosphoric acid is not coloured, although at high concentration (4.0×10^{-3} mol/100 g) a grey could be seen. The control curve shown in figure 87 represents the photo-oxygen absorption of unstabilised HIPS film extruded under similar conditions after the

Photoxidation of HIPS extruded film (50 µm) containing mono(o-hydroxy-phenyl)phosphoric acid only (oxygen absorption in oxygen)

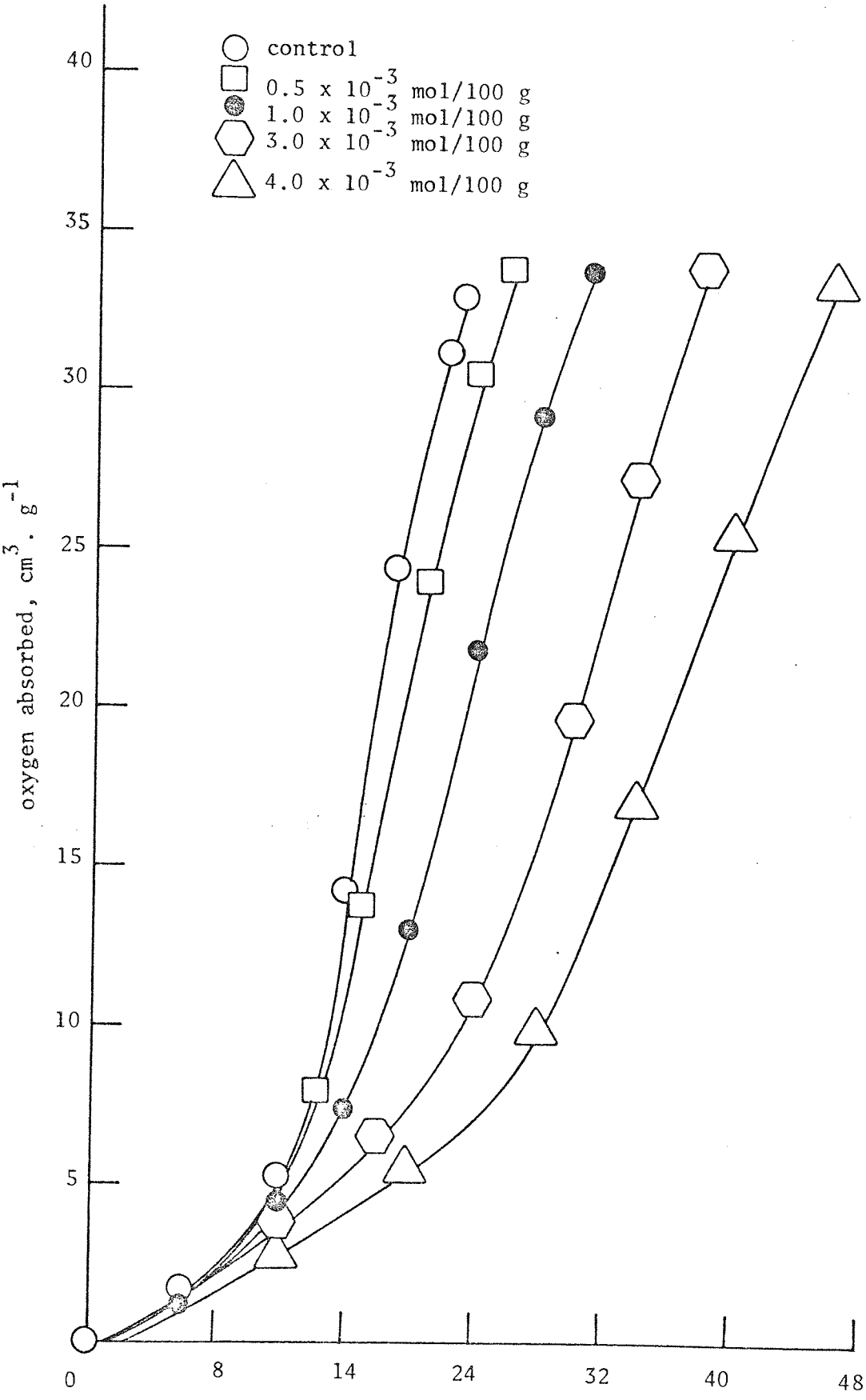

Figure 87.

extrusion mixing of mono-(o-hydroxy-phenyl)phosphoric acid. Nickel and cobalt metal complexes were, however, more effective UV stabilisers as shown by their ability to extend the induction period at equivalent molar concentration, Figure 84.

6.1.4 Chloranil

Figure 88 shows the effect of incorporation of chloranil (3,2,5,6-tetrachloro-1,4-benzoquinone) into unstabilised HIPS by a similar extrusion mixing to that used above. Photoxidation of HIPS film (50 μm) in oxygen was followed by oxygen absorption. Similarly the control curve shown in figure 88 represents unstabilised HIPS film extruded after the extrusion mixing of chloranil. Increasing the concentration of chloranil in HIPS from 0.1×10^{-3} mol/100 g to 10×10^{-3} mol/100 g results in an entirely analogous behaviour towards photoxidation as shown for Fe^{III}D4DC (figure 83). However, a higher molar concentration of chloranil is required to produce a similar pro-oxidant effect (1.0×10^{-3} mol/100 g). Furthermore, chloranil does not retard the photoxidation of HIPS extruded film to the same extent as Fe^{III}D4DC at equivalent molar concentrations. Chloranil imparts a dark brown colouration at high concentration (10^{-2}mol/100 g) and does appear to fade during photoxidation.

6.1.5 Dinonyl ketone

Figure 89 shows the effect of addition of dinonyl ketone to unstabilised HIPS by extrusion mixing. Photoxidation of HIPS film (50 μm) was followed by oxygen absorption in oxygen under identical conditions to those used above. At concentrations of 0.1×10^{-3} and 1.0×10^{-3} mol/100 g the oxygen absorption curves were identical

Photoxidation of HIPS extruded film (50 µm) containing chloranil only (oxygen absorption in oxygen)

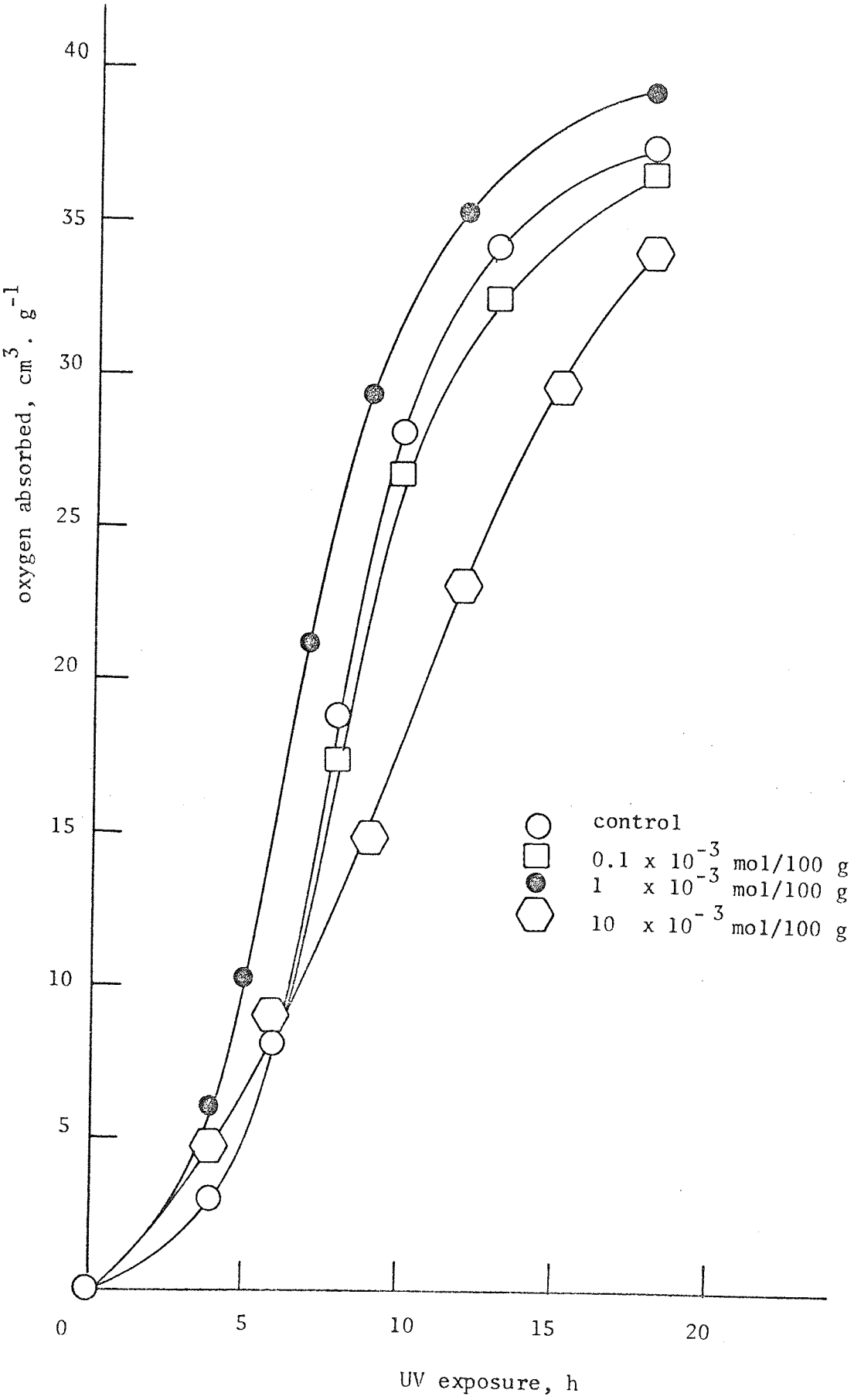

Figure 88.

Photoxidation of HIPS extruded film (50 μm) containing dinonyl ketone only (oxygen absorption in oxygen)

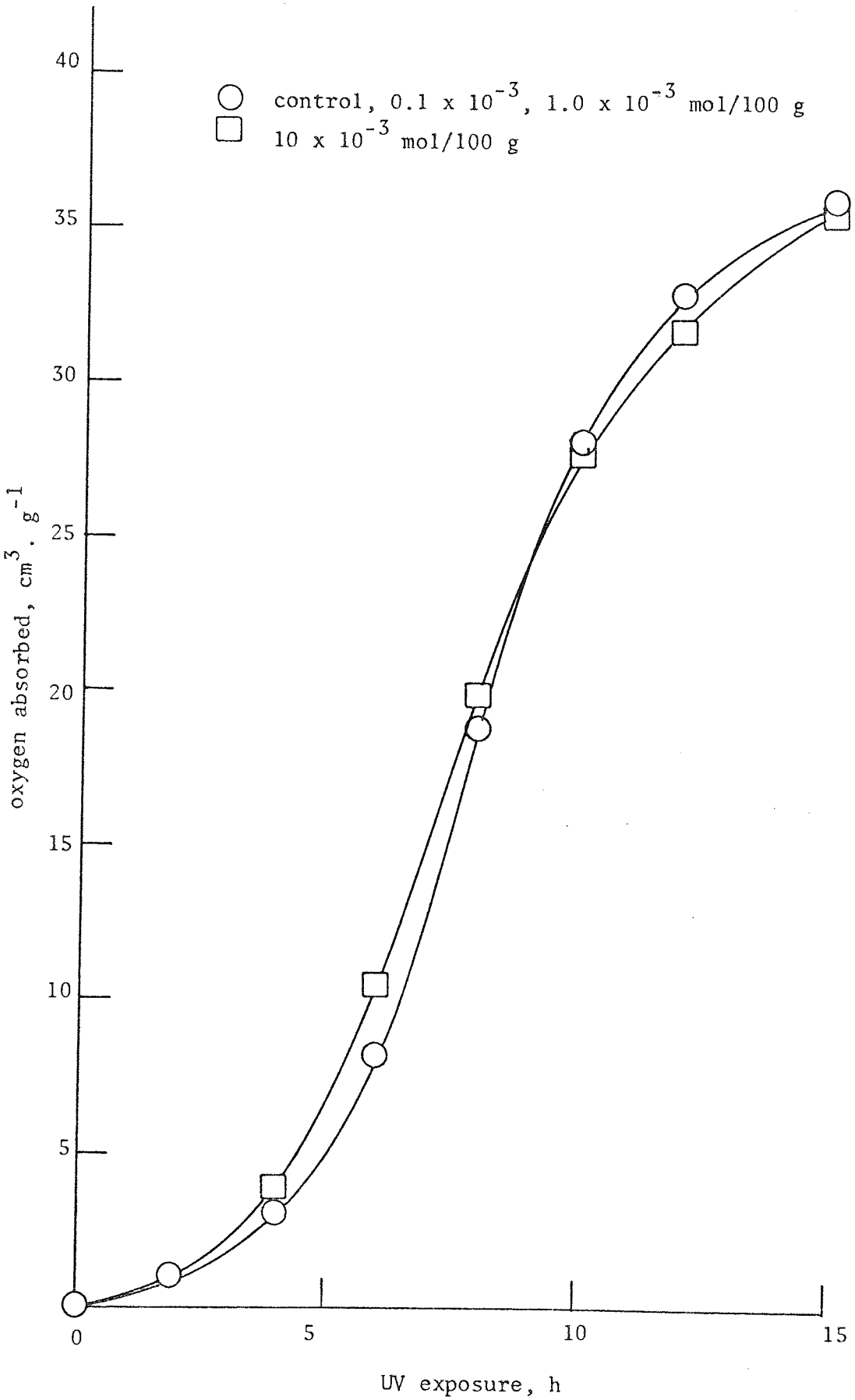

Figure 89.

to that of the control film which was extruded after extrusion mixing of dinonyl ketone. However, at a higher concentration of 10 x 10^{-3} mol/100 g a slight shortening of the auto-accelerating stage is obtained, although the initial rate of photoxidation is not altered. After the linear part of the oxygen absorption curve has been surmounted the rate of photoxidation of the sample containing dinonyl ketone falls slightly below that of the control. No colouration of HIPS extruded film is apparent even at a high concentration of dinonyl ketone (10^{-2} mol/100 g).

6.2 DISCUSSION

In the previous chapters experimental evidence has been sought with the aim of elucidating the possible photo-initiating mechanisms occurring during the UV degradation of HIPS, "crystal" PS and PBD. Accordingly the significance of hydroperoxide acting as a photo-initiator during the photo-oxidative degradation of HIPS has been established. In view of this evidence an understanding of the behaviour of different "types" of UV stabilisers and activators on the photoxidation of HIPS extruded film should be possible. Unfortunately the UV stabilising (and activating) mechanism of many commercial additives has not been fully developed and many reports in the literature[39,160] differ on basic UV mechanisms. This is especially true for metal complexes (chelates), typified in the present study by dithiocarbamates. Several workers have cited the well known UV stabilising action of nickel dibutyl dithiocarbamate [161, 162] to involve the quenching of photo-excited chromophores present in the polymer as oxidation product[35,163,164].

While others suggest that quenching of excited singlet oxygen by nickel dibutyldithiocarbamate is more important than quenching of chromophores[165]. Both of these reported mechanisms for the UV stabilisation of polymers by addition of nickel chelates are an extension of the original proposal for the photo-initiation of polymers involving carbonyl triplet states and subsequent quenching by oxygen forming singlet state oxygen[23]. This mechanism is at variance with evidence presented in the previous four chapters for the photo-initiation of HIPS, "crystal" PS and PBD. Consequently the evident UV stabilising ability of Ni^{II}D4DC in HIPS (figure 79) and other additives will be discussed with reference to hydroperoxidation.

From original work using tetralin as a model hydrocarbon it has been reported[166] that the effectiveness of zinc diethyldithiocarbamate (Zn^{II}DEDC) as a peroxide decomposer stems from the formation of a catalytic non-radical forming hydroperoxide decomposer. Furthermore, it was suggested[166] that sulphur dioxide (or sulphur trioxide[167]) derived from the breakdown of dithiocarbamate was responsible for the catalytic decomposition of hydroperoxide by acting as a Lewis acid. The ionic decomposition of cumene hydroperoxide (CHP) has been shown in Chapter Four, Scheme 6. It is possible, although no evidence is available, that other reaction products of dithiocarbamate may be involved as catalysts in the decomposition of hydroperoxide. It is believed that the observed auto-retardation of photoxidation of HIPS extruded film containing metal complexes of dithiocarbamate (see 6.1.1) towards the later stages of degradation

can be attributed to the formation of the above mentioned catalytic hydroperoxide decomposer after an initial stoichiometric reaction of hydroperoxide with the dithiocarbamate. It is postulated that the first step in the decomposition of hydroperoxide involves the formation of a sulphoxide with reduction of hydroperoxide to alcohol (see Scheme 19)[168]. With further reaction with hydroperoxide the thiocarbamate (sulphoxide) is oxidised to sulphone and finally to sulphonate. This may either breakdown to evolve sulphur dioxide[168] or undergo hydrolysis[167, 169] producing thiocarbamic acid, sulphur dioxide and metal sulphate. The thiocarbamic acid which is relatively stable may decompose to form isothiocyanate[167,169]. Furthermore, the sulphur dioxide may react stoichiometrically with hydroperoxide to give an alkyl acid sulphate[168].

SCHEME 19

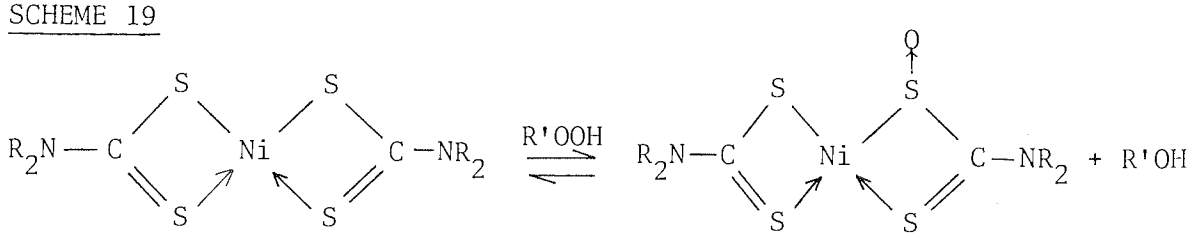

nickel dialkyl dithiocarbamate (sulphoxide)

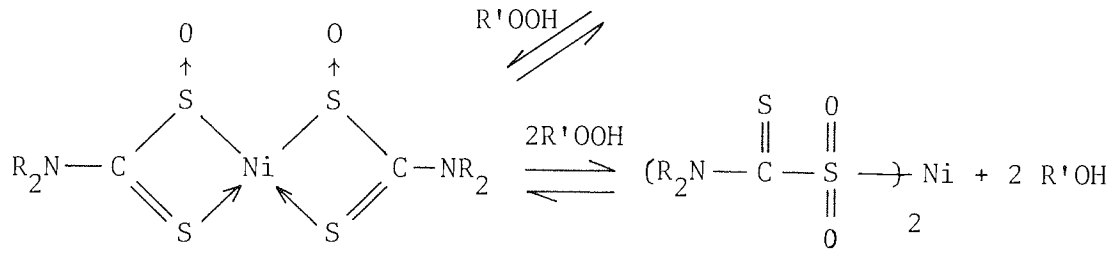

(sulphone)

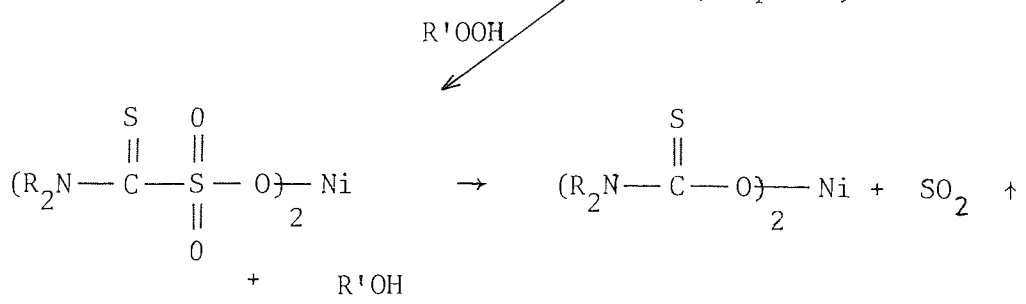

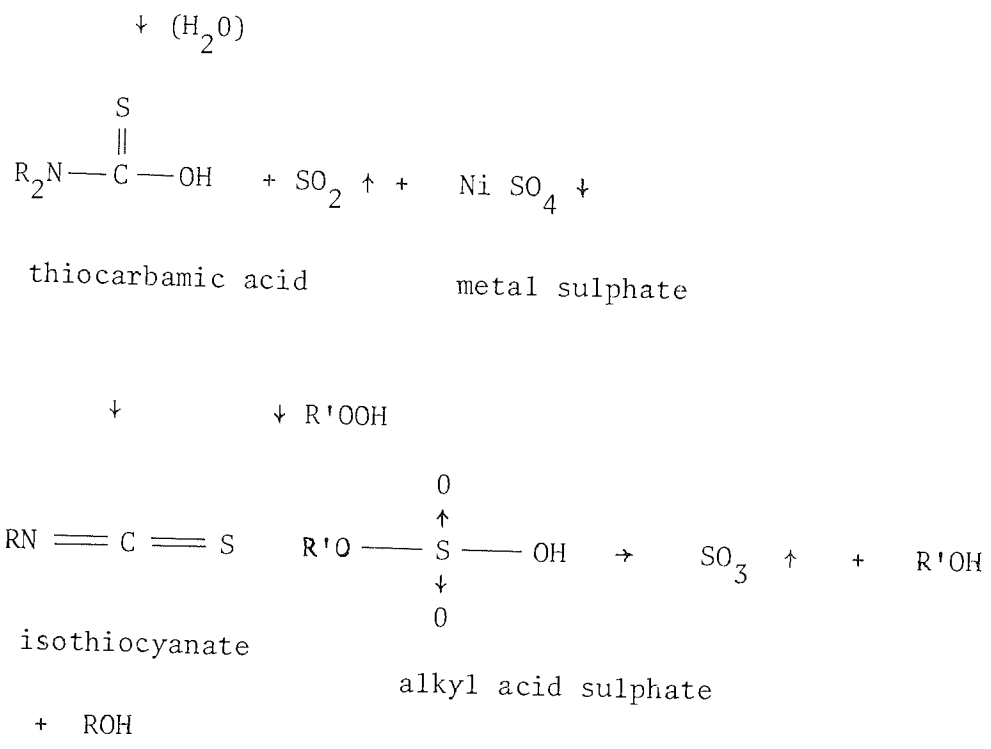

In the second stage of the hydroperoxide decomposing mechanism (see Scheme 20) the reaction products derived from Scheme 19 act as powerful hydroperoxide decomposers by virtue of their ability to destroy hydroperoxide by a catalytic (ionic) mechanism with formation of non-radical products[166]. Moreover, it is believed that this reaction (Scheme 20) supercedes the initial stoichiometric reaction (Scheme 19) and is thus responsible for the powerful UV stabilising ability of the thiocarbamates[166] observed in HIPS extruded film (see 6.1.1).

SCHEME 20

R'OOH + SO_2, SO_3, (R'O—SO_2—OH) → non-radical products.

It is likely that the observed variation in UV stabilising ability of the metal complexes arises from their differing stability to oxidative attack during processing in the extruder at 220°C (see 1.2.1.1) and subsequent exposure to UV. Nickel and cobalt complexes are known to be more stable than analogous copper and iron complexes towards melt-processing at high temperature [87,99] and, therefore, by virtue of their ability to survive thermal oxidation will become effective UV stabilisers[37, 167]. The technological usefulness of thiocarbamates lies in their ability to destroy hydroperoxides during the high temperature fabrication process involving contact with atmospheric oxygen by the same mechanism proposed for UV stabilisation (Schemes 19 and 20)[37,167]. However, under the conditions used for the extrusion of HIPS containing metal complexes (see 1.2.1.1) it is believed that the less stable copper and iron dibutyl dithiocarbamate remain substantially intact as evidenced by the pronounced colour of the extrudate when high concentration of additives were used. This is to be expected in view of the experimental conditions selected for this work. The residence time of the melt during extrusion mixing was approximately 5 minutes only, the temperature of the "feed" (barrel zone 1) was relatively low (160°C) and the extrudate was quench-cooled to 60°C (see 1.2.1.1). Consequently, it is likely that other factors influence the effectiveness of metal thiocarbamates as UV stabilisers. It has been shown by other workers that a substantial part of the UV stabilising ability of metal chelates is due to UV screening of incident light[170]. This is consistent with the observed progressive retardation of the maximum rate of photoxidation of HIPS film containing increasing concentration of

metal complexes (figure 85). Zn^{II}D4DC was the poorest retarder of photoxidation and it is likely that this is a result of a low UV screening efficiency (see 1.15.3) and may be associated with the inability of zinc to promote an $4S^2$ electron to the filled $3d^{10}$ orbital which accounts for the lack of colour of this complex.

The photolytic stability of metal thiocarbamates varies considerably, nickel and cobalt being the most stable and copper and iron complexes the least[162]. This is exemplified for Fe^{III}D4DC (figures 83 and 84) in which the breakdown product (dithiocarbamoyl radical[169]) may either dimerise or behave as a pro-oxidant[37,167] by abstracting a hydrogen from HIPS (probably the labile tertiary hydrogen of 1,2-polybutadiene) forming a thiol (see Scheme 21). The alkyl radical produced will combine rapidly with oxygen forming an alkylperoxy radical which will initiate further chain sequences (see Chapter Three). The transition metal ion (Fe^{3+}) may also be involved in the initial pro-oxidant effect observed for Fe^{III}D4DC in HIPS at different concentrations (figures 83 and 84). It is well known that transition metal ions decompose hydroperoxide in accordance with the redox reaction[169] shown in Scheme 22; the overall reaction being similar to the bimolecular decomposition of hydroperoxide. The auto-retardation of photoxidation of HIPS film containing Fe^{III}D4DC observed (figure 83) during the latter stages of UV exposure which also increases with increasing concentration of additive is reminiscent of the acid-catalysed decomposition of hydroperoxide and UV screening discussed above for the photolytically more stable metal complexes. Accordingly the thiol produced (see Scheme 21) may be

oxidised to thiocarbamic acid and sulphur dioxide through the intermediate sulphonic acid. This is because Fe^{III}D4DC persists during the photoxidation of HIPS (contrary to LDPE[87,99]) even beyond embrittlement (evidenced by the retention of colour) and is thus available for formation of the above catalytic hydroperoxide decomposer (see Scheme 20).

SCHEME 21

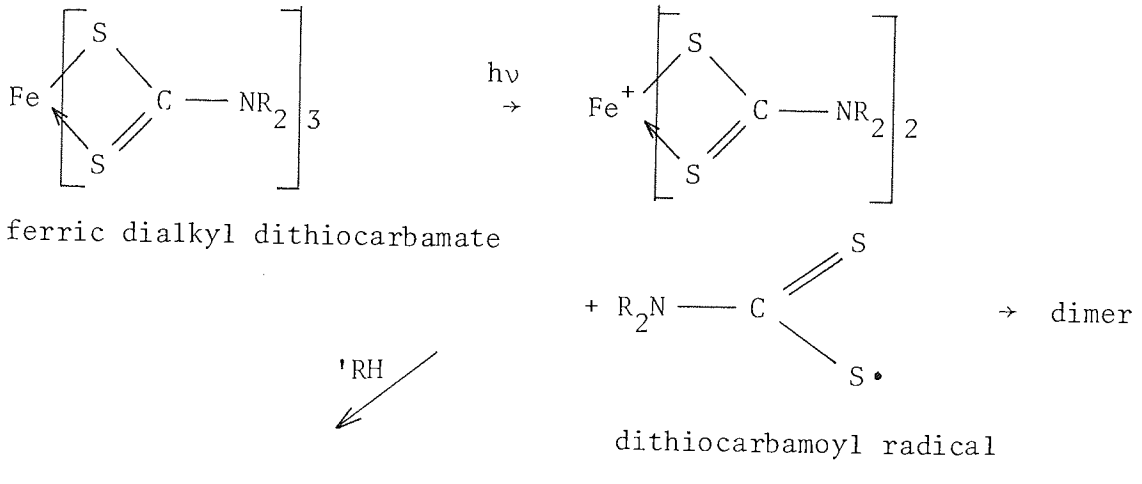

SCHEME 22

$$ROOH + Fe^{3+} \rightarrow RO\cdot + {}^{-}OH + Fe^{2+}$$

$$ROOH + Fe^{2+} \rightarrow ROO\cdot + H^{+} + Fe^{3+}$$

It has been reported that Cu^{II}D9DC behaves as a pro-oxidant during photoxidation when incorporated into LDPE[87,99]. In the present study Cu^{II}D4DC was found to stabilise HIPS at all concentrations used and to be more effective than Zn^{II}D4DC (figures 84 and 85). Furthermore, an initial UV stabilising period followed by loss of colour and rapid degradation leading to embrittlement has been reported during the photoxidation of LDPE containing between 0.01 and 0.1% w/w Fe^{III}D9DC[37,167]. No "delayed action" effect was observed when Fe^{III}D4DC was incorporated into HIPS (figure 83); the initial rate of oxygen absorption was always greater than that of the control over a wide range of concentrations. Therefore, it is deduced that the hydroperoxide decomposing ability of Fe^{III}D4DC is insufficient to suppress the powerful photo-pro-oxidant effect of PBD in HIPS during the early stages of photo-degradation. However, there would appear to be a concentration range at which the radical generating reactions (see Scheme 21) are optimumised resulting in a photo-activation[37,167] (figure 83, 0.05×10^{-3} mol/100 g). The pro-oxidant effect observed during photoxidation of HIPS containing Fe^{III}D4DC is further evidence against the reported role of singlet oxygen as a photo-initiator[26,30] for it is known that Fe^{III}D4DC is an efficient quencher of singlet oxygen[171].

The UV stabilising ability of N-oxyl compounds has, similar to

the nickel chelates, been attributed to quenching of excited triplet state carbonyl and the deactivation of singlet oxygen[172]. 2,2,6,6-tetramethyl-piperid-4-one-N-oxyl was chosen as the radical chemistry of this compound is well established in the literature[173]. Aliphatic nitroxides react selectively with alkyl radicals (a) to give stable non-radical products[173] (see Scheme 23). However, to be effective antioxidants by this mechanism alone they must compete with oxygen (b). Accordingly the rate of inhibited oxidation of HIPS containing an alkyl nitroxide will be proportional to the oxygen pressure and inversely proportional to the concentration of alkyl nitroxide[173] if the above mechanism is operative during photoxidation. Therefore, a plot of rate of absorption of oxygen (figure 86) against the initial concentration of nitroxide should be a straight line, as the change in concentration of oxygen is negligible (see 1.4.4). However, the maximum rate of photoxidation was retarded in a similar, non-linear manner to that observed for HIPS film containing metal complexes (figure 85). This would at first sight appear to support the quenching mechanisms proposed in the literature[172] as it is also reported that nickel chelates are more efficient quenches than N-oxyl derivatives. Nevertheless, it is believed that the effective UV stabilisation observed when alkyl nitroxide is incorporated into HIPS (figure 86) is due to UV screening of incident light; this was also suggested earlier to be partly responsible for the UV stabilising mechanism of metal complexes. 2,2,6,6-tetramethyl-piperid-4-one-N-oxyl was found to absorb strongly in the UV below 280 nm but the tail extends well into the visible region (> 500 nm) and accounts for the bright colour of N-oxyl derivatives, precluding them from

widespread commercial application[172]. The initial inhibition and the final auto-retardation of photoxidation observed for HIPS films containing Ni^{II}D4DC (figure 79) was absent during photoxidation of HIPS films containing alkyl nitroxide (figure 86). This indicates that, in contrast to the metal thiocarbamates, a hydroperoxide decomposing mechanism does not occur. Moreover, the radical trapping mechanism (a) fails to compete successfully with oxygen for alkyl radicals. Indeed an initial photo-activation of HIPS by the N-oxyl derivative was observed at high concentration (figure 86, 10^{-2} mol/100 g) and is possibly a result of photo-sensitisation via excitation of the carbonyl structure to the triplet state (see Scheme 23).

SCHEME 23

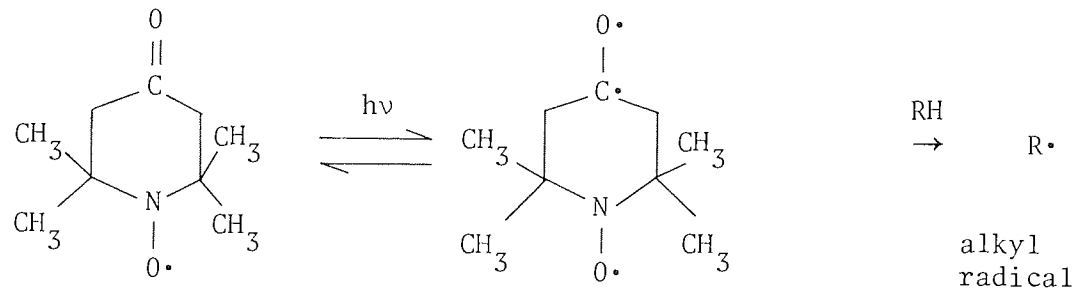

alkyl nitroxide

(a) ↓ R• $\xrightarrow{O_2}$ ROO•

(b) alkylperoxy radical

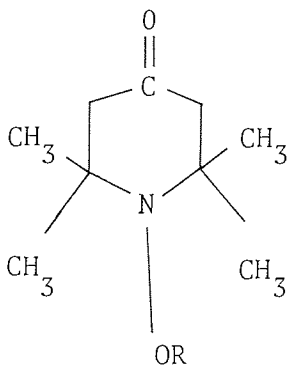

stable non-radical product

In order to separate the combined effect of UV screening and hydroperoxide decomposition attributed to the UV stabilising action of dithiocarbamates discussed earlier, a phosphate hydroperoxide decomposer was selected which does not possess significant UV screening ability. Mono-(o-hydroxy-phenyl)phosphoric acid has a weak absorption peak at 272 nm, and shows extensive absorption below 240 nm. Consequently, insufficient absorption of incident light will occur with UV $\geqslant$ 280 nm (see 1.4.1) for screening of UV to be an important mechanism, although at high concentrations of additive the absorption tail of this peak does extend into the visible region. The ineffectiveness of mono-(o-hydroxy-phenyl)phosphoric acid to behave as a UV screen was illustrated in figure 85 in which the nitroxide and thiocarbamate complexes except Zn^{II}D4DC (which is colourless) are better retarders of the linear (maximum) rate of photoxidation. The auto-retardation observed for the thiocarbamates (figure 79, 0.75×10^{-3} mol/100 g, et seq.) attributed to the generation of a catalytic hydroperoxide decomposer[166] was absent during photoxidation of HIPS containing the phosphate stabiliser. Therefore, it is believed that the mono-(o-hydroxy-phenyl)phosphoric acid is responsible for efficient hydroperoxide decomposition evident in figure 87 as an extension of the induction period, rather than an oxidation or photolysis product. Mono-(o-hydroxy-phenyl)phosphoric acid is itself an oxidation product of catechol hindered-phenyl phosphite[109,117,174]. It is postulated that mono-(o-hydroxy-phenyl)phosphoric acid decomposes hydroperoxide in an ionic,catalytic reaction (see Scheme 24) with the formation of non-radical products via an initial dehydration, (i)[175].

SCHEME 24

(i)

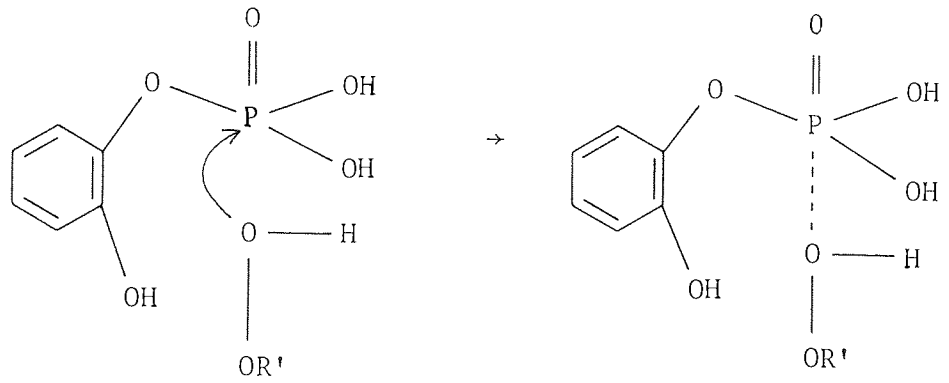

(ii)

mono-(o-hydroxy-phenyl)phosphoric acid

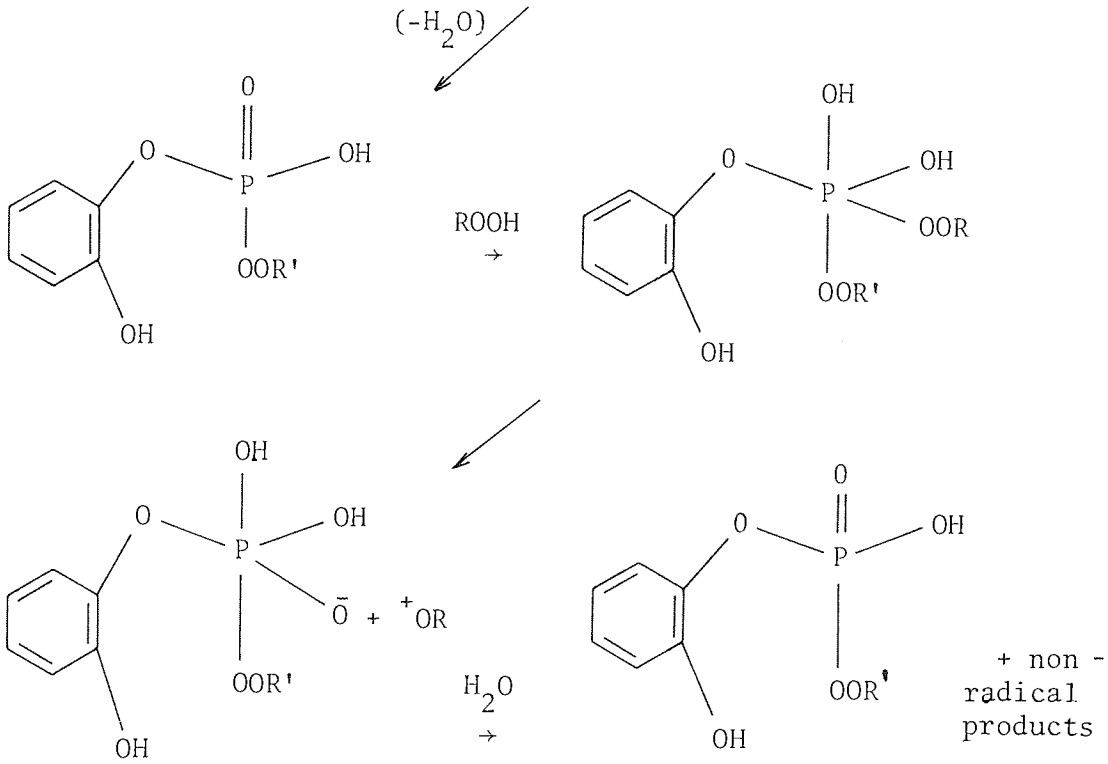

The phosphate hydroperoxide decomposer is, however, not such an effective UV stabiliser as the nickel and cobalt dithiocarbamates at the same molar concentration in HIPS (figure 84). It is likely that the hydroperoxide decomposing mechanisms proposed for thiocarbamate stabilisers (see Schemes 19 and 20) are more effective in decomposing hydroperoxide during the melt stage and during subsequent photoxidation. Moreover, it is not believed that deactivation of excited triplet states of carbonyl or singlet state oxygen is a contributory factor to the greater UV stabilising power of these additives. The experimental fact that mono-(o-hydroxy-phenyl)phosphoric acid, whose stabilising ability has not been reported to be associated with quenching[175], is an effective UV stabiliser during the initial stages of photoxidation of HIPS (figure 87) supports the mechanism of hydroperoxide initiation as it is known that hydroperoxide, not carbonyl , is formed during the early stages of photo-degradation (Chapter Two, figure 15).

The initial slow, linear rate of oxygen absorption observed during the photoxidation of HIPS extruded film containing the phosphate hydroperoxide decomposer (figure 87, 4.0×10^{-3} mol/100 g et seq.) is of some interest since the rate might be expected to approach zero in the inhibited system. It is possible that during this initial stage of inhibited photoxidation a direct photo-activation of the polymer makes a significant contribution to the chain-starting sequences. The mechanism of photo-activation of the PBD moiety has been discussed fully in Chapter Five. Moreover, this would account for the non-auto-accelerating character of the curves towards higher concentration of additive.

It has been suggested by other workers that photo-sensitisation of polymers by p-quinones may find useful application for the manufacture of photo-degradable material[106]. The merits of ferric dibutyldithiocarbamate as a photo-activator for polyolefins are well known[37, 167]. Indeed, addition of a chlorinated p-quinone (chloranil) to HIPS photo-sensitised the polymer (figure 88) in a similar manner to Fe^{III}D4DC (figure 83). However, it is believed that the mechanism of photo-sensitisation is different. Substituted p-quinones are known to undergo photo-excitation to the triplet state[106], (see Scheme 25). This may either abstract a hydrogen from the polymer hydrocarbon forming a chain-starting alkyl radical, or the carbonyl triplet state may be quenched by ground state triplet oxygen producing excited singlet state oxygen. The alleged photo-initiation of polymers by singlet oxygen has been reported by many workers[30]. Evidence for the singlet oxygen intermediate was presented by the same workers[106] to account for their observation that photo-sensitisation occurred only in the presence of oxygen. However, it is likely that oxygen "magnifies" the alkyl radical initiation mechanism (see Scheme 25) by producing many more radicals via the well established auto-accelerating chain mechanisms[3]. As an alternative (a) to photo-sensitisation via the triplet state, chloranil may accept an alkyl radical (see Scheme 25) with the formation of a more stable radical[176].

SCHEME 25

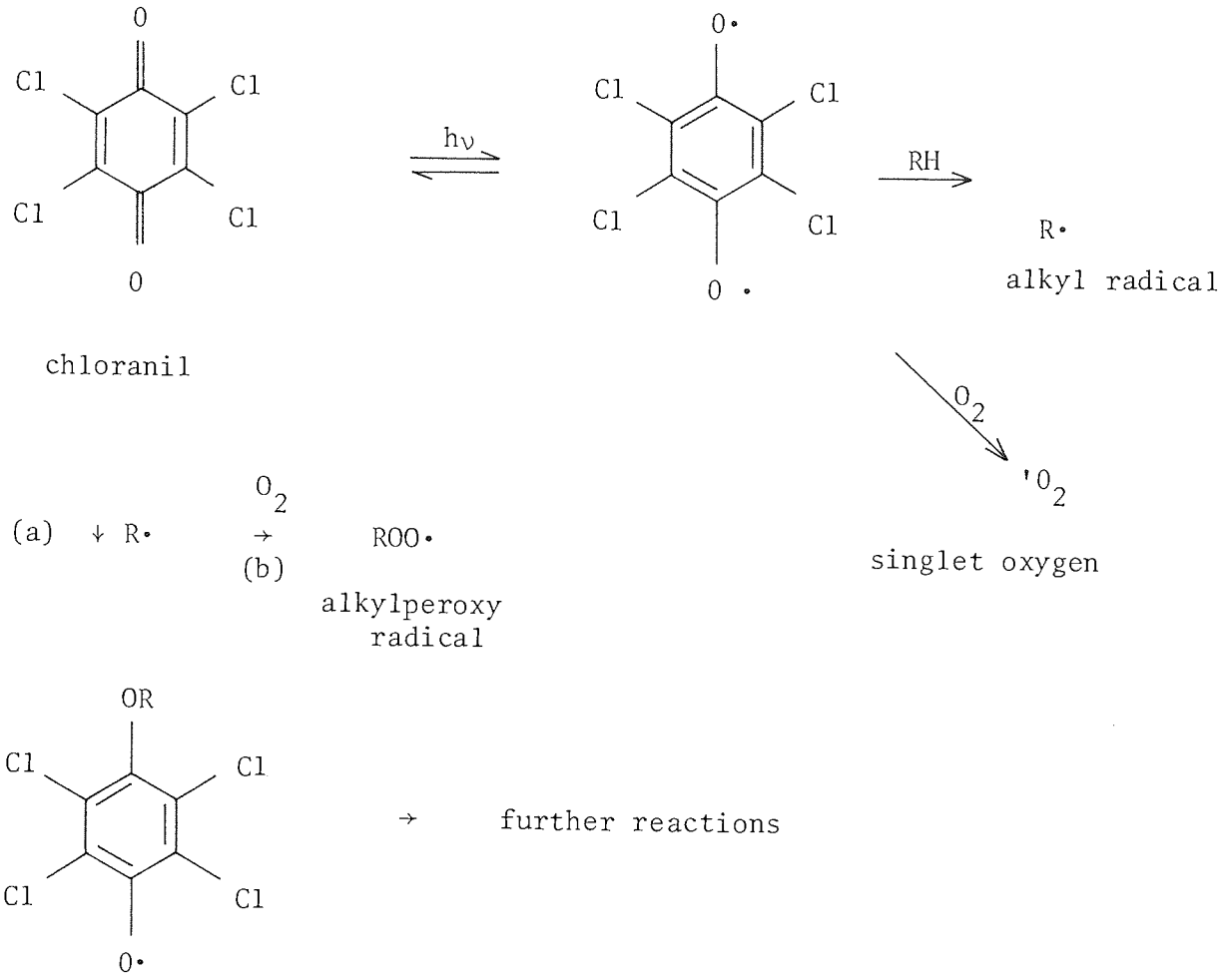

However, for this mechanism to be effective in stabilising the polymer during photoxidation it must compete not only with oxygen (b), similar to the nitroxide (Scheme 23) but also with the above mentioned photo-sensitisation mechanism. Indeed, no inhibition during the early stages of photoxidation of HIPS film containing chloranil was observed (figure 88). Furthermore, a retardation of the linear (maximum) rate of photoxidation was not apparent until a very high concentration of additive was used (10^{-2} mol/100 g). It is likely that chloranil behaves as a UV screen and UV absorber at this concentration. The

extinction coefficient of the UV absorption peaks at 293 nm and 375 nm are 10^4 - 10^5 and 10^2 - 10^3 respectively[177].

Inter-molecular photoreduction of the carbonyl group of the above p-quinone would appear to provide a feasible path for photo-sensitisation of HIPS during photoxidation. However, this mechanism and subsequent quenching by oxygen to give singlet oxygen is unlikely to be of significance during the photoxidation of similar HIPS film containing an equivalent molar concentration of a non-quinonoid carbonyl structure (dinomyl ketone) as the initial rate of oxygen absorption was not altered (figure 89, 10^{-2} mol/100 g). The small reduction of induction period during photoxidation of HIPS film containing the above high concentration of dinonyl ketone (equivalent to 25 hours of thermal oxidation at 98°C) is likely to be a consequence of the radical generating processes occurring via Norrish type I photolysis. The mechanism of which has been discussed fully in Chapter Four (see Scheme 9).

CONCLUSIONS

Photoxidation of HIPS, PBD and pure PS (and thermal oxidation of HIPS) was auto-catalytic, implying the build-up of an initiating species during UV irradiation. It is concluded that hydroperoxide (and peroxide) and not carbonyl are associated with autoxidation and are responsible for the oxidative degradation of the polymers studied. The progressive build-up of allylic hydroperoxide during processing or oven ageing photo-activated HIPS towards rapid photoxidation with a corresponding reduction of the auto-accelerating stage. The fastest rate (linear kinetics) was associated with the maximum concentration of hydroperoxide.

Additives which act by destroying hydroperoxides formed during thermal processing or subsequent exposure to UV lengthen the induction period to rapid oxygen absorption. This is exemplified by the metal complexes (Ni, Co, Cu and Zn) of dialkyldithiocarbamic acids which are known to destroy hydroperoxide by a catalytic (ionic) mechanism involving a Lewis acid (notably sulphur dioxide) generated in an initial stoichiometric reaction with hydroperoxide. The catechol phosphate peroxide decomposer used in this work was not as effective in stabilising HIPS towards photoxidation as the metal dithiocarbamates. Screening of incident UV by thiocarbamate stabilisers also makes a significant contribution to their effectiveness. Ferric dibutyl dithiocarbamate (and chloranil) behaved as pro-degradants for HIPS during photoxidation. However, the ferric complex was not photolysed completely before the

auto-accelerating stage but remained in the polymer and retarded the final photoxidation. This is because PBD is itself a powerful pro-oxidant and can be photolytically activated even in the presence of a peroxide decomposer.

Direct activation of PBD in the absence of oxygen and of initial hydroperoxide probably takes place via an initial photo-excited structural rearrangement with the formation of polyene chromophores. A commercial phenolic antioxidant present in HIPS behaved as a weak photo-activator during the auto-accelerating stage and a retarder of the maximum rate of photoxidation. Photo-activation was enhanced by prior photolysis.

Addition of a saturated aliphatic ketone (dinonyl ketone) to HIPS did not lead to photo-initiation during the initial stages of photoxidation at a concentration corresponding to extensive thermal oxidation. Moreover, addition of an α, β-unsaturated ketone (mesityl oxide) which absorbs more strongly in the UV, to a solution of PBD in chlorobenzene retarded the initial stages of photoxidation, probably by a radical scavenging mechanism. Therefore, it is concluded that neither intermolecular photoreduction of excited triplet state carbonyl (saturated or unsaturated) or excited singlet state oxygen formed by energy transfer from the ketone to ground state oxygen can be involved in the photo-initiation of HIPS even when ketone is added initially in the absence of hydroperoxide. Ozone which unlike singlet oxygen is a normal constituent of the earth's atmosphere did behave as a weak photo-initiator for the photoxidation

of HIPS by virtue of its peroxide formation during ozonisation. Carbonyl groups were not formed during ozonisation and hence not responsible for the observed photo-activation.

Even though the build-up of hydroperoxide during the oxidative degradation of HIPS was extremely rapid it was not the first chemical group to reach a maximum concentration. During photoxidation of HIPS, the gel content reached a maximum before hydroperoxide. The allylic peroxy radicals formed via initial hydrogen abstraction by alkylperoxy (or alkoxy) radicals from the tertiary allylic graft positions of HIPS will simultaneously produce allylic hydroperoxide by hydrogen abstraction and polymeric peroxy gel by addition to 1,2-polubutadiene. 1,2-polybutadiene is more reactive towards addition reactions and hydrogen abstraction by an alkylperoxy radical than 1,4-polybutadiene of which the cis is more reactive than the trans isomer. All isomeric modifications of PBD obeyed first order kinetics after an identical induction period. 1,2-polybutadiene was consumed at a faster rate and, therefore, accounts for the attainment of a maximum weight of gel before the maximum concentration of hydroperoxide. Both allylic hydroperoxide and polyperoxide are photolytically unstable and breakdown rapidly to give a common alkoxy radical. β-scission of the alkoxy radical severs the PS chain producing conjugated carbonyl which is reactive towards alkoxy radicals forming a relatively stable α-keto alkyl radical which either dimerises or undergoes further oxidative reaction leading to hydroperoxide. Addition of an alkoxy radical to α, β-unsaturated ketone destroys the conjugation double bond and constitutes the main reaction in the second stage of the gel formation. IR absorbance confirmed the presence of an ether.

Cross-linking in the rubber phase through an initial peroxidic linkage is responsible for the rapid destruction of the useful mechanical properties of HIPS. This was illustrated by the rapid depletion of the low temperature damping peak (tan δ) at -80°C during the photoxidation of HIPS prior to the formation of a significant quantity of stable oxidation products (carbonyl and hydroxyl). Indeed, the tan δ curve at 20°C was found (by inspection) to be similar to the gel curve representing both peroxy gel and the relatively stable ether gel which dominates the later stages of photoxidation of HIPS. The predominance of cross-linking in the early stages of photoxidation of HIPS was confirmed by the integral rise in complex modulus at 20°C which dropped slightly after extensive oxidation as a result of β-scission and formation of the secondary ether linkage. The selective chain scission of tie-bonds of grafted PBD-PS in HIPS was the only morphological change that occurred during photoxidation.

In the case of pure polystyrene, chain scission predominated during the early stages of photoxidation with the formation of carboxylic acid. This was confirmed by the drop in complex modulus and an increase in the appropriate IR absorbance. However, competitive cross-linking of PS does take place during photoxidation producing an insoluble ether gel with a similar absorbance in the IR to degraded HIPS. Low molecular weight cross-linked PS derived from the oxidative scission of the polymer was probably responsible for the low temperature damping peak (tan δ) found to increase during the photoxidation of pure polystyrene in contrast to the rubber peak of HIPS which decreased. Nevertheless a similar hydroperoxide initiation mechanism is responsible

for the oxidative degradation of pure polystyrene. Hydroperoxidation of PS was accelerated by the breakdown of allylic hydroperoxides derived from the photoxidation of the PBD moiety in HIPS; the rubber phase behaved as a chemical pro-oxidant.

SUGGESTIONS FOR FURTHER WORK

The evidence presented in this thesis suggests overwhelmingly that thermally-produced allylic hydroperoxides are responsible for the photo-instability of HIPS. However, the possibility of minute quantities of α, β-unsaturated carbonyl compounds (undetectable by transmission IR spectroscopy) derived from the breakdown of allylic hydroperoxide acting as photo-initiators still remains as these structures are powerful chromophores. Therefore, further experiments are required to correlate the effect of different concentrations of allylic hydroperoxide and α, β-unsaturated carbonyl on the initial rate of photoxidation of HIPS. The thermal decomposition in argon of thermally-produced hydroperoxides was attempted but the resultant gelation of the unsaturation complicated the subsequent photoxidation. It is suggested that a part of each sample of a series of HIPS films which have had different amounts of thermal oxidation and thus contain different concentrations of hydroperoxide and carbonyl is heated in argon under identical conditions until the hydroperoxide has been completely decomposed. The subsequent rate of photoxidation of each sample should then be compared with that of samples taken from the original series (containing hydroperoxide) which have similar (1) carbonyl index, (2) unsaturation, (3) gel content. Carbonyl and unsaturation (trans-1,4-polybutadiene) indexes are most conveniently measured by IR spectroscopy. Whereas gel content may be estimated accurately by measurement of complex modulus without destruction of the sample.

During the photoxidation of HIPS film which has had a mild processing operation carbonyl (and hydroxyl) were found to increase rapidly after an induction period while hydroperoxide concentration (measured by iodiometry)showed no induction period. This was consistent with the fact that a small quantity of hydroperoxide could be detected before exposure to UV. Confirmation of these observations using ATR rather than transmission spectroscopy is necessary as carbonyl compounds derived by the decomposition of hydroperoxide will be formed initially at the surface of the polymer film.

The maximum initial rate of photoxidation of HIPS was found to occur just before the maximum concentration of thermally-produced hydroperoxide which indicates the presence of a photolytically unstable peroxy gel. It is suggested that gel content should be estimated during the oven ageing of extruded HIPS film to confirm that an entirely analogous cross-linking process occurs during both thermal and photoxidation.

Pre-irradiation of HIPS film in argon was found to activate the polymer towards photoxidation. No carbonyl was detected by IR spectroscopy after photolysis. It is suggested that phosphorescence studies should be performed on pre-irradiated samples to see if a correlation exists between possible changes in the low concentration of α, β-unsaturated carbonyl presumably present, and the initial rate of photoxidation. In addition, a chemical estimation of the concentration of polyene chromophores present immediately after pre-irradiation of HIPS film in argon should provide useful information.

An attempt should be made at identification by ESR of the various radicals produced during photolysis by trapping at liquid nitrogen temperature. Cross-linking of HIPS during pre-irradiation was established by the changes in dynamic-mechanical properties measured at ambient temperature on the Rheovibron. However, it is necessary to confirm that the loss of useful mechanical properties (embrittlement) resulted through the destruction of the rubber phase by cross-linking. It is suggested that the low temperature damping peak (tan δ) should be measured with respect to photolysis.

Further information on the relative importance of photo-sensitisers on the rate of photoxidation and cross-linking may be obtained by the prior photolysis of HIPS film containing varying concentrations of suitable saturated and conjugated ketones.

REFERENCES

1. J.A.Kerr,Chem.Rev., 66, 465 (1966).
2. W.L.Hawkins, (Ed.) Polymer Stabilisation, Wiley-Interscience, New York and London (1972) p.31 et seq.
3. J.L.Bolland, Quart.Rev., London, 3, 1 (1949).
4. A.V.Tobolsky, D.J.Metz and R.B.Mesrobian, J.Am.Chem.Soc., 72, 1942 (1950).
5. A.Robertson and W.A.Waters, Trans.Faraday Soc., 201 (1946).
6. Z.Manasek, D.Berck, M.Micko, M.Lazar and J.Pavinec, Rubber Chem.Tech., 35, 532 (1963).
7. G.Scott, Atmospheric Oxidation and Antioxidants, Elsevier, New York and London (1965) p.92 et seq.
8. Reference 2, p.18.
9. E.H.Farmer and A.Sundralingarn, J.Chem.Soc., 1, 145, 125 (1943).
10. O.Cicchetti and F.Gratani, Eur.Poly.J., 8, 561 (1972).
11. L.R.Koller, Ultraviolet Radiation, 2nd Ed., Wiley, New York (1965) p.4.
12. J.C.W.Chien, J.Poly.Chem., 12, 69, 4317 (1965).
13. F.H.Winslow and W.L.Hawkins, Appl.Poly.Sym., 4, 29 (1967).
14. O.Cicchetti , Adv.Poly.Sci., 7, 70 (1970).
15. R.G.W.Norrish and M.H.Searby, Proc.Roy.Soc., London, A 237, 464 (1956).
16. N.J.Turro, Molecular Photochemistry, W.A. Benjamin, Inc., New York (1965) p.139 et seq.
17. G.Calvert and N.Pitts, Photochemistry, J.Wiley and Son, Inc. (1966) p.379 et seq.
18. G.H.Hartley and J.E.Guillet, Macromol., 1, 165 (1968).
19. P.J.Wagner and G.S.Hammond, J.Am.Chem.Soc., 87, 4009 (1965) and 88, 1245 (1966).

20. J.E.Guillet and R.G.W.Norrish, Proc.Roy.Soc., A 233, 153 (1955).

21. G.H.Hartley and J.E.Guillet, Macromol., 1, 413 (1968).

22. H. Kautsky, Trans.Faraday Soc., 35, 216 (1939).

23. A.M.Trozzolo and F.W.Winslow, Macromol., 1, 1, 98 (1968).

24. K.Kawaoka, A.V.Khan and D.R.Kearns, J.Chem.Phy., 46, 1842 (1967).

25. J.R.MacCallum and C.T.Rankin, Die Makromol. Chem., 175, 2477 (1974).

26. M.L.Kaplan and P.G.Kelleher, J.Poly.Sci., A-1, 8, 3163 (1970).

27. A.K.Breck, C.L.Taylor, K.E.Russell and J.K.S.Wan, J.Poly.Sci., Poly.Chem.Ed., 12, 1505 (1974).

28. G.A.George, J.Appl.Poly.Sci., 18, 117 and 419 (1974).

29. W. Klöpffer, Eur.Poly.J., 11, 203 (1975).

30. J.F.Rabek and B.Ranby, J.Poly.Sci., Poly.Chem.Ed., 12, 273 (1974).

31. J.R.Lawrence and N.A.Weir, J.Poly.Sci., Poly.Chem.Ed., 11, 105 (1973).

32. J.Shimada and K.Kabuki, J.Appl.Poly.Sci., 12, 671 (1968).

33. J.Shimada and K.Kabuki, J.Appl.Poly.Sci., 12, 655 (1968).

34. S.W.Beavan, D.Phillips, Eur.Poly.J., 10, 593 (1974).

35. S.W.Beavan, P.A.Hackett and D.Phillips, Eur.Poly.J., 10, 925 (1974).

36. K.Tsuji, Adv.Poly.Sci., 12, 131 (1973).

37. G.Scott, Sym. on Macromol, Helsinki, Special Publ. (1972).

38. Reference 37, p.9.

39. H.J.Heller, Eur.Poly.J., Suppl., 105 (1969).

40. G.P.Fratkina and E.I.Kirillova,Poly,Sci., USSR, 12, 2491 (1970).

41. K.T.Paul, RAPRA Bulletin, 2, 29 (1972).

42. D.J.Carlsson and J.C.Robb, Trans.Faraday Soc., 62, 3403 (1966).

43. M.S.Kharasch, A.Fono and W.Nudenberg, J.Org.Chem., 16, 113 (1951).

44. C.G.Hatchard and C.A.Parker, J.Phy.Chem., 63, 22 (1959).

45. Reference 17, p.780.

46. B.Ranby and J.F.Rabek, Photodegradation and Photostabilisation of Polymers: Principles and Applications, Wiley-interscience, London (1975) p.

47. N.Grassie and N.A.Weir, J.Appl.Poly.Sci., 9, 987 (1965)

48. Private Com., Building Research Establishment (BRE) Garston, Watford (1975).

49. C.R.Boss and C.W.Chien, J.Appl.Poly.Sci., A-1, 4, 1543 (1966).

50. J.A.Meyer, C.Rogers, V.Stannett and M.Szwarc, Tappi., 40,142 (1957).

51. L.Bateman, Quart.Rev., 8, 147 (1954).

52. N.Grassie and N.A.Weir, J.Appl.Poly.Sci., 9, 963 (1965).

53. Instruction mannual for Rheovibron, DDVII, Toyo Measuring Instruments Co.Ltd., Tokyo (1969).

54. M.Matsuo, C.Nozak and Y.Jyo, Prog.Eng.Sci., 9, 197 (1969).

55. K.Kato, Poly.Let., 4, 35 (1965).

56. H.Keskkula, Schmitt, J.A.Cobler, J.G. and J.W.Norton, Paper presented at Gordon Res. Conf., New London (1958).

57. F.J.Welcher, Standard Methods of Chemical Analysis, 8th Ed., B, 3, (1966) p.1592.

58. A.Anton, J.Appl.Poly.Sci., 9, 1631 (1965).

59. O.Cicchetti, R.De Simone and F.Gratani, Eur.Poly.J., 9 1205 (1973).

60. P.Bocek, Chem.Prum., 17, 8, 439 (1967).

61. C.D.Wagner, R.H.Smith and E.D.Peters, Anal.Chem., 19, 976 (1947).

62. N.A.Weir, J.Appl.Poly.Sci., 17, 401 (1973).

63. P.J.Flory and J.Rehner, J.Chem.Phys., 11, 512 (1943).

64. L.Mullins, J.Poly.Sci., 19, 225 (1956).

65. C.G.Moore and W.F.Watson, J.Poly.Sci., 19, 237 (1956).

66. R.L.Scott and M.Magat, J.Poly.Sci., 4, 555 (1949).

67. P.J.Flory, Ind.Eng.Chem., 38, 417 (1946).

68. J.P.Guillory and C.F.Cook, J.Poly.Sci., Poly.Chem.Ed., 8, 11, 1927 (1973).

69. A.I.Vogel, Quantitative Inorganic Analysis, Longmans (1966) p.443.

70. R.F.Vassilev, Mackromol. Chem., 126, 231 (1969).

71. F.R.Mayo and K.C.Irwin, Prog.Eng.Sci., 9, 282 (1969).

72. J.L.Bolland, Trans.Faraday Soc., 46, 358 (1950).

73. T.L.Cottrell, The Strengths of Chemical Bonds, Butterworths, London, 2nd Ed. (1958) p. 280 et seq.

74. L.Pauling, The Nature of the Chemical Bond, Cornell Univ. Press, Ithaca, New York, 3rd Ed., (1960) p.53

75. G.V.Hutson and G.Scott, Eur.Poly.J., 10, 45 (1973).

76. M.A.Salimov, Rub.Chem. and Tech., 36, 747 (1963).

77. D.Rysavy and Z.Slama, Chem.Prum., 12, 17, 652 (1967), RAPRA Tranl. 1619 (1968).

78. W.L.Hawkins, Preprints, SPE conf., 38 (1964).

79. N.V.Zolotova and E.T.Denisov, J.Poly.Sci., A-1, 9, 3311 (1971).

80. J.R.Shelton and D.N.Vincent, J.Am.Chem.Soc., 85, 2433 (1963).

81. D.J.Carlsson and D.M.Wiles, Macromol., 2, 4, 174 (1971).

82. Reference 7, p.25.

83. W.Kern and A.R.Heinz, Makromol.Chem., 16, 81 (1955).

84. Reference 7, p.390.

85. F.R.Mayo, J.Am.Chem.Soc., 80, 2465 (1958).

86. D.J.Carlsson and D.M.Wiles, Macromol., 3, 7, 259 (1974).

87. M.U.Amin, G.Scott and L.M.K.Tillekeratne, Eur.Poly.J., 11, 85 (1975).

88. P.I.Vincent, F.M.Willmonth and A.J.Cobbold, 2nd Int.Conf., Yield, deformation and fracture of polymers, Cambridge, 5, 3 (1973).

89. L.J.Bellamy, Infra-red Spectra of Complex Molecules, Methuen and Co.Ltd., London (1958) p.5 et seq.

90. J.R.Dyer, Applications of Absorption Spectroscopy of Organic Compounds, Prentice-Hall, Inc., New Jersey (1965) p.33 et seq.

91. P.M.Hay, The Science and Technology of Polymer films, Ed. O.J.Sweeting, Interscience Publ., 1 (1968) p.528.

92. K.Schmieder and K.Wolf, Kolloid-Z, 127, 65 (1952).

93. P.I.Vincent, Physics of Plastics, Ed. P.D.Ritchie, Iliffe Book Ltd., London (1965) p.98.

94. M.Gordon, Physics of Plastics, Ed. P.D. Ritchie, Iliffe Book Ltd., London (1965) p.224.

95. C.M.Blow, Rubber Technology and Manufacture, Ed. C.M.Blow, Butterworths, London (1971) p.20.

96. L.E.Nielsen, Mechanical Properties of Polymer, Reinhold Pub.Co., New York (1962) p.174.

97. R.F.Boyer, Poly.Eng.and Sci., 3, 8, 161 (1968).

98. Reference 7, p.145 et seq.

99. M.U.Amin and G.Scott, Eur.Poly.J., 10, 1019 (1974).

100. L.J.Broutman and T.Kobayashi, 2nd Int.Conf., Yield deformation and fracture of polymers, Cambridge, 10, 9 (1973).

101. K.H.Illers, Electrochem. 65, 679 (1961).

102. J.F.Fellers and M.Rahbar-Semanani, J.Poly.Sci.,Poly.Chem.Ed., 12, 2035 (1974).

103. V.R.Kosfeld, Kolloid-Z, 172 (1960).

104. S.L.Samuels and G.L.Wilkes, Poly.Eng.and Sci., 4, 13, 280 (1973).

105. G.Scott and M.Tahan, Preprints, Int.Sym.on Degradation and Stabilisation of Polymers, 47 (1974).

106. J.F.Rabek and B.Ranby, J.Poly.Sci., Poly.Chem.Ed., 12, 295 (1974).

107. Reference 7, p.250.

108. Reference 46, p.199.

109. K.J.Humphris and G.Scott, Pure and Appl.Chem., 36, 163 (1973).

110. M.S.Kharasch, A.Fono and W.Nudenberg, J.Org.Chem., 15, 748, 753, 763, 775 (1953).

111. H.S.Blanchard, J.Am.Chem.Soc., 81, 4548 (1959).

112. F.H.Seubold and W.E.Vaughan, J.Am.Chem.Soc., 75, 3790 (1953).

113. R.G.W.Norrish and M.H.Searby, Roy.Soc.Proc., A 237, 464 (1956).

114. W.E.Doering and W.R.Roth, Tetrahedron, 18, 67 (1962).

115. J.D.Roberts and M.C.Caserio, Basic Principles of Organic Chemistry, W.A.Benjamin Inc., New York, Amsterdam (1965) p.432.

116. Reference 7, p.107

117. K.J.Humphris and G.Scott, J.Chem.Soc., Perkin II, 6, 826 (1973).

118. Reference 7, p.33, 34.

119. Reference 5, p.208.

120. Reference 17, p.533.

121. Reference 17, p.379.

122. N.C.Yang and M.J.Jorgenson, Tet.Lett., 1203 (1964).

123. C.H.Bamford and R.G.W.Norrish, J.Chem.Soc., 1544 (1938).

124. Reference 90, p.12.

125. Reference 90, p.11.

126. E.Dyer, O.H.Beckett, S.E.Strause and H.E.Worrell, J.Am.Chem.Soc., 78, 3384 (1956).

127. Reference 17, p.382.

128. Reference 17, p.378.

129. D.J.Harper and J.F.McKellar, J.Appl.Poly.Sci., 17, 3503 (1973).

130. P.J.Burchill and G.A.George, J.Poly.Sci., Poly.Lett., 12, 497 (1974).

131. F.E.Blacet and R.D.Vanselow, Abstracts, Div.Phys.Chem., A.C.S. (1957).

132. Reference 7, p.12.

133. Reference 115, p.461.

134. A.P.Pivovarov and A.F.Lukovnikov, Khim.Vys.Energ., 2, 220 (1968); High Energ.Chem., 2, 188 (1968).

135. M.F.R.Mulcahy and I.C.Watt, Proc.Roy.Soc., A 216, 10, 30 (1953).

136. C.F.H.Tipper, Ind.Chem.35, 113 (1959).

137. Reference 7, p.88.

138. Reference 115, p.1039.

139. W.G.Herkstroeter, A.A.Lamola and G.S.Hammond, J.Am.Chem.Soc., 86, 4537 (1964).

140. D.J.Carlsson and D.M.Wiles, Macromol., 6, 2, 597 (1969).

141. J.L.Morand, Rub.Chem.Tech, 48, 481 (1972).

142. F.Sondheimer, D.A.Ben-Efraim and R.Wolovsky, J.Am.Chem.Soc., 83, 1675 (1961).

143. D.F.Evans, J.Chem.Soc., 2, 1735 (1960).

144. P.Carstensen, Die Mackromol. Chem., 142, 131 (1971).

145. L.Bateman and G.Gee, Proc.Roy.Soc., A 195, 376 (1948).

146. E.J.Hart and M.S.Matheson, J.Am.Chem.Soc., 70, 785 (1948).

147. M.A.Golub and C.L.Stephens, J.Poly.Sci., Part C, 16, 765 (1967).

148. K.J.Laidler, The Chemical Kinetics of Excited States, Oxford Univ. Press (1955) p.95.

149. J.Shimada, K.Kabuki and M.Ando., Rev.Elec.Com., 5-6, 20, 553 (1972).

150. Reference 7, p.145, 156 et seq.

151. Reference 2, p.217.

152. Air Pollution Foundation, Los Angeles (1955).

153. Reference 115, p.191 et seq.

154. Reference 7, p.478 et seq.

155. E.R.Erickson, R.A.Bernstein, E.L.Hill and P.Kusy, Sym., Effect of Ozone on Rubber, A.S.T.M. Spec.Publ., 11, 229 (1958).

156. F.H.Kendall and J.Mann, J.Poly.Sci., 19, 503 (1956); Rub.Chem.Tech., 29, 1332 (1956).

157. D.J.Carlsson and D.M.Wiles, J.Poly.Sci., Poly.Let.Ed., 12, 11, 759 (1973).

158. R.M.Badger, A.C.Wright and R.F.Whitlock, J.Chem.Phy., 43, 4345 (1965).

159. B.Schnuriger and J.Bourdon, Photochem. Photobiol., 8, 361 (1968).

160. G.Scott, Eur.Poly.J., Suppl., 189 (1969).

161. G.Scott, Macromol. Chem., 8, 319 (1973).

162. D.C.Mellor, A.B.Moir and G.Scott, Eur.Poly.J., 9, 219 (1973).

163. J.P.Guillory and C.F.Cook, J.Am.Chem.Soc., 95, 4885 (1973).

164. D.J.Carlsson, T.Suprunchuk and D.M.Wiles, J.Appl.Poly.Sci., 16, 615 (1972).

165. J.P.Guillory and R.S.Becker, J.Poly.Sci., Poly.Chem.Ed., 12, 993 (1974).

166. J.D.Holdsworth, G.Scott and D.Williams, J.Chem.Soc., 4692 (1964).

167. G.Scott, Am.Chem.Soc., (1972).

168. J.C.W.Chien and C.R.Boss, J.Poly.Sci., A-1, 10, 1579 (1972).

169. G.Scott, Chem.Brit. 6, 9, 267 (1973).

170. R.P.R.Ranaweera and G.Scott, J.Poly.Sci., Poly.Lett.Ed., 2, 13, 71, (1975).

171. D.J.Carlsson, T.Suprunchuk and D.M.Wiles, J.Poly.Sci., Poly.Lett.Ed., 11, 61 (1973).

172. H.J.Heller and H.R.Blattmann, Pure and Appl.Chem., 36, 141 (1973).

173. K.U.Ingold, Adv.,Chem.Ser., 75, 296 (1968).

174. G.V.Hutson and G.Scott, J.Poly.Sci., Sym., 40, 67 (1973).

175. K.J.Humphris and G.Scott, J.Chem.Soc., Perkin Trans.II, 617 (1974).

176. A.A.Yassin and A.M.El-Reedy, Eur.Poly.J., 7, 9, 657 (1973).

177. UV Allas of Organic Compounds, Butterworths, London (1971).

Reprinted from

THE CHEMICAL AND PHYSICAL CHANGES OCCURRING DURING U.V. DEGRADATION OF HIGH IMPACT POLYSTYRENE

A. GHAFFAR, A. SCOTT and G. SCOTT

Department of Chemistry, University of Aston in Birmingham, Birmingham B4 7ET, England

(*Received* 9 *August* 1974)

Abstract—Dynamic-mechanical measurements, i.r. spectroscopy and oxygen absorption techniques have been used to study structural changes in high impact polystyrene during its photo-oxidation under artificial weathering conditions. It was found, using a viscoelastometric technique, that the damping peak at −80° (corresponding to the β-transition temperature of polybutadiene) disappeared completely after irradiation for 14 hr; this was accompanied by a sharp increase in the complex modulus at 20°. A parallel change was observed in the rate of formation of carbonyl and hydroxyl groups as measured by i.r. spectroscopy. The results indicate that the polybutadiene part of the resin is selectively attacked by u.v. light during the initial stages of the process. Similar results have been reported for ABS [1].

PERGAMON PRESS
OXFORD · NEW YORK